X-RAY AND SPECTROSCOPIC STUDIES ON SOME LIQUID CRYSTALS

Thesis Submitted for the Degree of
Doctor of Philosophy (Science)
of the
University of North Bengal
1983

NORTH BENGAL
UNIVERSITY LIBRARY
RAJA RAMMOHUNPUR

BASANA BHATTACHARJEE
Department of Physics
Lady Keane Girls' College, Shillong
Meghalaya-793001
India

ST - VERE

STOCK TAKING - 2011

Ref
537.5352
B 575 St

T 83579
27 DEC 1983

DEPARTMENT OF PHYSICS
UNIVERSITY OF NORTH BENGAL

Phone : Siliguri 20223, 20273 PABX Extn. 28
NORTH BENGAL UNIVERSITY
Dist. DARJEELING, WEST BENGAL.
INDIA PIN-734430

Ref No Phy/C-7/Cert-83

Date 25. 2. 1983

This is to certify that the research work reported in the dissertation "X-ray and Spectroscopic studies on some Liquid Crystals" has been performed by Mrs. Basana Choudhury (neé Bhattacharjee) under my supervision. Some part of this work has been done in collaboration with other research workers, however, even there her contribution is very substantial. In character and disposition Mrs. Basana Choudhury (neé Bhattacharjee) is fit to submit her thesis for the Ph.D. degree of the University of North Bengal.

Ranjit Paul

(Ranjit Paul)

Professor of Physics & Supervisor.

ACKNOWLEDGEMENTS.

I wish to express my deep sense of gratitude to Professor Ranjit Paul, Department of Physics, University of North Bengal for his constant guidance and active supervision throughout the period of my research work. I also wish to extend my gratefulness to Dr. (Mrs.) Sukla Paul for many valuable suggestions and whole hearted co-operation in this regard.

I also record my gratefulness to Professor S.N.Sen, Sr.Prof. & Head of the Department of Physics, N.B.U. for his help in many respect. Thanks are due to University Grants Commission, New Delhi and the Physics Department, University of North Bengal for providing me with a Teacher Fellowship in the Faculty Improvement Programme, Principal, Lady Keane Girls' College, Shillong is also thankfully acknowledged for granting me study leave.

I am grateful to Prof. M. Wada of Tohoku University, Sendai and also to Prof. A. de Vries, Liquid Crystal Institute, Kent State University, U.S.A. for sending us the samples MBBA and BBA respectively. Thanks are also due to Prof. M.Schadt of M/s. Hoffmann-La-Roche, Basel, Switzerland for supplying us the samples (CPBD, 500B and 800B and the liquid crystal No. III in chapter 12).

M/s. Imperial Chemical Company, London is also thankfully acknowledged for sending me two dyes (Dispersal scarlet B and Dispersal Rubine B). Thanks are also conveyed to Prof. H. Schenk of the University of Amsterdam for providing

us with the molecular model Kit. Dr. K.L. Chopra of I.I.T. Delhi (India) is thankfully acknowledged for taking troubles in preparing some transparent conductive glass plates for us.

I like to extend my sincere thanks to Dr. G.S.S. Murti, Mr. N. De, Mr. A. Majumdar, Mr. R. Mukherjee, Dr. A. Sengupta, Dr. S. L. Datta, Dr. S. Saha and Mr. S. Talapatra of Chemistry Department, University of North Bengal for their help in purifying samples, synthesising two dyes and taking I.R. spectra of one sample and also for their help and co-operation in many other factors.

Grateful acknowledgement is due to Dr. T. N. Misra of the Optics Department, Indian Association for the Cultivation of Science (IACS), Jadavpur, Calcutta - 32, for permitting me to use the Spectrophotometer to study the Guest Host interactions and to Dr. S. Chakraborty of the same department for his helpful co-operation in this regard.

Mrs. E.B. Mirza of Bhabha Atomic Research Centre, Chemistry Division is thankfully acknowledged for performing DSC of two samples.

I wish to express my thankfulness to Mr. B. Jha, Mr. A.K.Zeminder and Mrs. A. Nandi for their help in the laboratory and also their collaboration in the works with samples CBOOA, PCBAV and Guest Host interactions.

I am thankful to Meghalaya College Teachers' Association and also to N.B.U. Research Scholars' Association for the help rendered to me in solving several problems during the tenure of my fellowship.

I desire to record my appreciation for the sincere help rendered to me by Mr. R. K. Datta of Physics Deptt.,N.B.U. I also take the opportunity to extend my thanks to Mr. B.Majumdar, Mr. P. Mandal, Mr. M.Mitra, Mrs. K. Bhattacharjee, Mr.S.K.Ghosh of Physics Department,N.B.U. and Mr. D. Lahiri of Polytechnique Institute, Kurseong and R.Chatterjee of Siliguri for their help and co-operation during the progress of my work.

Mr. S. Sarkar, Senior Technical Assistant of Physics Department,N.B.U. and Mr. B.K.Nag, Mr. G.C. Basak of Central Workshop,N.B.U. are thankfully acknowledged for their help in maintainance and repair of different instruments and fabrication of different apparatus needed for experimental purpose. I am also thankful to Mr. N.K.Samanta, Mr. C. Nayak of Research Service Centre, NBU for many help in using the computer.

I like to express my thankfulness to Mr. S. Choudhury for typing the thesis and also to Mr. N. Ghosh and Mr.B.Bagchi for drawing the figures.

Sincere gratitude is expressed to Miss. J.Sen, Ex-Vice-Principal, Lady Keane Girls' College, Shillong for the inspiration I received from her.

Lastly, I wish to express my gratefulness to my beloved parents, my husband and my brothers and sister for the constant encouragement and inspiration I received from them.

Basana Bhattacharjee.

Dated The 4th March,1983, (Basana Bhattacharjee)

North Bengal University.

CONTENTS.

		Page
CHAPTER 1		
General Introduction ...	...	1-51
1.1.	What is liquid crystal... ...	2
1.2.	Classification of liquid crystals ...	3
1.3.	Chemical constitution of mesomorphic compounds... ...	13
1.4.	Theories of nematic liquid crystals.... ...	19
	Phase transitions... ...	22
	Orientational distribution functions... ...	27
	Orientational order parameters ...	28
	McMillan's theory of Smectic A ...	33
1.5.(a)	Alignment of nematic mesophases ...	35
1.5.(b)	Alignment of Smectic phases ...	37
1.6.	Texture analysis by polarising microscope... ...	38
1.7.	Motivation and scope of the work ...	42
	References... ...	44
CHAPTER 2		
Introduction to X-ray work ...	...	52-68
1.1.	Sample used... ...	53
1.2.	Experimental procedure... ...	54
	Recrystallization... ...	54
	Polarizing microscopic study for identification of different phases and transition temperatures... ...	55

			Page
	Apparatus...	...	56
1.3.	Alignment of samples...	...	61
1.4.	Conversion of optical density into X-ray intensity...	...	62
	References...	...	68

CHAPTER 3

Theoretical Background for X-ray work...	...	69-85
Average Intermolecular distance, Apparent length of the molecules and layer thickness (in case of smectics)...	...	74
Orientational distribution function and order parameter...	...	76
Pseudopotential...	...	81
References...	...	84

CHAPTER 4

Experimental procedure and data Analysis...	...	86-109
References...	...	102
Computer programme...	...	103

CHAPTER 5

X-ray diffraction studies on unoriented mesophases of (-)-2-Methylbutyl-p-n-(p-methoxy benzylidene) Amino) Valerophenone	...	110-137
1. Introduction...	...	111
2. Experimental methods...	...	112

		Page
3.	Experimental results and discussions....	112
	Tables.. ...	124
	References... ...	137

CHAPTER 6

X-ray diffraction studies on ordered sample of 4-Methoxy 4'-n-Butylbenzylidene-Aniline (MBBA in short) at room temperature... ... 138-155

1.	Introduction... ...	139
2.	Results and discussions... ...	140
	Tables... ...	150
	References... ...	155

CHAPTER 7

X-ray diffraction studies of 4-Cyanophenyl 4'-n-Heptylbenzoate in the nematic phase (CPHB in short) in magnetic field.... ... 156-193

1.	Introduction... ...	157
2.	Results and discussions... ...	158
	Tables... ...	170
	References... ...	193

CHAPTER 8

X-ray diffraction studies on the nematic phase of 4'-pentyloxy-4-cyanophenyl (50CB in short) in magnetic field... ... 194-222

1.	Introduction... ...	195

		Page
2.	Results and discussions... ...	196
	Tables... ...	204
	References... ...	222

CHAPTER 9

X-ray diffraction studies on the mesophases of 4'-Octyloxy-4-cyanobiphenyl(8OCB in short) in magnetic field... ... 223-254

1.	Introduction... ...	224
2.	Results and discussions... ...	225
	Tables... ...	233
	References... ...	254

CHAPTER 10

X-ray diffraction studies on Smectic phase of 4'-(n-(p-Pentyloxy Carbonyloxy-Benzylidene) Amino) Valerophenone... ... 255-278

1.	Introduction... ...	256
2.	Experimental Results and discussions...	257
	Tables... ...	268
	References... ...	278

CHAPTER 11

X-ray diffraction studies on the mesophases of n-p-Cyanobenzylidene p-Octyloxy-Aniline (CBOOA in short) in magnetic field... ... 279-322

		Page
1.	Introduction... ...	280
2.	Experimental results and discussions...	281
	Tables.. ...	295
	References... ...	322

CHAPTER 12

The order parameter of Dye molecules as Guest in nematic liquid crystalline host in presence of electric field... ... 323-344

1.	Introduction and outlines of theoretical background.... ...	324
2.	Experimental... ...	332
3.	Results and discussions... ...	338
	Tables... ...	341
	References... ...	344

CHAPTER 13

Summary and conclusion... ...	345-352
References... ...	352
List of Publications... ... 353-354	353-354

CHAPTER 1

GENERAL INTRODUCTION.

CHAPTER 1

GENERAL INTRODUCTION

1.1. What is liquid Crystal

The term liquid crystal was not known to us before 1888. Reintzer[1,2] and O.Lehmann[2] observed unusual melting behaviour in certain organic compound and it was O.Lehmann who designated a state of matter that is intermediate between solid crystalline and the isotropic liquid phase in 1890 and used the term "Liquid Crystals". Because of their intermediate nature liquid crystals are also called mesophase or mesomorphic phase[4a,4b] that lies between the rigidly ordered solid phase where the mobility of the individual molecule is restricted and the isotropic phase where the molecular mobility and a general lack of molecular order exists. On reaching a certain temperature the solid undergoes transformation into a turbid condition, where there is no correlation between the directions or centres of mass of the molecules (as in isotropic liquid), but adopts a structure where although ~~3-dimensional~~ lattice structure is broken the molecules still retain some sort of order regarding direction of their long axes that is both birefringent and fluid. At a higher temperatures called the clearing temperature, the turbid condition disappears and the isotropic liquid state is formed. These changes take place in reverse order on cooling for most of the liquid crystalline substances.

Almost all liquid crystalline materials are organic compounds. Several thousands of organic compounds are now known

to form liquid crystals[4,5]. Kelker[6] has written a historical summary about liquid crystals. Numerous review articles have been appeared including those of Bragg[7] and Brown & Shaw[8]. Some other review articles and books on liquid crystals are also referred here[9-17] where details about various types of liquid crystals, their theory, experimental data and applications are given.

1.2. Classification of liquid crystals:

The two major categories of liquid crystals are identified as 'thermotropic' and 'lyotropic'. Thermotropic liquid-crystals are obtained by heating certain chemical compounds. Lyotropic liquid crystals occur in solution. The best known representative of this group are aqueous soap solutions. However, we will not discuss about lyotropic liquid crystals further as only thermotropic liquid crystals concern us in this thesis.

Thermotropic liquid crystals are obtained when some organic substances are melted. They are formed at the stage of melting when insufficient heat has been supplied to bring about the transition into normal isotropic liquid.

Thermotropic liquid can be classified into three types - Nematics, Smectics and cholesterics[18]. The classification system proposed by Sackman and Co-workers[19] was expanded by de Vries[20,21] to included three kinds of nematic, two cholesterics, eight distinguishable smectic phases ranging from A to H. A columnar phase has also been recently observed in certain disc like molecules.

Nematics

The word nematic comes from the Greek word thread and refers to certain thread like defects which commonly observed in these materials. Nematic liquid crystals differ from ordinary isotropic liquid by a long range orientational order of the long axes of the rod like molecules i.e. the molecules tend to align parallel to a preferred direction $\bar{n}$ usually ~~xix~~ called the director. The preferred direction usually varies from point to point in the medium. Nematic liquid crystal has no long range translational order, i.e. there is no long range correlation of the molecular centre of mass positions and thus the nematic phase is fluid. Fig. 1.1 shows the schematic representation of molecules in nematic and isotropic phase. The molecules are allowed to rotate freely about their long axis. In the state of thermal equilibrium the nematic phase has the axis of symmetry which is identical with the director direction. Nematic phase is optically uniaxial. The nematic phase is mobile and markedly affected by the external fields and forces; the molecules therefore possess a high degree of mobility and are capable of rotational movement. According to the molecular statistical theory of Maier and Saupe[22] the anisotropy of the molecular polarisability is responsible for the occurrence of the liquid crystalline phase. The relation between molecular structure has been discussed in details by Gray and Winsor[23] and Jen and Van der Veen[24].

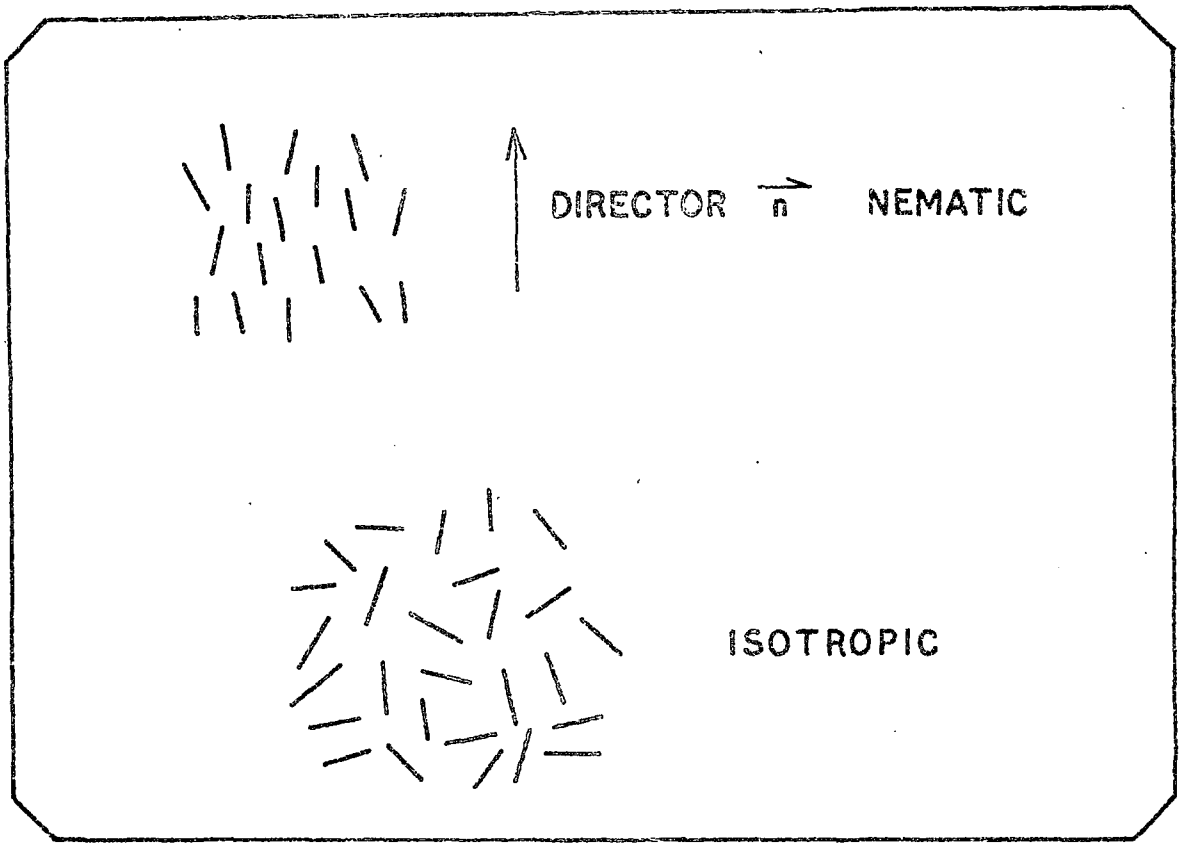

FIG. I.I. SCHEMATIC REPRESENTATION OF MOLECULES IN NEMATIC AND ISOTROPIC STATES.

Molecular ordering within a classic nematic phase is such that there is no regular arrangement between neighbouring molecules. de Vries[25,26] has proposed more than one type of nematic phase from his experimental observations namely -

(1) Normal Nematic phase,

(2) Cybotactic phase, and

(3) Skew cybotactic phase.

Smectics:

All smectic liquid crystals have a layered structure. The centre of gravity of the elongated molecules are arranged in equidistant layers. The long axes of the molecules are parallel to a preferred direction $\bar{n}$ which may be normal to the plane as in case smectic A (S_A) (Fig. 1.2 a) or tilted in case of smectic C (S_C)(Fig. 1.2 b). The arrangement of the centres of gravity within the planes may be regular or at random in the liquid like fashion. The thickness of the layer is of the order of the length of the free molecule. The interlayer attractions were weak as compared with the lateral forces between the molecules and in consequence the layers are able to slide over one another easily.

Information about the molecular ordering has been obtained from X-ray analysis. In case of S_A and S_C, the centres of mass of the molecules in each layer may be arranged randomly. S_B phase differs from the S_A phase by the fact that in S_B type the centres of mass of molecules in each layer form a two-dimensional hexagonal closed packed structure [Fig - 1.2 c].

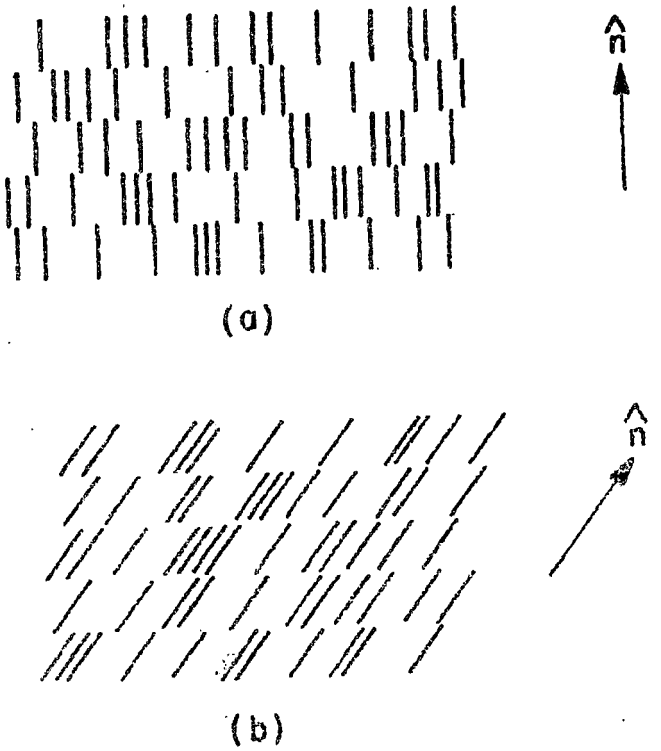

Fig. 1.2. Schematic representation of two types of smectic order: (a) smectic A order; (b) smectic C order.

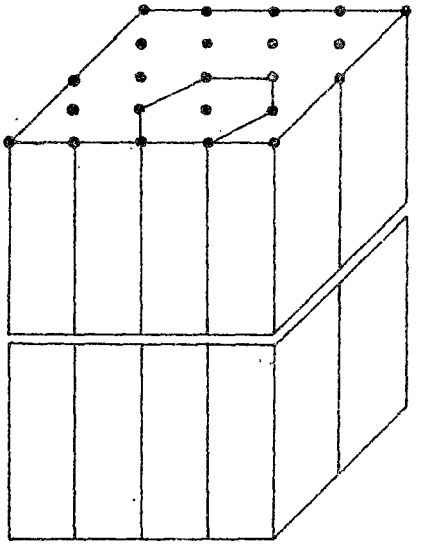

(a)

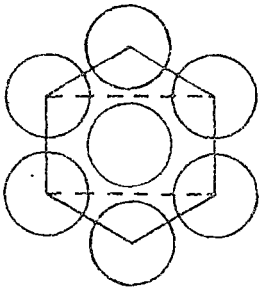

(b)

(a) TWO LAYERS (b) SECTIONS IN THE BASIC PLANE, THE ROTATING MOLECULES HAVE CIRCULAR CROSS SECTIONS.

FIG.1.2(c).STRUCTURE OF HEXAGONAL SMECTIC B.

The various types of smectic phase have been identified by texture analysis in a polarising microscope. Polymorphism in smectic phase is obvious and the classification and characteristics of different phases have been investigated by Sackman and many workers[28,29,30]. At least five other distinct modifications have been identified. These are S_D S_E S_F S_G and S_H[31,32,33,34,20].

Smectic phases can be arranged in sequences as follows[35]

S_A

S_D

S_C

S_B

S_E

$S_{F,C.H.}$ ....

where the lower temperature phase stand further to the right.

From reports of recent workers[36-39] the existences of some other smectic phases as S_I, S_J and S_K are also found. Since in the present work we are concerned with only S_A and S_B phase, detailed discussion of other phases has been omitted.

Cholesterics

In 1888 Reintzer[1,2] reported the synthesis and thermal behaviour of a series of cholesteryl esters. Among these are the first recognised example of liquid crystals, specifically cholesteric liquid crystals. Cholesteric liquid crystals are denominated after cholesterol since many cholesterol esters form type of liquid crystals (cholesterol itself exhibits no mesomorphic phase).

The cholesteric mesophase is also a nematic type of liquid crystal except that it is composed of optically active molecules, which can be described[40-42], as a twisted nematic Fig. 1.3. The cholesteric structure has a screw axis super imposed normal to the preferred molecular direction. The structure of cholesteric liquid crystal is periodic with a spatial period given by $L = \frac{\pi}{|q_0|}$

The sign of q_0 (the sign of rotation of the helix) may be left handed (type "leavo") or right handed (type "dextro") and its magnitude determines the spatial period. With infinite pitch, i.e. $q_0 = 0$ a cholesteric liquid crystal is nothing, but a nematic liquid crystal. A necessary condition for the formation of the cholesteric mesophase is that the molecules are chiralic. Another type of liquid crystals was discovered by Chandrasekhar et al[43] the columnar phase, where the molecules are stacked in columns and so the plane of the molecules are perpendicular to the director, but in earlier cases we have

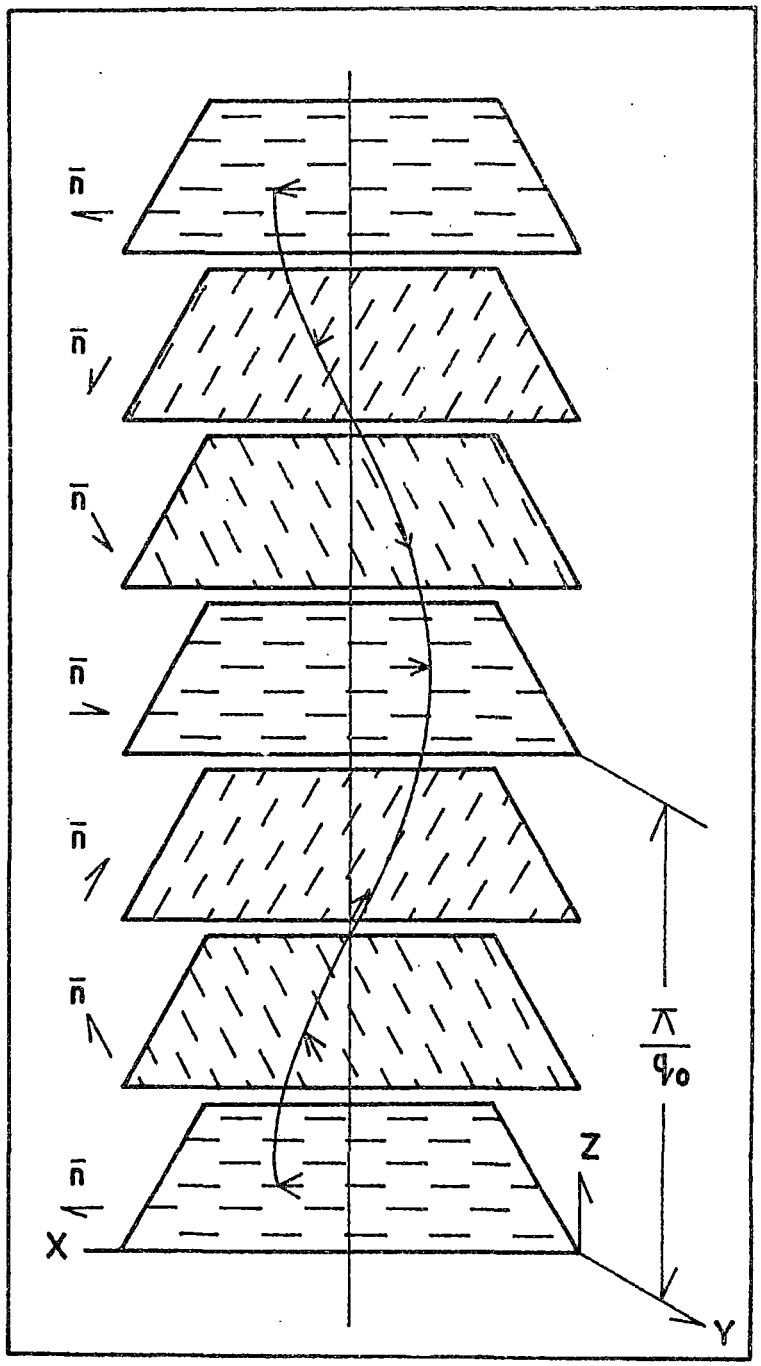

FIG. 1.3.

observed rod or lath like molecules with their long axes parallel to the director[44]. However, we will not discuss any more about this columnar phase here.

A liquid crystalline sample may possess more than one mesomorphic phase i.e. smectic, nematic and cholesteric.

A typical example for a compound forming a smectic phase is

p-(p'-ethoxybenzylidene amino)-ethylcinnamate

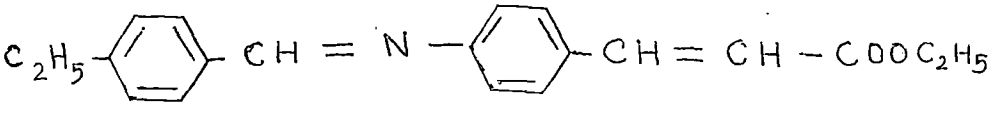

which has the following transition path and temperatures (in °C)

$$C \underset{81}{\rightleftharpoons} S_B \underset{118.5}{\rightleftharpoons} S_A \underset{156.5}{\rightleftharpoons} N \underset{159}{\rightleftharpoons} I$$

The abbreviations used are defined as[45]

C - Crystal

S - Smectic liquid crystal

N - Nematic liquid crystal

Ch- Cholesteric liquid crystal

I - Amorphous isotropic liquid.

Any substance possessing smectic and cholesteric phases has the following transition path

$$C \rightleftharpoons S \rightleftharpoons Ch \rightleftharpoons I$$

Nematic and cholesteric phases do not occur in the same sample though cholesteric can undergo a transition to nematic phase under the action of electric or magnetic field.

Normally in phase transition the higher temperature phase is less ordered i.e. more symmetric than the lower temperature phase[46]. However, as a counter example, the re-entrant nematic phase[47] is one where the more symmetric phase reφoccuring at a lower temperature than the less symmetric smectic A phase[47a].

It was discovered by Cladis[47] that binary mixtures of certain mesogenic cyano compounds that exhibited the following transition path during cooling

Isotropic - Nematic - Smectic A - Nematic

The low temperature nematic phase below the smectic phase is called re-entrant nematic phase[47]. At elevated pressure Cladis et al[48,49] have observed this phenomenon.

A mechanism which lead to the reentrant nematic at lower temperature has been explained by Cladis[50]. Recently the reentrant nematic phase has been observed in some pure compounds[51,52,53] and their mixtures at atmospheric pressure. Reentrant smectic phases have also been reported.[102]

1.3. Chemical Constitution of Mesomorphic Compounds:

The molecular architecture for thermotropic liquid crystalline compounds is generally two or more planar ring system e.g. aromatic nuclei (or more rarely heteroatomic and/or cycloaliphatic) joined by central linkage and having appropriate flexible terminal groups like -

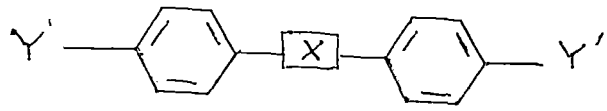

structure 1.1.

where X represents the central linkage and Y & Y' the terminal groups (mostly alkyl or alkoxy chains) may be same or different usually on the long axis of the molecule. The terminal groups frequently determines which mesophase will be observed[55].

It is evident that intermolecular attractive forces play an important role in the mesophase stability from the fact that the various mesophases differ from each other and from isotropic liquid by the degree of freedom of molecular motion. The long range ordering of molecules would more clearly be encountered more often as the molecules become less spherical in shape. Thus it is more evident that the mesophases will be observed more easily for rod like molecules. Thermal stability (i.e. the maximum temperature of the mesomorphic substance at which the particular liquid crystalline behaviour is observed) of the mesophase is favoured by the molecular rigidity, permanent dipoles within the molecule and a high level of molecular polarizability along the long axis of the molecules in addition to the molecular shape (linear molecule i.e. considerable longer than it is wide). Generally most of the molecules contain multiple bonds along their long axis, aromatic nuclei and either polar or long chain terminal groups (as shown in structure 1.1). In addition to thatmelting point must not be too high, otherwise only supercooled metastable mesophases be found monotropically. Monotropic liquid crystals are those formed by cooling from the isotropic state, a mesomorphic state is formed below the melting temperature of the liquid crystal (i.e. supercooled region),

but when the crystal melts directly to isotropic state on heating. The other type of mesomorphic phase formed both by heating the crystal and cooling the isotropic liquid is called enantiotropic.

Thus an essential requirement for the mesomorphism to occur is that the molecules must be highly geometrically anisotropic (i.e. the intermolecular forces are also likely to be anisotropic), usually long and narrow.

In structure 1.1, the aromatic rings are joined by a central group X. The aromatic nuclei are rigid, polarizable and planar. Mesophase is formed if the central groups that joins the ring is itself rigid in nature, e.g. involves a multiple bond, a system of conjugate double bonds or a ring formed by dimerization of carboxyl groups and if the rings are parasubstituted. The more extended the rigid central part of the molecule the more thermally stable the liquid crystal will be. The two rings and the central group should constitute a lath or rod like core of the molecule.

Following the structural principle Vörlander first formulated the list of the known molecular building blocks in detail[56].

Common central linkage of mesogenic compounds of structure 1.1 are shown as follows[55]

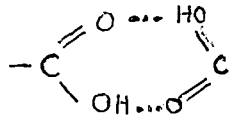

Acid dimers

$-CH=CH-$

Olefin

$-C\equiv C-$

Acetylene

NORTH BENGAL UNIVERSITY LIBRARY 83579 Dated 7 DEC 1983

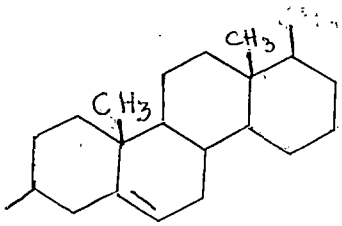

Δ^5-Steroid

$-CH=N-$

Azomethine

$-CH=\overset{\downarrow}{N}(\rightarrow O)-$

Nitrone

$-N=N-$

Azo

$-\overset{\downarrow}{N}(\rightarrow O)=N-$

Azoxy

$-C(=O)-O-$

Esters

The aromatic rings are sometimes connected directly[57] as in

4-cyano-4'-n-pentylbiphenyl

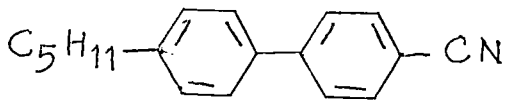

Here C - N = 22.5°C and N - I = 35°C.

When an additional phenyl ring is added to the rigid core increasing its length forms the substance.

4-Cyano-4'-npentylterphenyl- the mesomorphic behaviour is greatly influenced.

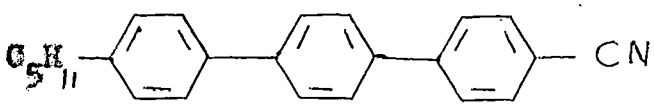

C - N = 130°C, N - I = 239°C.

Gray has discussed[58] several other examples how the length of the molecule can be increased and in consequence the anisotropy and polarizability by ~~an~~ extending the rigid core structure. The thermal stability of the mesophase increases by this process.

Because of lateral attractions the possibility of formation of a layered arrangement increases due to the existence of dipoles acting transverse to the molecular axis[55]. Smectic phases are expected to occur from a layered crystal lattice[59].

The effect of broadening of a molecule by introducing one or more substituents in place of hydrogen along the side of the core structure is given in detail by Gray[59].

When hydrogen is replaced by substituents the molecule is broadened reducing anisotropic polarizability and consequently the intermolecular attraction.

Young et al[60] had studied the following structure:

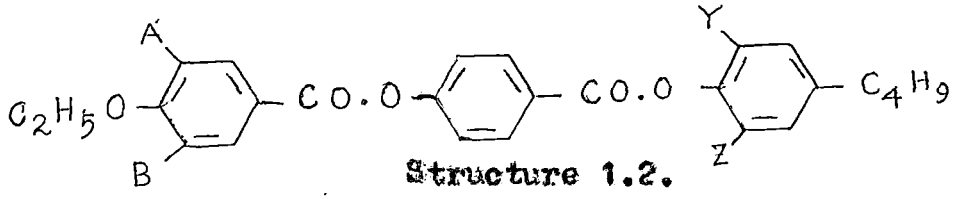

Structure 1.2.

and found a systematic decrease in N-I temperature as the number of CH_3 groups introduced at positions A,B, or Y, Z was increased.

To obtain a mesophase it is generally (but not essentially) required that the terminal group of the molecule contain permanent dipoles. Other than ~~xxx~~ smectics if a terminal hydrogen is replaced by a substituent the thermal stability of the mesophase is increased generally. It was established by Gray[58,59] that the plots of transition temperature versus the number of carbon atoms in n-alkyl groups of a homologous series gives some smooth curves though the melting points do

not show any regularity.

(a) So called odd even[59] effect is obtained when we find that the N-I temperatures fit in two curves, one for even and the other for odd numbers of carbon atoms in n-alkyl chains. The N-I temperature alternates as we pass on serially to different members of the homologous series.

(b) With increasing chain length the mesophase to isotropic transition temperatures usually falls. There are exceptions to this rule, possibly because the aromatic nuclei in this cases do not adopt coplanar conformation, and so termini of one molecule may interact strongly with one of the rings of another molecule giving rise to additional attractions. The thermal stability of the molecule increases because of the increase in additional attack attraction when the length of the terminal group increases.

(c) The plot of the clearing points of smectics and their transition points to nematics usually reaches a maximum at a moderate chain length and decreases gradually with further elongation of the chain. Normally no distinct odd-even effect is observed in this point.

(d) In a homologous series, smectics are rarer with shorter chains. But becomes more common with longer chains increasing the nematic thermal stability. Longer molecules are prevented from sliding, favouring the formation of smectic phase, whereas the flexibility of longer chains generally hinders the parallel orientations. Chemical cons-

titution of different mesophases are listed by Kelker and Hatz[59(a)].

1.4. Theories of Nematic Liquid Crystals:-

Before starting the deduction of molecular mean field theory of mesophases the term "Order Parameter" must be explained.

It has been already stated that nematic liquid crystal differ from ordinary isotropic liquid by a long range orientational order of the long axes of the rod like molecules. In any system in which long range orientational order exists, for convenience, it is customary to introduce an order parameter, a quantity that vanishes in the disordered isotropic phase, but is different from zero in the ordered phase and will be unity when the molecules of the substance are perfectly ordered. Thus a suitable order parameter which describes the ordering in a nematic phase must be defined.

Order parameter -

In a homogeneously ordered nematic liquid crystal sample the long axes of the molecules are all almost parallel to the preferred direction which is represented by $\bar{n}$ the director. Assuming the molecules as rigid rods, the orientation of a particular molecule with respect to the director $\bar{n}$ (taken to be the z direction) be completely defined by three Eulerian angles θ , ϕ & ψ ,(Fig. 1.4 (a)). Due to the thermal energy the individual molecules or small

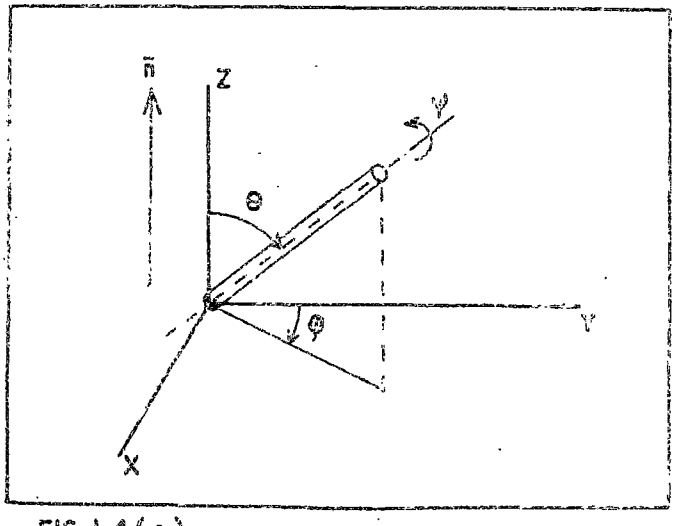

FIG. I.4(a).

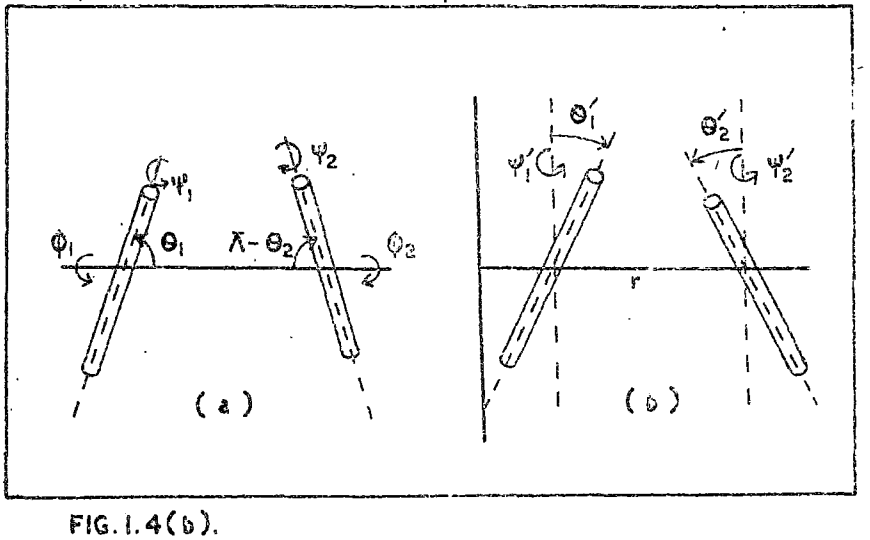

FIG. I.4(b).

groups of molecules tumble about the preferred direction. The efficiency of the molecular orientation in the nematic phase along $\bar{n}$ can be described by a single order parameter. It is also assumed that the director $\bar{n}$ and $-\bar{n}$ are equivalent and the molecules are cylindrically symmetric. But in practice none of the above assumption are strictly realisable, i.e. (i) molecules are not perfectly rigid some flexibility are also there (ii) $\bar{n}$ and $-\bar{n}$ are not equivalent i.e head and tails of a molecule can be distinguished in some cases. (iii) The molecules are more lath-like than cylindrical.

Considering that deviations from the idealised case are small the molecules are assumed to rotate freely around the long molecular axes. In order to maintain the cylindrical symmetry no order could exist for ϕ and ψ and under the most simplified consideration θ becomes the only quantity that characterises the orientational ordering about the director $\bar{n}$.

Simple scalar form of order parameter for nematic is defined as

$$\langle P_2 \rangle = \frac{1}{2}\left(3\langle \cos^2\theta \rangle - 1\right) = \langle P_2(\cos\theta) \rangle$$

The brakets indicate the ensemble average i.e. the average is carried over all the molecules. $P_2(\cos\theta)$ is the Legendre polynomial of the second order. $P_2 = 1$ for perfectly parallel alignment (i.e. $\theta = 0$) and $P_2 = 0$ for

random orientation of molecules (isotropic phase). In the nematic phase it has an intermediate value which decreases rapidly with temperatures and drops abruptly to zero at the nematic isotropic point T_{NI} in a weak first order transition.

Phase transitions -

The order of the phase transition is related to the degree of abruptness of change in physical properties which takes place during a phase transition. In a first order transition e.g. melting or condensation away from the critical point there is a finite jump in the enthalpy, the entropy and in the 1st.derivative of the free energy. In a higher order transition, however, the entropy changes is continuous across the transition. The nematic - isotropic phase transition is a 1st. order with a small latent heat. For this reason it is often called a weak 1st. order phase transition. Such transitions are generally accompanied by pre-transitional effect which are the characteristic of the 2nd. order phase transition and are not usually seen at 1st. order transitions. It is the weakness of the forces responsible for the long range orientational ordering as reflected in small change in enthalpy, that gives rise to the pre-transition effect. At nematic isotropic transitions the forces responsible for long range orientational ordering disappears. Because of this pre-transitional effects sometimes confusion arises to the 1st. order phase transition of nematic phase to isotropic phase.

Chandrasekhar could show that the N-I transition is always of the 1st. order, and there always remains a short range order in the isotropic phase in spite of sudden disappearance of any long range order at the clearing point[61].

Molecular field theories for nematic mesophases:-

As early as in 1916 M. Born[62] proposed the first mean field theory of nematic state in which the medium has been treated as an assembly of permanent electric dipoles. When the temperature is lowered a transition from an isotropic to an anisotropic phase is possible. This result is however, only qualitative importance because it is now established that the permanent dipole moments are not necessary for the existence of liquid crystals. According to this theory the aligned phase should be ferroelectric, which in fact does not appear even in polar molecule. Maier and Saupe[63] have developed a statistical theory for the phase transition in a nematic liquid crystal. The theory says that the occurrence of liquid crystalline phase is due to the anisotropy of the molecular polarizability. The theory is mainly based on these assumptions - (i) The molecules interact through an attractive orientation dependent Vander Waals interaction. (ii) The orientation dependent interaction does not effect the configuration of the centre of mass and (iii) The mean field approximation - each molecule is assumed to be in an average orientating field due to its environment, but other-

wise uncorrelated with its neighbours. As a result a given molecule feels an effective potential of the mean field or single molecule potential or pseudopotential .

The interaction potential between the molecule 1 & 2 is taken as the starting point for the derivation of pseudopotential for a rod like molecule. The intermolecular pair potential V_{12} is a function of five co-ordinates[64],

$$V_{12} = V_{12}(r, \theta_1, \phi_1, \theta_2, \phi_2) \ldots.$$

Fig. 1.4 (b) represents the different coordinates required to describe the interaction between a pair of assymetric molecules. Where r is the separation of the centre of gravity and θ_i , ϕ_i , ψ_i are three Eulerian angles. Since, in case of nematics the molecules have no ordering about their long axis the angles ψ_i are eliminated.

Pople[65] expanded the two body interaction potential as

$$V_{12} = V_{12}(r, \theta_1, \phi_1, \theta_2, \phi_2)$$

$$= 4\pi \sum_{L_1 L_2 m} U_{L_1 L_2 m}(r)\, Y_{L_1 m}(\theta_1, \phi_1)\, Y^{*}_{L_2 m}(\theta_2, \phi_2) \quad \ldots (1)$$

where $Y_{Lm}(\theta, \phi)$ are the usual spherical harmonics.

The expression is convenient because it not only separates the distance and angular part of the potential, but in addition to the expansion coefficient $U_{L_1 L_2 m}(r)$ are found to decrease rapidly with increasing L_1 and L_2.

In order to derive mean field approximation to the potential first we have to express V_{12} in terms of polar co-ordinate system based on the director $\bar{n}$ as the polar axis.

The rotation of the molecule 1 and 2 is required and mathematically rotation of the coordinate axes transforms the spherical harmonic into the form

$$Y_{Lm}(\theta,\phi) = \sum_{P} D^{L}_{Pm} Y_{LP}(\theta',\phi') \qquad \ldots (2)$$

where D^{L}_{Pm} are the elements of Wigner rotation matrices. Therefore eqn. (1) can be transformed using Wigner rotation matrices[66] from the coordinate system containing the intermolecular vector to this spatial axis system we get

$$V_{12} = 4\pi \sum_{L_1,L_2,m} \sum_{Pq} U_{L_1,L_2,m}(r)\, Y_{L_1P}(\theta_1',\phi_1')\, Y^{*}_{L_2q}(\theta_2',\phi_2') \left(D^{L_1}_{Pm}\right)\left(D^{L_2}_{qm}\right)^{*} \qquad \ldots (3)$$

Primed angles represents the orientation of the molecule with respect to the new rotated coordinate system (space fixed coordinate system).

Pseudopotential from the pairwise intermolecular potential can be obtained by taking three averages[64]. First average is over all orientations of the intermolecular vector $\bar{r}$ in the spatial coordinate system, then we average over all orientations of the molecules 2 (which has influence only on the spherical harmonics in θ_2', ϕ_2') and finally we average V_{12} over all values of the intermolecular separation $|r|$.

The potential obtained after taking the above mentioned averages is given as

$$\langle\langle\langle V_{12}\rangle\rangle\rangle = \sum_{Lm} \langle U_{LLm}(r)\rangle P_L(\cos\theta_i')\langle P_L\rangle \quad \ldots (4)$$

where P_Ls are the Lth. order legendre polynomials. The desired single molecule potential in the mean field approximation, which can be written by dropping the pined as

$$V_1(\cos\theta) = \sum_L U_L \langle P_L\rangle P_L(\cos\theta)$$

$$U_L = \sum_m \langle U_{LLm}(r)\rangle \quad \ldots (5)$$

Since for most nematic liquid crystals director directions $\bar{n}$ and $-\bar{n}$ are indistinguishable, averages over all odd powers of Cos θ vanish, then only the even values of L are required in equation (5). L = 0 term being a mere additive constant can be neglected. The eqn. (5) can be written as

$$V_1(\cos\theta) = U_2\langle P_2\rangle P_2(\cos\theta) + U_4\langle P_4\rangle P_4(\cos\theta) + U_6\langle P_6\rangle P_6(\cos\theta) + \cdots \ldots (6)$$

The equation for the pseudopotential is equivalent to that in the Maier-Saupe theory if the summations are restricted to terms with L = 2 i.e. the 1st. term only in equation (6)

$$V_1(\cos\theta) = U_2\langle P_2\rangle P_2(\cos\theta) \quad \ldots (6\,a)$$

Accordingly to Humphrie et al[67] if we consider the true cylindrical symmetry of the distribution function for the orientation of the intermolecular Vector the <u>single molecular potential</u> will contain the terms which are proportional to

$$\langle U_{L_1 L_2 m}(r)\rangle \left(P_{L_1}\langle P_{L_2}\rangle + P_{L_2}\langle P_{L_1}\rangle\right)$$

Thus the equation for pseudopotential is equivalent to that in the Maier Saupe theory[63] if the summation are restricted to term with $L = 2$.

<u>Orientational distribution function</u> $(f_1(\cos\theta))$

Orientational distribution function $(P_1(\cos\theta))$ gives the probability of finding a molecule whole axis makes an angle θ with the director $\bar{n}$.

Orientational distribution function corresponding to the single molecule potential has the form

$$f_1(\cos\theta) = Z_1^{-1} \exp\left[-\beta V_1(\cos\theta)\right], \qquad \ldots (7)$$

$$Z_1 = \int_0^1 \exp\left[-\beta V_1(\cos\theta)\right] d(\cos\theta), \qquad \ldots (8)$$

where Z_1 is the single molecule partition function and $\beta = \frac{1}{KT}$ (k is the Boltzmann's constant and T is the temperature in absolute unit).

Since both V_1 and f_1 are even functions of $\cos\theta$ as $\bar{n}$ and $-\bar{n}$ are indistinguishable over all possible orientations can be restricted to $0 \leqslant \cos\theta \leqslant 1$.

The orientational order parameter

The orientational order parameter has already been defined as

$$\langle P_2 \rangle = \frac{1}{2} \left(3 \langle \cos^2\theta \rangle - 1 \right) = \langle P_2 (\cos\theta) \rangle$$

This holds either in time or space average. This is one of the earliest definition of the orientational order parameter which was given by Zwetkoff[68] in proposing the semi empirical theory of nematogens.

In eqn. (7) and (8) the functions V_1 and hence φ_1 contains the order parameter $\langle P_L \rangle$ which is as yet undetermined functions of temperatures, so average values cannot be calculated from the eqns. (5) and (7). Its temperature dependence can be obtained as follows:

$\langle P_L \rangle$ is the average value of Lth. Legendre function for a given molecule. Therefore, from eqn. (7)

$$\langle P_L \rangle = \int_0^1 P_L (\cos\theta)\, \varphi_1 (\cos\theta)\, d(\cos\theta) \qquad \ldots (9)$$

combining this equation with eqn. (7) we get

$$\langle P_L \rangle = \frac{\int_0^1 P_L (\cos\theta) \exp\left[-\beta V_1 (\cos\theta)\right] d(\cos\theta)}{\int_0^1 \exp\left[-\beta V_1 (\cos\theta)\right] d(\cos\theta)} \qquad \ldots (10)$$

which is a self consistent equation for the determination of the temperature dependence of $\langle P_L \rangle$.

From a simultaneous solution of equations (6) and (10) we get the temperature dependence of all the P_L s originally included in the potential V_1. For L = 2 we get the solution

of $\langle P_2 \rangle$ and from the solution of $\langle P_2 \rangle$ we get the traditional order parameter in the nematic phase. $\langle P_2 \rangle = 0$ is at all temperatures which is disordered normal isotropic liquid phase; below certain temperatures determined by $KT/v = 0.22284$, two other solutions appear. Of the three solutions below the critical temperature the one which satisfies the thermodynamic condition of minimum free energy will give the stable phase.

The free energy is given by $F = E - TS$. Where E is the internal energy and S the entropy.

For a system of N molecules we have the following expressions for E, S and F[64].

$$E = \frac{1}{2} N \langle V_i \rangle = \frac{1}{2} N \sum_L U_L \langle P_L \rangle^2,$$

$$S = -Nk \langle \ln \rho_i \rangle = \frac{N}{T} \sum_L U_L \langle P_L \rangle^2 + Nk \ln Z_1$$

$$F = E - TS = -N k T \ln Z_1 - \frac{1}{2} N \sum_L U_L \langle P_L \rangle^2.$$

It is found that for $KT/v = 0$ to $KT/v = 0.22019$ from the condition of minimum free energy (64.a) (calculated by using the obtained $\langle P_2 \rangle$ values for each T) the positive values of $\langle P_2 \rangle$ (i.e. the molecules tend to align parallel to the director) gives the stable nematic phase. While for T corresponding to $KT/v > 0.22019$ the solution $\langle P_2 \rangle = 0$ gives the stable isotropic phase. $\langle P_2 \rangle$ decreases from unity to 0.43 from $T = 0$ to $T = 0.22019\ v/k$ and then suddenly it decreases to zero $[\langle P_2 \rangle = 0]$ at $T = 0.22019\ v/k$. Accompanied by latent heat of transition, discontinuous entropy and volume changes, a 1st. order transition from nematic to isotropic phase takes place at

this temperature (T_{NI}). As the temperature is lowered down in the nematic phase, however, the substance attains smectic phase or solid crystalline phase long before $\langle P_2 \rangle$ can attain the value of unity at absolute zero. This theory predicts that $\langle P_2 \rangle$ is same at T_{NI} for all substance[63].

It is observed that the mean field theory of Maier-Saupe is obtained by the retention of only the 1st. term in the equation (6). Maier and Saupe[63] first attempted to elucidate the nature of intermolecular forces in nematics. The character of which is contained in the parameter of the one molecule potential V_1 (orientation dependent part only). It was assumed by them that the nematic order is mainly due to dispersion forces (i.e. induced dipole-induced dipole). This restriction gives[64].

$$V_1 = -\frac{A}{v^2}\langle P_2 \rangle P_2(\cos\theta)$$

Where, A is a constant to be determined which is a character of the substance (related to the polarisability) can be calculated from the transition temperature if the molar volume of the nematic and isotropic liquid at clearing point is known. v is the mean molecular volume. This volume dependence comes from the fact that the potential of dispersion force is dependent on the intermolecular separation as r^{-6} (whether between symmetric or assymetric molecules). It is assumed from M.S. theory[63] that $V_1 \propto v^{-2}$.

In their development of the mean field theory Humphries et al[67] decided the volume dependence as $v^{-\gamma}$, γ being an adjustable parameter. Experimental data[69] on the pressure dependence of the order parameter of PAA indicates that $V_1 \propto v^{-4}$. On the other hand a recent argument due to Cotter[70] (referred by Chandrasekhar[70.a]) suggests that thermodynamic consistency of the mean field theory requires v^{-1} dependence. A force fitting experimental results with theory however yielded values of γ in some cases[71] which are neither thermodynamically self consistent nor the values are expected to come from the consideration of dispersion forces (v^{-2} dependence).

Chandrasekhar and Madhusudan[72] obtained an average of v^{-3} dependence after calculation considering to permanent dipole-permanent dipole forces, induced dipole-induced quadrupole part of the dispersion forces.

In order to avoid all these ambiguities regarding a knowledge of volume dependence, it is preferable to assume that the coefficients of V_1 in eqn. (6) are independent of volume and to restrict the fitting of the theory to experiment to a narrow range of temperature T_{NI}. Finally different forms of volume dependence may be included.

According to M.S. theory plot of $\langle P_2 \rangle$ versus T/T_{NI} is a universal curve for all substances. Experimentally these are small but systematic derivations from this curve[8a,73] and the need of higher order terms in the potential function has been emphasized by Chandrasekhar et al[72] and Humphries et al[67]. When theoretical values of $\langle P_2 \rangle$ and $\langle P_4 \rangle$ obtained

from M.S. potential are compared with some experimental results.

The temperature dependence of the $\langle P_2 \rangle$ and $\langle P_4 \rangle$ of MBBA are determined by Jen et al[74] using Raman Scattering technique and found that $\langle P_4 \rangle$ values are much lower than that predicted by M.S. theory and even negative near the transition. Kabinata et al[75] in more recent work reported the results of measurement of $\langle P_2 \rangle$ and $\langle P_4 \rangle$ by resonance Raman polarization measurements of all trans β -carotene dissolved in MBBA and 5CB (utilised as orientational probe). The value of $\langle P_4 \rangle$ obtained for MBBA is not negative in their case while for 5 CB becomes negative (within experimental uncertainity) just before the transition temperature.

These values of $\langle P_4 \rangle$ are also much lower than those predicted by MF theories. The negative values of $\langle P_4 \rangle$ are not predicted even if the higher term in the mean field potential is included although the inclusion improves the agreement to some extent.

Further the long wavelength orientational fluctuations in the medium which diminish the effective order parameter and this has to be taken into the theory according to Luckhurst[76]. The assumption that the molecule is a rigid rod is also an over simplification. A realistic calculation has been made by Marcelja[77] of the contribution of flexible end chain in the ordering process, which accounts for the alternation in the transition temperatures, the order parameter and other related properties of the successive members of a homologous series. Recent theoretical work by Luckhurst[78] shows that

the effect of the flexibility of molecules on order parameter is only marginal.

McMillan's theory for Smectic A (SA)

Contribution to the theory of S_A liquid crystals have been made by a number of Investigations[79-83]. All the treatments are extensions of the Maier-Saupe[63] theory of nematics. Here we will discuss the theory as given McMillan.

The McMillan form of the single molecule potential is deduced starting from the Kobayashi form of the potential[79,80] and using the formal development presented earlier[64.a, 64].

The McMillan model of the potential[84] is given in the form

$$V_m(\cos\theta, z) = -v\left[\delta\alpha\tau\cos(2\pi z/d) + \eta + \alpha\sigma\cos(2\pi z/d)\,P_2(\cos\theta)\right]$$

The smectic A liquid crystals possess both orientational and translational order. The centre of mass of the molecule tends to lie on a plane perpendicular to the Z direction (i.e. to the director). The molecular distribution function must therefore describe both the tendency of the molecule to orient along $\bar{n}$ Fig. 2(b) and form layers perpendicular to $\bar{n}$. The distribution function is thus a function of both Cos θ and Z and can be expanded in a double series

$$f(\cos\theta, z) = \sum_{L=0\,(\text{even})}^{\infty}\sum_{n=0}^{\infty} A_{Ln}\,P_L(\cos\theta)\cos(2\pi nz/d), \quad \text{and}$$

$$\int_{-1}^{+1}\int_{0}^{d} f(\cos\theta, z)\,dz\,(d\cos\theta) = 1.$$

The coefficients A_{Ln} are found after integrating and recognizing the definition of averages[84].

The results are

$$A_{00} = \frac{1}{2d},$$

$$A_{0n} = \frac{1}{d}\left\langle \cos\left(2\pi n z/d\right)\right\rangle, \quad (n \neq 0),$$

$$A_{L0} = \frac{2L+1}{2d}\left\langle P_L(\cos\theta)\right\rangle; \quad (L \neq 0), \qquad \ldots(11)$$

$$A_{Ln} = \frac{2L+1}{2d}\left\langle P_L(\cos\theta)\cdot\cos\left(2\pi n z/d\right)\right\rangle; \quad (L, n \neq 0)$$

In addition to the purely orientational and translational order parameter, the $\langle P_L(\cos\theta)\rangle$ and $\langle\cos(2\pi n z/d)\rangle$ we find a set of mixed order parameters, $\langle P_L(\cos\theta)\cos(2\pi n z/d)\rangle$

This describes the correlation coupling between the degree of orientational and translational order. The three order parameters of lowest degree in eqn. (11) of the S_A phase have been given symbols

$$\eta \equiv \langle P_2(\cos\theta)\rangle,$$

$$\tau \equiv \langle\cos(2\pi z/d)\rangle,$$

$$\sigma \equiv \langle P_2(\cos\theta)\cos(2\pi z/d)\rangle$$

In the isotropic phase, $\eta = \tau = \sigma = 0$

In the nematic phase $\eta \neq 0$, $\tau = \sigma = 0$

In the smectic A phase $\eta \neq 0$, $\tau \neq 0$, $\sigma \neq 0$

For perfect order all three tend to unity.

1.5. (a) Alignment of nematic mesophases-

In a large volume of a nematic liquid crystal the preferential direction $\bar{n}$ is in general not uniform but changes from place to place under the action of disturbing forces such as convention flow, wall effects etc. However, even large samples can be aligned by both magnetic and electric field. The field induced alignment of a liquid crystal is a strong effect. This is due to the particular intermolecular forces responsible for the mesomorphic state and lead to a co-operative behaviour of the molecules.

An anisotropic dielectric or diamagnetic component will tend to align such that the largest component of dielectric or diamagnetic constants lie in the direction of the applied field. Nematic molecules behave as dipolar species with $\epsilon_{\parallel} \neq \epsilon_{\perp}$ ($\chi_{\parallel} \neq \chi_{\perp}$) where ϵ and χ are dielectric and diamagnetic susceptibilities parallel and perpendicular to the long molecular axis. When $\epsilon_{\parallel} > \epsilon_{\perp} (\chi_{\parallel} > \chi_{\perp})$ the nematic liquid crystal along molecular axis will tend to align with the applied field.

For example, p-methoxy-p'-cyanobenzylideneaniline is a highly polarizable molecule with positive dielectric aniso-

trony, i.e. $\epsilon_{\parallel} > \epsilon_{\perp}$, that will align its long molecular axis with an applied field. On the other hand p-methoxy-p-n-butylbenzylideneaniline with $\epsilon_{\perp} > \epsilon_{\parallel}$, will tend to align its long molecular axis perpendicular to the applied field.

Thin films of liquid crystals upto 100 μm can be aligned by surface generated orienting forces which results from physico chemical processes, e.g. hydrogen bonding, Vander waals, interactions or dipolar interactions and from mechanical interactions as a result of the anisotropic elasticity of the liquid crystals[85].

Ordered layers of nematic phases upto about 0.1 mm thickness can be prepared by sandwiching the liquid crystal between flat glass plates. If the surface is rubbed with a piece of cotton, paper or leather a number of times in a particular direction the molecules are aligned in the direction of rubbing (i.e. homogeneous[85], alignment. By depositing suitable chemical at particular angle on the surface the alignment can be made more uniform. Homeotropic orientation (perpendicular to the surface) can also be obtained in the same way[85]. Homogeneous oriented nematic layers have been used for UV and infrared spectroscopic studies[85].

A variety of electro-optic effects of liquid crystals are based on the electric field molecular re-alignment. Using the surface treatment to produce a molecular alignment which is orthogonal to that produced by the applied field the molecular reorientations can readily be intereconverted within a

millisecond response time. The alignment of nematic liquid crystals by external electric field has been recently reviewed by Gray[86] and was first observed by Freedericksz[87]. Variation of the linear birefrengence or light absorption (linear dichroism) can be observed by reorientating nematic molecules with positive dielectric anisotropy $(\epsilon_{\parallel} > \epsilon_{\perp})$.

Nonliquid crystalline dye molecules may be aligned by the nematic molecules to produce display applications[88].

Nematic liquid crystals can easily be oriented by static magnetic fields. Two cases have to be distinguished depending on the sign of the diamagnetic anisotropy $(\chi_{\parallel} - \chi_{\perp})$ of the molecules forming the liquid crystals. The aromatic nematogens are examples of compounds with positive diamagnetic anisotropy i.e. $(\chi_{\parallel} - \chi_{\perp}) > 0$. The long axis of the molecule tend to align parallel to the direction of the magnetic field. The nematic liquid crystals orient in the magnetic field $\overline{H}$ in such a way that the directors of the spontaneously ordered domains are all aligned uniformly in one direction (parallel to $\overline{H}$). In general field strength of several hundred gauss are sufficient to produce uniform orientation i.e. monodomain sample.

1.5. (b) Alignment of smectic phases:-

Meiboom and Luz[89] have ma shown that smectic liquid crystals of compounds which exhibit a nematic and a smectic phase may be oriented uniformly by the application of a magnetic field in the following way: First the nematic phase is oriented

in the magnetic field. Then the sample is slowly cooled below the nematic to smectic transition while it is kept in the magnetic field. In this way all the three smectic phases A,B,C, of ~~X~~ TBBA can be ordered uniformly.

1.6. Texture analysis by polarising microscope:

When liquid crystals are studied with a polarising microscope, they are usually observed as thin films between glass plates.

Nematics:-

On cooling from the amorphous isotropic liquid circular birefringent areas appear at first in case of nematics. The appearance of the textures that form after the completed transitions often depend considerably on the layer thickness. Thicker nematic layers may show the typical threaded schelieren textures. The well defined thread like textures may move and float around in the ~~xxxxxxxx~~ nematic. The term nematic refers to these features, being derived from the Greak word "nema" a thread. The threads have elastic properties. In thinner layers the threaded texture changes to the schliern texture. By a suitable surface treatment it is possible to obtain films with ~~xxx~~ uniform molecular alignment. A film that has been aligned between the rubbed surface is shown by Saupe. With untreated surface, the surface effect may produce an irregular marble texture. It is also possible to obtain uniformly aligned films with the optic axis normal to the surface.

Pseudo isotropic textures are often obtained with compounds that form, in addition to the nematic phase, a smectic A phase at lower temperatures[90].

Cholesterics:-

Cholesteric liquid crystal -- can occur in three textures. On cooling, an isotropic texture or modification can be obtained first at the liquid to cholesteric liquid crystal transition, which at a lower temperature changes to a birefringent texture. Transition point is not easily observed in this case. Where in other cases when the birefringent texture is formed directly, transition can be easily observed. Elongated banana shaped forms may appear first (referred to as a batonnets).

The photograph of birefringent "focal-conic" texture of a cholesteric phase is given by Saupe[91]. When the cover glass is shifted focal conic texture is shifted to planner texture. Wedge Shaped samples, when the surfaces are prepared for a parallel alignment, show a particular feature called Grandjean steps or threads. The variation of pitch is directly observable by the colour change in the sample that show reflection colours.

Smectics:-

Typical texture obtained with smectic A liquid crystals are focal conic textures. The appearance of the focal conic texture is directly related to the focal conic layered structure of the smectic. In thinner layers the focal conic texture changes its appearance and gives the fan texture or more accurately the fan-shaped focal-conic textures. A shift of the cover glass often changes the fan texture suddenly to a pseudo-isotropic texture.

In contrast to nematics, a slight shift of the cover glass has no optical effects on a pseudo-isotropic smectic - A film. This type of texture can also form spontaneously at the phase transition during cooling from a pseudo-isotropic nematic. Disappearance of Brownian motion can only indicate the transition in such cases. Smectic A phases shows 'batonnates' when it is formed directly from amorphous isotropic liquid. They float in normal liquid and on cooling they merge resulting into a fan texture.

Typical textures of smectic are the 'broken fan' and 'broken focal - conic textures. They are less regular and disturbed by additional disclinations in comparison with S_A phase. Schlieren textures of smectic C are also observed which corresponds to pseudopotentic-isotropic texture of S_A. At the transition from a normal isotropic liquid to S_C batonnets appear first to those of S_A phase.

The characteristic of liquid crystals with structured layer is the "mosaic" texture. The most common smectic with structured layer is smectic B. The mosaic texture has been observed with S_B and slightly modified also with other smectics with structured layers. A modification of fan textures and of Schlieren textures can also be observed with smectic B films that are obtained on cooling from a S_A or a S_C. The pseudo-isotropic textures can also be observed with S_B the existence of the texture shows directly that the corresponding S_B phase is uniaxial and has upright layers.

Photographs of all the typical textures discussed above are given by Saupe[91].

Demus and Richter[92] have discussed details about texture analysis with several photographs of different mesomorphic phases with their typical textures.

Order parameters of different mesophases (specially for nematics) have been determined by many workers by employing various experimental techniques including diamagnetic anisotropy[93] optical anisotropy[93,94] magnetic resonance spectroscopy. Raman scattering[96,97], Infrared spectroscopy[97], UV and visible spectroscopy[96], Mössbauer spectroscopy[98], Neutron scattering[98], positron annihilation[98], dielectric anisotropy[98], Guest host interaction[99,100], X-ray diffraction etc. Comparison of these results with the Maier Saupe theory is briefly discussed in Brown's book[101].

The details about all the experimental techniques are reviewed by different workers[98]. In this thesis we are not going to discuss about all the techniques other than the use of X-ray diffraction in determination of order parameters of different mesophases and the orientation of different non-liquid crystalline azo dyes doped in different nematic mesophases by spectroscopic method (Guest Host effect). Details about the X-ray and spectroscopic works on liquid crystalline phase made by us will be presented in next few chapters.

1.7. MOTIVATION AND SCOPE OF THIS WORK

While enormous advances in the technical applications of liquid crystals have been made, the basic reason for the formation of various mesophases is not fully understood. There are several theories of liquid crystals based on Mean field approximation. My aim was to test these theories from my X-ray and spectroscopic data. I have been able to analyze my X-ray diffraction data from several aligned liquid crystal samples (nematic and smectic A) to give the orientational distribution function, $f(\beta)$, which in turn provides the angular part of the Mean field potential. This experimentally obtained distribution function has been compared with those obtained from different theories and large discrepancies have been found for cyano compounds having strong terminal dipole moment.

X-ray data have also been analyzed for apparent molecular length and intermolecular distances. The apparent molecular lengths for cyano compounds were found to be larger than molecular model lengths, showing formation of association in the mesophase. I have also calculated the orientational order parameters $\langle P_2 \rangle$ and $\langle P_4 \rangle$ for aligned nematic and smectic A phases and contrary to some earlier works my $\langle P_4 \rangle$ values are always positive.

The $\langle P_2 \rangle$ value can be obtained experimentally using various techniques, viz. refractive index, magnetic susceptibility anisotropy, NMR, Raman Spectra, etc., and the calculation of $\langle P_2 \rangle$ from the experimental data involve

certain assumptions in each case. By comparing $\langle P_2 \rangle$ values obtained from different methods, we can get an idea about the accuracy of these assumptions. With this motivation, I wanted to measure $\langle P_2 \rangle$ by a spectroscopic method using a guest dye in an aligned liquid crystalline host. However, the $\langle P_2 \rangle$ values obtained by this method did not agree at all with the values obtained from our X-ray studies. The ~~problem~~ probable reasons for this discrepancy have been discussed.

REFERENCES.

1. F.Reintzer, Monatsch, 9, 421 (1888).
2. F.Reintzer, Ann. Physik, 27; 213 (1908).
3a. O.Lehmann, Z. Physik, Chem. 4, 462 (1889).
3b. O.Lehmann, Z. Physik, Chem. 5, 427 (1890).
3c. O. Lehmann, Z.Physik, Chem. 56 750 (1906).
4a. G.Friedel - In colloid chemistry ed. J.Alexander, Vol. 1, p. 102, The Chemical catalogue company, Inc. N.Y. (1926).
4b. G. Friedel and F.Friedel, Z. Krist. 79; 1 (1931).
5. H. Kelker, R. Hatz, Hand Book of Liquid Crystals, Chapt. 2, Verlag Chemie (1980), p. 33.
6. H. Kelker, Mol.Cryst.Liq.Cryst. 21 (1973).
7. W. Brag, Nature (London) 133, 445 (1934).
8. Brown & Show, Chem Rev. 57 1043 (1957).
9. A. Saupe - Angew, Chem. Internat.Edit. 7, No.2 (1968).
9a. H. Kelker and R.Hatz, Handbook of Liquid Crystals Verlag Chemie (1980).
10. G.W.Gray, "Molecular Structure and the properties of Liquid Crystals" Academic Press, N.Y. (1962).
11. G.W.Gray, The Molecular Physics of Liquid Crystals ed. G.R.Luckhurst and G.W.Gray, Academic Press, Chapt. 12 (1980).
12. J.A.Castellano - Liquid Crystals the Fourth State of Matter, Macel Dekkar Inc. (N.Y.) ed.F.D.Saeva Chap.12.
13. W.H.de Jen in Liquid Crystals (Solid State Phys. Suppl. (14) Academic Press (1978).
14. G.Maier, E.Sackman and J.Grabmaier, Applications of Liquid Crystals, Springer Verlag (1975).

15. G.W.Gray in Advances in Liquid Crystals, Ed.G.H.Brown, Vol. 1 (1976).

16. M.J.Stephen and J.P.Straley - The Physics of Liquid Crystals. Rev.Mod. Phys. 46 No.4, 617-704 (1974).

17. W.H. de Jen in Physical Properties of Liquid Crystalline Materials, Gordown and Breech, Chapt. 5 (1980).

18. G.Friedel, Ann. Physique 18 273 (1922).

19. H.Sackmann & D.Demus, Fortscher. Chem.Forsch. 12 349 (1969); Molecular Crystals 2 81 (1966).

20. A. devries Pramanna Suppl. on Liquid Crystals (Proceedings of the International Conference held at Bangalore December 3-8, 1973, Ed.S.Chandrasekhar, p.93-113 (1975).

21. A. de Vries, in Liquid Crystals - The Fourth State of Matter, Marcel' Dekker INC (N.Y.) Ed. F.D.Saeva Chap.1. (1979)

22. W.Maier, A. Saupe, Z.Naturforsch, 13a 564 (1958), 14a 882 (1959); 15a, 287 (1960).

23. G.W.Gray, Molecular structure and the properties of Liquid Crystals London, Academic Press (1962).

24. de Jen, W.H. Vander Veen, J. Philips, Res. Reports, 27 172 (1972).

25. A. de Vries, Acta Crystallography; A 25:S.135 (1969).

26. A. de Vries, Mol. Cryst. Liq.Cryst. 10:31 (1970).

27. A. de Vries, Mol. Cryst. Liq. Cryst. 10:219 (1970).

28. E.Alexander & K. Z.Herrmann. Kristallogr. Con.Abt. A69 285 (1928).

29. H.Sackmann & D.Demus. Mol.Cryst.Liq.Cryst.21 239 (1973).

30. S. Diele, P. Brand and H. Sackmann, Mol.Cryst.Liq. Cryst. 17 163 (1972).

31. D. Demus, G.Kunicke, J. Nelson and H. Sackman, Z. Naturforsch 23a, 84 (1968).

32. D. Demus, S. Diele, M. Klapperstruck, V.Link, and H. Zaschke, Mol.Cryst.Liq.Cryst. 15 161 (1971).

33. A. de Vries, Mol.Cryst.Liq.Cryst. 24 337 (1973).

34. D. Demus, H. Demus, Flussige Kristalle in Tabellen, VEB Deutsch, Verlag Fur Grund. Stoffindustrie Leipzig, Leipzing, (1973).

35. H. Kelker and R. Hatz, Handbook of Liquid Crystals, Verlag Chemie, Chapt. 1, page 6 (1980).

36. A de Vries in Liquid Crystals (Proc. of International Symposium), Bangalore, India, Dec. 3-8, 1979, Ed. S. Chandrasekhar.

37. E.M.Barrall, J.W. Goodby and G.W.Gray, Mol.Cryst.Liq. Cryst. Lett. 49 319 (1979).

38. S. Diele, D. Demus and H.Sackmann, Mol.Cryst.Liq.Cryst. 56 217 (1980).

39. P.A.C.Gane, A.J.Leadbetter and P.G.Wrigton, Mol.Cryst. Liq. Cryst. 66, 247 (1981).

40. G.W.Brown, Amer. Scientists 60, 64 (1972).

41. T. Kakagini, H. Kodane and K.K.Kobayashy, Phys. Lett. A 27 564 (1971).

42. I.G.Chistyakov, Sov.Phys.Upsekk 9 551 (1967).

43. S.Chandrasekhar, B.K.Sadashiva and K.A.Suresh, Pramanna 9, 471 (1977).

44. C.Beatrade, M.C. Bernand, H. Gasparoux, A.M. Levelut and N.H.Tinh, Liquid Crystals, Proc. of Int.Conf. Bangalore, India, Dec 3-8, 1979; Ed.S.Chandrasekhar, Heyden, P. 29, 1980.

45. G.W. Gray, Mole. Cryst., 2, 189 (1966).

46. L.D.Landau & E.M.Lifaitz, "Statistical Physics" Addision-Wesley publishing Co., Reading Mas 1965, Chapt. XIV.

47. P.E.Cladis, Phys. Rev. Letts. 35 48 (1975).

47a. G.Riblet & K.Winzer, Sol.St.Comm. 9 1663 (1971); 11 175 (1972).

48. P.E.Cladis, R.K.Bogardus, W.Daniels and G.N.Taylor Phys. Rev.Lett. 39 720 (1977).

49. P.E.Cladis, R.K.Bogardus and D.Aadsen, Phys. Rev.A18; 2292 (1978).

50. P.E.Cladis, Proc. Int.Liq.Cryst. Conf. Bangalore Dec. 3-8, 1979, Ed.Chandrasekhar, p. 105,Heyden (1980).

51. N.V.Madhusudana, B.K.Sadashiva and K.P.L.Moodithaya, Curr.Sci. 48 613 (1969).

52. F.Hardouin, G.Sigaud, M.F.Achard and H.Gasparoux, Phys. Lett. 71A 347 (1979).

53. N.H.Tinh and H.Gasparoux, Mol.Cryst.Liq.Cryst.Lett. 49 237 (1979).

54. K.P.L.Moodithaya and N.V.Madhusudana, Proc.Int.Liq. Cryst. Conf. Bangalore, Dec. 8, 1979,Ed.Chadrasekhar, p. 121, Heyden (1980).

Some other articles on reentrant x nematic phases are also there in this book.

55. A.W.Levine - in Introduction to Liquid Crystals. Plenum. Ed. E.B.Priestley, Peter J.Wojtwicz and Ping Sang. Chapt. 2.

56. D. Vorlainder, In Hand Book of liquid Crystals Verlag Chemie Chapt. 2 (1980).

57. G.W.Gray- In Liquid Crystals and Plastic Crystal Vol.1, Chapt.4, Ed.G.W.Gray and Winsor.

58. G.W.Gray - The Molecular Physics of Liquid Crystals, Academic Press, Ed.G.R.Luckhurst and G.W.Gray,p.6,1979.

59. G.W.Gray - Advances in Liquid Crystals, II Academic Press, Ed.G.H.Brown (1976).

59a. Chapt. 2 of ref. 35.

60. W.R.Young, I.Haller and D.C.Green, J. Organic Chem. 37 3707 (1972), W.R.Young and D.C.Green, Mol.Cryst. Liq.Cryst. 26, 7, (1974).

61.H. Kelker and R. Hatz - Handbook of Liquid Crystals Verlag Chemie, Chapt. 8 (1980).

62. M. Born, Sitz d. Phys. Math. 25 614 (1916).

63. W. Maier & A. Saupe, Z. Naturforsch 13a, 564 (1958); ibid, 14a 882 (1959); ibid 15a 287 (1960).

64. F.J.Wojtowicz in Introduction to Liquid Crystals. Plenum Ed. E.B.Priestley, Chpt. 4 (1974).

64a. Chapt. 3 of ref. 64.

65. J.A.Pople, Proc. Roy Soc. Vol. A221, p. 498 (1954).

66. M.E.Rose, Elementary Theory of angular momentum John Wiley & Sons, New York (1957).

67. R.L.Humphries, P.G.James and G.R.Luckhurst, J.Chem. Soc. Faraday Trans. II, 68, 1031 (1972).

68. Zwetkoft, Acta. Physicochemic, USSR, 16, 132 (1942).

69. J.R.Mc Call & C.S.Shih, Phys. Rev.Lett. 29, 85 (1972).

70. M.A.Cotter, Mol.Cryst.Liq.Cryst. 39, 173 (1977).

70a. M.A.Cotter, referred by Chandrasekhar, Chap. 14, Progress in Liq.Cryst. ed. Clive Croxton, John Wiley & Sons (1978).

71. G.R.Luckhurst in the Molecular Phys. of Liq.Crystals, Academic Press, ed. G.R.Luckhurst and G.W.Gray Chap.4 (1979).

72a. S.Chandrasekhar and N.V. Madhusudan, Acta. Cryst. A27 303 (1971).

72b. S. Chandrasekhar, N.V. Madhusudan and K.Subba, Faraday Soc. Suppl. No.5, 26 (1972).

73 S.Chandrasekhar and N.V.Madhusudan, J.de.Physique,30(1969).

74a. S.Jen, N.A.Clark, P.S.Pershan. and E.B.Priestley, Phys. Rev.Lett. 31 No. 26, 1552 (1973).

75a. S.Kabinata, Y.Nakajima, H.Yoshida and S.Maeda, Mol. Cryst. Liq.Cryst. 66 No. 1-4 (1981).

75b. Y.Nakijima, H.Yoshida, S.Kabinata and S.Maeda, Phys. Soc. Japan, 49, 1140 (1980).

76. G.R.Luckhurst, Quart.Rev. 22 179 (1968); M.C.L.C. 21 125 (1975).

77. S.Marcelja, J.Chem.Phys. 60 3599 (1974).

78. G.R.Luckhurst, M.C.L.C. Vol.72 (Letts.) 201 (1981).

79. K.K.Kaboyashi, J.Phys. Soc. Japan, 21, 201 (1970).

80. K.K.Kobayashi, Mol.Cryst.Liq.Cryst. 13 137 (1971).

81. W.L.McMillan, Phys. Rev. A4 1238 (1971).

82. W.L.McMillan, Phys. Rev. A6 936 (1972).

83. F.T.Lee, H.T. Tan, Y.M. Shih and C.W.Woo, Phys. Rev. Lett. 31, 1117 (1973).

84. P.J. Wojtowicz, Introduction to Liquid Crystals Chapt. 7, p. 83, Ed. E.B. Priestley, P.J. Wojtowics, and Ping Seng, Chapt. 7 (1974).

85. Gerhard Meier - Application of Liquid Crystals, Page 2, Ed. G. Maier, E. Sackmann, J.G. Grabmmier (1975), Springer Verlag.

86. G.W.Gray, Molecular Structure and properties of Liquid Crystals, Academic, London (1962).

87. Freedericksz and V.Zolina, Appl. Phys. Lett. 13, 91 (1968).

88. J.A.Castellano, Liquid Crystals. The Fourth State of Matter, Chapt. 12, Ed.F.D.Saeva. Marcal dekker Inc.(1979).

89. S. Meiboom, Z.Luz. Fourth International Liquid Crystal Conference, Kent Ohio (1972).

90. D. Demus & H.J. Sackman, Phys. Chem. 238, 215 (1968).

91. A. Saupe, Liq. Crystals and Plastic Crystals, Vol.1, Chapt. 2, Ed. G.W.Gray and P.A.Winsor, John Wiley & Sons, Inc. (1974).

92. D. Demus and Richter, Textures of Liquid Crystals, Verlag Chemie (1978).

93. A. Saupe, W.Maier, Z.Naturforsch 16a 816 (1961).

94a. P.Chatelain, Bull.Soc.France, Miner, Cryst.78 262 (1955).

94b. S. Chandrasekhar and N.V.Madhusudan, J. de Physique 30 C4-24 (1969).

94c. S. Chandrasekhar, Mol.Cryst.Liq.a Cryst.16 21 (1972).

95. P. L. Nordio and U. Segre, The Molecular Physics of Liq. Cryst. Ed. by G.R.Luckhurst and G.W. Gray, Academic Press (1979).

96. P. S. Pershan - The Molecular Physics of Liquid Crystal Chap. 17, 384, ed. G.R.Luckhurst and G.W.Gray, Academic Press (1979).

97. V.D. Neff - Chap. in Liquid Crystal and Plastic Crystals - Vol. II, Ed. G.W.Gray and P.A. Winsor, John Wiley and Sons, Inc. (1974).

98. Handbook of Liquid Crystals - Chap. 5, H.Kelker and R.Hatz, Verlag Chemie (1980).

99. G.H. Heilmier and L.A.Zanoni, Appl.Phys. Lett. 91, (1968).

100. Robert J. Cox, Mol. Cryst. Liq. Cryst. 55, p.1-32 (1979).

101. G.W.Smith, Advances in Liquid Crystals Vol.I, Ed. G.H.Brown, Acedemic Press (1975).

102. Nguyen Huu Tinh, C. Destrade, F. Hardoin, M.F. Achard. Ninth International Conference on Liquid Crystals, Bangalore, India (1982). Abstract No C-8.

CHAPTER 2

INTRODUCTION TO X-RAY WORK.

CHAPTER 2.

INTRODUCTION TO X-RAY WORK:-

1.1. Samples used -

X-ray diffraction studies have been made on seven different samples possessing nematic, Smectic A, Smectic B and cholesteric phases.

They are as follows:

(i) 'MBAC'-
(-)-2-Methylbutyl-p-[n-(p-Methoxy benzylidene)amino]-Cinnamate]

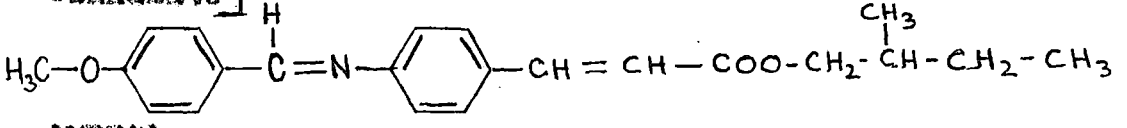

(ii) 'MBBA'-
p-Methoxybenzylidene-p-n-butyl aniline

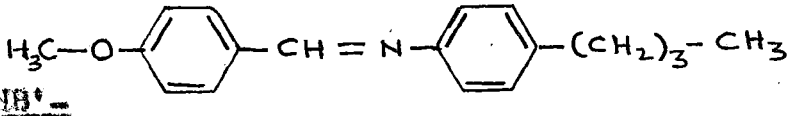

(iii) 'CPHB'-
p-Cyanophenyl-p-n-heptylbenzoate

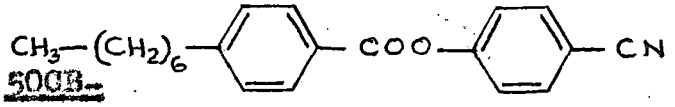

(iv) 5OCB-
p-n-Pentyloxy-p-biphenyl carbonitrile

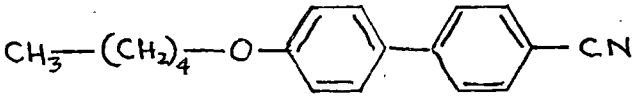

(v) 8OCB-
p-n-octyloxy-p-biphenylcarbonitrile

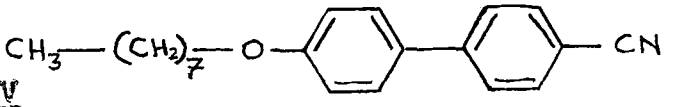

(vi) PCBAV
p-n-(p-Pentyloxy carbonyloxy benzylidene) amino) valerophenone

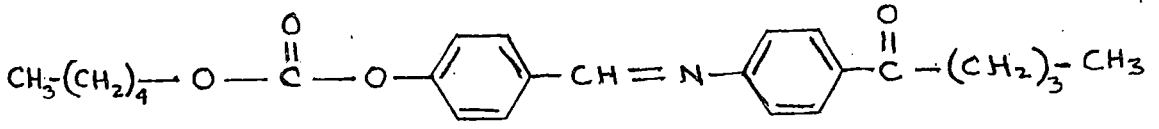

(vii) CBCOA

n-p-Cyanobenzylidene-p-Octyloxyaniline

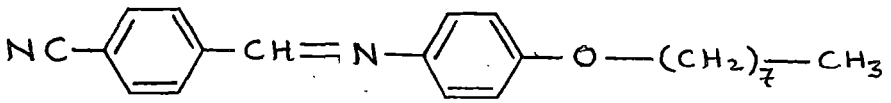

1.2. Experimental Procedure

(i) Recrystallisation:-

Before starting any experiment with the liquid crystalline samples, generally it is necessary to recrystallize the same from different organic solvents several times in order to get the sample in the purest form.

The sample MBAC was recrystallized from ethanol, but after recrystallization some chemical changes were observed, so the original sample was used for X-ray diffraction studies without further purification.

The sample MBBA which was given by Prof. N.Weda of Tohoku University, Sendai, was also used for experimental purpose without further purification.

The samples CPHB, 5OCB and 8OCB were obtained from M/s. F.Hoffmann-La-Roche & Co. and all the samples were recrystallized from ethanol.

The samples CBCOA, PCBAV and MBAC was purchased from M/s. Eastman Kodak & Company.

PCBAV was recrystallised from a mixture of benzene and petroleum ether solution (1:2) in the chemistry dept. of NBU.

CBCOA was used for experimental purpose without further purification.

All the samples were dried in vacuum desiccator for several hours and then used for experimental purpose.

(ii) Polarizing microscopic study for identification of different phases and transition temperatures:-

To identify the different mesomorphic phases the texture analysis is highly useful. Demus & Richter have described in detail ~~about~~ the texture analysis with several photographs of different textures of different mesophases[1]. A polarizing microscope [Towa, India] with magnification 150 X equipped with a hot stage which has been fabricated in our laboratory, has been used to examine the melting behaviour of the different liquid crystals. The sample was kept between the cover slips and the observations were performed under the a crossed polarizers. Temperatures were regulated and recorded with a pre-calibrated thermocouple within an accuracy of ± 0.5°C.

Observing the different textures under the crossed polarizer we could identify the different phases of the liquid crystalline compounds and also the transition temperatures. First we observed the phase transitions of the particular liquid crystalline sample with polarizing microscope and then etarted the experimental study with X-ray diffraction.

(iii) Apparatus - Apparatus required for X-ray diffraction:

Three different Flat plate cameras were used for taking the X-ray diffraction photographs of different mesomorphic phases at different temperatures with Radon House (India), X-ray generator. A copper target was employed in the X-ray generator. The three different cameras with different sample holders are

described below -

1. X-ray diffraction photographs were recorded on a flat plate camera with a high temperature attachment and modified collimating system. The attachment was designed and fabricated in our laboratory. The sectional diagram of the attachment is shown in the fig. 2.1. The sample in the powder form was contained in a glass capillary of 1 mm. diameter. A brass disc had a hole drilled along its diameter and the capillary was inserted in the hole and the brass disc in the specimen container is kept inside the brass block. Then it is covered with a brass cover insulated with asbestos having a hole of 2 mm. diameter for the passage of X-ray. No external magnetic field was used in this set up during the exposure.

The temperatures were regulated with the help of a pre-calibrated copper-constantan thermocouple inserted in the brass block close to the specimen.

The X-ray diffraction studies of unoriented MBAC sample was performed with this high temperature camera.

2. A Universal Camera (UNK 3) was used for taking the X-ray diffraction of the sample MBBA. MBBA has a mesomorphic phase at room temperature. No high temperature attachment was there and the camera was used for taking the photographs of the samples which possess mesomorphic phases at room temperatures. The specimen was enclosed in a glass capillary of 1mm in diameter. The sample was aligned by repeated heating and cooling process i.e. recycling the sample from its isotropic state to solid state several times.

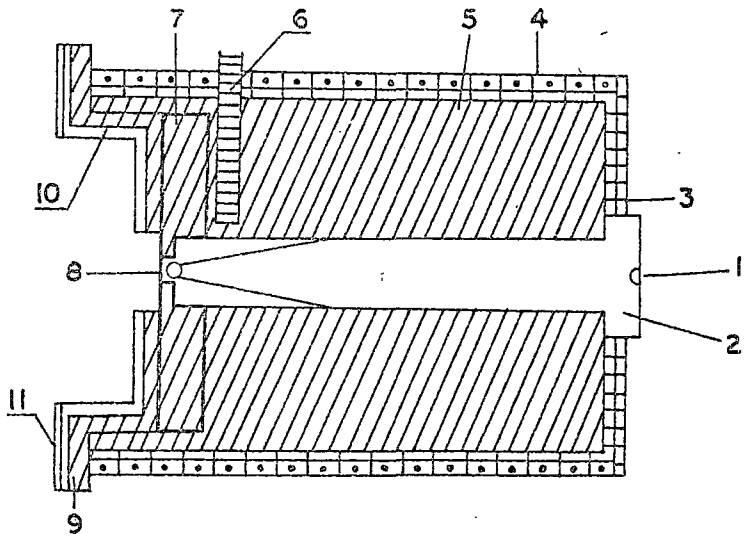

1. DIRECTION OF X-RAY, 2. COLLIMATOR,
3. ASBESTOS, 4. INSULATION AND HEATER WINDING,
5. CYLINDRICAL BRASS CHAMBER, 6. THERMOCOUPLE,
7. SPECIMEN CONTAINER BRASS DISC, 8. SPECIMEN,
9. BRASS COVER FOR SPECIMEN CONTAINER,
10. LEAD, 11. ASBESTOS INSULATION.

FIG. 2.1(a). SECTIONAL DIAGRAM OF THE SAMPLE HOLDER.

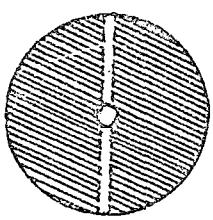

FIG. 2.1(b). CAPILLARY HOLDER.

3. In order to determine the orientational distribution functions and order parameters of different samples (CPNB, 50OB, 80OB, PCBAV and CBOOA), thirdly, we used another camera with high temperature attachment. This attachment has been designed and fabricated in our laboratory by B.Jha et al[2] with a view to study the alignment of the liquid crystals in presence of a magnetic field. Vainshtein et al[3] also studied alignment of several liquid crystals in presence of magnetic field. The whole arrangement is schematically shown in the fig. 2.2.

Here the sample holder contains interchangable metallic (brass or nonmagnetic steel) specimen container, where the samples can be contained in the molten state in the form of a bead by surface tension. The thickness of the sample holder with the ak asbestos insulation is only 1 cm. so that the pole-pieces of the electromagnet which are properly shaped can be brought very close, thus producing a strong field at the specimen position. The cylindrical brass chamber has heating coils which are insulated by asbestos. The temperature is regulated through a pre-calibrated copper-constantan thermocouple which can be attached to the specimen container. The sample holder is well insulated by sindanyo board and asbestos sheet. The film cassette is mounted on a cassette holder. In order to provide magnetic shielding the iron container (which is magnetic), where the X-ray tube is mounted in the Radon House X-ray generator, was retained. Wooden blocks were kept over the pole pieces in between the magnet and the pole pieces to avoid the attraction of the X-ray tube by the magnet.

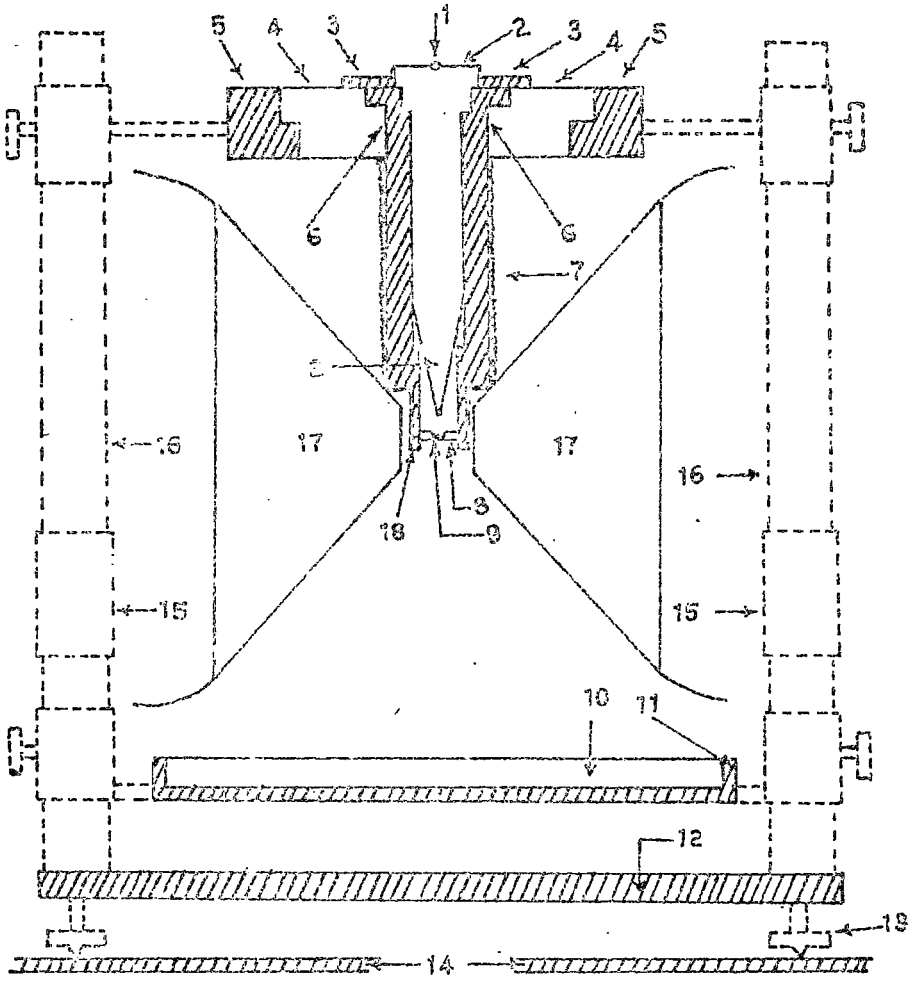

Fig. 2·2. Sectional diagram of the camera:
(1) X-Ray; (2) Collimator; (3) Brass Ring; (4) Ring of Syndanio Board; (5) Brass Ring; (6) Cylindrical Brass Chamber; (7) Asbestos Insulation and Heater Winding; (8) Specimen Holder and Thermocouple; (9) Specimen; (10) Film Cassette; (11) Film Cassette Holder; (12) Base Plate; (13) Levelling Screw; (14) Brass Plates over the Coils of Electromagnet; (15) Removable Spacer; (16) Supporting Brass Stands; (17) Polepieces; (18) Asbestos Insulation.

A sensitive galvanometer attached with a lamp and scale arrangement with a Cu-constantan thermocouple was used for the measurement of temperature. Temperature was regulated within 0.5°C by supplying variable voltages to the heating coils from a stabilized power supply. Both the sample holders can be heated upto 250°C.

A sensitive Gaussmeter (ECIL Model GM 867) is used for the measurement of the strength of the magnetic field for the different distances between the pole pieces of the electromagnet as maintained during the exposures.

In both the cases thermocouples were calibrated with three different pure samples of known melting point. These are -

1. Benzilic acid (m.p. 150°C)
2. P-nitrotoluene (m.p. 54°C)
3. O-Toluic acid (m.p. 102°C)

In all the three cases for the X-ray diffraction photographs Ni filter of thickness 0.009 mm. was used to obtain nearly monochromatic CuK_{α} radiation of wavelength 1.542 Å. The X-ray generator was operated at a Cu target voltage of 30 KV and a tube current of 10 mA. for a long time. The X-ray beam was collimated by using collimators of different apertures 0.5 mm, 0.8 mm and 1 mm. in different cases. For all the set ups, the exact distance between the sample and the film was determined by taking photographs with Al powder.

The unit cell dimension 'a' of a cubic crystal for reflections from (h k l) plane, is related to the Bragg angle θ' by[4]

$$\sin\theta' = \frac{\lambda}{2a}\sqrt{h^2+k^2+l^2}$$

[a for Al. is 4.04 Å, and λ for Cuk$_\alpha$ radiation with Ni-filter of thickness 0.009 mm is 1.542 Å]

Measuring the diameter of the diffraction rings corresponding to both (111) and (200)[5] reflections and the value of Bragg angle from the above relation, the exact distance between the sample and the film in Aluminium photograph can be obtained from the relation $\tan 2\theta' = \frac{\text{Radius}}{\text{distance}}$. A correction term is calculated by comparing the mean distance from the two i.e. (111) & (200) reflections with the spacer separation employed, for each of the three above mentioned sets and thus the exact distance could be determined for any spacer separation between the sample holder and the film cassette.

1.3. Alignment of samples:

In order to get monodomain sample i.e. aligned sample several methods can be adopted. Here we used two processes to produce monodomain mesomorphic samples.

(i) Simple recycling process

(ii) Application of magnetic field perpendicular to the direction of the X-ray ~~tube~~.

(I) Recycling process - The sample in a glass capillary is slowly heated upto isotropic phase and then cooled down to the solid phase slowly. The process is repeated several times

and the aligned samples could be obtained. The sample MBBA was aligned by this process.

(II) Application of magnetic field:- The smectic sample was first heated into the isotropic phase and a magnetic field of about 5.81 K.Gauss was applied to the sample. After the magnetic field had stabilised (about 30 min.) the sample was allowed to cool slowly just below the smectic - nematic transition temperature. After the stabilization of the desired temperature the magnetic field was lowered. In this way we can get the oriented smectic liquid crystals samples.

Nematic phases can be oriented by the application of magnetic field. The sample could be oriented by the application of magnetic field. The monodomain sample could be obtained by applying sufficiently strong magnetic field.

For all the samples other than MBBA and MBAC alignments were made by the application of the magnetic field.

1.4. Conversion of optical density into X-ray Intensity:-

The optical density obtained from the densitometer scanning of the X-ray diffraction photograph was converted into relative intensity value by a method as given by Klug and Alexander[6].

For an experimental purpose a graded intensity scale was prepared in our laboratory by the following method. Two sets of photographs were taken with double films in each set with films of length 25 cm. and 2 cm. width. The films were wrapped in a light tight paper envelope, which slides freely in a jacket made of lead which protects the film from the X-ray beam except the portion exposed by 2 mm. wide rectangular

aperture. The film holder was kept at a distance of 15 cm. from the X-ray slit and the slit used was large so that the entire area of the aperture was irradiated with X-rays of uniform intensity. Under such condition care was taken to protect the unexposed part of the film from direct and scattered X-rays by means of suitable absorbing shields of lead. A nickel filter was used to reduce the intensity of the X-ray beam sufficiently, so that the exposure time may be of practicable length. The X-ray beam was adjusted by setting proper applied target 25 KV, tube current of 5 mA and a Ni filter of thickness 0.027 mm. A manually operated lead shutter was used for the regulation of exposures using CuK_α radiation (1.542 Å) from the X-ray generator at a constant voltage and tube current a number of exposures were taken at 2, 4, 6, 8, 10... secs. The film used was fresh and of the same brand and type used in the experimental purpose.

Optical densities (O.D.) were measured with an optical densitometer Model No. EM 803 (ECIL). With the front film of 1st. set of series an O.D. versus time in seconds (X-ray intensity) graph was drawn. Corresponding to measured ≅ O.D. of the second film of the 1st. set X-ray intensities were recorded from this graph. The average of the ratios of these intensities corresponding to all the exposures gives the film factor. The intensities of the 2nd. film multiplied by the film factor converts the reading of to those of the front film.

The film factor for the second set was determined exactly in the same process. By comparing the intensities

corresponding to the same time of exposures of the two front films of the two sets, the readings are converted to those of first set.

The unexposed film O.D. of these films were 0.31.

A graph is drawn by plotting the optical density values (obtained by subtracting 0.31 from the O.D. values of the graph drawn from different films ~~same~~ as mentioned above) against corresponding intensities as shown in fig. 2.3.

Intensities noted were in arbitrary unit.

The developing time has a pronounced effect upon both the Optical density (O.D.) and the film factor of the response curve. Increase in developing time will increase both the O.D. and film factor within certain limit with the result that a change takes place in the ratio of the intensities. Thus the scale processed in one developing time will lead to errors if applied to a film developed for different period of time. So the time used for developing the films of the liquid crystalline sample was kept the same as that used for developing the film for graded intensity scale. Moreover, the developing temperature and composition of the developer used were also kept constant throughout the series of experiments reported here in.

While developing the photographs ~~of the photographs~~ of the liquid crystalline samples a separate small piece of film was also developed in each case in order to get the O.D. of the

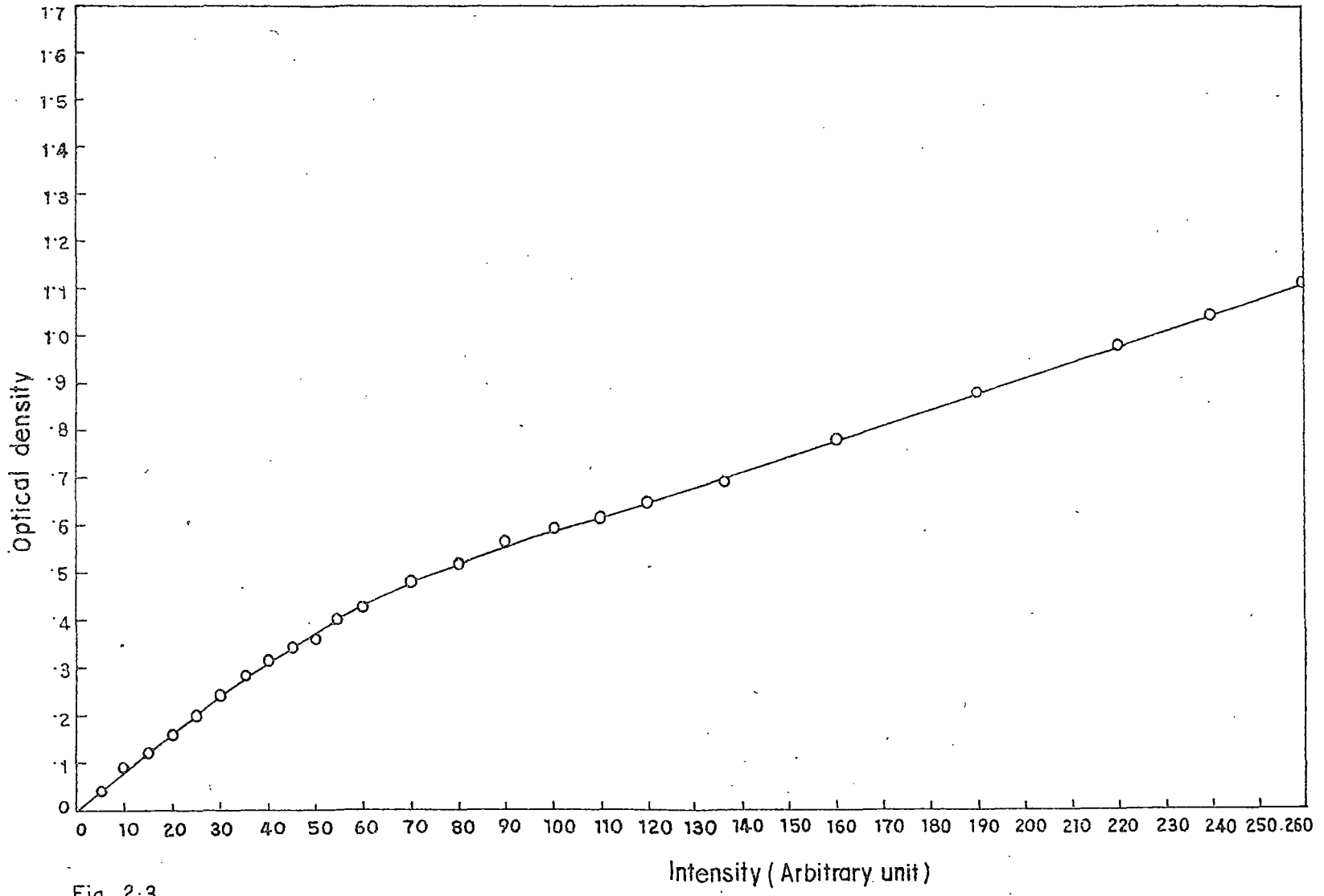
Optical density
1·7
1·6
1·5
1·4
1·3
1·2
1·1
1·0
·9
·8
·7
·6
·5
·4
·3
·2
·1
0
0 10 20 30 40 50 60 70 80 90 100 110 120 130 140 150 160 170 180 190 200 210 220 230 240 250 260
Intensity (Arbitrary unit)

Fig. 2·3

unexposed film. In spite of all possible cares taken it was found that O.D. of the unexposed film was different (depending on the temperature and developing time) from that of the standard strip (0.31). The O.D. ~~density~~ of the unexposed film is here termed as background O.D. Then the background O.D. for each photograph is subtracted from the measured O.D. of the particular photograph and then the corresponding X-ray Intensity was determined from the graph 2.3.

Another O.D. vs. Intensity curve is drawn in Fig. 2.4 by exactly following the same procedure. Here the unexposed O.D. for the standard strip was 0.34 and for the sample MBBA the intensity conversion is done from this curve as the background O.D. for MBBA is also 0.34 and the film used was also of the same brand.

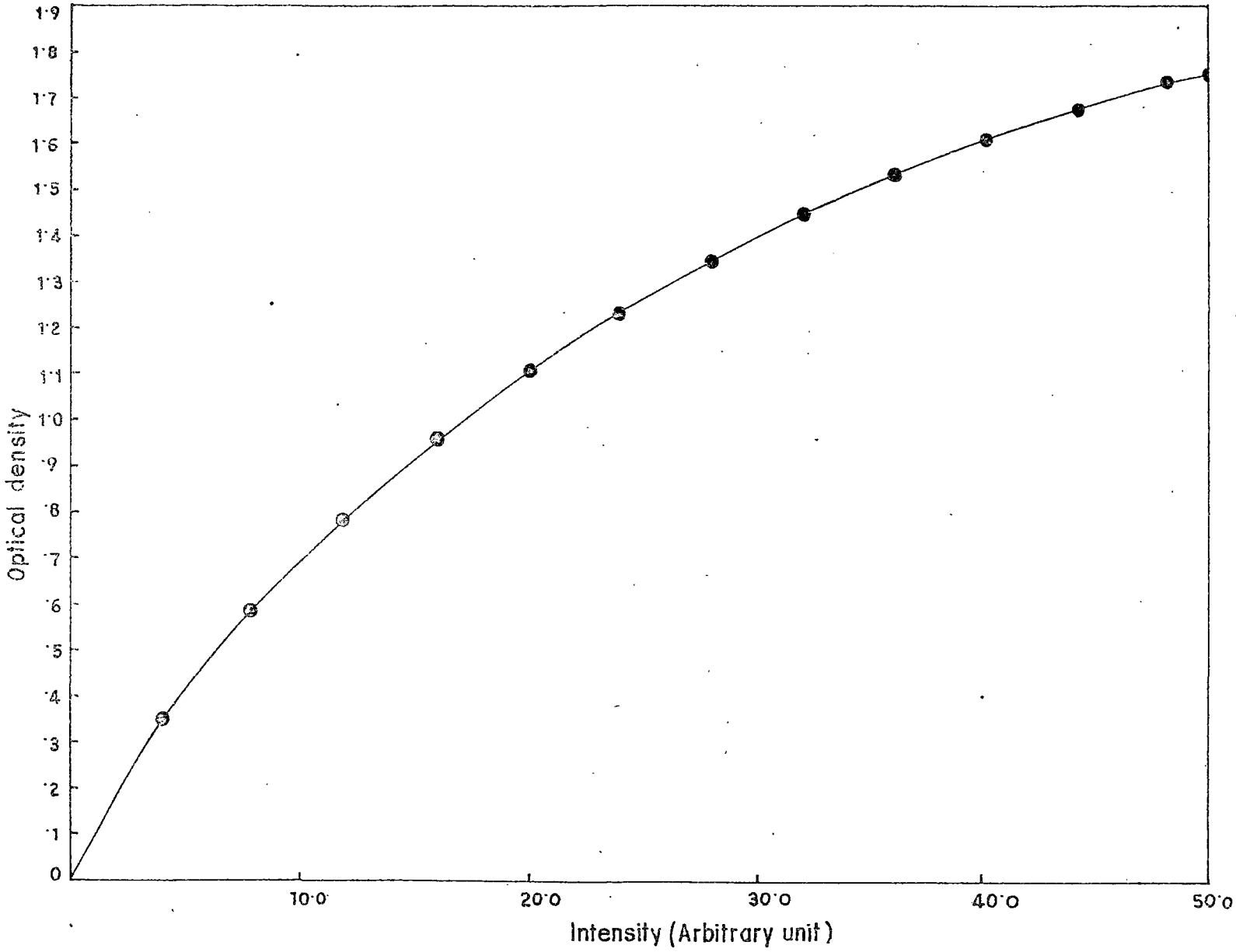
1·9
1·8
1·7
1·6
1·5
1·4
1·3
1·2
1·1
1·0
·9
·8
·7
·6
·5
·4
·3
·2
·1
0
Optical density
10·0
20·0
30·0
40·0
50·0
Intensity (Arbitrary unit)

Fig. 2·4

REFERENCES.

1. D. Demus & L. Richter, Texture of Liquid Crystals, Verlag Chemie, (1978).
2. B. Jha, R. Paul, Proc. Nucl. Phys. Solid State Phys. Symp. India, 19C, 491 (1976).
3. V.M.Chakovskii & I.G.Chistykov, Kristallografiya, (USSR) 13, No. 1, 158 (1968).

   &: Eng. Tr. in Sov. Phys. Cryst. (USA).
4. C. Kittle, Introduction to Solid States Physics, Wiley Eastman, Chapter 2 (1976).
5. H.P. Klug & L.E.Alexander, X-ray Diffraction Procedures, John Wiley & Sons, Chapt. 3 (1974).
6. H.P. Klug & L.E. Alexander, X-ray Diffraction Procedures, John Wiley & Sons, New York, Page 114 & 473 (1974).

CHAPTER 3

THEORETICAL BACKGROUND FOR X-RAY WORK.

CHAPTER 3

THEORETICAL BACKGROUND FOR X-RAY WORK:

X-ray scattering technique is a good tool to give an idea of the molecular interactions in liquid crystals. The first attempts to study liquid crystals by X-ray analysis followed immediately the discovery of X-ray diffraction[1,2]; they indicated that the X-ray diffraction patterns for mesomorphic phase and the corresponding liquids were similar. Thus it was stated that there was no three dimensional periodicity in structure of these phases. Some difference between X-ray patterns of amorphous isotropic liquids and mesophases was experimentally detected afterwords. X-ray patterns of nematic phase oriented by the application of external magnetic or electric field showed that the main diffuse ring split into two crescents[3]. Falgueirettes made the first quantitative study of X-ray scattering by a single domain sample of nematic liquid crystal of PAA[4].

By considering the scattering from an isolated molecule and then that from molecules arranged parallel to one another in a cluster, he proved that intermolecular interference were possible only when the scattering vector was perpendicular to the major axis of the cluster: (a Such cluster of molecules has no physical existence, but by considering such bundles, it is possible to describe the short range order in the nematic and to interprete the X-ray diffraction data. By this result it was possible to find a relation between the

intensity of the crescent with the number of molecules taking part in the intermolecular scattering and to deduce the molecular angular distribution function. For PAA distribution functions obtained in this way lead to values of the degree of order, which agree with values obtained by other methods.

Then Delord has studied other nematic compounds with a diffractometer[5]. His results confirmed those of Falgueirettes.[4]

Working with long chain molecules Vainshtein[6] provided a quantitative interpretation of equatorial diffraction by an oriented nematic or smectic by use of cylindrical distribution functions.

X-ray diffraction studies of mesomorphic phases have been reviewed by many authors[7-10]. Theoretical considerations are given by Vainshtein[6] and Leadbetter[11].

Unoriented nematic phase shows X-ray diffraction pattern which is a uniform halo just like that of an ordinary liquid. This is due to the fact that, generally, nematic liquid crystal samples consists of large number of domains, the molecules being ordered within each domain in a preferred direction i.e. the director (optic axis), but there is no preferred direction for the specimen as a whole and naturally X-ray diffraction pattern has a symmetry of revolution around the direction of X-ray beam.

The principle feature of the X-ray pattern of a sample which is oriented perpendicular to the incident X-ray is that the main halo (ring) splits into two crescents for each

of which intensity is maximum in the equatorial section i.e. perpendicular to the director (optic axis). These crescents are mainly due to the intermolecular scattering[4]. Fig.3.1(a) and Fig.3.1(b) represent schematically the X-ray diffraction pattern of oriented nematic and oriented smectic A phase respectively.

In the meridional section i.e. parallel to the optic axis some other rings are also observed; these are due to intramolecular scattering. These rings which are less intense than the crescents due to intermolecular scattering appear disintly only on patterns obtained after long exposure times. From such an X-ray diffraction photograph the main optic axis can be located easily.

Additional rings of maximum intensity in the equatorial section are observed some times in experiments employing very strong magnetic fields or with very sensitive detector. These are due to inter molecular scattering - interference between waves scattered by atoms in the equatorial plane of individual molecules.

The first of the meridional rings (halo) (this ring is also called the inner ring) corresponds to the molecular length.

Chistyakov's[7] review gives a detailed descriptions of methods which permit the cylindrical distribution functions. The methods involve an integration of the scattering vector from zero to infinity which can never be fulfilled by photographic methods with a flat plate camera, where the plate is normal to the incident X-ray.

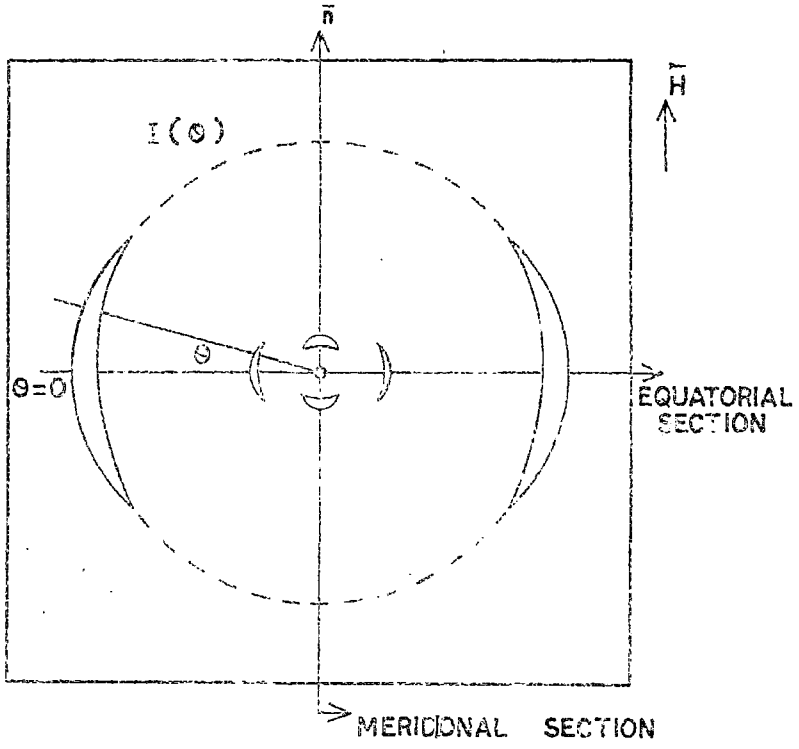

FIG. 3.1(a). X-RAY PATTERNS OF THE MAIN TYPES OF ORIENTED NEMATIC MESOPHASE. (SCHEMATIC REPRESENTATION).

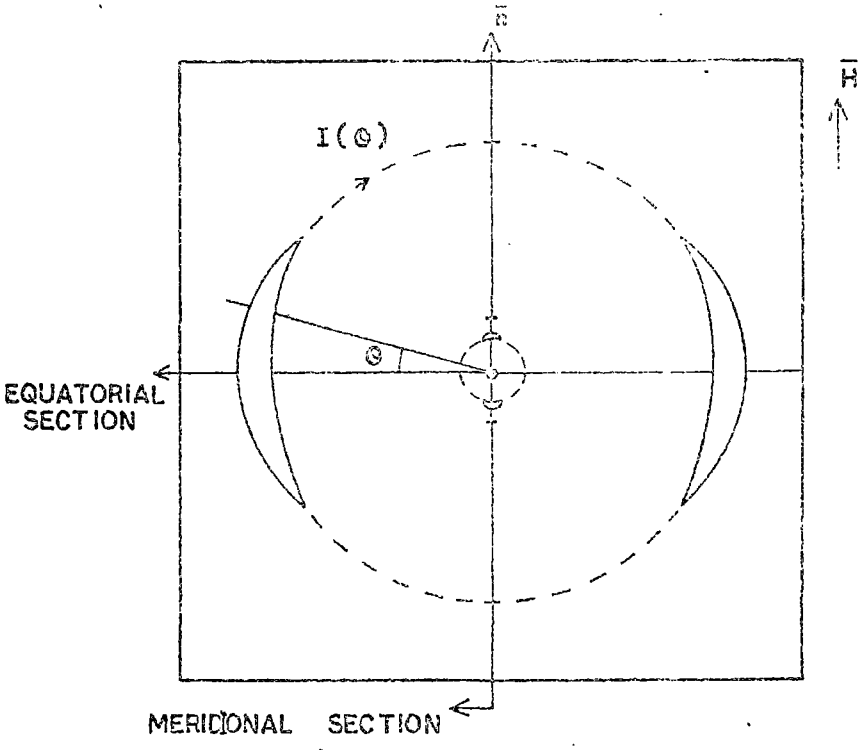

FIG. 3.1(b). SCHEMATIC REPRESENTATION OF THE X-RAY PATTERN OF ORIENTED SMECTIC A PHASE. (IN PRESENCE OF MAGNETIC FIELD $\bar{H}$).

From X-ray diffraction calculation of cylindrical distribution function and order parameter has been done by de Vries[12]. Orientational distribution function and order parameter were obtained by many workers by X-ray diffraction on ordered mesophases[13-18].

By the X-ray diffraction technique on different mesomorphic phases we are going to find out the different molecular parameter (viz. average intermolecular distance, apparent length of the molecule and layer thickness in case of smectics) and the singlet orientational distribution function $f(\beta)$ which gives the probability of finding a molecule of a particular orientations (β) with respect to the director and from that the order parameter $\langle P_L \rangle$ (L = 2 and 4). In one particular case we have calculated ~~down~~ the translational order parameter of smectic A phase and also the mean square displacement of the molecular centre in the direction perpendicular to the layer plane.

Average Intermolecular Distance. Apparent Length of the Molecules and Layer Thickness (In case of Smectics).

In our measurements from X-ray diffraction photographs wer are concerned with two spacings. A long spacing l (i.e. the apparent length of the molecule and layer thickness in case of smectics) and the short spacings 'D' values - the average lateral distance between the two molecules.

In general it is possible to calculate a spacings X, from the position of a diffraction maxima by a formula of the type[19].

$$2X \sin\alpha = K_1 n\lambda \qquad \ldots (1)$$

Here 2α is the diffraction angle measured between the incident and diffracted beams, λ is the wavelength of radiation employed, n is the order of reflection (generally n assumed to be unity) and K_1 is a constant depending on the shape and arrangement of the molecule[20], i.e. the choice of K_1 value depends on the orientational order within a phase and the particular spacings we are concerned with.

De vries has discussed the equations, their applications and their limit in details[21,22].

In our cases we used $K_1 = 1$ in eqn. (1) for the long spacings (i.e. for l values) i.e. Bragg's law.

For both oriented and unoriented samples we used $K_1 = 1.117$ in equation (1) for the calculation of intermolecular distance. This is because of the fact that, considering the scattering from a pair of molecules at a distance 'D' apart; - if the chains are allowed to rotate freely around each other, the positions of the maxima along the equator are determined by the function,

$$J_0(x) = \int_0^{2\pi} \cos(x\cos\delta)\, d\delta \qquad \left[\text{where, } x = \frac{4\pi}{\lambda} d\sin\alpha\right]$$

which gives for the position of the 1st. maximum

$$2d\sin\alpha = 1.117\lambda \quad \text{i.e.} \quad K_1 = 1.117$$

Wenderff[19] et al have calculated the K values from the photographs of some cholestrol esters by taking X values in eqn. (1) from completely extended form of the molecule and found that K_1 lies between 1 (for perpectly ordered molecules) and 1.229 (for completely random orientation of the molecule).

In some cases the long spacings which corresponds to the molecular length are found to be greater than the measured molecular length in the completely extended form which seem to arise from the antiparallel associations of the molecules[23] or from bilayered structures. Again in some cases where the molecules are arranged in layers with the molecules tilted at same definite angles with the layer normal in case of smectics, the long spacings are found to be much shorter than the actual length of the molecule measured in its form[23,24].

Orientational distribution function and order parameters:-

The average state of orientation for a system of cylindrically symmetric molecules can be sufficiently described by a distribution function, $f(\beta)$ depending only on the angle β between the molecular symmetry axis and the director[15]. The X-ray diffraction photographs record intensities averaged over a relatively long time and over the

irradiated volume which is sufficiently large so the molecules may have assumed to have an average cylindrical symmetry, even if the molecules are not rotating about their long axes[16]. The order parameters $\langle P_L \rangle$ for a system of rigid rods in a unaxial phase are defined by

$$\langle P_L \rangle = \frac{\int_0^{\pi/2} P_L(\cos\beta)\, f(\beta) \sin\beta \, d\beta}{\int_0^{\pi/2} f(\beta) \sin\beta \, d\beta} \qquad \ldots(2)$$

with $L = 2$ & 4 we will get $\langle P_2 \rangle$ and $\langle P_4 \rangle$ [$P_L(\cos\beta)$ is the Legendre polyomial of Lth. order].

By X-ray method the measurements of $f(\beta)$ have been reported by Leadbetter et al[17,18]. Assuming the molecules as rigid rods perfectly aligned in cluster of small number of molecules ($\gtrsim 10$) Leadbetter and Morris[17] obtained a relationship between $I(\theta)$ and $f(\beta)$ where $I(\theta)$ is the intensity around the diffuse equatorial are as

$$I(\theta) = c \int_{\beta=\theta}^{\pi/2} f_d(\beta) \sec^2\theta \left[\tan^2\beta - \tan^2\theta\right]^{-1/2} \sin\beta \, d\beta \qquad \ldots(3)$$

where, $f_d(\beta)$ now describes the distribution function for the orientation β of a local cluster of molecules perfectly aligned with respect to the director, rather than the true singlet distribution function. In the derivation they have assumed that for a perfectly aligned samples [$f_d(\beta) = \delta(\beta)$], the scattering is zero

except for the direction of the scattering vector perpendicular to the cluster axis. Leadbetter et al have however, calculated the effects and shown that the deviations are very small in general which can be neglected except for highly ordered phases ($\langle P_2 \rangle \geq 0.8$) . Comparing the values of $f_d(\beta)$ with $f(\beta)$ of the same samples obtained by other methods they have shown that the value of the true singlet orientational distribution function $f(\beta)$ may be taken to be the same as the value of $f_d(\beta)$ Thus, $f_d(\beta)$ or $f(\beta)$ values can be obtained from equation (3) with the measured intensity distribution I (Θ) values, and hence order parameters $\langle P_L \rangle (L = 2,4)$ can also be obtained.

The intensity I (Θ) values are obtained after the conversion of the optical density values measured on the film and after background correction for different factors which will be described in next chapter.

These intensity values also contain the background intensity arising due to the thermal vibration of the molecules.

The peak intensity position which would correspond to $\Theta = 0$ was determined at the position where the height of the $I(\Theta) \leftarrow \Theta$ (intensity - angle) curve above the background tangent line was maximum Eqn. (2) & (3) shows that the evaluation of the integrals requires angular scanning for one quadrant i.e. from $\Theta = 0$ to $\Theta = \pi/2$.

As molecular distribution in the nematic phase is centro symmetric ($\bar{n}$ & $-\bar{n}$ are indistinguishable), so the distribution function and the intensity distribution can be expanded as a power series with only even terms of Legendre Polynomial 6,18

$I(\theta)$ and $f(\beta)$ can be expressed as

$$I(\theta) = \sum_{n=0}^{\infty} A_{2n} \cos^{2n}\theta \qquad \ldots (4)$$

$$f(\beta) = \sum_{n=0}^{\infty} B_{2n} \cos^{2n}\beta \qquad \ldots (5)$$

Substituting $\sin\alpha = (\cos\beta \cdot \sec\theta)$ in equation (3)

$$I(\theta) = c \int_0^{\pi/2} f_1(\alpha) \sin\alpha \, d\alpha \qquad \ldots (6)$$

From eqn. (4), (5) & (6) we have,

$$\sum_0^{\infty} A_{2n} \cos^{2n}\theta = \int_0^{\pi/2} \sum_0^{\infty} B_{2n} \cos^{2n}\theta \sin^{2n+1}\alpha \, d\alpha \qquad \ldots (7)$$

$\sin\theta$ is arbitrary, the coefficients of $\cos^{2n}\theta$ must be equal. The integral

$$\int_0^{\pi/2} \sin^{(2n+1)}\alpha \, d\alpha = \frac{2^{2n}(n!)^2}{(2n+1)!}$$

and so

$$B_{2n} = A_{2n} \frac{(2n+1)!}{2^{2n}(n!)^2} \qquad \ldots (8)$$

The series in equation (4) and (5) converges rapidly. Retaining eight terms in the truncated series, a least square fitting is made to obtain the coefficients from equation (4), with the intensity values as obtained after background correction.

The agreement w between the observed and calculated intensity values are found nearly perfect in all the calculations taking the eight terms in series.

The value of the coefficients B_{2n} in the truncated series for $f(\beta)$ in equation (5) are calculated with the help of equation (8) by putting the values of A_{2n}

By calculating the integral

$$\int_0^{\pi/2} f(\beta) \sin\beta \, d\beta = K \quad (\text{say})$$

and then deviding all the B_{2n} values by K we obtain the normalized values for the orientational distribution function.

$$\int_0^{\pi/2} f(\beta) \sin\beta \, d\beta = 1 \qquad \ldots (9)$$

Subetituting (4) in (1) we get

$$\langle P_2 \rangle = \frac{1}{2} \frac{\int_0^1 (3\cos^2\beta - 1) \sum_0^r B_{2n} \cos^{2n}\beta \, d(\cos\beta)}{\int_0^1 \sum_0^r B_{2n} \cos^{2n}\beta \, d(\cos\beta)} \qquad \ldots (10)$$

$\langle P_2 \rangle$ can be calculated by writing this equation in the form of standard integrals and similarly $\langle P_4 \rangle$ can also be calculated.

Pseudopotential:-

The normalised singlet distribution function can be written as (described earlier in chap 1)

$$f(\beta) = Z^{-1} \exp\left[-\frac{V(\beta)}{kT}\right] \qquad \ldots (11)$$

where Z is the orientational partition function which at a particular temperature treated as a constant and $V(\beta)$ is the angular part of the intermolecular potential.

We have fitted our $f(\beta)$ values to the form

$$f(\beta) = Z^{-1} \exp\left[\sum_{L(\text{even})} a_L P_L(\cos\beta)\right] \qquad \ldots (12)$$

or

$$\ln f(\beta) = \sum_{L(\text{even})} a_L P_L(\cos\beta) + \text{Constant} \qquad \ldots (\;)$$

$$= \sum_{L(\text{even})} a'_L \cos^L(\beta) \qquad \ldots (13)$$

For a particular temperature, Z is taken to be constant. A least square fitting of equation (13) with the calculated $f(\beta)$ values for different β for a particular photograph gives a_L ... In order to obtain a good idea about pseudopotential six term in the series (L upto 10 with L even) are retained in this fitting.

For the sample CPHB we analysed[23c] the errors in calculating the coefficients a_L ($a_0 \equiv -\ln Z$) and estimated the percentage errors for a_L (L upto 10 with L even) i.e. a_0, a_2, a_4, a_6, a_8 and a_{10} as 2, 1, 4, 5, 20 and 25 percents respectively. Except the last two values all the coefficients are well defined within an accepted range of values.

A general anisotropic pair potential may be constructed by using the equation (1.6) for pseudopotential

$$V(\beta) = \sum_{L\,(even)} b_L \langle P_L \rangle P_L(\cos\beta) \qquad \ldots (14)$$

Where b_L is obtained by comparing equation (12) and (14) as

$$b_L = -\frac{k a_L T}{\langle P_L \rangle} \qquad \ldots (15)$$

and so the coefficients b_L can be determined.

For different temperatures the values of b_2 and b_4 have been calculated. Since the coefficients b_L determine the strength of the intermolecular forces it is expected that they should depend on intermolecular separation and so on temperature.

Initially b_L were treated as constants independent of temperatures and the pseudopotential[17] was constructed by taking averages of the value of b_2 and b_4 obtained for different temperatures and then included density dependence.

With the pseudopotential thus constructed the normalised distribution function $f(\beta)$ values were calculated both by retaining P_2 term only and also by retaining P_2 and P_4 terms using equation (11).

Using the eqn. (9), distribution function values obtained were normalised. The normalised distribution function values thus obtained are then compared with experimental $f(\beta)$ values.

Vainshtein[6] obtained a fairly good approximation for the order parameters by replacing $f(\beta)$ with $I(\beta)$ the X-ray intensity along the arc of the main equational reflection, keeping the Bragg angle constant ($\beta = 0$ at the maximum intensity position). We have also calculated the order parameter values using Vainshtein's approximation and the values will be denoted by $\langle P_2 \rangle_v$ and $\langle P_4 \rangle_v$.

REFERENCES.

1. J.S.V.D. Lingen, Ber. dt. Chem. Ges. 15 913 (1913).
2. G. Friedel, Annls. Phys. 18, 273 (1922).
3. P.W.Glamann, K. Herrmann, and A.H.Z. Krummacher, Kristallogr. Kristallgeom, 74 73 (1930).
4. J. Falgueirettes, Diffusion des Rayons X Par un Monocristal Liquide dn. Type Nematique, Thesis University of Montpellier, France, C.N.R.S. No. 160 (1958).
5. P. Delord and J. Falgueirettes, Cr. hebd. Seane Acad. Sci. Paris 260, 2468 (1965).
6. B.K. Vainshtein, Diffraction of X-rays by Chain Molecules, Elsevier Publishing Co. (1966).
7. I.G.Chistyakov, Sov. Phys. USP, 9, 531 (1967).
8. J. Falgueretteo & P. delord: In liquid crystals and Plastic crystals. Ed.G.W.Gray and P.A.Winsor, vol.2, Chapt. 3, Ellis Norword (1974).
9. H.Kelker & R.Hatz, Habdbook of Liquid Crystals, Chapt.5, Verlag Chemic, (1980).
10. L.V.Azaroff, Mol.Cryst. Liq.Cryst. 60, 73 (1980).
11. A. J. Leadbetter in the Molecular Physics of Liquid Crystals. Ed. G.R. Luckhurst & G.W.Gray, Chapt. 13, Academic Press (1979).
12. A. de Vries, J. Chem. Phys. 56, 4489 (1972).
13. P. Delord & J. Falguierettes, C.r.hebd. Seanc. Acad. Sci. Paris 260, 2468 (1965).

14. J. Falgueirettes, Bull. Soc. fr. miner cristallogr. 82, 171 (1956).

15. C.Zanoni, in the Molecular Physics of Liquid Crystals. Ed.G.R.Luckhurst & G.W.Gray, Chapt.3, Academic Press (1979).

16. A.J.Leadbetter & E.K.Norris, Mol.Phys. 38, No.3, 669 (1979).

17. A.J. Leadbetter and P.G.Wrighton, J. De Physique Collogue, 40 C 3-234 (1979).

18. P.G.De Gennes, The Phys. of Liq.Cryst. Chapt.2, Oxford (1974).

19. J.H. Van Wendorff and P.P. Price, Mol. Cryst.Liq. Cryst. 24 129-144 (1973).

20. I.G. Chistyakov, R.I. Schabischev, R.I., Jarenov, & L.A.Gusakova, [illegible]. Mol.Cryst. Liq. Cryst. 7, 279 (1969).

21. A. de Vries, Mol. Cryst. Liq. Cryst. 10 31, (1970).

22. A. de Vries, ibid..... 10, 219 (1970).

22a. A. de Vries, Ibid.....11, 361 (1970).

22b. A. de Vries..ibid. 20, 119 (1973).

23a. A. J. Leadbetter, R.M. Richardson, [illegible] and C.N. Colling, J.Phys. Paris, 36, C-1, 37 (1975).

23b. J.E.Lydon and C.J.Coakley J.Phys.(Paris) 36 C-1, 45(1975).

23C. B.Bhattacharjee, S. Paul & R. Paul, Mol.Phys. 44 6, 1391 (1981).

24. A. de Vries - Advances in Liquid Crystal Research and Applications. Ed.-Lajos Bata Pergamon Press, Oxford(1980).

CHAPTER 4.

EXPERIMENTAL PROCEDURE AND DATA ANALYSIS

CHAPTER 4.

EXPERIMENTAL PROCEDURE AND DATA ANALYSIS

The typical X-ray diffraction photographs for the unoriented and oriented nematic phase (CPHB at 34°C) are shown in the Fig. 4.1 and Fig. 4.2 respectively.

Generally, randomly oriented nematic phase consists of a large number of domains, the molecules being ordered within each domain in a preferred direction i.e. along the director, but there is no preferred direction for the specimen as a whole so that the X-ray diffraction pattern has a symmetry of rotation around the direction of the X-ray beam which is evident from the uniform diffuse outer halo or ring as in fig. 4.1, which is similar to the X-ray diffraction photograph from isotropic liquid. The diffraction photograph also contains a diffuse inner halo (in case of isotropic phase inner ring is generally more diffuse).

Nematic and isotropic phases can be distinguished by X-ray diffraction by using an oriented nematic sample. Fig. 4.2 shows the photograph of sample CPHB in the supercooled oriented nematic phase at 34°C in presence of a magnetic field of 5.8 K. Gauss. The outer halo splits up into two crescents along the equator for each of which the intensity is a maximum in the equatorial nn section which is absent in case of isotropic or randomly oriented mesophase. The inner ring is also splitted into two crescents for which the intensity has a maximum in the meridian section.

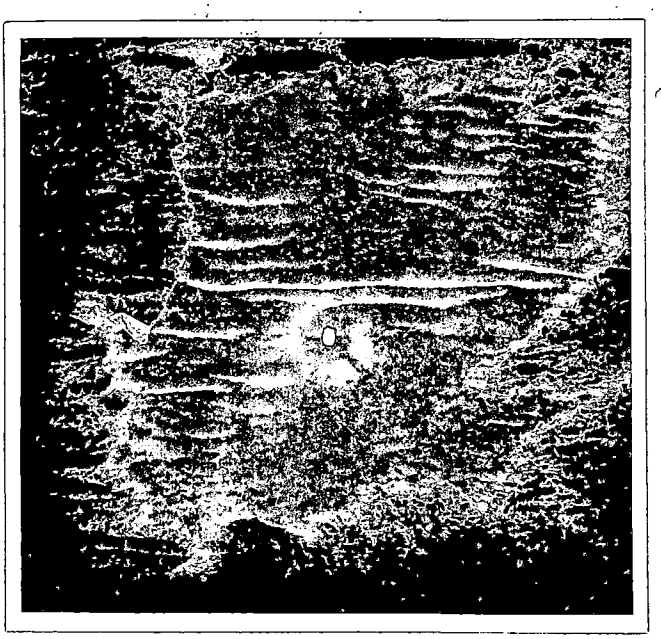

Fig. 4.1. Photograph of unoriented CPHB (nematic phase) at 34°C

Fig. 4.2. Photograph of oriented CPHB (Nematic phase) at 34°C.

In order to determine the various parameters the film containing the X-ray diffraction patterns were scanned (both linearly and circularly)by an optical densitometer (ECIL Model DM 803), with the help of a linear cum rotatory stage designed by us and constructed in our workshop.

Optical density obtained from the densitometer readings were converted to X-ray intensities wherever necessary with the help of a calibration curve [Fig. 2.3]prepared by the method as described in chapter 2.

It is found that intensity (I) is linear with O. D. values in the lower region of the curve and for this reason in case of determination of the diameters of the halos or crescents, the optical density values have not been converted to X-ray intensity values.

Linear scanning is required for the calculation of different molecular parameters.

In order to calculate the average intermolecular distance the diameter of the outer diffuse halo in case of unoriented sample and the diameter of the outer crescents at its maxima in case of oriented nematics is to be determined. The optical densities obtained from the linear scanning of the outer ring through the centre (central spot) is plotted against the linear scale readings (L in cm.). A typical graph (linear scan) for the diffraction photograph (Fig. 4.1) is shown in the Fig. 4.3(a).

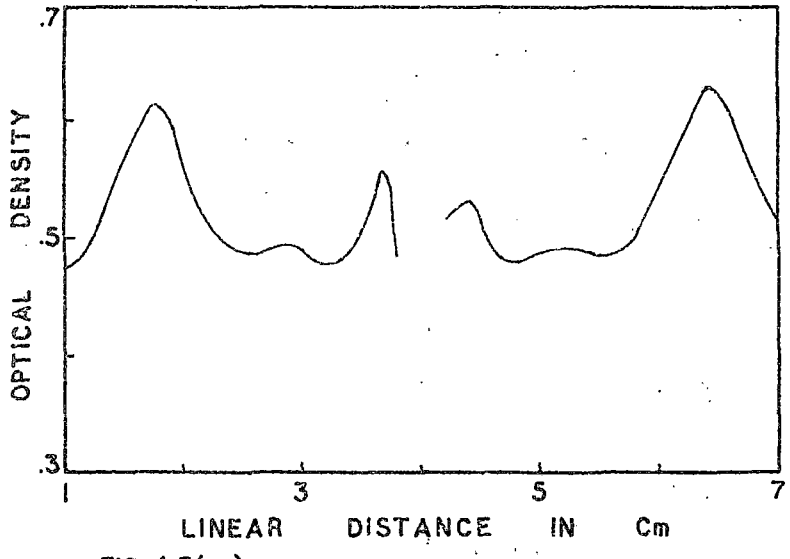

FIG. 4.3(a).

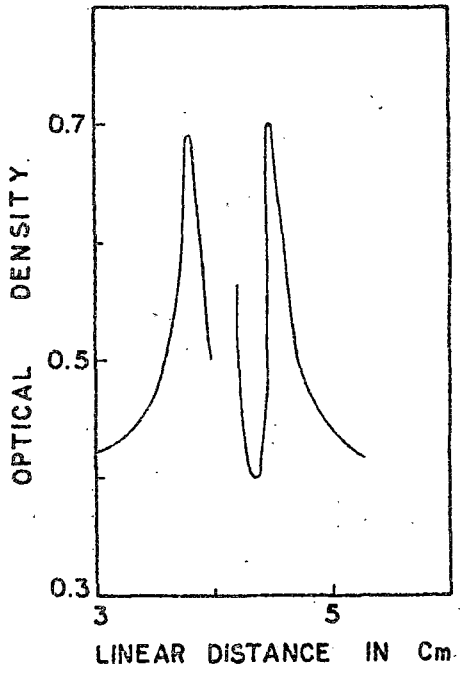

FIG. 4.3(b).

The difference between the two peak points of the outermost halo gives the diameter of the outer halo, (which is necessary for the determination of the half angle between the incident X-ray beam and diffracted beam).

Location of peak position:-

There are different methods[1] for locating the peak position from L-O.D. curve as shown in Fig. 4.3(A). P_o is the apperent maximum of the line profile. It has the drawback that statistical uncertainity in the intensity values at and in the immediate vicinity of the maximum makes its precise location uncertain. In order to avoid this problemm a commonly employed device is to locate the peak of P_x, the point of intersection of two straight lines projected from the most nearly linear portions of the sloping sides of the profile. Another method is to assign the peak position to the mid points of a chord drawn parallel to the background and located at one half of the maximum peak intensity $P_{1/2}$, or better at higher levels such $P_{2/3}$ or $P_{3/4}$.

Some times different methods give somewhat different values for the peak position despite the relative sharpness of the line profile.

In our case the peak position is located by one of the above mentioned methods, taking care that the method is convenient for the particular case. Generally, where the peak is well defined we simply take the P_o position but in some cases we used the other methods.

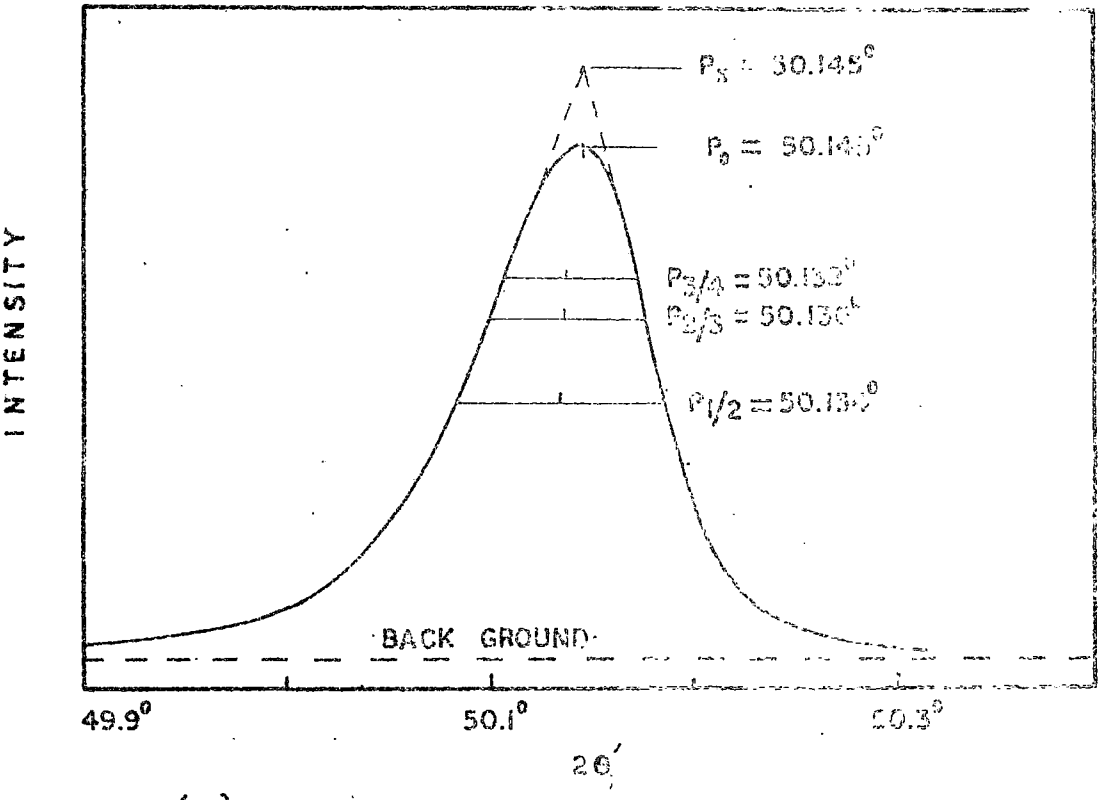

FIG. 4.3(A). VARIOUS METHODS OF LOCATING THE PEAK POSITION OF A LINE PROFILE.

The diameter of the outer crescents or halo is determined by taking the linear distance between the two peaks. The exact distance between the sample to film is determined as described in Chapt. 2 and value of the Bragg angle is determined.

Then the average intermolecular distance is calculated by using the formula 3.1 following the theory described in Chapter 3. As described in Chapt. 3, the diameter of the inner ring or halo (shown in fig. 4.1) is also to be determined in order to get the apparent molecular length.

A typical linear scanning through the diameter of the inner ring (halo) is shown by plotting O.D. against linear distance (L in cm.) as shown in Fig. 4.3 (b). The peak positions are located by the methods described earlier, though here the peaks are well defined and it is easy to locate.

Knowing the diameter of the inner halo the apparent molecular length is determined by calculating the Bragg angle α with the help of the actual distance between sample and film as given by deVries (Eqn. 3.1 in Chapt. 3).

Now let us consider the case of diffraction pattern of oriented sample (as in Fig. 4.2). Here both linear and angular scanning are required. Angular scanning is required for getting the intensity distribution.

The average intermolecular distance and the apparent length of the molecule are determined by the same process described in case of unoriented sample.

In order to get the diameter of the outer crescents accurately the linear scanning was made on different angular positions (θ values), [Fig. 4.4].

Considering $\theta = 0°$ at the maximum intensity position the linear scanning is done [Fig. 4.5(a)]. The peak difference between the two maxima is obtained i.e. the diameter of the outer halo is obtained at maximum intensity. Then linear scanning is done at two other positions at $\theta = 30°$, [Fig.4.5(b)] and $\theta = -30°$, [Fig. 4.5(c)]. The difference between the two peaks positions are obtained from both the θ positions and it was found that diameter of the outer most halo (crescents) of the diffraction pattern are same in all the three cases.

Linear scanning is done at $\theta = 90°$ and the nature of the curve is shown in the Fig. 4.5 (d). A smooth line is obtained without any prominent peak position at the diameter of the outer halo. The O.D. at the maxima of the outer ring positions for the scanning at $\theta = 90°$ is corrected for fogging factor by subtracting a factor which is the optical density of the unexposed portion called the background O.D. After correction the O.D. value at maxima of the outer ring position (at $\theta = 90°$) is converted to intensity value I with the help of calibration curve described earlier.

The values of optical density obtained from the densitometeric circular scanning (scanned along the arc of main equatorial reflection) of the diffraction pattern are converted to X-ray intensity value with the help of the calibration curve. The converted intensity is then plotted against

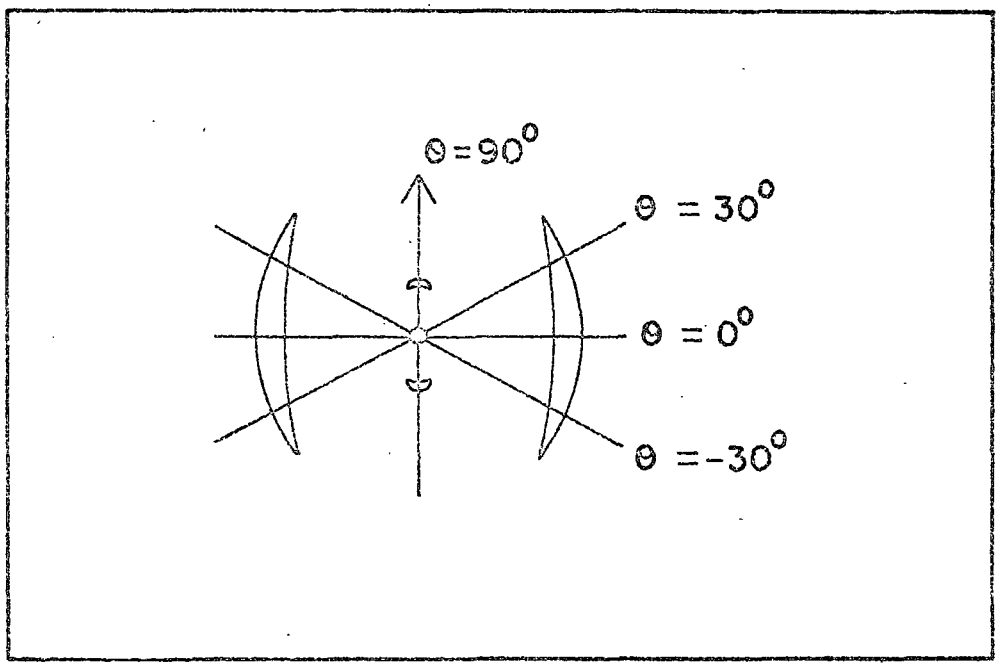

FIG. 4.4.

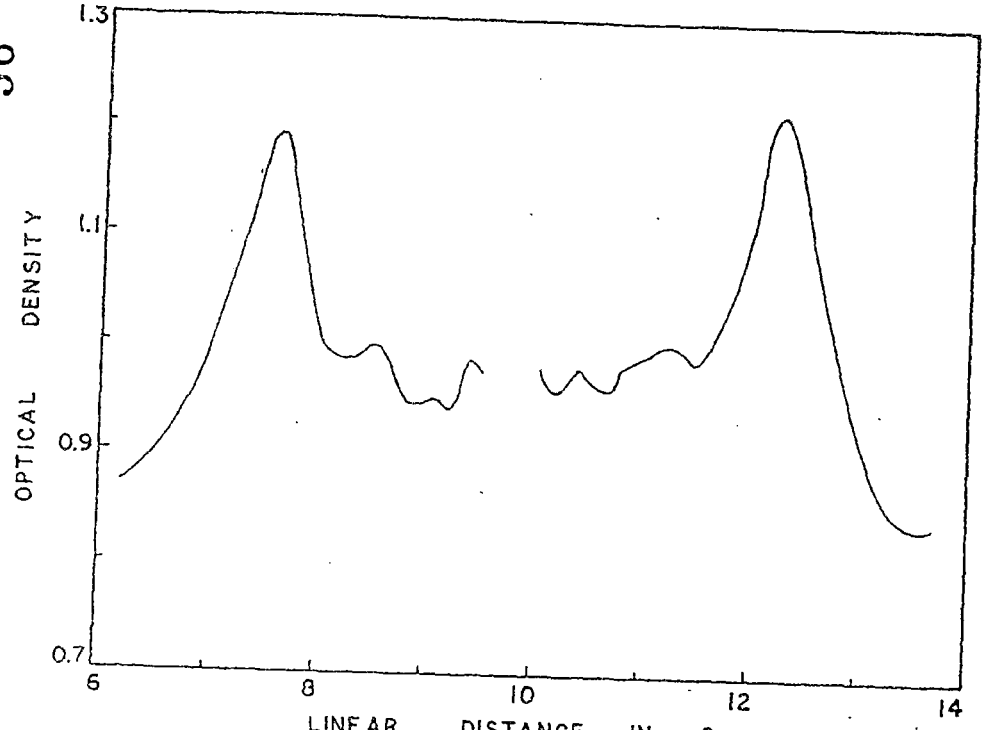

FIG. 4.5(a).

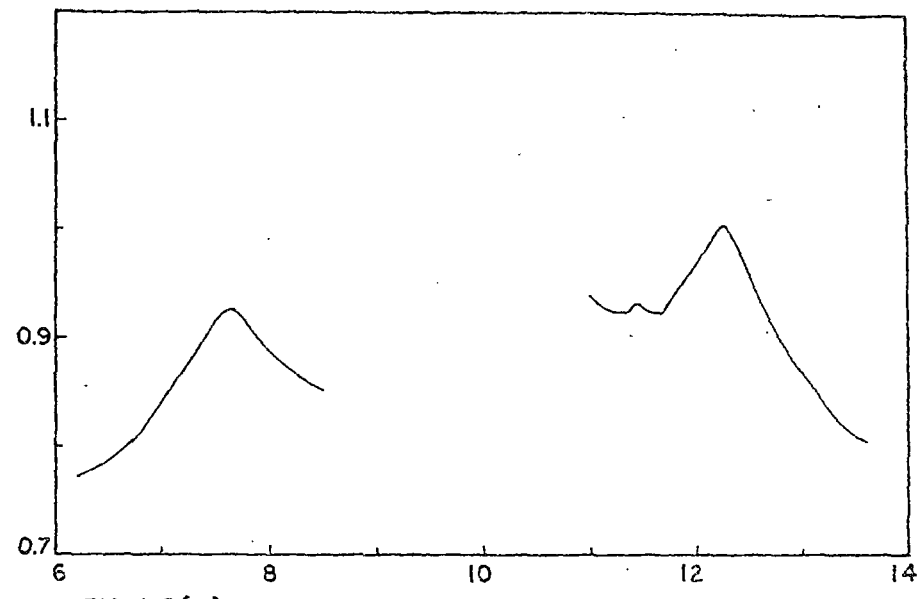

FIG. 4.5(c).

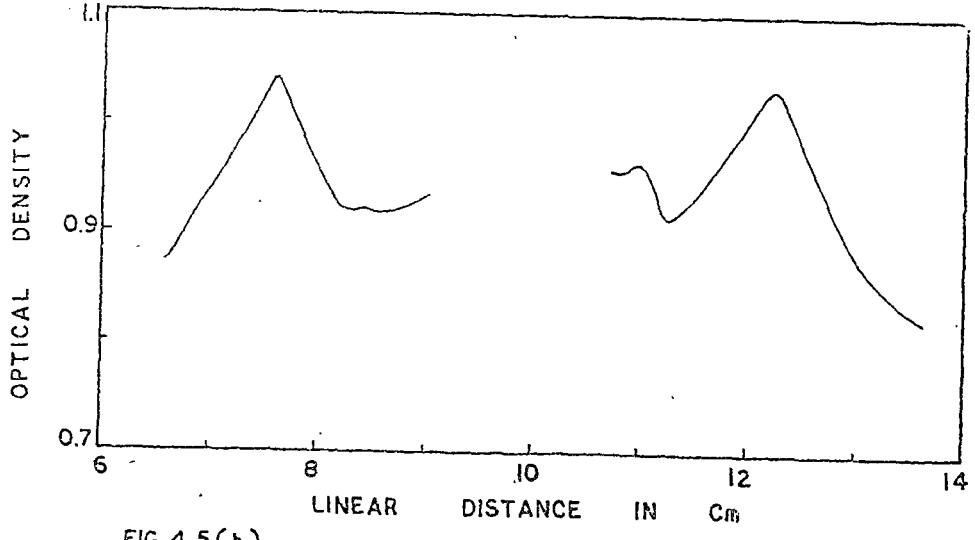

FIG. 4.5(b).

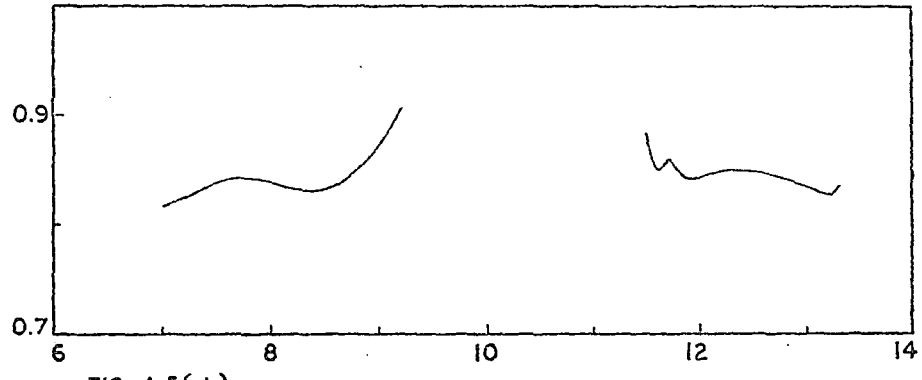

FIG. 4.5(d).

different angular positions θ.). The background intensity arising due to the thermal vibration of the molecule and air scattering is eliminated by subtracting the converted intensity value of the O.D. at the smooth curve obtained at $\theta = \frac{\pi}{2}$ position from the converted intensity values of the corrected optical density value of the angular scanning at the diametrical position of the outer halo.

The scanning of the photograph then gives the background intensity which is normally a tangent at $\theta = \frac{\pi}{2}$ i.e. minimum of the intensity distribution curve, [I (θ) versus θ curve] .

Leadbetter et al[2] also had similar intensity distribution with their X-ray diffraction photograph of the aligned sample.

The typical plot of I (θ) against θ is shown in the Fig. 4.6. Four equivalent sets of data from the four quadrants i.e. ($\theta = 0$ to 2π) are shown separately in fig. 4.6(a) and 4.6 (b) and the average I (θ) of these four quadrants is also plotted against θ as shown in fig. 4.6(c).

The dotted lines show the level of the background scattering intensity.

For our calculation the angular scanning for four quadrants (i.e. $\theta = 0$ to $\theta = \pi/2$) is required. We have obtained I (θ) vs θ distribution for all four quadrants separately and calculated order parameters for each of the four quadrants separately and then took the average.

We have at the same time calculated order parameter values by using the mean I (θ) values for the four quadrants.

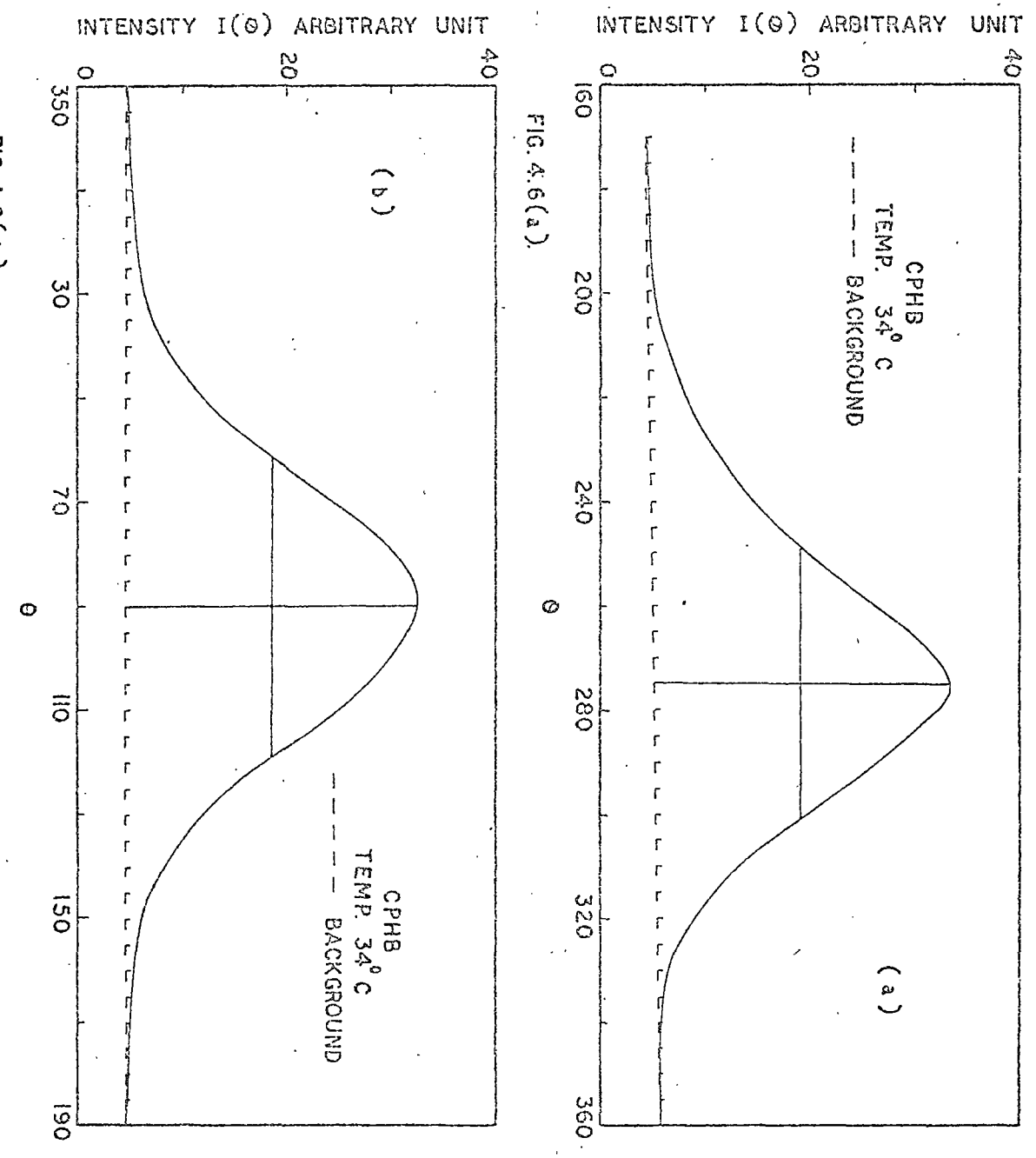

FIG. 4.6(a).

FIG. 4.6(b)

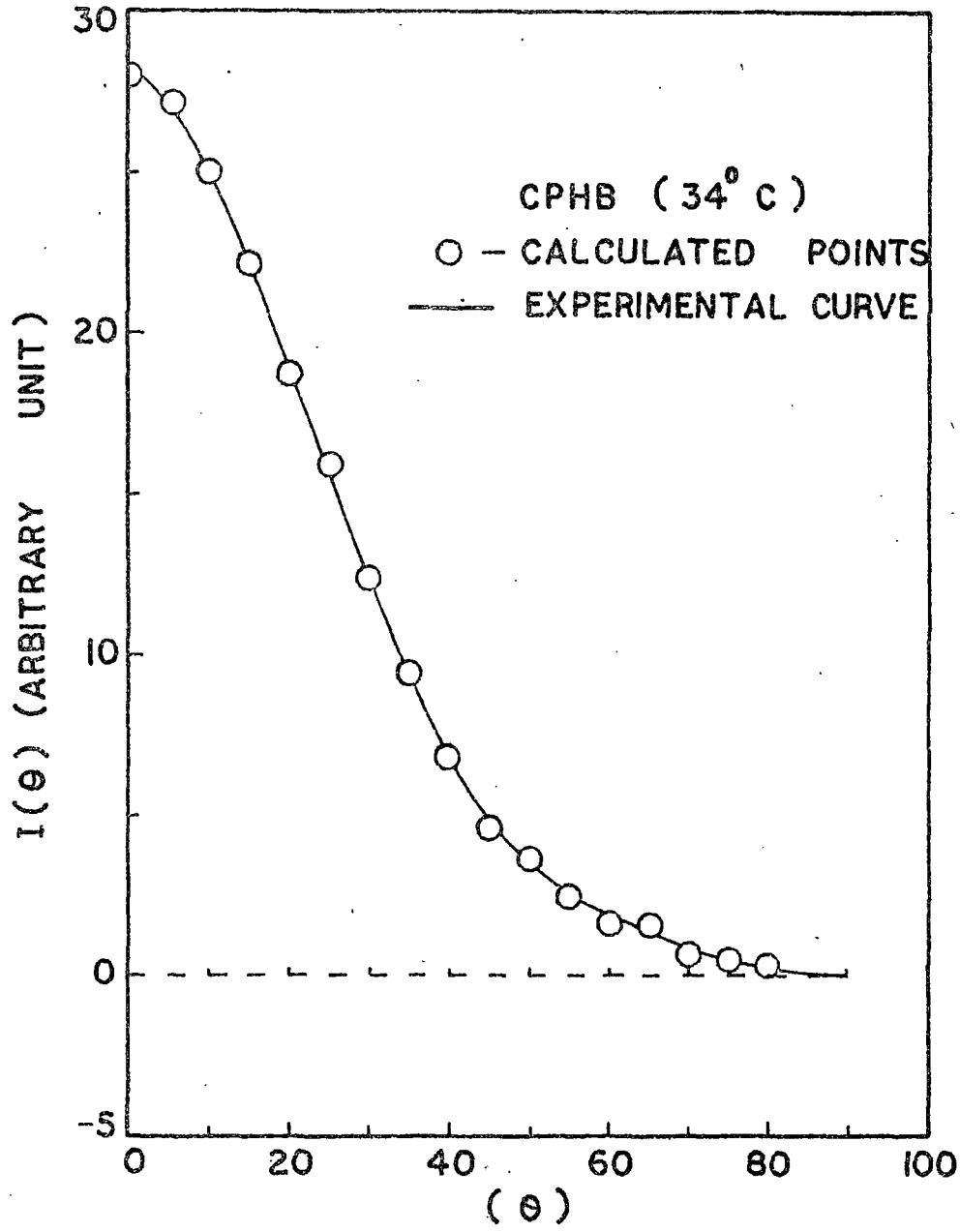
CPHB (34° C)
O – CALCULATED POINTS
EXPERIMENTAL CURVE
I(θ) (ARBITRARY UNIT)
30
20
10
0
-5
0
20
40
60
80
100
(θ)

FIG. 4.6(c).

The difference between the two methods gave nearly equal results for the order parameters, better than the experimental uncertainity. Therefore, we have calculated the distribution functions and order parameters (as described in chapt. 3) from only the mean I (θ) value of the four quadrants.

The calculated intensity values are shown in the fig. 4.6 (c) by points inside the circles (chap 3, eqn 4, eight terms).

Calculating $f(\beta)$ values from I (θ) values by a programme from the computer the $f(\beta)$ values are plotted against (β) at different temperatures [Fig. 4.7] . The programme used has been given at the end of this chapter.

The results were analysed (as described in chapt.3) to give $f(\beta)$ from which order parameters i.e. $\langle P_L \rangle$ values [$\langle P_2 \rangle$ & $\langle P_4 \rangle$] were calculated.

Uncertainity in O. D. value obtained from our densitometric scanning is .0025 which gives rise to the uncertainity in intensity value is 0.3.

Three different curves are obtained by plotting I (θ), (I+0.3) (θ) and (I - 0.3) (θ) against θ . $f(\beta)$ values were calculated from these three different intensity values (by the method described earlier) and $f(\beta)$ values were plotted against (β). The uncertainity in distribution function obtained in this way is only 1%.

The order parameters obtained from these three values are found to be accurate within 0.02.

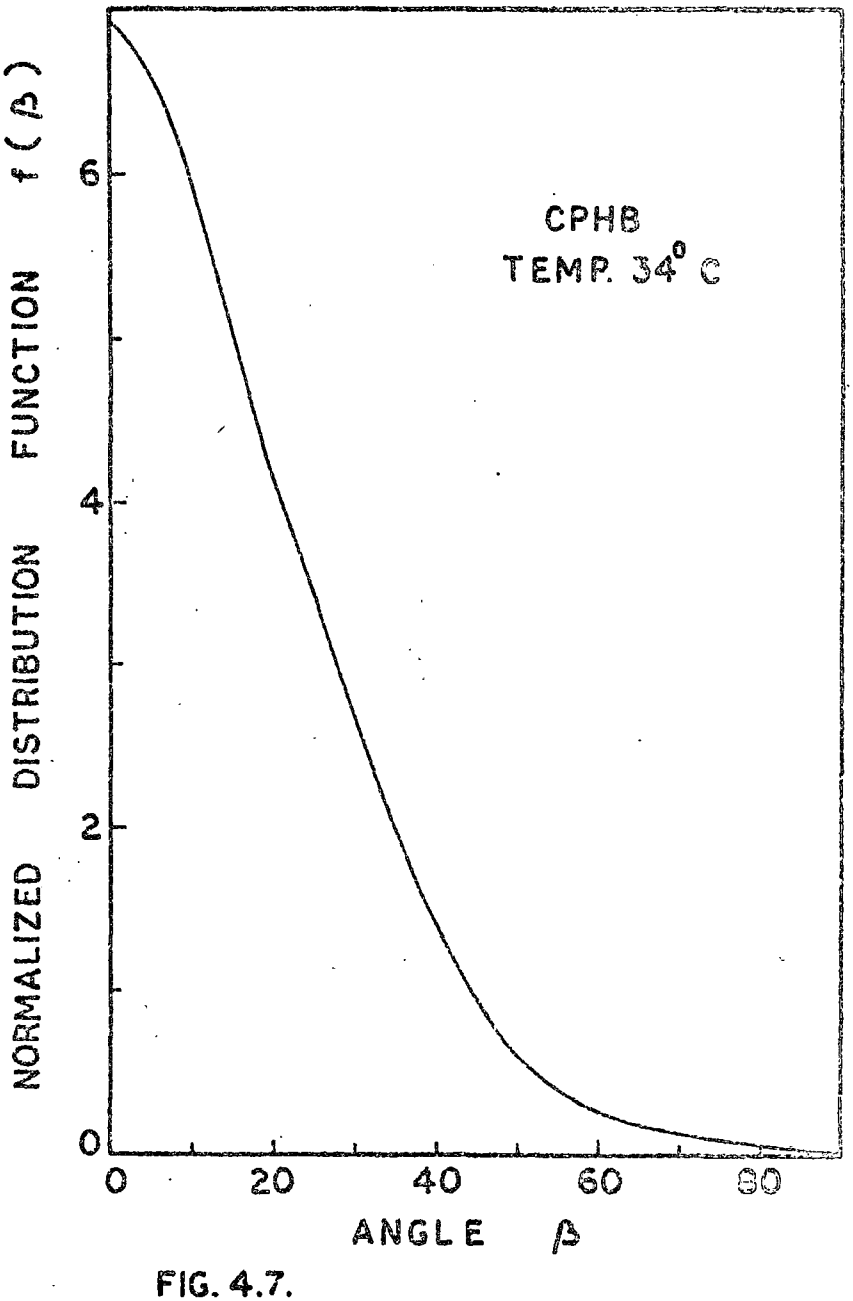
NORMALIZED DISTRIBUTION FUNCTION f(β)
CPHB
TEMP. 34° C
0
2
4
6
0
20
40
60
80
ANGLE β

FIG. 4.7.

REFERENCES

1. H. P. Klug and L.E. Alexander, - X-ray Diffraction Procedures. p. 308, John Wiley & Sons (1954).

2. A. J. Leadbetter and E. K. Norris, Mol. Phys. 38 669 (1979).

COMPUTER PROGRAMME

The calculations for the order parameters and distribution functions were done with a DCM (India) Spectrum 1 Microcomputer incorporated with a slightly different form of BASIC Language (HI-BASIC), and situated in the Research Service Centre, North Bengal University. The programmes are given below:

I. RAPAL01.BAS

```
1:        REM CALCULATION OF ORDER PARAMETERS
2:  1     INPUT"MORE JOB?"; Y$
3:        IF Y$="N" THEN STOP
4:        INPUT"IDENTIFICATION"; ID$
5:        INPUT"NO. OF POINTS";NP
6:        DIM IN(NP)
7:        NY=NP-1:JA=0
8:        CONSOLE
9:        FOR I = 0 TO NY
10:       PRINT IN(I):INPUT "INTEN VAL="; IN(I)
11:       NEXT I
12:2.01   INPUT"NO. OF VARIABLES";NV
13:       LPRINTER WIDTH 40
14:       IF JA > .5 THEN GOTO 2.11
15:       PRINT TAB(5); ID$
16:       PRINT "INTENSITY VALUES"
17:       FOR I=0 TO NY
18:       PRINT USING"-####.##   ";IN(I);
19:       NEXT I
20:2.11.  IF NV> NP THEN PRINT"TOO MANY VARIABLES"
          ELSE GOTO 2.02
21:       GOTO 2.01
22:2.02   CON=ATN(1)/9:NX=NV-1:NS=2*NX
23:       DIM C(NS),D(NS),B(NX),A(NX,NX),X(NX)
```

```
24:         I=1 TO NS
25:         D(I)=ϕ
26:         IF I LE NX THEN B(I) =ϕ
27:         NEXT I
28:         C(ϕ)=1:D(ϕ)=NP:B(ϕ)=ϕ
29:         FOR M=ϕ TO NY
3ϕ:         ANG=CON+M:CSQ=COS(ANG):CSQ=CSQ+CSQ
31:         B(ϕ)=B(ϕ)+EN(M)
32:         FOR K = 1 TO NS
33:         C(K)=C(K-1)+CSQ
34:         D(K)=D(K)+C(K)
35:         IF K LE NX THEN B(K)=B(K)+C(K)+IN(M)
36:         NEXT, K,M
37:         FOR I =ϕ TO NX
38:         FOR J = ϕ TO NX
39:         A(I,J)= D(I+J)
4ϕ:         NEXT J,I
41:         FOR NL=NX TO 1.ϕ STEP -1.ϕ
42:1.ϕ4     TERM=A(ϕ,NL):IMAX=ϕ
43:         FOR I=1 TO NL
44:         IF A(I,NL) < TERM THEN 1.ϕ5
45:         TERM=A(I,NL):IMAX=I
46:1.ϕ5     NEXT I
47:         FOR K=ϕ TO NL
48:         P=A(IMAX,K):A(IMAX,K)=A(NL,K):A(NL,K)=P
49:         NEXT K
5ϕ:         P=B(IMAX):B(IMAX)=B(NL):B(NL)=P:NK=NL-1
51:         FOR I=ϕ TO NK
52:         FT=A(I,NL)/TERM
53:         FOR J=ϕ TO NK
54:         A(I,J)=A(I,J)-A(NL,J)*FT
59:         NEXT J
```

```
56:       B(I)=B(I)-B(NL)*PT
57:       NEXT I,NL
58:       X(ϕ)=B(ϕ)/A(ϕ,ϕ)
59:       PRINT TAB(5);"COEFFICIENT";PRINT"X ϕ=";X(ϕ)
6ϕ:       FOR I = 1 TO NX
61:       SUM = ϕ
62:       FOR J=ϕ TO (I-1)
63:       SUM=A(I,J)*X(J)+SUM
64:       NEXT J
65:       X(I)=(B(I)-SUM)/A(I,J)
66:       PRINT"X";I;"=";X(I):NEXT I
67:       PRINT
68:       IF JA>ϕ THEN 1.ϕ7
69:       PL$="VAINSHTEIN"
7ϕ:       FOR IK=ϕ TO 1
71:       GOSUB 3.ϕ1
72:        GOSUB 4.ϕ1
73:       IF IK>.5 THEN 1.ϕ6
74:       GOSUB 5.ϕ1
75:       PL$="LEADBETTER"
76:       NEXT IK
77:1.ϕ6   JA=1:GOTO 2.ϕ1
78:1.ϕ7   IK=2
79:       GOSUB 4.ϕ1
8ϕ:1.ϕ9   GOSUB 6.ϕ1
81:       GOSUB 7.ϕ1
82:       INPUT "CONVERGENCE?"; X$
83:       IF X$="Y" THEN 2.ϕ1
84:         PRINT:PRINT:PRINT:GOTO 1
85:3.ϕ1   DIM  SI(2)
86:       FOR I=ϕ TO 2
87:       SI(I)=ϕ
88:       NEXT I
89:       FOR I=ϕ TO 2
9ϕ:       FOR M=ϕ TO NX
```

```
91:      SI(I)=X(M)/(2+(M+I)+1)+SI(I)
92:      NEXT M,I
93:      PRINT:PRINT"INTEGRALS":PRINT SI(ϕ),SI(1),SI(2)
94:      P2=1.5+SI(1)/SI(ϕ)-.5
95:      P4=((35+SI(2))/SI(ϕ)-(3ϕ+SI(1)/SI(ϕ))+3)/8
96:      PRINT PL3;" ORDER PARAMETERS"
97:      PRINT"P2=";P2;" P4= ";P4
98:      RETURN
99:4:ϕ1  DIM Z(NY)
1ϕϕ:     IF IK < .5 THEN PRINT"CALCULATED INTENSITY VALUES":
         GOTO 4.11
1ϕ1:     PRINT "DISTRIBUTION FUNCTION VALUES"
1ϕ2:4:11 FOR M=ϕ TO NY
1ϕ3:      ANG=CON+M:CSQ=COS↑2(ANG):CSQ=CSQ+CSQ
1ϕ4:     SUM=ϕ
1ϕ5:     FOR J=MX TO 1.ϕ STEP -1.ϕ
1ϕ6:     SUM=(SUM+X(J))+CSQ
1ϕ7:     NEXT J
1ϕ8:     Z(M)=SUM+X(ϕ)
1ϕ9:     NEXT M
11ϕ:     IF IK < 1.5 THEN 4.ϕ2
111:     FOR M=ϕ TO NY
112:     Z(M)=EXP(Z(M))
113:     NEXT M:GOTO 4.ϕ3
114:4.ϕ2 IF IK < .5 THEN 4.ϕ3
115:     FOR M=ϕ TO NY
116:     Z(M)=Z(M)/SI(ϕ)
117:     NEXT M
118:4.ϕ3 FOR M=ϕ TO NY
119:      PRINT USING"-###.### ";Z(M);
12ϕ:     NEXT M:PRINT
121:     IF IK NE 1 THEN ϕ.ϕ4.
122:     FOR M=ϕ TO NY
123:     IF Z(M) < ϕ THEN 4.ϕ5
124:     IN(M)=LOG (Z(M))
125:     NEXT M
```

```
126:4.Ø4  RETURN
127:4.Ø5  NP=M:NY=NP-1:GOTO 1.06
128:5.Ø1  PRO=1:PRINT:PRINT"COEFFICIENT" PRINT"X 0 =";X(Ø)
129:      FOR M=1 TO NX
13Ø:      PRO=PRO*(M+.5)/M
131:      X(M)=PRO*X(M):PRINT X(M)
132:      NEXT M
133:      RETURN:STOP
134:6.Ø1  DIM T(NX,NX)
135:      T(Ø,Ø)=1
136:      FOR I=1 TO NX
137:      T(I,Ø)=-T(I-1,Ø)*(I-.5)/I
138:      NEXT I
139:      FOR I=1 TO NX
14Ø:      FOR J=1 TO I
141:      T(I,J)=T(I,J-1)*(1+J-.5)*(J-I-1))/(J*J-.5*J)
142:      NEXT J,I.
143:      RETURN
144:7.Ø1  DIM Y(NX)
145:      Y(NX)=X(NX)/T(NX,NX).
146:      FOR J=(NX-1) TO Ø.Ø STEP -1.Ø
147:      SUM =Ø
148:      FOR I=(J+1) TO NX
149:      SUM=SUM+T(I,J)*Y(I)
15Ø:      NEXT I
151:      Y(J)=(X(J)-SUM)/T(J,I)
152:      NEXT J
153:      PRINT:PRINT "COEFFS OF LEGENDRE POLYNOMIALS"
154:      FOR I =Ø TO NX
155:      PRINT"Y";I;"=";Y(I)
156:      NEXT I
157:      RETURN
```

II. R:PALO6.BAS

```
1:        REM CALCULATION FOR NORMALISED DISTRIBUTION FUNCTION
2:1.ϕ1    INPUT "MORE JOB?"Y$
3:        IF Y$="N" THEN STOP
4:        INPUT "IDENTIFICATION"; ID$
5:        INPUT  "NO OF TERMS";NP
6:        NX=NP-1
7:        DIM A (NX), B(NX), FUN (18)
8:        FOR I=ϕ TO NX
9:        INPUT "A(I) =";A(I)
1ϕ:       NEXT I
11:       LPRINTER WIDTH 4ϕ
12:       PRINT TAB(5);ID$
13:       CON=ATN(1)/9
14:       GO SUB 6.ϕ1
15:       FOR NY =ϕ TO NX
16:       SUM =ϕ
17:       FOR I=NY TO NX
18:       SUM=SUM+A(I)+I(I,NY)
19:       NEXT I
2ϕ:       B(NY)=SUM
21:       NEXT NY
22:       FOR N=ϕ TO 18
23:       ANG=CON+N:CSQ:COS(ANG):CSQ:CSQ+CSQ
24:       SUM=B(NX)
25:       FOR N=(NX-1) TO ϕ.ϕ STEP -1.ϕ
26:       SUM=SUM+CSQ+B(N)
27:       NEXT N
28:       FUN(N)=EXP(SUM)
29:       NEXT N
3ϕ:       DIM W(6)
31:       W(ϕ)=1:W(1)=5:W(2)=1:W(3)=6:W(4)=1:W(5)=5:W(6)=1
32:       PRINT "NO OF TERMS =  ";NP
33:       PRINT "COEFFS"
34:       FOR I=ϕ TO NX
35:       PRINT "X";I;"=";A(I)
36:       NEXT I
37:       extnt PRINT
```

```
38:         PRINT "DISTRIBUTION FUNCTION VALUES"
39:         FOR M=Φ 18
4Φ:         PRINT USING "-###.### "; FUN(M);
41:         NEXT M
42:         PRINT
43:         SUM=Φ
44:         FOR M=Φ TO   2
45:         FOR N=Φ TO 6
46:         PA=6+M+N
47:         SUM=SUM+W(N) +FUN(PA)+SIN(PA+CON)
48:         NEXT N,M
49:         SUM=SUM+Φ.3+CON:SUM=1/SUM
5Φ:         PRINT "NORMALISING CONSTANT= ";
51:         PRINT "NORMALISED DISTRIBUTION FUNCTION"
52:         FOR M=Φ TO 18
53:         FUN(M)=SUM+FUN(M)
54:         PRINT USING "-###.### ";FUN(M);
55:         NEXT M
56:         PRINT:PRINT:PRINT
57:         GO TO 1.Φ1
58:6.Φ1     DIM T(NX,NX)
59:         T(Φ,Φ)=1
6Φ:         FOR I=1 TO NX
61:         T(I,Φ)=-T(I-1,Φ)+(I-Φ.5)/I
62:         NEXT I
63:         FOR I=1 TO NX
64:         FOR J=1 TO 1
65:         T(I,J)=T(I,J-1)+(I+J-.5)+(J-I-1)  /(J+J-.5+J)
66:         NEXT J,I
67:         RETURN.
```

CHAPTER 5.

X-RAY DIFFRACTION STUDIES ON UNORIENTED MESOPHASES OF (-)-2-METHYLBUTYL-p-n(p-METHOXY BENZYLIDENE) AMINO) CINNAMATE (MBAC IN SHORT).

CHAPTER 5.

X-RAY DIFFRACTION STUDIES ON UNORIENTED MESOPHASES OF (-)-2-METHYLBUTYL-p-n-(n-METHOXY BENZYLIDENE) AMINO) CINNAMATE (MBAC IN SHORT).

1. Introduction

X-ray diffraction studies of MBAC at different temperatures have been performed by us. Liao et al[1] have studied Brillouin scattering for this sample. They have attributed a smectic A and Smectic B modification of the substances. Steady flow-viscosity data have been given for this by Friedman et al[2]. Gray[3] has given the transition temperatures of (-)-2-methyl butyl p-(n-methoxy benzylidene)-amino) α cinnamate along with the transition temperatures of other n-alkoxy homologues. The transition temperatures from solid to smectic, smectic to cholesteric and cholesteric to isotropic as given by them are 53°C, 78°C and 98°C respectively. Leclercq et al[4] have also studied the phase transitions of this compound. The existence of two smectic phases has also been observed by them. Till now, no X-ray diffraction data have been published for this substance. We have identified the various mesomorphic phases of MBAC by microscopic, calorimetric and X-ray diffraction studies. The molecular structure of the substance is given in chapter 2.

According to the literature[5] the sample MBAC has the following mesomorphic range -

Solid $\xrightarrow{53^\circ C}$ Smectic $\xrightarrow{78^\circ C}$ Cholesteric $\xrightarrow{97^\circ C}$ Isotropic

On the basis of our X-ray and microscopic studies it is found to have the following ~~crystallization~~ transition path

$$\text{Solid} \underset{\sim 16^{\circ}C}{\overset{53^{\circ}C}{\rightleftharpoons}} S_B\,(Sm\,II) \underset{}{\overset{59^{\circ}C}{\rightleftharpoons}} S_A\,(Sm\,I) \underset{}{\overset{78^{\circ}C}{\rightleftharpoons}} Ch \underset{}{\overset{97^{\circ}C}{\rightleftharpoons}} I$$

2. Experimental methods:-

Details of experimental procedure including X-ray technique and polarising microscopy has been described in chapter 2 Flat plate photographs of unoriented sample have been taken at different temperatures in the set up no.1 of chapt. 2. (Fig.2.1).

The sample was then allowed to get oriented in presence of magnetic field of 5.81 K.Gauss. But unfortunately we could not get the monodomain sample. This may be due to the presence of cholesteric phase, because, cholesteric phase requires magnetic field of much higher strength for orientation.

3. Experimental results and discussions:-

The melting behaviour of the sample was examined by polarising microscope as described in chapt. 2. The sample melts at 53°C. During heating we could not observe a phase change at 59°C on our first attempt. About 59°C we got focal conic texture characteristic of S_A[6,7] phase, below 59° we could not identify the x texture which looked somewhat like broken focal conic type. Our microscopic observation missed the B phase while heating. We started with a fresh sample. A phase change was observed at 59°C while heating, but the texture characteristic of S_B phase could never be detected. At

78°C the change of colour having fan shaped texture with focal conics[6] of cholesteric phase was observed. The isotropic phase was found at 97°C. During cooling focal conic textures of cholesteric phase with several colours were observed. Below 87°C textures of S_A both the focal conic[6a, 7] and fan type[6b,7] were observed very distinctly. We had not been successful with our conoscopic measurement, so we cannot say definitely whether the phase is uniaxial or biaxial, but from our texture studies we identify this phase to be S_A. From 58°C to room temperatures 22°C the sample showed mosaic and fan textures of S_B[6c,7,8] phase. The sample in the cover slips was then kept in ice for a few hours and the texture observed was found to be that of solid phase. Heating and cooling runs did not yield identical results indicating that super cooling was present.

The X-ray diffraction photographs of the sample were taken at different temperatures, starting from the solid phase at room temperatures to isotropic phase. The melting point is found to be 53°C. Below 53°C we got powder patterns of polycrystalline sample. Photographs below 78°C showed that the sample was in the smectic phase and above 78°C cholesteric phase was observed. The compound changed to isotropic liquid at 98 97°C. X-ray photographs showed the existence of two smectic phases, SmII and SmI. Photographs of SmII phase showed one sharp outer ring and are sharp inner ring (and its ~~second order one~~) characteristic of the SmB phase. The Sm II phase is therefore a B phase, which was confirmed by our

polarising microscopic study also. Photographs of SmI phase showed one sharp inner ring and one diffuse outer ring. The phase may be S_A or S_G phase. The substance was then cooled down to room temperature, it was found to be very sticky. A diffraction photograph was taken at room temperature. The pattern obtained in this photograph was interesting. We no longer got a powder photograph but a pattern of one sharp inner ring and a sharp outer ring as shown in fig. 5.1. This phase is same as the SmII phase that is S_B phase. Another series of photographs of the sample in the same capillary was taken while heating as well as while cooling. We never got a powder photograph below 53°C while cooling, even at room temperature. The process was repeated with fresh sample. In each and every case it was found that once the sample is heated above 53°C the solid phase could not be observed at room temperature again. If it is not heated we get photographs of polycrystelline sample. Confirmation of the fact that there was no change in chemical composition was performed by taking the infra-red spectra of the sample (first with the original sample at room temperature and then with the sample which was cooled down to room temperature after heating upto 53°C). DSC (differential Scanning Calorimetry) was done for the sample and phase changes were observed approximately at 98°C, 80°C and 59°C. Existence of supercooled state of MBAC below 47°C was reported by Liao et al[1]. As we do not have any arrangement for taking X-ray diffraction photographs below room temperature, the sample holder with the sample was kept vertically in a thermoflask containing fm ice and the temperature was observed. At about

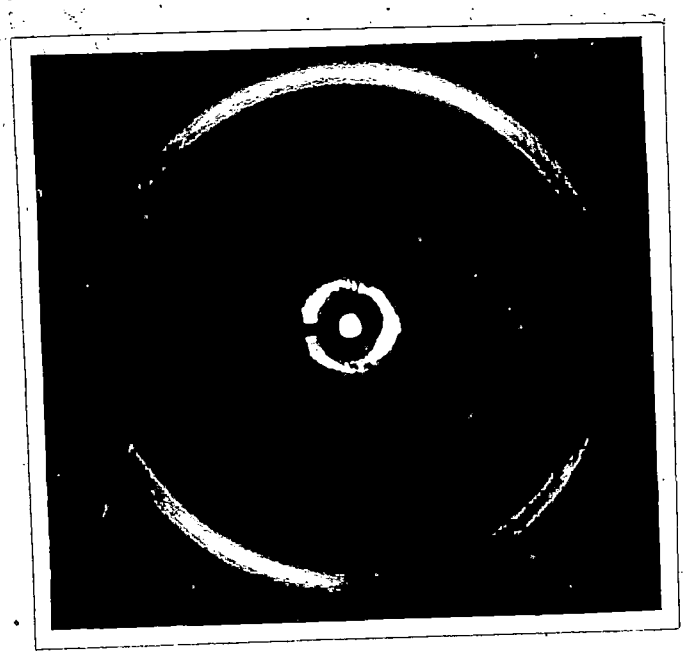

Fig. 5.1. X-ray diffraction photograph of S_B phase 'MBAC' at room temperature 25°C (during cooling).

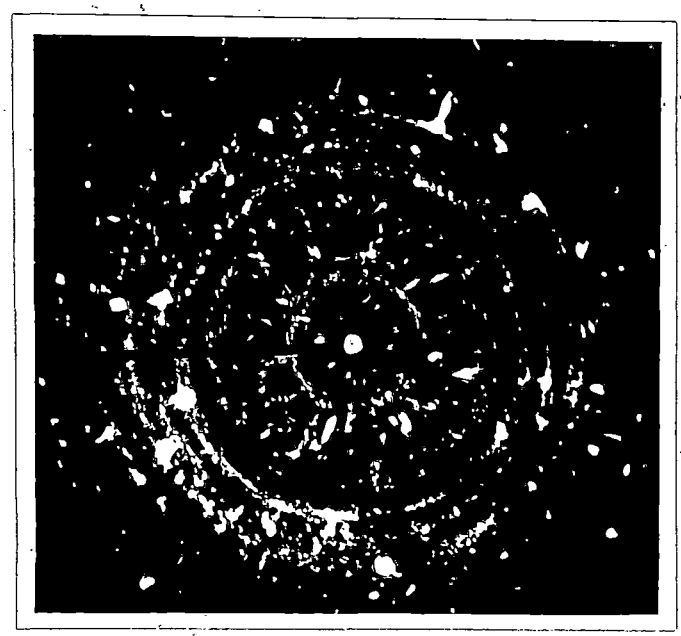

Fig. 5.2. X-ray diffraction photograph of the solid phase of MBAC at room temperature 25°C.

16°C there was a marked change in the appearance of the substance. The substance changed its phase at this temperature. An X-ray diffraction photograph was then taken at room temperature (22°C) and we got a solid phase photograph as shown in fig.5.2. We repeated the whole process with fresh sample and X-ray diffraction photographs were taken while cooling. Photograph at 45°C, 52°C, 55°C and 60°C taken while heating are shown in fig. 5.3, 5.4, 5.5 and 5.6 respectively.

Photographs of 55°C and 60°C taken while cooling are exactly the same as while heating. But patterns at 45°C and 52°C are just like the photographs shown in fig. 5.1 i.e. the photograph of S_B phase.

All the photographs were scanned linearly by the method described in chapt. 4. As all the photographs are of unoriented sample, angular scanning is not necessary. Optical densities (O.D.) corresponding to linear scale reading in cm.(L) are shown in the tables (Table 5.1 - 5.18).

Typical plots of O.D. versus L of S_B and S_A and cholesteric phases are shown in the fig. 5.7, 5.8 and 5.9 respectively. Average distance between the neighbouring molecules (D) and apparent molecular length in cholesteric phase and layer thickness in the smectic phase (ℓ) are calculated by using the equation 3.1 (with K = 1.117 and 1 respectively as described in chapt. 3).

The results are given in the Table 5.19.

The variation of D and 'ℓ' with temperatures are given in fig. 5.10 and 5.11 respectively. These are the values

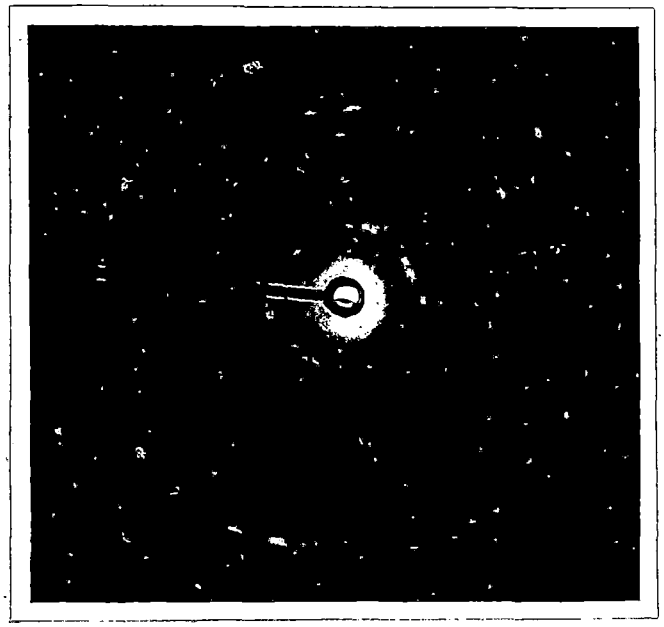

Fig. 5.3. X-ray diffraction photograph at MBAC at 45°C during heating.

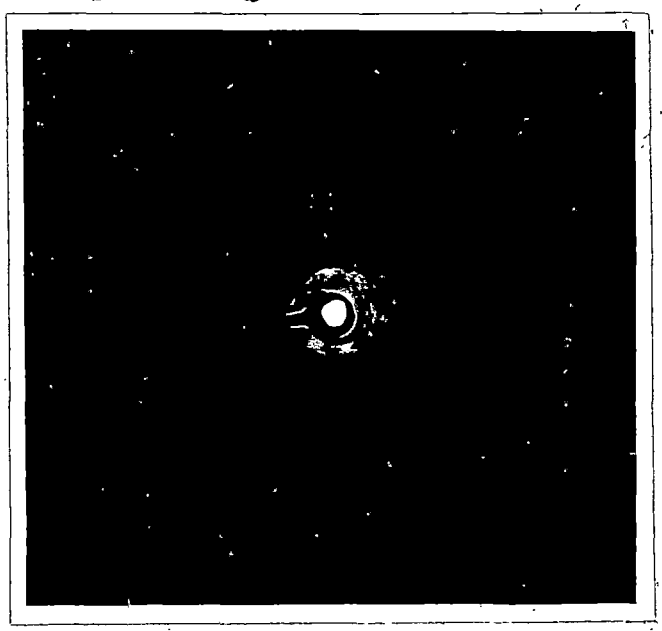

Fig. 5.4. X-ray diffraction photograph of MBAC just before transition from solid phase at 52°C (during heating).

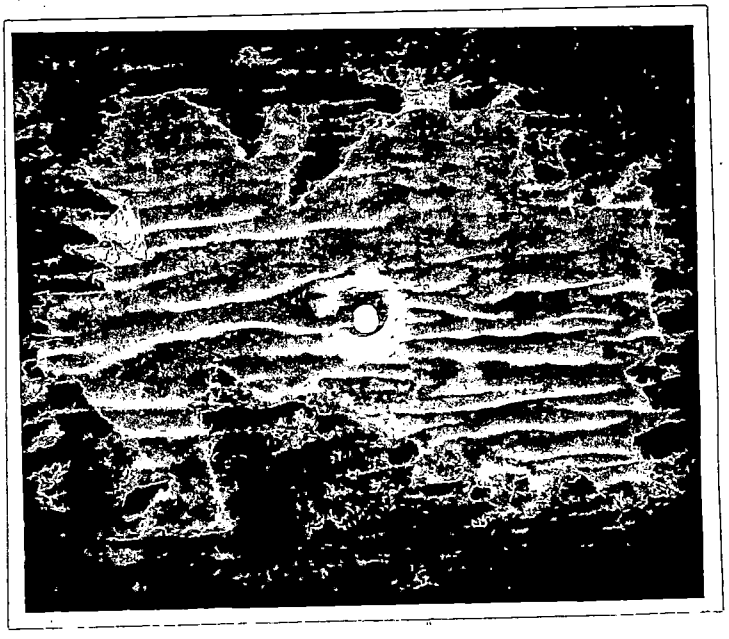

Fig. 5.5. X-ray diffraction photograph of S_B phase of MBAC at 55°C (during heating).

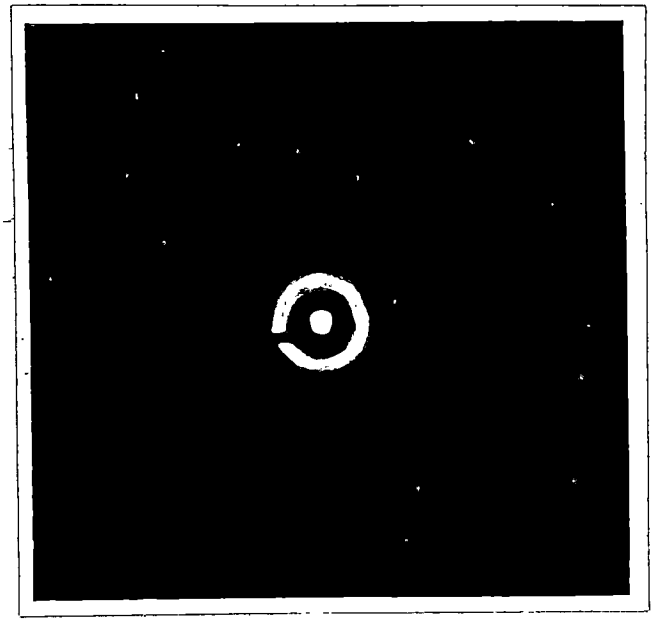

Fig. 5.6. X-ray diffraction photograph of S_A phase of MBAC at 60°C (during heating).

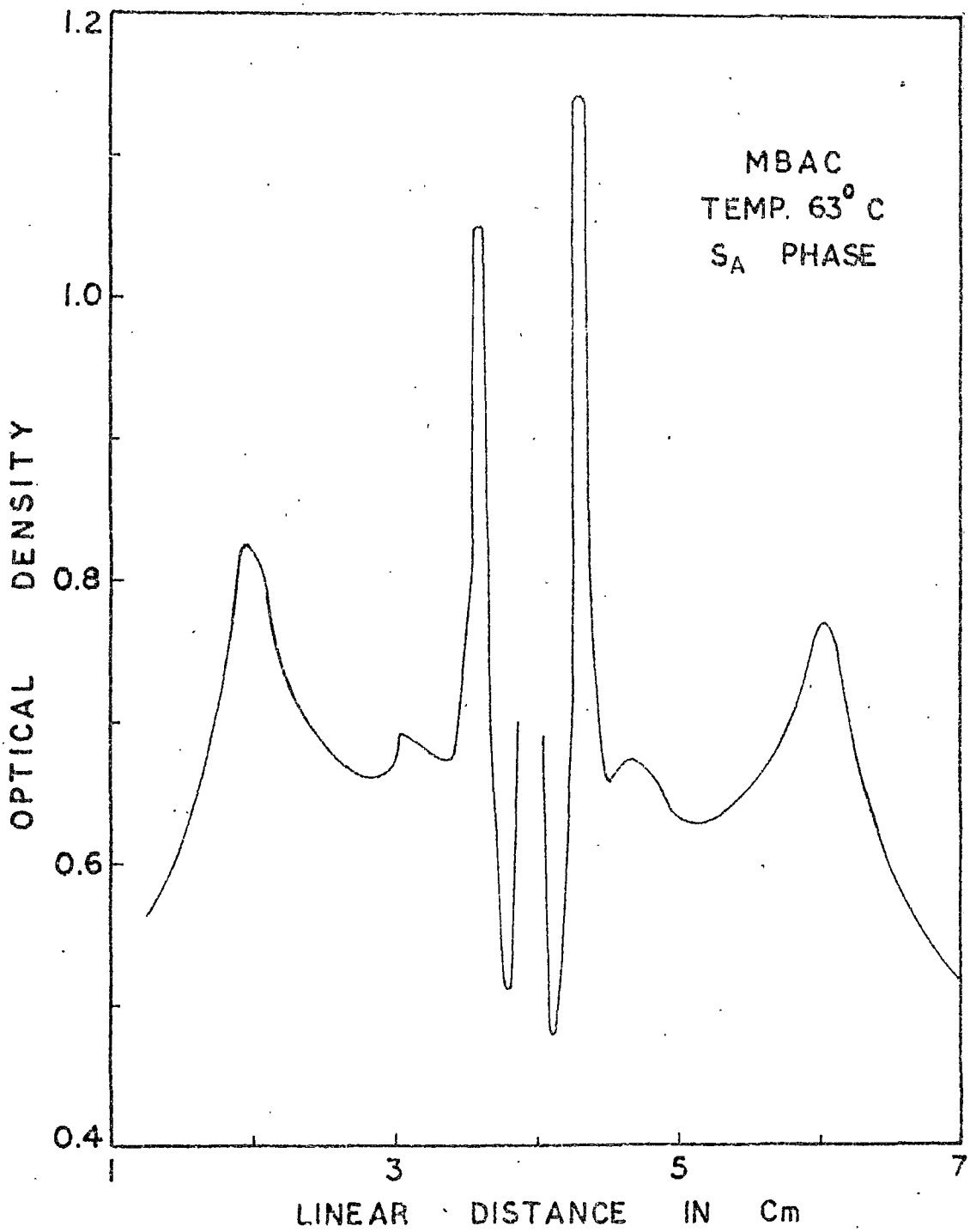
MBAC
TEMP. 63° C
S_A PHASE
OPTICAL DENSITY
1.2
1.0
0.8
0.6
0.4
1
3
5
7
LINEAR DISTANCE IN Cm

FIG. 5.7.

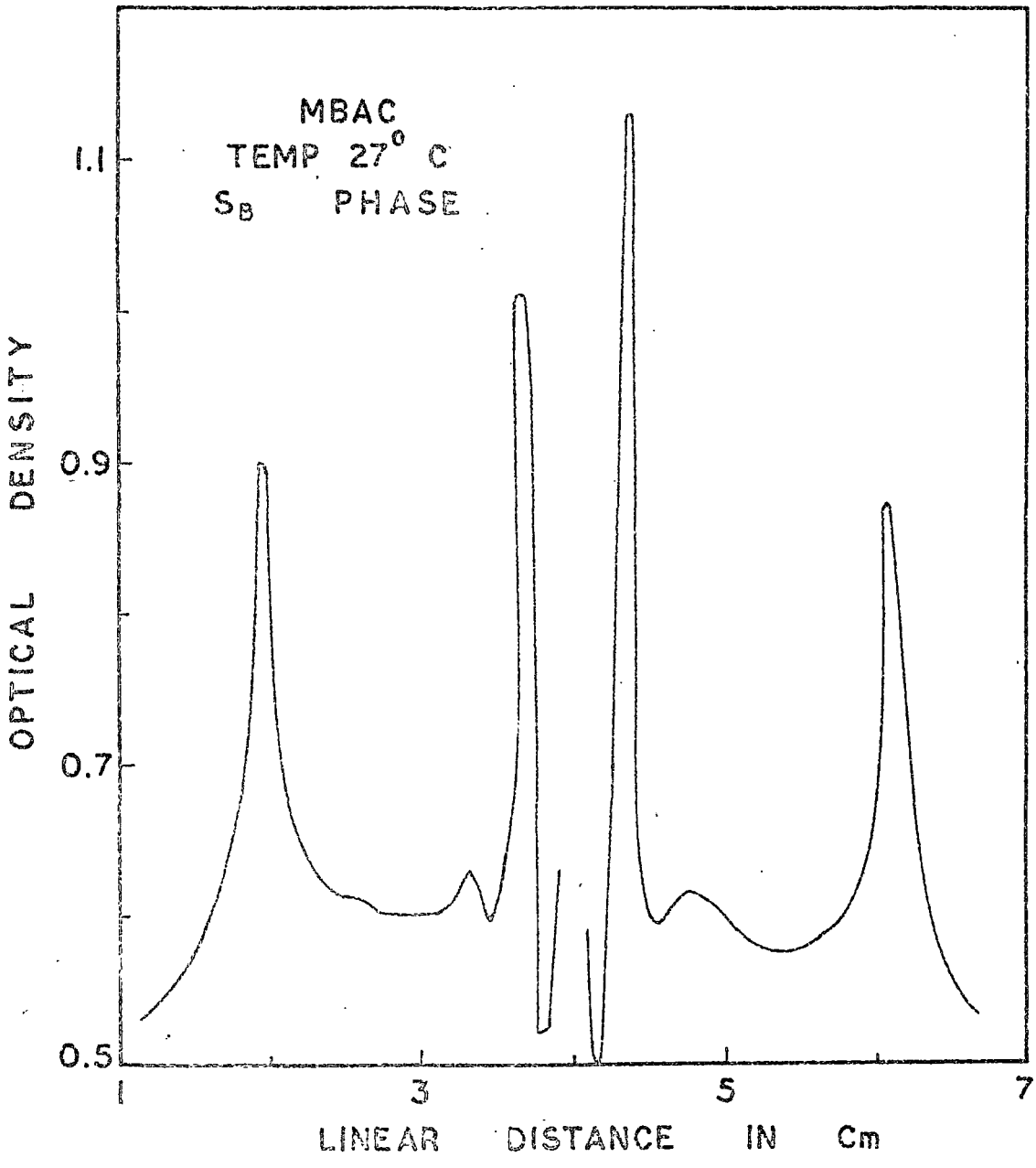
MBAC
TEMP 27° C
S_B PHASE
OPTICAL DENSITY
1.1
0.9
0.7
0.5
3
5
7
LINEAR DISTANCE IN Cm

FIG. 5.8.

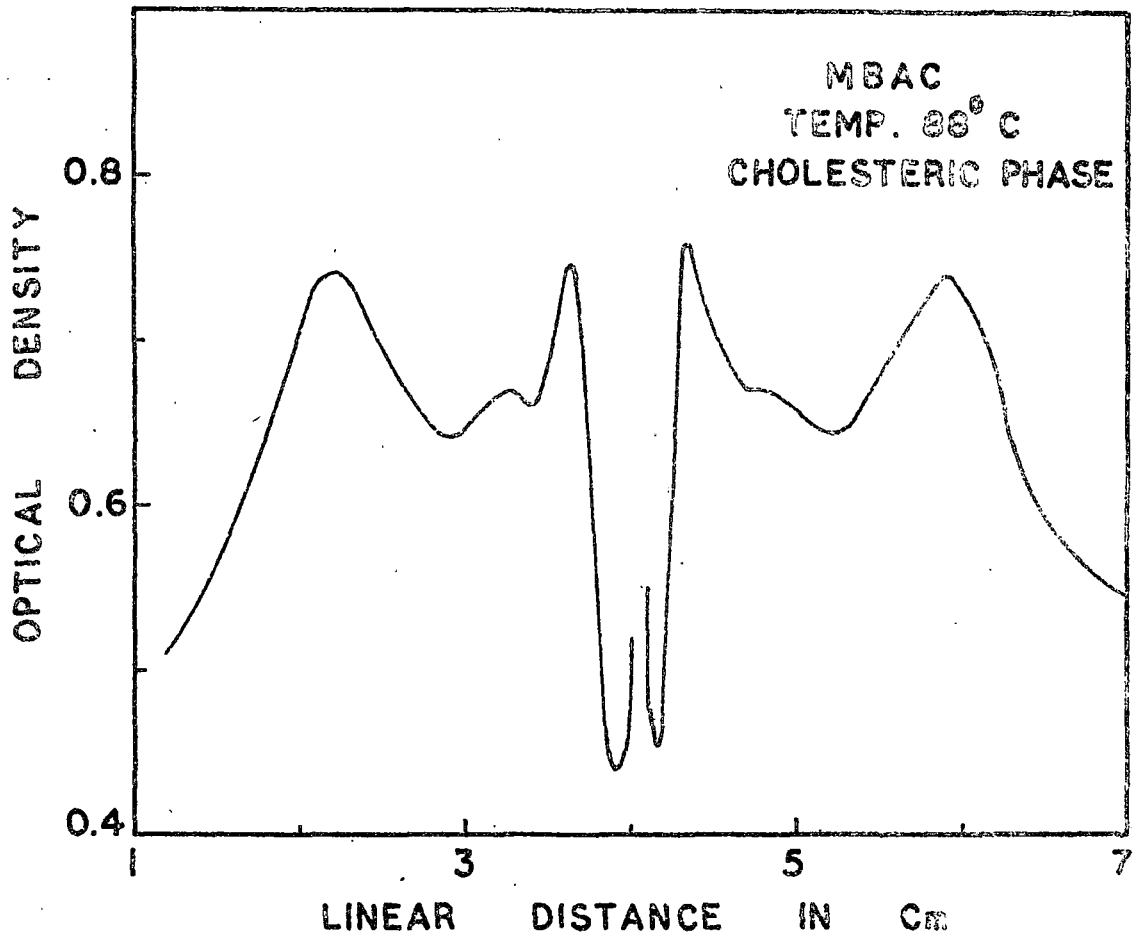
MBAC
TEMP. 88° C
CHOLESTERIC PHASE
OPTICAL DENSITY
0.8
0.6
0.4
1
3
5
7
LINEAR DISTANCE IN Cm.

FIG. 5.9.

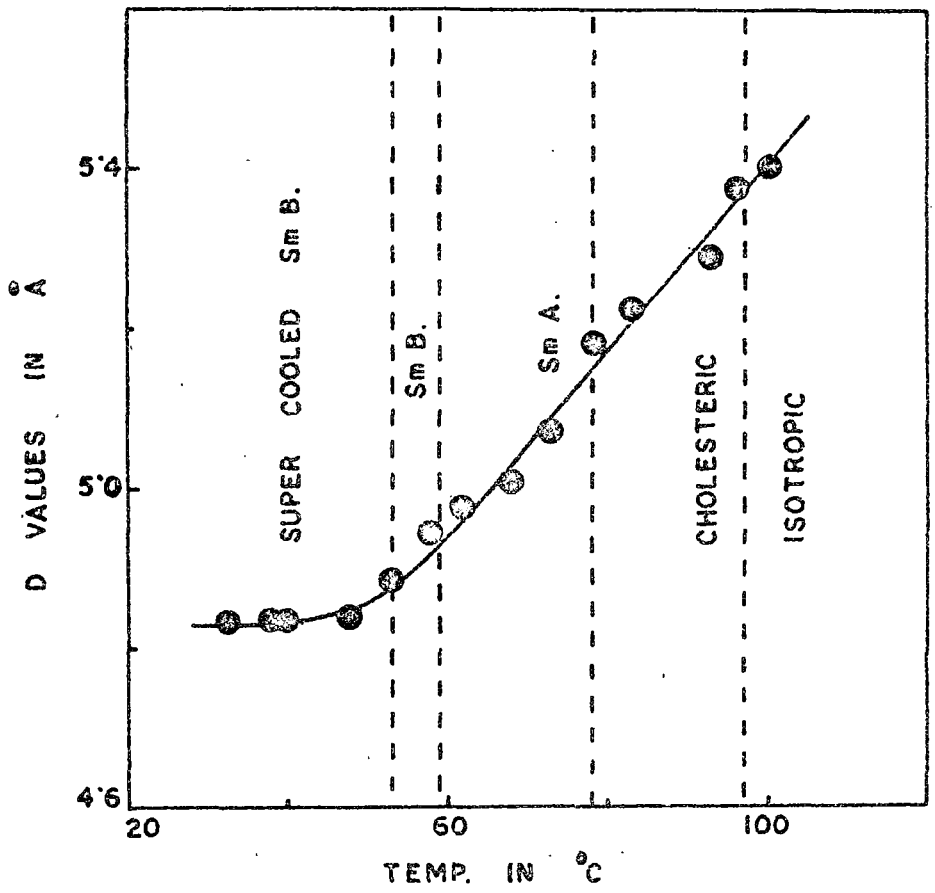

FIG. 5.10.

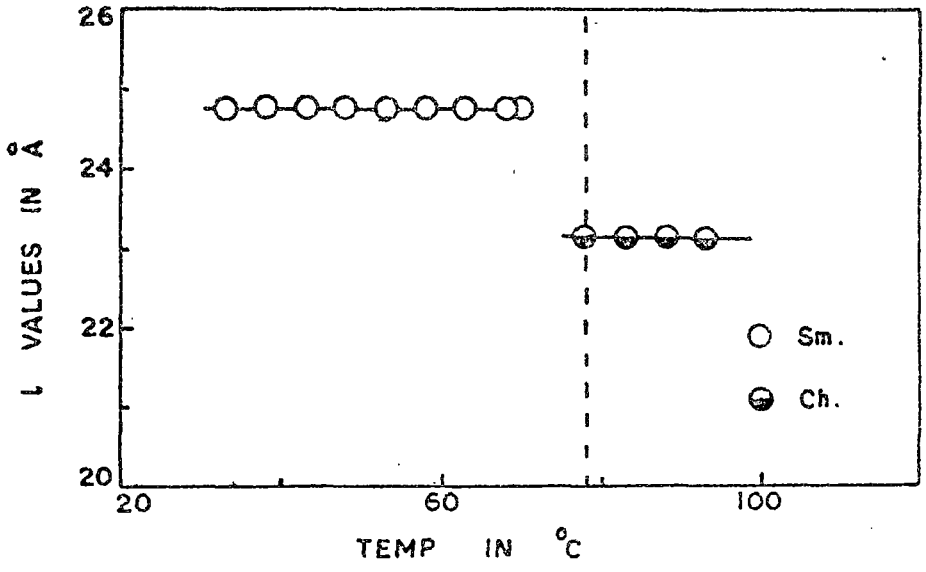

FIG. 5.11.

calculated from the photographs taken while cooling. Variation of D and ℓ with temperature in different Sm phases has been discussed by de Vries[9]. In our case it is found that D increases with temperatures except in the supercooled region, where it remains fairly constant. ℓ values remain the same in the smectic region, but there is a sharp decrease in the cholesteric region as shown in fig. 5.11. With the help of the stereomodel units (W.Bochi glass aparate febrik 920 Flawil), we have constructed the possible structure of MBAC and measured the molecular length L in its completely extended form which is 23.14 Å. In the Smectic range the ~~molecular~~ layer thickness is found to be 24.78 Å, which is little larger than L. Leadbetter et al[10] in their study of the structure of smectic phase of some compounds found L to be much smaller than ℓ . They expleined it to be due to some form of bilayered structure. In our case difference of ℓ and L is not so large and in our opinion this may be due to the staggered parallel orientations of the molecules in the layers. This staggering is due to the hindrance caused by branching of hydrocarbon chains.

Thus microscopy and X-ray studies confirmed that the sample MBAC has S_B phase, S_A phase and cholesteric phase. The result is in very good agreement with the observation of Liao et al[1]. In accordance with the observation of Friedman et al[2] a viscosity maximum is observed at the cholesteric-isotropic transition (during microscopic study).

TABLE 5.1

Sample: MBAC, Temperature 27°C
Sample to Film distance 5.618cm.

LINEAR SCANNING			
L in cm.	O. D.	L in cm.	O. D.
6.9	0.515	3.85	0.535
6.8	0.52	3.8	0.49
6.7	0.53	3.75	0.525
6.6	0.54	3.7	0.965
6.5	0.55	3.65	1.01
6.4	0.57	3.6	0.99
6.3	0.615	3.55	0.64
6.25	0.642	3.5	0.62
6.2	0.75	3.45	0.60
6.175	0.865	3.4	0.61
6.1	0.80	3.35	0.61
6.0	0.64	3.3	0.63
5.9	0.61	3.25	0.62
5.8	0.6	3.2	0.605
5.7	0.5	3.15	0.60
5.6	0.585	3.1	0.60
5.5	0.58	3.0	0.60
5.4	0.578	2.9	0.60
5.3	0.572	2.8	0.60
5.2	0.58	2.7	0.60
5.1	0.59	2.6	0.61
5.0	0.59	2.5	0.612
4.9	0.595	2.4	0.62
4.8	0.60	2.3	0.63
4.75	0.615	2.2	0.65
4.7	0.612	2.1	0.660
4.65	0.608	2.05	0.73
4.6	0.600	2.0	0.768
4.55	0.598	1.95	0.9
4.5	0.605	1.9	0.885
4.45	0.63	1.8	0.68
4.4	0.885	1.7	0.63
4.35	1.03	1.6	0.60
4.3	0.84	1.5	0.57
4.25	0.688	1.4	0.555
4.2	0.47	1.3	0.55
4.15	0.5	1.2	0.54
4.1	0.59	1.15	0.53
4.05	0.80		
4.0	0.835		
3.95	0.78		
3.9	0.63		

TABLE 5.2

Sample: MBAC, Temperature 38°C
Sample to Film distance 5.618cm.

LINEAR SCANNING			
L in cm.	O. D.	L in cm.	O. D.
6.9	0.47	3.85	0.51
6.8	0.485	3.8	0.44
6.7	0.49	3.75	0.478
6.6	0.50	3.7	0.835
6.5	0.51	3.65	0.95
6.4	0.53	3.6	0.95
6.3	0.55	3.55	0.615
6.2	0.615	3.5	0.59
6.1	0.75	3.45	0.55
6.075	0.765	3.4	0.55
6.05	0.75	3.35	0.555
6.0	0.70	3.3	0.572
5.9	0.60	3.25	0.572
5.8	0.57	3.2	0.56
5.7	0.56	3.1	0.56
5.6	0.552	3.0	0.55
5.5	0.55	2.9	0.54
5.4	0.542	2.8	0.54
5.3	0.535	2.7	0.532
5.2	0.535	2.65	0.535
5.1	0.535	2.6	0.54
5.05	0.54	2.55	0.55
5.0	0.54	2.5	0.55
4.95	0.542	2.4	0.552
4.9	0.545	2.3	0.552
4.85	0.55	2.25	0.555
4.8	0.552	2.2	0.565
4.75	0.555	2.15	0.565
4.7	0.57	2.1	0.568
4.65	0.57	2.0	0.595
4.6	0.456	1.95	0.72
4.55	0.55	1.9	0.77
4.5	0.55	1.85	0.78
4.45	0.565	1.8	0.672
4.4	0.69	1.7	0.562
4.35	0.80	1.6	0.548
4.3	0.78	1.5	0.53
4.25	0.61	1.4	0.51
4.2	0.455	1.2	0.50
4.15	0.415		
4.1	0.418		
4.05	0.565		
4.0	0.69		
3.95	0.77		
3.9	0.565		

TABLE 5.3

Sample: MBAC, Temperature 33°C. Sample to film distance = 6.618 For Outer Ring, 5.618 For Inner Ring.

LINEAR SCANNING

L in cm.	O. D.	L in cm.	O. D.	L in cm.	O. D.
OUTER RING		4.25	0.815	1.55	0.85
		4.2	0.655	1.5	0.835
		4.15	0.55	1.45	0.82
7.0	0.6	4.10	0.6	1.35	0.68
6.95	0.61	4.05	1.04	1.3	0.66
6.9	0.615	4.0	1.314		
6.85	0.62	3.95	1.58	INNER RING	
6.8	0.63	3.9	1.03		
6.75	0.65	3.85	0.87	5.0	0.562
6.7	0.675	3.8	0.55	4.9	0.57
6.65	0.71	3.75	0.57	4.8	0.575
6.6	0.74	3.7	0.59	4.7	0.585
6.55	0.84	3.65	0.86	4.65	0.60
6.5	0.86	3.6	0.94	4.6	0.595
6.45	0.81	3.55	1.01	4.55	0.575
6.4	0.74	3.5	0.9	4.5	0.58
6.35	0.698	3.45	0.82	4.45	0.585
6.3	0.665	3.4	0.66	4.4	0.74
6.2	0.65	3.35	0.655	4.35	0.86
6.1	0.64	3.3	0.655	4.3	0.875
6.0	0.642	3.25	0.66	4.25	0.725
5.9	0.645	3.2	0.665	4.2	0.472
5.8	0.645	3.15	0.685	4.15	0.49
5.7	0.642	3.10	0.68	4.1	0.53
5.6	0.64	3.05	0.67	4.05	1.04
5.5	0.64	3.0	0.67	4.0	1.18
5.4	0.64	2.95	0.67	3.95	1.29
5.3	0.642	2.9	0.665	3.9	0.99
5.2	0.65	2.85	0.665	3.85	0.84
5.1	0.652	2.75	0.66	3.8	0.47
5.0	0.655	2.7	0.66	3.75	0.47
4.95	0.655	2.65	0.65	3.7	0.57
4.9	0.652	2.6	0.65	3.65	1.04
4.85	0.652	2.5	0.64	3.6	1.04
4.8	0.66	2.4	0.64	3.55	0.68
4.75	0.66	2.3	0.64	3.5	0.63
4.7	0.66	2.2	0.645	3.45	0.565
4.65	0.64	2.15	0.65	3.4	0.562
4.6	0.64	2.1	0.65	3.35	0.565
4.55	0.66	2.05	0.655	3.3	0.585
4.5	0.67	2.0	0.66	3.25	0.585
4.45	0.73	1.9	0.662	3.2	0.57
4.4	1.04	1.8	0.68	3.15	0.57
4.35	1.18	1.7	0.68	3.1	0.57
4.3	1.01	1.6	0.77	3.05	0.57

TABLE 5.4

Sample: NBAC, Temperature 40°C
Sample to Film distance 6.618 cm.

LINEAR SCANNING			
L in cm	O. D.	L in cm	O. D.
7.0	0.58	3.85	0.675
6.8	0.6	3.8	0.55
6.65	0.65	3.75	0.58
6.55	0.74	3.7	0.96
6.5	0.74	3.65	1.11
6.45	0.72	3.6	1.21
6.4	0.685	3.55	1.02
6.35	0.65	3.5	0.92
6.3	0.63	3.45	0.66
6.1	0.62	3.4	0.65
6.0	0.62	3.35	0.65
5.9	0.62	3.3	0.655
5.8	0.618	3.25	0.665
5.7	0.615	3.2	0.68
5.6	0.615	3.15	0.678
5.5	0.612	3.1	0.67
5.3	0.615	3.0	0.65
5.2	0.62	2.85	0.65
5.15	0.625	2.8	0.64
5.1	0.628	2.7	0.64
5.05	0.63	2.6	0.63
5.0	0.632	2.5	0.62
4.95	0.635	2.4	0.62
4.9	0.64	2.3	0.62
4.85	0.65	2.2	0.615
4.8	0.66	2.1	0.64
4.75	0.65	2.05	0.642
4.7	0.64	2.0	0.642
4.65	0.63	1.95	0.642
4.6	0.63	1.9	0.645
4.55	0.7	1.8	0.65
4.5	0.78	1.65	0.685
4.45	1.02	1.6	0.725
4.4	1.39	1.55	0.72
4.35	1.38	1.5	0.72
4.3	0.77	1.45	0.65
4.25	0.67	1.35	0.63
4.2	0.55	1.3	0.605
4.15	0.56	1.2	0.59
4.1	0.68		
4.05	1.9		
4.0	1.08		
3.95	1.04		
3.9	0.745		

TABLE 5.5

Sample: NBAC, Temperature 43°C
Sample to Film distance = 5.618 cm.

LINEAR SCANNING			
L in cm.	O. D.	L in cm.	O. D.
7.0	0.535	3.25	0.635
6.8	0.55	3.2	0.61
6.6	0.565	3.15	0.61
6.4	0.59	3.1	0.60
6.2	0.725	3.0	0.595
6.1	0.865	2.9	0.59
6.05	0.775	2.8	0.588
6.0	0.71	2.7	0.58
5.9	0.64	2.6	0.59
5.8	0.625	2.5	0.595
5.7	0.615	2.4	0.595
5.6	0.61	2.35	0.602
5.4	0.60	2.3	0.605
5.2	0.59	2.25	0.61
5.1	0.592	2.2	0.625
5.05	0.598	2.15	0.625
4.9	0.60	1.95	0.795
4.8	0.605	1.9	0.825
4.7	0.62	1.875	0.83
4.6	0.61	1.85	0.72
4.5	0.60	1.8	0.68
4.4	0.70	1.65	0.59
4.35	0.96	1.5	0.55
4.3	1.01	1.4	0.535
4.25	0.855	1.3	0.52
4.2	0.478	1.2	0.505
4.15	0.47		
4.1	0.58		
4.05	0.75		
4.0	0.89		
3.95	0.93		
3.9	0.88		
3.85	0.51		
3.8	0.478		
3.75	0.48		
3.7	0.885		
3.65	1.02		
3.6	1.03		
5.55	0.73		
3.5	0.682		
3.45	0.61		
3.4	0.61		
3.35	0.628		
3.3	0.632		

TABLE 5.6

Sample: MBAC, Temperature 48°C
Sample to Film distance
5.618 cm.

LINEAR SCANNING			
L in cm	O. D.	L in cm.	O. D.
7.0	0.525	3.8	0.5
6.9	0.53	3.75	0.52
6.8	0.535	3.7	0.96
6.7	0.545	3.65	1.115
6.6	0.535	3.6	0.83
6.5	0.57	3.55	0.73
6.4	0.585	3.5	0.685
6.3	0.615	3.45	0.615
6.2	0.72	3.4	0.612
6.1	0.815	3.35	0.615
6.05	0.76	3.3	0.64
6.0	0.69	3.25	0.64
5.9	0.625	3.2	0.62
5.8	0.61	3.1	0.61
5.7	0.605	3.0	0.61
5.6	0.60	2.9	0.60
5.4	0.59	2.7	0.60
5.3	0.585	2.6	0.61
5.2	0.588	2.5	0.615
5.15	0.59	2.4	0.618
5.05	0.595	2.3	0.62
5.0	0.60	2.2	0.642
4.9	0.602	2.1	0.675
4.8	0.605	2.0	0.7
4.7	0.622	1.95	0.82
4.65	0.62	1.9	0.83
4.6	0.618	1.85	0.72
4.55	0.61	1.8	0.69
4.5	0.615	1.7	0.61
4.4	0.785	1.6	0.58
4.35	1.10	1.5	0.57
4.3	0.98	1.4	0.55
4.25	0.78	1.3	0.54
4.2	0.485	1.2	0.525
4.15	0.52	1.15	0.52
4.1	0.93		
4.05	1.36		
4.0	1.78		
3.95	1.5		
3.9	1.1		
3.85	0.725		

TABLE 5.7

Sample: MBAC, Temperature 58°C
Sample to Film distance
5.618 cm.

LINEAR SCANNING			
L in cm	O. D.	L in cm.	O. D.
6.9	0.50	3.8	0.98
6.7	0.52	3.25	1.04
6.5	0.55	3.7	0.73
6.3	0.605	3.65	0.665
6.2	0.645	3.6	0.61
6.15	0.65	3.55	0.575
6.1	0.645	3.5	0.57
6.05	0.63	3.45	0.58
6.0	0.62	3.4	0.582
5.95	0.605	3.35	0.58
5.9	0.605	3.3	0.595
5.8	0.58	3.25	0.572
5.7	0.57	3.2	0.57
5.5	0.55	3.15	0.565
5.4	0.56	3.1	0.562
5.35	0.558	3.05	0.56
5.25	0.56	2.95	0.562
5.2	0.562	2.9	0.552
5.15	0.57	2.85	0.55
5.1	0.572	2.8	0.55
5.05	0.58	2.75	0.552
5.0	0.58	2.7	0.56
4.95	0.58	2.65	0.56
4.9	0.582	2.6	0.57
4.85	0.59	2.55	0.57
4.8	0.592	2.5	0.57
4.75	0.59	2.45	0.58
4.7	0.585	2.4	0.58
4.65	0.585	2.35	0.59
4.6	0.60	2.3	0.60
4.55	0.675	2.25	0.60
4.5	0.75	2.2	0.63
4.45	0.95	2.15	0.632
4.4	0.82	2.1	0.66
4.35	0.69	2.05	0.662
4.3	0.485	2.0	0.662
4.25	0.515	1.95	0.63
4.2	0.76	1.9	0.62
4.15	0.995	1.8	0.575
4.1	1.18	1.7	0.55
4.05	0.985	1.6	0.535
4.0	0.91	1.5	0.52
3.95	0.53	1.45	0.52
3.9	0.53	1.4	0.51
3.85	0.56	1.2	0.49

TABLE 5.8

Sample: MBAC, Temperature 53°C, Sample to Film distance 6.618 cm For Outer Ring and 5.618cm for Inner Ring.

LINEAR SCANNING

L in cm.	O. D.	L in cm.	O. D.	L in cm	O. D.
OUTER RING					
6.95	0.6	4.25	0.55	1.8	0.71
6.9	0.61	4.2	0.52	1.75	0.715
6.85	0.61	4.15	0.495	1.7	0.77
6.8	0.63	4.1	0.51	1.65	0.8
6.75	0.635	4.05	0.70	1.6	0.82
6.7	0.645	4.0	0.79	1.55	0.9
6.65	0.665	3.95	0.83	1.5	0.9
6.6	0.69	3.9	0.62	1.45	0.815
6.55	0.73	3.85	0.59	1.4	0.79
6.5	0.77	3.8	0.515	1.35	0.77
6.45	0.82	3.75	0.55	1.3	0.70
6.4	0.825	3.7	1.0	1.25	0.69
6.35	0.78	3.65	1.12	INNER RING	
6.3	0.74	3.6	1.21	4.9	0.562
6.25	0.71	3.55	0.96	4.85	0.57
6.2	0.69	3.5	0.845	4.8	0.58
6.1	0.67	3.45	0.66	4.70	0.57
6.0	0.66	3.4	0.65	4.6	0.575
5.9	0.65	3.35	0.65	4.55	0.59
5.8	0.65	3.3	0.66	4.5	0.62
5.7	0.65	3.25	0.665	4.4	0.982
5.6	0.645	3.2	0.685	4.35	0.88
5.55	0.64	3.15	0.685	4.3	0.66
5.5	0.64	3.1	0.685	4.25	0.57
5.4	0.64	3.05	0.68	4.2	0.468
5.35	0.645	3.0	0.68	4.15	0.54
5.3	0.65	2.95	0.678	4.1	0.645
5.2	0.655	2.9	0.678	4.05	0.715
5.15	0.66	2.85	0.67	4.0	0.77
5.05	0.665	[illegible]2.7	0.655	3.95	0.485
5.0	0.668	2.65	0.65	3.9	0.455
4.95	0.67	2.6	0.65	3.85	0.415
4.9	0.678	2.55	0.65	3.8	0.48
4.85	0.68	2.5	0.65	3.75	0.53
4.8	0.685	2.48	0.65	3.7	0.92
4.75	0.68	2.35	0.65	3.65	0.855
4.7	0.66	2.3	0.66	3.6	0.60
4.65	0.63	2.25	0.66	3.55	0.58
4.6	0.63	2.15	0.66	3.5	0.572
4.55	0.60	2.1	0.66	3.4	0.58
4.5	0.61	2.05	0.665	3.3	0.58
4.45	0.625	2.0	0.670	3.2	0.57
4.4	0.615	1.95	0.68	3.15	0.565
4.35	0.615	1.9	0.685	3.1	0.56
4.3	0.565	1.85	0.690	3.0	0.56

TABLE 5.9.

Sample: MBAC, Temperature 63°C, Sample to Film distance 6.618 cm. for Outer Ring, 5.618 cm. for Inner Ring.

L I N E A R		S C A N N I N G			
L in cm.	O. D.	L in cm.	O. D.	L in cm.	O. D.
	OUTER RING				INNER RING
7.0	0.58	4.15	0.61	5.0	0.635
6.8	0.605	4.1	0.52	4.9	0.65
6.7	0.62	4.05	0.53	4.8	0.66
6.6	0.64	4.0	0.58	4.7	0.67
6.5	0.675	3.95	0.780	4.65	0.672
6.4	0.7	3.9	0.87	4.6	0.67
6.35	0.72	3.85	0.645	4.55	0.66
6.25	0.69	3.8	0.58	4.5	0.66
6.2	0.675	3.75	0.49	4.45	0.712
6.15	0.665	3.7	0.515	4.4	0.78
6.1	0.655	3.65	0.825	4.35	0.905
6.0	0.64	3.6	1.025	4.3	1.14
5.95	0.635	3.55	0.84	4.25	0.972
5.9	0.63	3.5	0.755	4.2	0.565
5.85	0.63	3.45	0.63	4.15	0.49
5.8	0.625	3.4	0.63	4.1	0.48
5.7	0.615	3.35	0.63	4.05	0.69
5.6	0.618	3.3	0.635	4.0	0.78
5.55	0.615	3.2	0.65	3.95	0.925
5.5	0.612	3.15	0.65	3.9	0.96
5.45	0.612	3.1	0.65	3.85	0.70
5.4	0.61	3.0	0.645	3.8	0.51
5.3	0.61	2.9	0.64	3.65	0.885
5.25	0.61	2.8	0.635	3.6	1.05
5.2	0.615	2.7	0.62	3.55	0.862
5.15	0.62	2.6	0.61	3.5	0.815
5.1	0.62	2.5	0.605	3.45	0.68
5.05	0.63	2.4	0.61	3.4	0.675
5.0	0.63	2.3	0.615	3.35	0.675
4.95	0.63	2.2	0.62	3.3	0.68
4.9	0.635	2.1	0.625	3.2	0.68
4.85	0.635	2.0	0.63	3.1	0.69
4.8	0.632	1.9	0.64	3.0	0.69
4.75	0.631	1.8	0.65		
4.7	0.63	1.7	0.67		
4.65	0.628	1.6	0.685		
4.6	0.62	1.55	0.685		
4.55	0.62	1.5	0.685		
4.5	0.622	1.45	0.67		
4.45	0.68	1.4	0.66		
4.4	0.74	1.35	0.66		
4.35	0.815	1.3	0.63		
4.3	1.08	1.25	0.62		
4.25	1.02	1.2	0.6		
4.2	0.93	1.15	0.59		

TABLE 5.10

Sample: MBAC, Temperature 68°C
Sample to Film distence 5.618 cm.

LINEAR SCANNING			
L in cm.	O. D.	L in cm.	O. D.
6.9	0.512	4.25	0.735
6.8	0.515	4.2	0.628
6.6	0.528	4.15	0.49
6.5	0.535	4.1	0.49
6.4	0.55	4.05	0.70
6.35	0.57	4.0	0.85
6.3	0.57	3.95	1.02
6.25	0.58	3.9	0.92
6.2	0.585	3.85	0.835
6.15	0.595	3.8	0.51
6.1	0.61	3.75	0.51
6.05	0.615	3.7	0.65
6.0	0.625	3.65	0.72
5.95	0.62	3.6	0.765
5.9	0.62	3.55	0.695
5.85	0.612	3.5	0.66
5.8	0.605	3.45	0.60
5.75	0.602	3.4	0.60
5.65	0.59	3.2	0.60
5.6	0.59	3.10	0.60
5.55	0.58	3.05	0.59
5.50	0.58	3.0	0.59
5.45	0. 575	2.95	0.582
5.4	0.57	2.9	0.58
5.35	0.57	2.85	0.58
5.3	0.568	2.70	0.58
5.25	0.568	2.65	0.582
5.2	0.562	2.6	0.582
5.15	0.562	2.5	0.582
5.1	0.562	2.45	0.59
5.05	0.565	2.4	0.59
5.0	0.568	2.35	0.595
4.95	0.57	2.3	0.60
4.9	0.57	2.25	0.60
4.85	0.578	2.2	0.61
4.8	0.58	2.15	0.61
4.75	0.58	2.10	0.63
4.6	0.58	2.0	0.635
4.55	0.58	1.9	0.63
4.5	0.582	1.8	0.64
4.45	0.60	1.7	0.64
4.4	0.625	1.5	0.57
4.35	0.665	1.4	0.56
4.3	0.78	1.2	0.54

TABLE 5.11

Sample: MBAC, Temperature 70°C
Sample to Film distance 5.618 cm.

LINEAR SCANNING			
L in cm.	O. D.	L in cm.	O. D.
7.0	0.56	3.85	0.53
6.8	0.58	3.8	0.49
6.6	0.605	3.75	0.52
6.4	0.63	3.7	0.84
6.3	0.652	3.65	0.88
6.2	0.70	3.6	0.86
6.1	0.74	3.55	0.66
6.05	0.75	3.50	0.64
6.0	0.75	3.45	0.62
5.95	0.74	3.4	0.62
5.9	0.73	3.35	0.62
5.85	0.715	3.3	0.625
5.8	0.705	3.25	0.625
5.7	0.682	3.2	0.62
5.6	0.65	3.15	0.615
5.5	0.632	3.1	0.61
5.45	0.625	3.05	0.61
5.3	0.62	2.95	0.60
5.2	0.62	2.9	0.60
5.15	0.62	2.85	0.60
5.1	0.618	2.8	0.59
5.05	0.612	2.7	0.59
5.0	0.612	2.6	0.59
4.95	0.615	2.55	0.595
4.9	0.62	2.50	0.60
4.85	0.622	2.45	0.605
4.8	0.625	2.4	0.605
4.75	0.628	2.3	0.615
4.7	0.63	2.2	0.63
4.65	0.63	2.15	0.63
4.6	0.63	2.1	0.645
4.55	0.63	2.0	0.65
4.5	0.635	1.95	0.635
4.45	0.72	1.9	0.63
4.35	0.815	1.8	0.60
4.3	0.65	1.65	0.56
4.25	0.562	1.60	0.56
4.2	0.46	1.50	0.55
4.15	0.476	1.40	0.54
4.10	0.52	1.3	0.525
4.05	0.93	1.2	0.51
4.0	1.11		
3.95	1.32		
3.9	0.65		

TABLE 5.12

Sample: MBAC, Temperature 73°C, Sample to Film distance 6.618 cm. for Outer Ring, 5.618 cm. for Inner Ring

L I N E A R S C A N N I N G					
L in cm.	O. D.	L in cm.	O. D.	L in cm.	O. D.
OUTER RING		4.5	0.71	1.9	0.74
		4.4	0.885	1.8	0.77
		4.35	0.9	1.7	0.775
6.9	0.63	4.3	0.755	1.65	0.785
6.8	0.645	4.25	0.67	1.6	0.782
6.7	0.675	4.2	0.625	1.55	0.762
6.6	0.71	4.15	0.57	1.45	0.75
6.5	0.745	4.1	0.66	1.4	0.76
6.4	0.77	4.05	1.65	1.35	0.75
6.35	0.775	4.0	2.05	1.3	0.69
6.3	0.77	3.95	2.17	1.2	0.64
6.25	0.762	3.9	1.31	1.1	0.44
6.2	0.75	3.85	1.02	INNER RING.	
6.15	0.74	3.8	0.53	4.9	0.65
6.1	0.73	3.75	0.54	4.8	0.66
6.05	0.715	3.7	0.79	4.75	0.66
6.0	0.705	3.60	0.835	4.7	0.658
5.95	0.69	3.55	0.89	4.65	0.665
5.9	0.685	3.5	0.855	4.6	0.668
5.85	0.68	3.45	0.82	4.5	0.678
5.8	0.67	3.4	0.7	4.45	0.70
5.75	0.67	3.35	0.698	4.4	0.72
5.7	0.665	3.3	0.688	4.35	0.732
5.65	0.66	3.25	0.69	4.3	0.732
5.6	0.66	3.2	0.69	4.25	0.688
5.55	0.66	3.15	0.705	4.2	0.535
5.5	0.66	3.1	0.705	4.15	0.50
5.45	0.66	3.05	0.705	4.1	0.612
5.4	0.66	3.0	0.705	4.05	0.72
5.35	0.66	2.95	0.705	4.0	0.885
5.3	0.67	2.9	0.702	3.95	0.84
5.25	0.67	2.85	0.70	3.9	0.72
5.2	0.678	2.8	0.69	3.85	0.62
5.15	0.68	2.7	0.685	3.8	0.49
5.1	0.685	2.6	0.675	3.75	0.492
5.05	0.69	2.5	0.665	3.7	0.635
5.0	0.69	2.45	0.668	3.6	0.725
4.95	0.695	2.4	0.67	3.5	0.685
4.9	0.69	2.35	0.67	3.45	0.65
4.85	0.692	2.3	0.678	3.4	0.65
4.8	0.69	2.25	0.68	3.35	0.635
4.75	0.69	2.2	0.686	3.3	0.635
4.7	0.685	2.15	0.69	3.2	0.631
4.65	0.680	2.1	0.69	3.1	0.628
4.6	0.682	2.05	0.71	3.0	0.62

TABLE # 5.13

Sample: MBAC, Temperature 75°C
Sample to film distance
5.618 cm.

LINEAR SCANNING			
L in cm.	O. D.	L in cm.	O. D.
7.0	0.51	3.6	0.64
6.8	0.515	3.55	0.69
6.6	0.53	3.5	0.68
6.4	0.555	3.45	0.65
6.2	0.60	3.4	0.65
6.0	0.648	3.35	0.642
5.95	0.655	3.3	0.64
5.9	0.652	3.25	0.642
5.85	0.65	3.2	0.64
5.8	0.645	3.15	0.64
5.75	0.64	3.1	0.635
5.7	0.64	3.05	0.63
5.65	0.638	3.0	0.63
5.6	0.63	2.95	0.615
5.55	0.62	2.85	0.615
5.5	0.618	2.75	0.615
5.45	0.612	2.7	0.622
5.4	0.61	2.65	0.625
5.35	0.608	2.6	0.64
5.3	0.602	2.55	0.64
5.25	0.602	2.5	0.64
5.2	0.602	2.45	0.66
5.1	0.605	2.4	0.665
5.0	0.61	2.3	0.695
4.9	0.62	2.20	0.72
4.8	0.63	2.15	0.72
4.7	0.632	2.1	0.73
4.6	0.635	2.05	0.73
4.5	0.65	2.0	0.725
4.4	0.69	1.95	0.71
4.35	0.715	1.9	0.71
4.3	0.72	1.8	0.67
4.25	0.695	1.65	0.625
4.2	0.52	1.55	0.60
4.15	0.478	1.45	0.57
4.1	0.455	1.35	0.562
4.05	0.60	1.25	0.55
4.0	0.765	1.2	0.53
3.95	0.65		
3.9	0.605		
3.85	0.57		
3.8	0.44		
3.75	0.44		
3.7	0.525		
3.65	0.585		

TABLE 5.14

Sample: MBAC, Temperature 88°C
Sample to film distance
5.618 cm.

LINEAR SCANNING			
L in cm.	O. D.	L in cm.	O. D.
7.0	0.545	4.1	0.505
6.9	0.552	4.05	0.65
6.75	0.562	4.0	0.665
6.65	0.57	3.95	0.45
6.55	0.588	3.9	0.44
6.5	0.60	3.85	0.45
6.4	0.62	3.8	0.585
6.3	0.652	3.75	0.64
6.2	0.66	3.7	0.74
6.1	0.71	3.6	0.74
6.0	0.73	3.5	0.69
5.9	0.742	3.45	0.665
5.85	0.74	3.4	0.66
5.8	0.73	3.35	0.66
5.75	0.725	3.3	0.67
5.7	0.712	3.2	0.662
5.65	0.70	3.1	0.66
5.6	0.69	3.0	0.65
5555	0.68	2.9	0.64
5.5	0.68	2.8	0.645
5.45	0.68	2.75	0.645
5.4	0.66	2.7	0.66
5.35	0.65	2.65	0.66
5.3	0.645	2.6	0.68
5.25	0.642	2.5	0.69
5.2	0.642	2.4	0.71
5.15	0.65	2.3	0.735
5.1	0.65	2.2	0.74
5.05	0.65	2.15	0.74
5.0	0.65	2.1	0.725
4.95	0.662	2.05	0.72
4.9	0.665	2.0	0.72
4.85	0.67	1.9	0.68
4.8	0.67	1.8	0.63
4.75	0.67	1.7	0.60
4.7	0.67	1.6	0.59
4.65	0.672	1.5	0.565
4.6	0.68	1.4	0.55
4.55	0.70	1.3	0.53
4.5	0.71	1.2	0.51
4.35	0.735		
4.3	0.735		
4.25	0.728		
4.2	0.57		
4.15	0.45		

TABLE 5.15

Sample: MBAC, Temperature 83°C, Sample to Film distance 6.618 cm. for Outer Ring, 5.618cm. for Inner Ring.

LINEAR SCANNING

L in cm.	O. D.	L in cm.	O. D.	L in cm	O. D.
OUTER RING					
7.0	0.61	3.65	0.69	4.7	0.77
6.8	0.63	3.6	0.73	4.6	0.79
6.6	0.66	3.55	0.765	4.5	0.81
6.4	0.71	3.5	0.76	4.4	0.865
6.3	0.722	3.4	0.705	4.35	0.87
6.25	0.722	3.35	0.70	4.3	0.75
6.20	0.72	3.3	0.68	4.25	0.69
6.15	0.715	3.15	0.68	4.2	0.50
6.1	0.715	3.0	0.68	4.15	0.50
6.05	0.71	2.95	0.68	4.1	0.55
6.0	0.705	2.8	0.665	4.05	0.98
5.8	0.68	2.75	0.662	4.0	1.27
5.6	0.668	2.7	0.66	3.95	0.875
5.5	0.662	2.65	0.66	3.9	0.75
5.45	0.662	2.6	0.66	3.85	0.61
5.4	0.66	2.55	0.65	3.8	0.49
5.3	0.66	2.55	0.65	3.75	0.52
5.25	0.66	2.4	0.65	3.7	0.815
5.2	0.662	2.35	0.652	3.65	0.86
5.1	0.675	2.3	0.662	3.6	0.862
5.0	0.685	2.25	0.662	3.55	0.83
4.9	0.69	2.2	0.67	3.5	0.82
4.8	0.698	2.1	0.678	3.45	0.795
4.75	0.698	2.0	0.685	3.4	0.79
4.7	0.695	1.9	0.702	3.35	0.79
4.65	0.698	1.8	0.72	3.3	0.78
4.6	0.7	1.75	0.72	3.2	0.775
4.55	0.715	1.7	0.725	3.15	0.77
4.5	0.72	1.65	0.725	3.1	0.775
4.45	0.73	1.6	0.725	3.0	0.77
4.4	0.76	1.55	0.722		
4.35	0.77	1.5	0.72		
4.3	0.75	1.45	0.718		
4.25	0.71	1.4	0.7		
4.2	0.66	1.3	0.675		
4.15	0.56	1.2	0.665		
4.1	0.565	1.1	0.645		
4.05	0.63				
4.0	1.01	INNER RING			
3.95	1.18				
3.9	0.98	5.0	0.74		
3.85	0.85	4.95	0.745		
3.8	0.555	4.9	0.75		
3.75	0.545	4.85	0.76		
3.7	0.55	4.8	0.77		

TABLE 5.16

Sample: MBAC, Temperature 93°C, Sample to Film Distance 6.618 cm. for Outer Ring, 5.618 cm. for Inner Ring

LINEAR SCANNING

L in cm.	O. D.	L in cm.	O. D.	L in cm.	O. D.
OUTER RING		3.7	0.65	4.65	0.82
		3.65	0.72	4.6	0.82
		3.6	0.775	4.55	0.84
6.9	0.67	3.55	0.815	4.5	0.85
6.7	0.72	3.5	0.81	4.45	0.885
6.5	0.77	3.45	0.77	4.4	0.895
6.4	0.792	3.4	0.765	4.35	0.90
6.3	0.802	3.35	0.76	4.3	0.89
6.2	0.802	3.3	0.74	4.25	0.87
6.15	0.8	3.25	0.745	4.2	0.62
6.05	0.78	3.2	0.748	4.1	0.515
6.0	0.775	3.1	0.75	4.05	0.55
5.9	0.76	3.05	0.75	4.0	0.59
5.7	0.74	3.0	0.75	3.95	0.61
5.6	0.73	2.95	0.742	3.9	0.54
5.5	0.72	2.9	0.74	3.85	0.525
5.4	0.72	2.85	0.738	3.8	0.61
5.3	0.72	2.8	0.725	3.75	0.66
5.25	0.725	2.75	0.72	3.7	0.93
5.2	0.73	2.7	0.715	3.65	0.935
5.1	0.74	2.65	0.715	3.6	0.94
5.0	0.75	2.6	0.71	3.55	0.91
4.9	0.76	2.55	0.71	3.5	0.905
4.8	0.755	2.45	0.71	3.45	0.87
4.75	0.755	2.4	0.715	3.4	0.87
4.7	0.758	2.35	0.72	3.35	0.86
4.65	0.76	2.2	0.74	3.3	0.85
4.6	0.765	2.0	0.76	3.25	0.855
4.55	0.78	1.8	0.782	3.2	0.858
4.5	0.79	1.7	0.782	3.15	0.855
4.45	0.82	1.65	0.78	3.1	0.85
4.4	0.845	1.6	0.778	3.05	0.84
4.35	0.85	1.5	0.75	3.0	0.838
4.3	0.825	1.3	0.68		
4.25	0.775	1.15	0.65		
4.2	0.58				
4.15	0.565	**INNER RING**			
4.1	0.65				
4.05	0.90	5.0	0.765		
4.0	1.04	4.95	0.775		
3.9	0.88	4.85	0.790		
3.85	0.81	4.8	0.802		
3.8	0.52	4.75	0.81		
3.75	0.52	4.7	0.815		

TABLE 5.17

Sample: MBAC, Temperature 96°C
Sample to Film distance
6.618 cm.

LINEAR SCANNING			
L in cm.	O. D.	L in cm.	O. D.
7.0	0.61	3.7	0.695
6.8	0.63	3.65	0.735
6.6	0.67	3.6	0.755
6.4	0.72	3.55	0.75
6.2	0.742	3.5	0.75
6.15	0.742	3.45	0.73
6.1	0.74	3.4	0.72
6.05	0.735	3.35	0.72
6.0	0.73	3.3	0.705
5.8	0.70	3.25	0.700
5.6	0.685	3.2	0.705
5.55	0.682	3.15	0.71
5.5	0.682	3.1	0.71
5.4	0.684	3.05	0.71
5.35	0.688	3.0	0.71
5.3	0.698	2.95	0.708
5.25	0.70	2.9	0.705
5.2	0.70	2.85	0.705
5.15	0.702	2.8	0.695
5.1	0.71	2.75	0.69
5.05	0.715	2.65	0.670
5.0	0.715	2.6	0.675
4.95	0.72	2.55	0.675
4.9	0.72	2.5	0.68
4.85	0.72	2.45	0.69
4.8	0.72	2.4	0.69
4.7	0.718	2.35	0.691
4.65	0.72	2.3	0.07
4.6	0.72	2.25	0.705
4.55	0.738	2.2	0.715
4.5	0.74	2.15	0.715
4.45	0.752	2.1	0.72
4.4	0.76	2.05	0.74
4.35	0.762	2.0	0.742
4.3	0.70	1.9	0.77
4.25	0.655	1.8	0.77
4.15	0.54	1.7	0.77
4.1	0.605	1.6	0.77
4.05	0.92	1.55	0.75
4.0	1.11	1.45	0.735
3.95	1.19	1.35	0.71
3.9	0.79	1.3	0.685
3.85	0.695	1.2	0.67
3.8	0.52	1.15	0.655
3.75	0.53		

TABLE 5.18

Sample: MBAC, Temperature 100°C
Sample to Film distance
6.618 cm.

LINEAR SCANNING			
L in cm.	O. D.	L in cm.	O. D.
6.9	0.64	3.6	0.815
6.8	0.66	3.55	0.812
6.7	0.672	3.5	0.80
6.65	0.685	3.4	0.77
6.6	0.702	3.3	0.75
6.55	0.72	3.25	0.745
6.5	0.73	3.1	0.745
6.4	0.755	3.05	0.748
6.3	0.77	3.0	0.75
6.2	0.78	2.95	0.742
6.1	0.78	2.9	0.72
6.05	0.775	2.8	0.73
6.0	0.77	2.7	0.725
5.9	0.75	2.6	0.715
5.8	0.735	2.5	0.712
5.7	0.725	2.45	0.72
5.6	0.71	2.4	0.72
5.5	0.695	2.3	0.735
5.4	0.695	2.2	0.75
5.35	0.698	2.1	0.76
5.3	0.7	2.0	0.775
5.2	0.7	1.9	0.79
5.1	0.71	1.8	0.792
5.0	0.715	1.75	0.79
4.95	0.72	1.7	0.788
4.9	0.722	1.6	0.778
4.8	0.722	1.5	0.75
4.7	0.725	1.4	0.71
4.6	0.732	1.3	0.675
4.5	0.76	1.2	0.66
4.4	0.79	1.15	0.64
4.3	0.77		
4.25	0.77		
4.2	0.67		
4.15	0.59		
4.1	0.625		
4.05	0.91		
4.0	1.01		
3.95	1.04		
3.9	0.83		
3.85	0.79		
3.8	0.59		
3.75	0.60		
3.7	0.63		
3.65	0.795		

TABLE 5.19.

Sample: MBAC.

Intermolecular distance (D) and layer thickness in Smectic phase (length of the molecule in Cholesteric phase) 'l'.

Temp. °C.	Sample to film distance in cm.	Outer halo: Dia. in cm.	Outer halo: Bragg angle (deg.)	Outer halo: 'D' in Å	Inner halo/ring *: Dia. in cm.	Inner halo/ring *: Bragg angle (deg.)	Inner halo/ring *: l in Å	Phase
27	5.6181	4.225	10.304	4.815	0.70	1.782	24.78	
33	6.6181	4.95	10.252	4.838	0.70	1.782	"	
38	5.6181	4.225	10.304	4.815	0.70	1.782	"	S_B
40	6.6181	4.95	10.252	4.838	-			
43	-	-	-	-	0.70	1.782	"	
46	5.6181	4.2	10.248	4.841	0.70	1.782	"	
53	6.6181	4.9	10.157	4.885	0.70	1.782	"	
58	5.6181	4.1	10.023	4.948	0.70	1.782	"	
63	6.6181	4.8	9.966	4.975	0.70	1.1782	24.78	
68	5.6181	4.25	9.911	5.004	0.70	1.782	"	S_A
70	5.6181	4.0	9.798	5.061	0.70	1.782	"	
73	6.6181	4.7	9.775	5.072	0.70	1.782	"	
78	5.6181	3.9	9.571	5.18	0.75	1.909	23.14	
83	6.6181	4.55	9.485	5.226	0.75	1.909	"	
88	5.6181	3.8	9.343	5.305	0.75	1.909	"	Ch
93	6.6181	4.475	9.340	5.306	0.75	1.909	"	
96	6.6181	4.4	9.194	5.389	0.75	1.909	"	
100	6.6181	4.375	9.145	5.417	-			I

* The sample to film distance is 5.6181 Å for all the temperatures in case of inner ring/halo.

References

1. Y. Liao, M.A., Clark & P. S. Perschan, Phys. Rev. Lett., 30, 639 (1973).
2. E.M. Friedman and R.S. Porter, Mol. Cryst. Liq.Cryst. 31 47 (1975).
3. G.W. Gray, Mol. Cryst.Liq.Cryst. 7, 127 (1969).
4. M. Leclereq, J. Billard and J. Jacques, Mol.Cryst.Liq. Cryst. 8, 367 (1969).
5. Catalogue Eastman Kodac Co., Catalogue, No. 11236.
6. D. Demus, & L. Richter, Textures of Liquid Crystals Verleg Chemie, P. 120 Plate 30, (1978).

6a. Ref. 6 p. 127, plate 43, 44.

6b. Ref. 6 p. 128, plate 45.

6c. Ref. 6 p. 202, 208, plate 194 and 206 respectively.

7. A. Saupe, Liq.Cryst. Plastic Cryst., Vol. I, Ed. G.W. Gray and P.A.Winsor, John Wiley and Sons INC (1974), p. 36, 38, 45.
8. N. Hun Tinh, A. Zann and J.C. Dubois, Mol.Cryst. Liq. Cryst. 53, 43 (1979).
9. A. de Vries, A. Ekachi and N. Spilberg, J. Phys. Colloque, 40c, 147 (1979).
10. A. J. Leadbetter, J.C. Frost. J.P. Gaughan, G.W.Gray and A. Mosley, J. Phys. 40, 375 (1979).

CHAPTER 6.

X-RAY DIFFRACTION STUDIES ON ORDERED SAMPLE OF 4'-METHOXY-4-n-BUTYLBENZYLIDENE-ANILINE (MBBA IN SHORT)

CHAPTER 6

X-RAY DIFFRACTION STUDIES ON ORDERED SAMPLE OF 4-METHOXY-4-n-BUTYLBENZYLIDENE-ANILINE (MBBA) (IN SHORT) AT ROOM TEMPERATURE

1. Introduction

The sample MBBA was supplied to us by Prof. M.Wada of Tohoku University, Sendai. The sample was recrystallised in their laboratory and purified by vacuum distillation. The transition temperature of the sample as given by Wada is shown below.

$$C \xrightarrow{18^{\circ}C} N \xrightarrow{42.5^{\circ}C} I$$

The transition temperatures of MBBA in its purest form obtained from standard books are $C \xrightarrow{21^{\circ}C} N \xrightarrow{48^{\circ}C} I$ As it is very difficult to purify the sample MBBA, we have not tried for further purification of the sample.

The chemical structure of MBBA has been given in chapter 2. In last few years a number of experiments have been performed to calculate the order parameters from aligned nematic liquid crystalline sample of MBBA. Shen Jen et al[1] have measured order parameters from Raman Scattering and have reproduce all other theoretical and experimental values of order parameters. Kabimata et al[2] also calculated order parameters using Resonance Raman effect. Terauchi et al[3] have studied X-ray halo scattering of MBBA and have calculated statistical distribution function.

In this chapter, the order parameters values of MBBA at room temperature have been determined by Leadbetters method[4] by calculating the orientational distribution function. Order parameter values are also determined by Vainshteins approximation[5]. We have discussed the interaction among the molecules and the nature of the variation of the intermolecular potential with the intermolecular distance is shown.

The details of experimental technique is described in chapter 2. The specimen was enclosed in a glass capillary of 1 mm. diameter and was aligned by simple heating cooling process. Flat plate X-ray diffraction photograph of the sample at room temperature 30°C was taken with an exposure time of 4 hours in the set up No.2 (in chapt. 2).

2. Results and Discussions:-

X-ray diffraction photograph of the sample shows that the sample is well aligned. It shows two diffuse outer maxima and two inner maxima perpendicular to the outer ones (fig.6.1)

Full circle scanning starting from the main equatorial reflexion and also linear scanning of the film were made with ECIL densitometer. The optical densities obtained from the densitometric scanning were converted into X-ray intensity values with the help of the calibration curve Fig. 2.4 prepared by the method described in chapter 2.

The linear distance - O.D. - Intensity values and also the angle - O.D. - Intensity values for the film are given in Table 6.1.

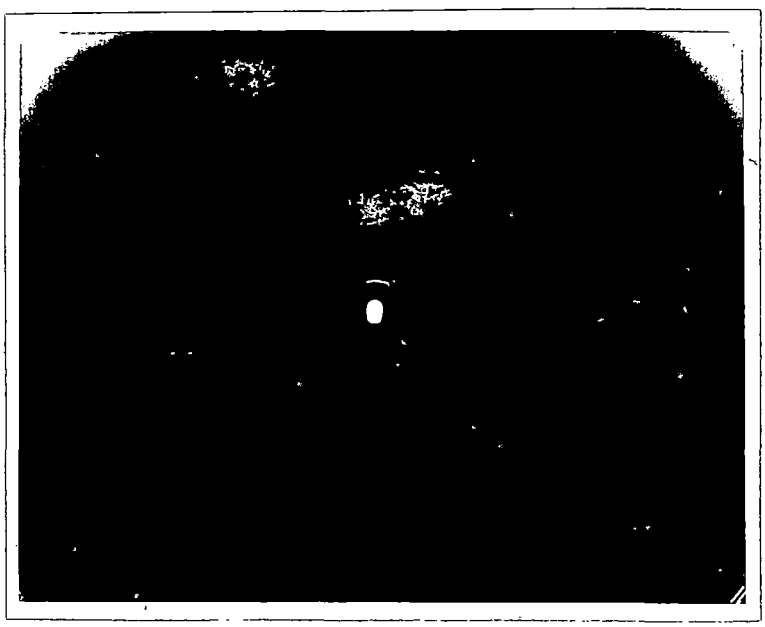

Fig. 6.1. Photograph of oriented sample of MBBA at 30°C.

The average intermolecular distance was calculated by using the eqn. 3.1. For this calculation distance between the two outer maxima, the corresponding Bragg angle and the actual distance between the film and the sample obtained respectively as 4 cm., 9.463 deg. and 5.833 cm. The average intermolecular distance is found to be equal to 5.24 Å. This value is little larger than the value given by Terauchi et al[3].

The converted intensity values of the O.D. for the angular scanning are plotted against corresponding angles. The background correction for each of the four quadrants has been done with the help of an empty capillary sample holder. A plot of Θ - I (Θ) is shown in the fig. 6.2. Background is shown by dotted line. At the maximum intensity position the angle is taken to be 0° and after 5° interval of Θ , I (Θ) was determined after background correction. The mean I (Θ) of four quadrants for each Θ from 0° to 90° was determined for the film. Θ - I(Θ) values are given in table 6.2. The calculated intensity values are also included in the same table. The experimental and calculated intensity values show a nearly perfect agreement. Calculated intensity values are obtained from the least square fitting with equation 3.4 with the series truncated after eight terms.

The normalized distribution function $f(\beta)$ are plotted against β - the angle with respect to the director in fig. 6.3. $f(\beta)$ values and also the calculated ~~and the~~ $f(\beta)$ values are given in table 6.2. $f(\beta)$ values are calculated by using the a_L values as described in chapter 3.

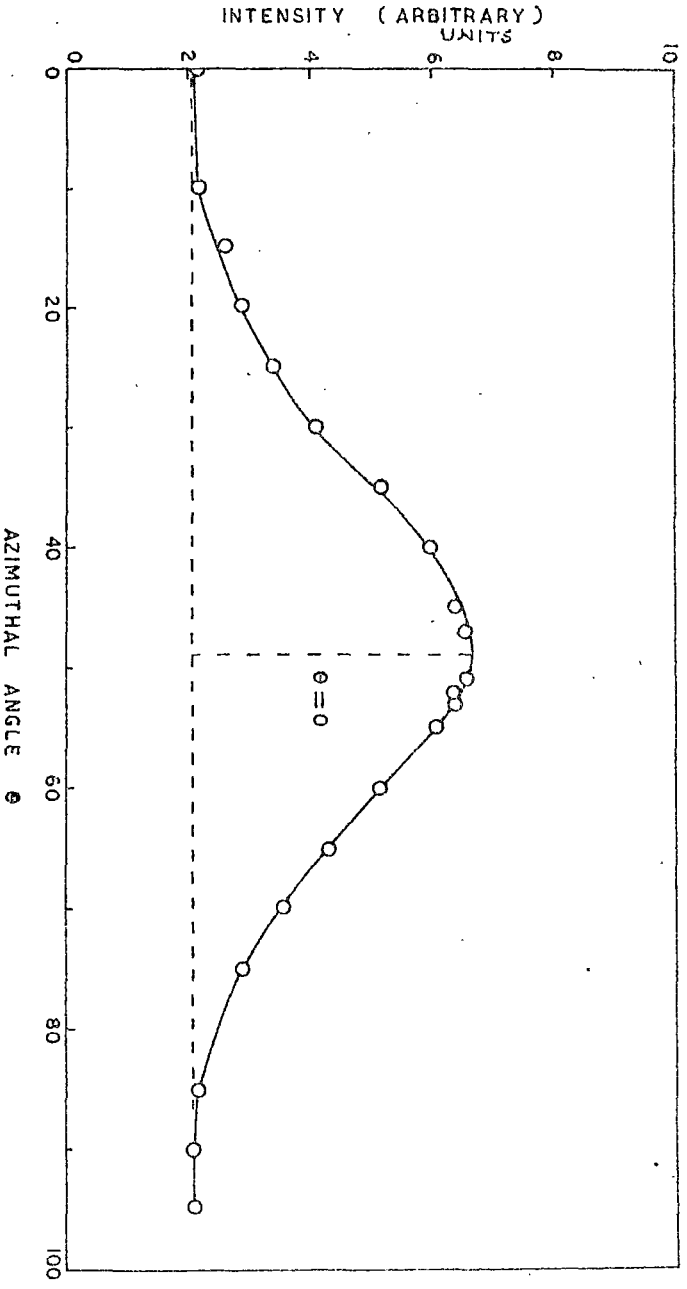
INTENSITY (ARBITRARY) UNITS
0
2
4
6
8
10
0
20
40
60
80
100
θ=0
AZIMUTHAL ANGLE θ

FIG. 6.2.

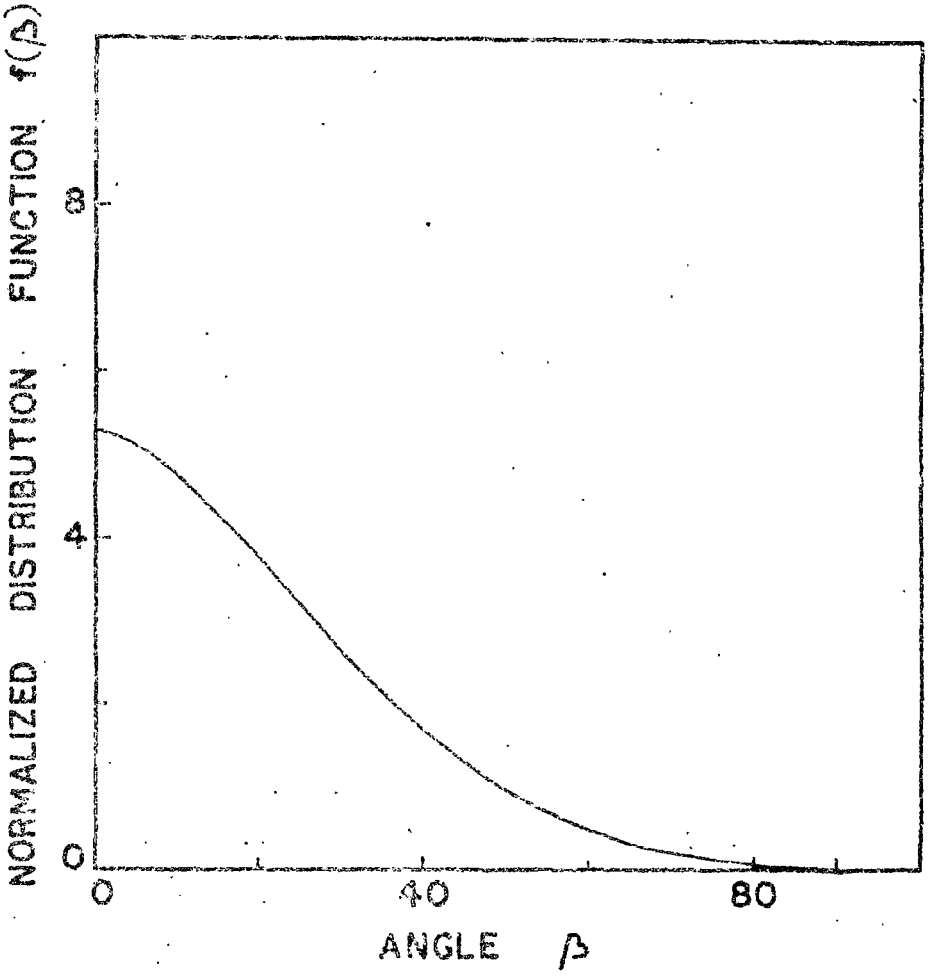

FIG. 6.3.

In our earlier paper on MBBA[5] we have calculated order parameter $\langle P_2 \rangle$ only by using Vainshtein's approximation as described in chapter 3, but afterwards we have calculated orientational order parameters $\langle P_2 \rangle$ and $\langle P_4 \rangle$ by Leadbetters method as described in chapter 3 by calculating the orientational distribution function $f(\beta)$. The order parameter values for MBBA are of great interest, since Shen Jen et al[1], using Raman effect have found $\langle P_4 \rangle$ values to be negative near T_c, the nematic - Isotropic phase transition temperature; whereas Kabinata et al[2], using Resonance Raman effect, failed to get any negative value for $\langle P_4 \rangle$ even within 0.5°C of T_c. Shen Jen et al[1] have reproduced all other theoretical and experimental values of $\langle P_2 \rangle$ and also the theoretical values of $\langle P_4 \rangle$ which is presented in fig. 6.4. $\langle P_2 \rangle$ and $\langle P_4 \rangle$ values obtained by Kabinata et al and also by us are plotted in the same figure. From our X-ray data at $T_c - T = 12.5°C$ we calculated $\langle P_2 \rangle = 0.54 \pm 0.02$ and $\langle P_4 \rangle = 0.12 \pm 0.02$. Our $\langle P_2 \rangle$ is in good agreement with both the previous studies[1,2]. Though our $\langle P_4 \rangle$ values are much larger than that of Shen Jen et al[1], it is in good agreement with Kabinata et al[2] value. The order parameter values are given in Table 6.3 and the coefficients a_L and b_L/k (L = 2 and 4) values are given in table 6.4. b_L values are calculated by using the formula $b_L = - \frac{a_L kT}{\langle P_L \rangle}$.

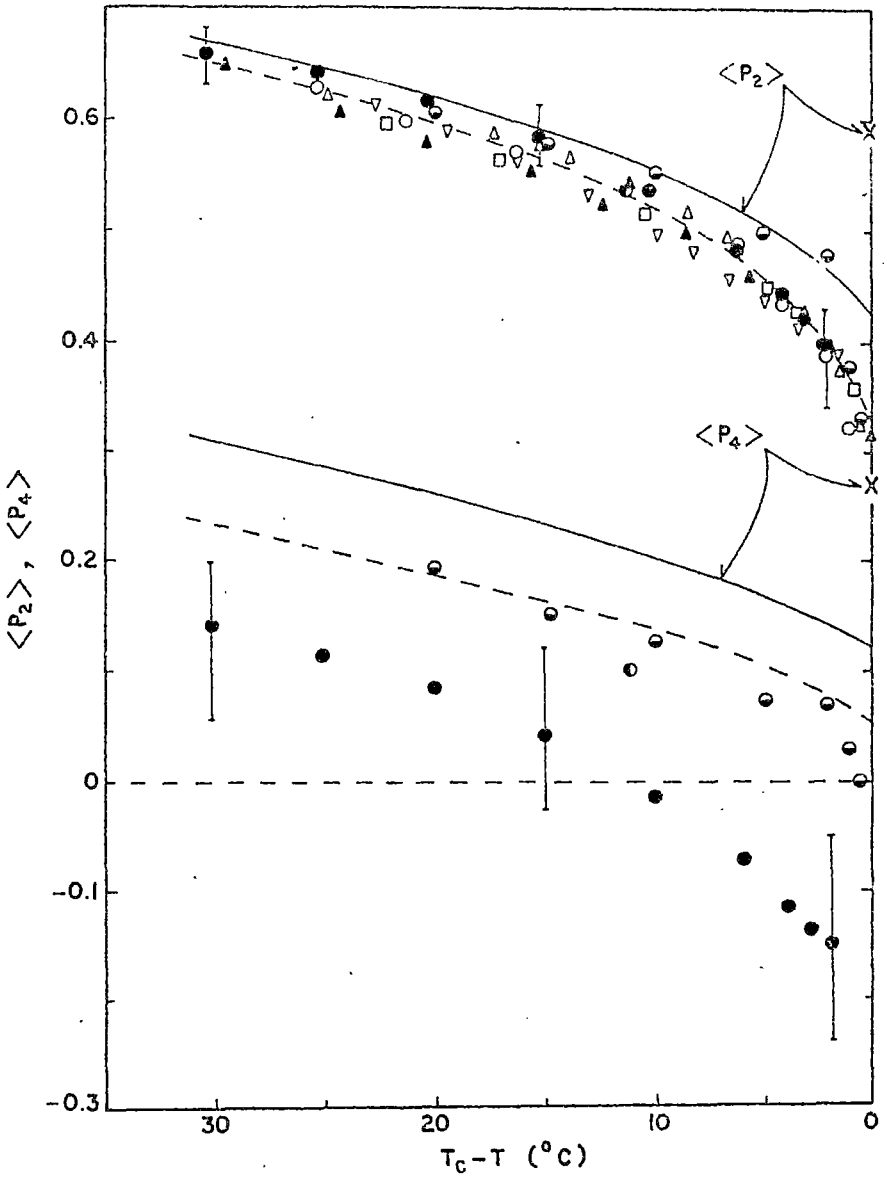

FIG. 6.4.

Theoretical and experimental values of nematic order parameters $\langle P_2(\cos\theta) \rangle$ and $\langle P_4(\cos\theta) \rangle$

Solid line - Theoretical results of simple mean field theory[6];

Dashed line - Theoretical results of HJL theory[7]; with $\lambda = 0.55$ and $\sqrt{=}10$

Crosses - Onsagar-Lakatos theory[8],

Filled circles - Raman scattering measurement[1] on MBBA

Open circles - NMR data on partially deuterated MBBA[9];

Squares - Relative values obtained from the measurement of optical anisotropy[1,10] of MBBA.

Triangles - Relative values obtained from the measurement of diamagnetic anisotropy of MBBA (Inverted triangles[11]; Open triangles[12]; filled triangles[13]).

◒ Data obtained from resonance Raman effect[2] on MBBA.

◐ Data obtained from present X-ray diffraction studies on MBBA.

Putting these values in the expression for pseudopotential we get

$$V(\beta)/k = -(2600)\langle P_2\rangle P_2(\cos\beta) + (7000)\langle P_4\rangle P_4(\cos\beta)$$

From the value of the order parameter it seems that single domain sample has been formed by alignment.

We have tried to determine the linear part of the intermolecular potential $V(r)$ between the two parallel molecules of MBBA as a function of distance (r), near the potential minimum by the following procedure.

The average number of molecules parallel to a molecule and at a distance between r and $r + dr$ from it is approximately given by

$$f(r)dr = 2\pi r \exp\left[-\frac{V(r)}{kT}\right] dr,$$

where, r is near the potential minimum disregarding the potential due to interaction of the other molecules. Now, the X-ray diffraction intensity distribution along the equatorial direction after correction for polarization factor and background correction is approximately proportional to the number of parallel molecule pairs (pointing to the mean field direction) at a distance r where θ' and r are related by the Bragg am condition. Polarization correction is made by using the formula $I_2 = I_1 \left[\frac{1}{2}\cos^2\theta' + \frac{1}{2}\right]$ where I_1 is the X-ray intensity converted from a O.D. value. Intensity after back-

ground correction is denoted by I and which is made by eliminating the intensity due to empty glass capillary sample holder. Table 6.5 includes the distance from the central spot, corresponding Bragg angle θ', Intensity values I_1 , I_2 and I and also the intermolecular distance r in Å.

The variation of intensity I with r is shown in fig. 6.5. The X-ray intensity distribution has been utilized to derive the intermolecular potential as a function of near potential minimum. $\left[V(r) = \frac{\log I(r)\, kT}{\langle P_2 \rangle}\right]$ The variation of potential V (r) with r near the potential minimum is shown in the fig. 6.6. The values r and corresponding I (r) taken from the graph 6.5 are given table 6.6. This table also includes the corresponding V (r) values.

No exact mathematical expression for the value of V (r) has been given so far, and we have not tried to formulate it. Anyway from the nature of the graph it can be inferred that there is anharmonicity in the intermolecular potential.

As MBBA breaks down very easily it was not possible to take X-ray diffraction photographs at other temperatures.

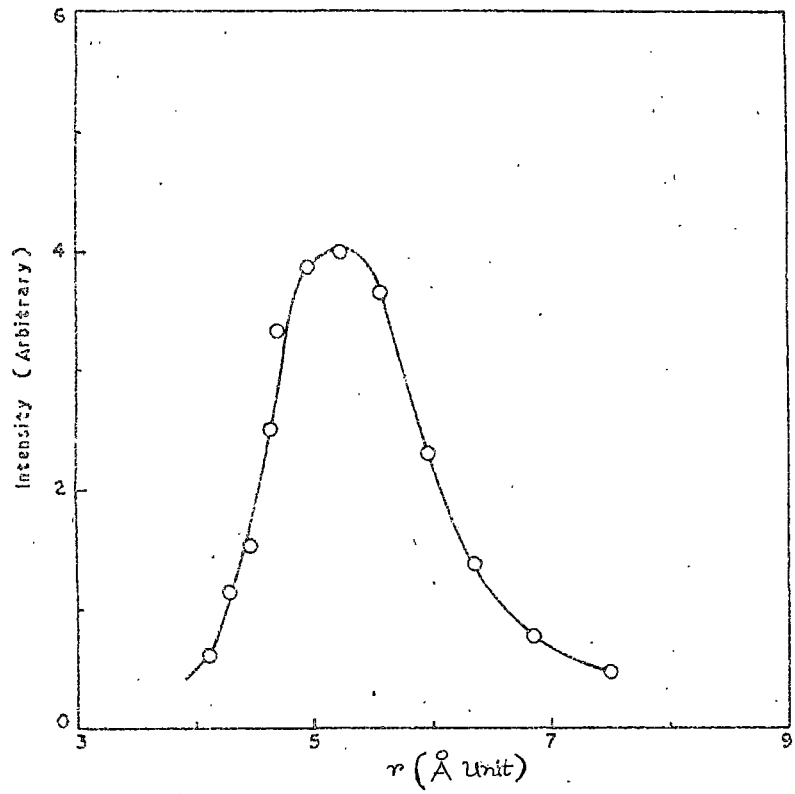
Intensity (Arbitrary)
6
4
2
0
3
5
7
9
r (Å Unit)

FIG. 6.5.

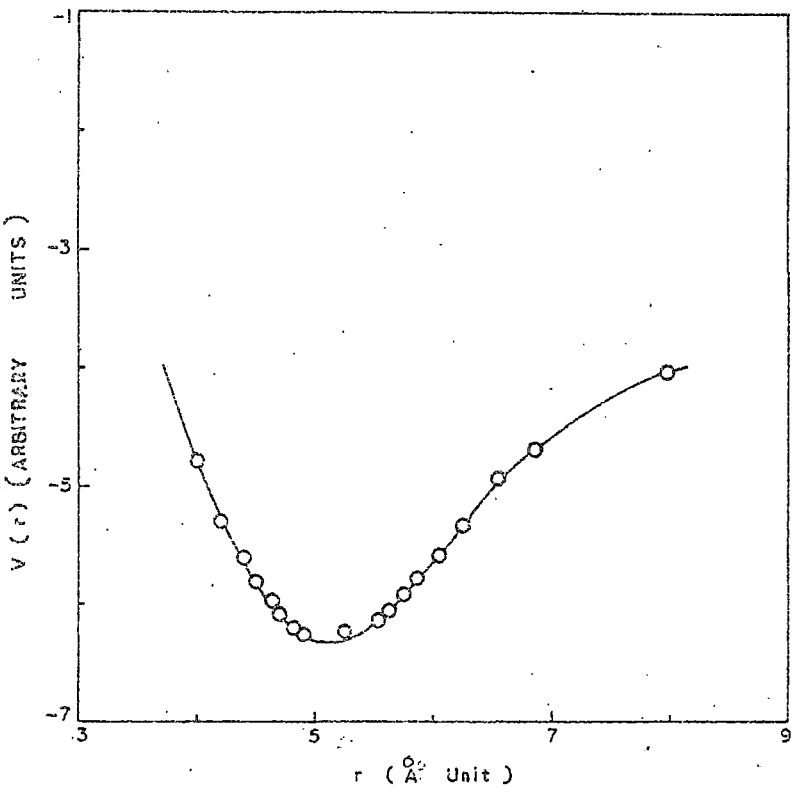
V (r) (ARBITRARY UNITS)
-1
-3
-5
-7
3
5
7
9
r (Å Unit)

FIG. 6.6.

TABLE 6.1

Sample: MERA. Temperature = 30°C, Background Optical Density 0.45.

LINEAR SCANNING						ANGULAR SCANNING		
L in cm.	O. D.	Intensity	L in cm.	O.D.	Intensity	θ in (deg.)	O. D.	Intensity.
OUTER HALO.			4.35	0.14	1.5	0	0.19	2.1
6.8	0.22	2.4	4.3	0.31	3.6	10	0.19	2.1
6.7	0.25	2.8	4.25	0.49	6.3	25	0.19	2.1
6.6	0.29	3.3	4.2	0.85	13.3	30	0.19	2.1
6.5	0.33	3.8	4.15	—	—	40	0.2	2.2
6.45	0.37	4.4	4.1	—	—	50	0.23	2.6
6.4	0.39	4.8	4.05	—	—	60	0.25	2.8
6.35	0.42	5.2	4.0	—	—	70	0.30	3.4
6.3	0.45	5.7	3.95	1.06	18.8	80	0.36	4.2
6.25	0.47	6.0	3.85	0.61	8.4	90	0.41	5.05
6.2	0.49	6.3	3.75	0.52	6.8	100	0.45	5.7
6.15	0.50	6.4	3.65	0.48	6.1	106	0.46	5.8
6.1	0.50	6.4	3.45	0.42	5.2	108	0.465	5.9
6.05	0.49	6.3	3.35	0.40	4.9	110	0.48	6.1
6.0	0.47	6.0	3.25	0.375	4.5	112	0.47	6.0
5.95	0.39	4.9	3.15	0.35	4.1	120	0.44	5.6
5.9	0.42	5.2	3.05	0.34	4.0	130	0.39	4.8
5.85	0.39	4.8	3.0	0.33	3.8	140	0.35	4.1
5.8	0.36	4.3	2.9	0.315	3.6	150	0.30	3.4
5.75	0.34	4.0	2.85	0.32	3.7	160	0.26	2.9
5.7	0.32	3.7	2.8	0.32	3.7	170	0.23	2.6
5.65	0.31	3.6	2.75	0.32	3.7	180	0.22	2.4
5.6	0.30	3.4	2.7	0.33	3.8	190	0.2	2.2
5.55	0.29	3.3	2.65	0.33	3.8	200	0.2	2.2
5.5	0.29	3.4	2.6	0.34	4.0	210	0.2	2.2
5.45	0.29	3.4	2.55	0.35	4.1	215	0.21	2.3
5.4	0.30	3.5	2.5	0.37	4.4	225	0.24	2.7
5.35	0.305	3.6	2.45	0.39	4.8	240	0.30	3.4
5.3	0.31	4.0	2.4	0.42	5.2	250	0.35	4.1
5.2	0.34	4.1	2.35	0.45	5.9	260	0.42	5.2
5.15	0.35	4.3	2.3	0.48	6.1	270	0.47	6.0
5.1	0.365	4.6	2.25	0.50	6.4	275	0.49	6.3
5.05	0.38	4.6	2.2	0.51	6.6	280	0.50	6.4
5.0	0.40	4.9	2.15	0.53	7.0	284	0.51	6.6
4.95	0.41	5.1	2.1	0.53	7.0	286	0.51	6.6
4.9	0.42	5.4	2.05	0.52	6.8	290	0.51	6.6
4.8	0.43	5.5	2.0	0.50	6.4	296	0.50	6.4
4.75	0.44	5.6	1.95	0.48	6.1	300	0.48	6.1
4.7	0.44	5.6	1.9	0.45	5.7	310	0.42	5.2
4.65	0.44	5.6	1.8	0.41	5.1	320	0.36	4.3
4.6	0.44	5.6	1.7	0.35	4.1	330	0.31	3.6
4.55	0.42	5.4	1.6	0.31	3.6	335	0.29	3.3
4.5	0.39	4.8	1.5	0.28	3.2	340	0.26	2.9
4.45	0.31	3.6				345	0.25	2.8
4.4	0.20	2.2				350	0.23	2.6

TABLE 6.2

Sample: MBBA.

Intensity and Normalized distribution function values.

θ/β (deg.)	$I(\theta)$	Calculated $I(\theta)$	$f(\beta)$	Calculated $f(\beta)$
0	4.2	4.169	5.266	5.595
5	4.05	4.084	5.117	5.353
10	3.84	3.85	4.727	4.444
15	3.53	3.515	4.213	3.706
20	3.13	3.123	3.674	3.357
25	2.68	2.697	3.133	3.225
30	2.26	2.255	2.583	2.946
35	1.85	1.827	2.038	2.310
40	1.40	1.448	1.551	1.556
45	1.18	1.140	1.171	1.017
50	0.89	0.891	0.898	0.75
55	0.65	0.674	0.686	0.656
60	0.48	0.471	0.494	0.591
65	0.30	0.290	0.313	0.415
70	0.14	0.149	0.163	0.179
75	0.06	0.06	0.066	0.047
80	0.01	0.016	0.018	0.010
85	0	0.001	0.002	0.003
90	0	-0.003	0.002	0

TABLE 6.3

Sample: MBBA.

Order Parameter Values.

Temp. °C.	Temp. °K.	$\langle P_2 \rangle_V$	$\langle P_2 \rangle$	$\langle P_2 \rangle_{M.F}$	$\langle P_4 \rangle_V$	$\langle P_4 \rangle$	$\langle P_4 \rangle_{M.F}$
30	303	0.51	0.53	0.54	0.09	0.12	0.22

TABLE 6.4

Sample: MBBA.

a_L and b_L (L = 2 and 4) values.

Temp. °C.	Temp. °K.	a_0	a_2	a_4	a_6	a_8	a_{10}	b_2/k	b_4/k
30	303	-1.479	4.594	-2.823	2.355	-1.897	1.007	−2626	7128

TABLE 6.5.

Sample: MBBA.

Actual sample to film distance = 5.833 cm

Distance from the spot in cm.	Bragg angle $\theta/$ (deg.)	Intensity I_1	Intensity I_2	Intensity I	Intermolecular distance in Å
1.375	6.632	3.3	3.192	0.49	7.46
1.5	7.211	3.5	3.616	0.765	6.86
1.625	7.784	4.0	4.155	1.355	6.36
1.75	8.350	4.85	5.068	2.318	5.93
1.875	8.91	6.0	6.309	3.653	5.56
2.0	9.463	6.4	6.583	3.983	5.24
2.125	10.009	6.0	6.398	3.848	4.95
2.25	10.547	4.95	5.318	3.318	4.70
2.375	11.077	3.8	3.952	1.502	4.48
2.5	11.599	3.225	3.52	1.15	4.28
2.625	12.115	2.65	2.918	0.618	4.10

TABLE 6.6

Sample: MBBA.

Intensity (I) - Intermolecular distance and Intermolecular potential.

I	r in Å	$V(r)$ x 10^{-12}
0.5	4.0	-4.783
1.0	4.25	-5.294
1.5	4.4	-5.593
2.0	4.5	-5.807
2.5	4.625	-5.966
3.0	4.7	-6.099
3.5	4.825	-6.203
3.75	4.9	-6.246
4.0	5.25	-6.243
3.75	5.55	-6.146
3.5	5.625	-6.079
3.25	5.7	-6.009
3.0	5.75	-5.937
2.5	5.855	-5.775
2.0	6.05	-5.668
1.5	6.25	-5.31
1.0	6.55	-4.944
0.75	6.855	-4.675
0.5	7.98	-4.225

References

1. Jen Shen, A. Noel, P.S. Clark and E.B.Priestley, Phys. Rev. Lett. 31 p. 1552 (1973).
2. Shunsuke, Kabinata, Yuko Nakajima, Hiroshi Yoshida and Shir Maeda, Mol.Cryst.Liq.Cryst. 66, 387 (1981).
3. T. Takenchi, H. Terauchi, K. Nakatsu and H. Maryama: Jap. J. Appl. Phys. 13, p. 203 (1974).
4. Basana Bhattacharjee, Sukla Paul and Ranjit Paul, Presented at Ninth International Conference on Liquid Crystals, Bangalore, India (1982). Abstract No. B-21-P
5. Basana Bhattacharjee, Ranjit Paul and Sukla Paul, Jap. J. Appl. Phys. Vol. 18, No. 5; (1979).
6. P.J.Wojtowicz, Introduction to liquid crystals. Chap.4, Ed. E.B. Priestley, Plenum Press (1974).
7. R.L.Humphries, P.G.James and G.R.Luckhurst, J.Chem.Soc. Faraday Trans. II, 68, 1031 (1972).
8. K. Lakatos, J. Status Phys. 2, 121 (1970).
9. Y.S. Lee, Y.Y.Hsu, and D. Dolphin, Presented at the American Chem.Society Symposium on ordered fluids and liquid crystals, Chicago, Illinois (1973).
10. N.V.Madhusudan, R.Sashidhar and S.Chandrasekhar, Mol. Cryst.Liq.Cryst. 13, 61, (1971).
11. P.I. Rose, Presented at the fourth International Liquid Crystal Conference, Kent State University, Kent, Ohio (1972).
12. I. Haller, J.Chem. Phys. 57 1400 (1972).
13. G. Sigaud and Gasproux, J.Chem.Phys. Physicochim Biol. 70, 669 (1973).

CHAPTER 7.

X-RAY DIFFRACTION STUDIES OF 4-CYANOPHENYL-4'-n-HEPTYL BENZOATE IN THE NEMATIC PHASE (CPHB IN SHORT) IN MAGNETIC FIELD.

CHAPTER 7.

X-RAY DIFFRACTION STUDIES OF 4-CYANOPHENYL-4'-n-HEPTYL BENZOATE IN THE NEMATIC PHASE (CPHB IN SHORT) IN MAGNETIC FIELD

1. Introduction

The structure of CPHB has been given in chapter 2.

According to the literature[1] CPHB has the transition temperatures

$$C \xrightarrow{43.5^{\circ}C} N \xrightarrow{56^{\circ}C} I$$

The temperatures as determined by us from X-ray diffraction and texture studies are identical to these although the nematic phase can be supercooled to 33°C i.e. the transition path is

$$C \underset{\sim 33^{\circ}C}{\overset{43.5^{\circ}C}{\rightleftharpoons}} N \overset{56^{\circ}C}{\rightleftharpoons} I$$

Orientational distribution function and order parameters values of CPHB by X-ray diffraction have not been reported so far. In this chapter details of intermolecular distance, degree of ordering in different magnetic field strength, apparent length of the molecule, orientational distribution function and order parameters of aligned sample of CPHB have been reported.

The details of experimental procedure has been discussed in chapter 2.

The X-ray diffraction photographs of the sample were taken at different temperatures starting from the solid phase at room temperature to the isotropic phase and also at supercooled nematic phase. The photographs of the unoriented sample were taken in the set up No.1 described in chapter 2 and the photographs of oriented samples were taken in presence of

magnetic field in the set up No. 3 (Chapter 2). Photographs were also taken at a particular temperature with the variation of the magnetic field strength in order to get an idea about the magnitude of the field needed for complete alignment.

2. Results and Discussions.

Two typical photographs of OPHB at the unoriented and oriented state at temperature 34°C, are shown in fig. 4.1 and fig. 4.2 respectively. The photographs of the oriented sample have two diffuse outer maxima and two inner maxima perpendicular to the outer ones- the direction of the preferred orientation of the molecule is along the line of the magnetic field $\bar{H}$, and the incident X-ray beam is perpendicular to the plane of the paper. The optical densities obtained from densitometric scanning as described in chapter 4 both for linear and angular positions for all the temperatures are given in table 7.1 - 7.18. In case of angular scanning the converted intensity values of the corresponding optical densities are also produced in those tables. The method of conversion of optical density into intensity has been described in chapter 2. For conversion the graph No.2.3 is used.

Average Intermolecular distance, apparent length of the molecule and degree of ordering.

Average intermolecular distance 'D' and the apparent molecular length 'l' are calculated by using the formula 3.1 (with K = 1.117 and 1 respectively as described in chapter 3).

Calculation for 'D' requires the diameter of the outer crescents/halo which is measured by the distance between the two intensity maxima and for 'l' the diameter of the inner ring is required.

In table 7.19 D and l values are given against different

temperatures along with the diametrical distance between outer maxima and inner maxima and the corresponding Bragg angles. The sample to film distance is given above the table.

The variation of D with temperature is shown in Fig.7.1 and the variation of ℓ with temperature is shown in Fig. 7.2. The temperature dependence of these parameters has been discussed by de Vries[2,3]. From the fig. 7.1 it can be observed that 'D' increases with temperature and remains fairly constant in the supercooled region. The experimental uncertainty for the measurement of D is nearly ± 0.05 Å near 5 Å. The dependence of on temperature is not very clear, it varies between 27 Å to 29 Å. Experimental uncertainty in the measurement of ℓ near 25 Å is $\pm$ 1.25 Å. With the help of stereomodel units (Prentice Hall,Inc, West Nyack, New York 10984) we have constructed a possible conformation for CPHB and measured the molecular length L in its completely extended form. This gives L = 21 Å. The value is seen to be much smaller than the experimental value which is attributed to the antiparallel association of the molecule in the nematic phase. It has been found that cyano compounds with alkyl a end groups have very large dipole moment along their major axis. The antiparallel ordering of the molecule may be due to dipole-dipole interactions. Similar results have been observed from X-ray diffraction studies by Leadbetter[4] and Lydon[5].

The table 7.20 shows the intermolecular distance and the degree of ordering at different magnetic fields at temperature 50°C. The variation of 'D' with different magnetic field is shown in the fig. 7.3 and fig. 7.4 represents the degree of ordering (not order parameter) calculated by Leadbetters methods[6]. From the graph (Fig. 7.3) it is found that for

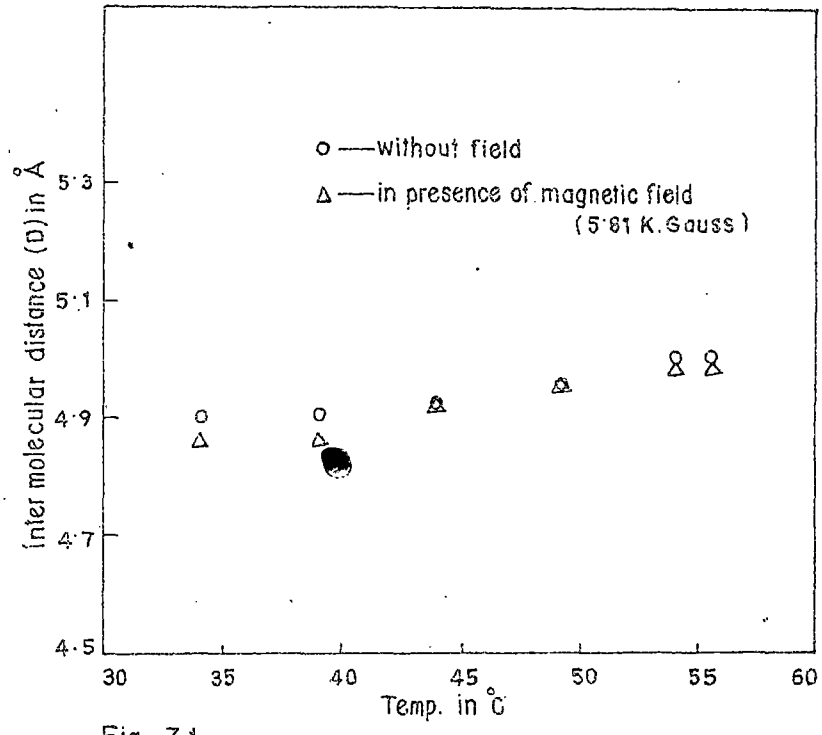
o —without field
Δ —in presence of magnetic field
(5·81 K.Gauss)
Inter molecular distance (D) in Å
5·3
5·1
4·9
4·7
4·5
30
35
40
45
50
55
60
Temp. in °C

Fig. 7·1

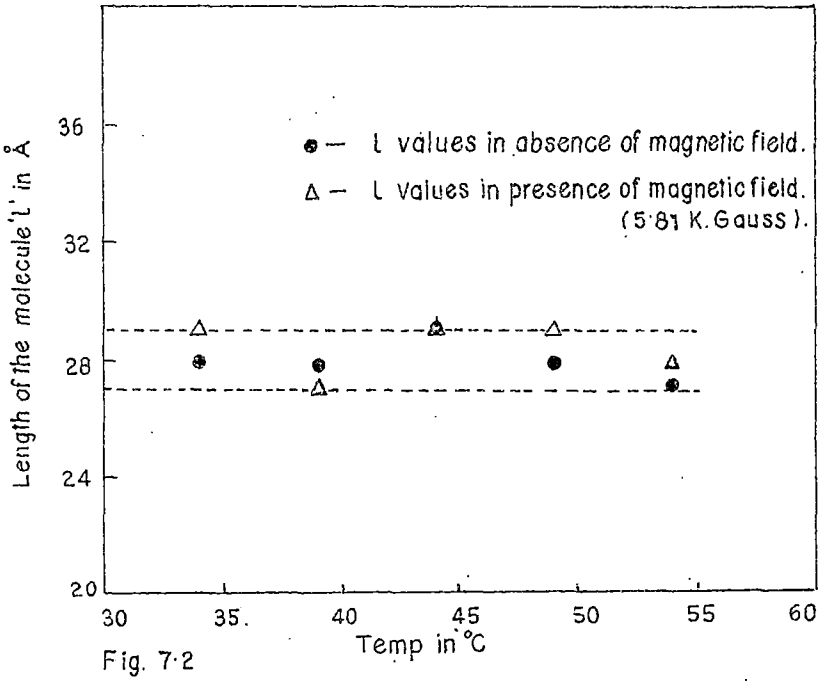
● — l values in absence of magnetic field.
Δ — l values in presence of magnetic field.
(5·81 K.Gauss).
Length of the molecule 'l' in Å
36
32
28
24
20
30
35
40
45
50
55
60
Temp in °C

Fig. 7·2

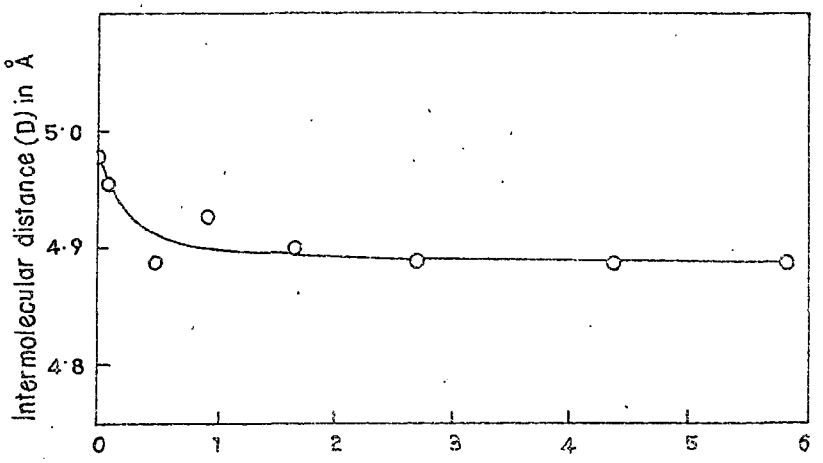

Fig. 7·3 Field in Kilo Gauss.

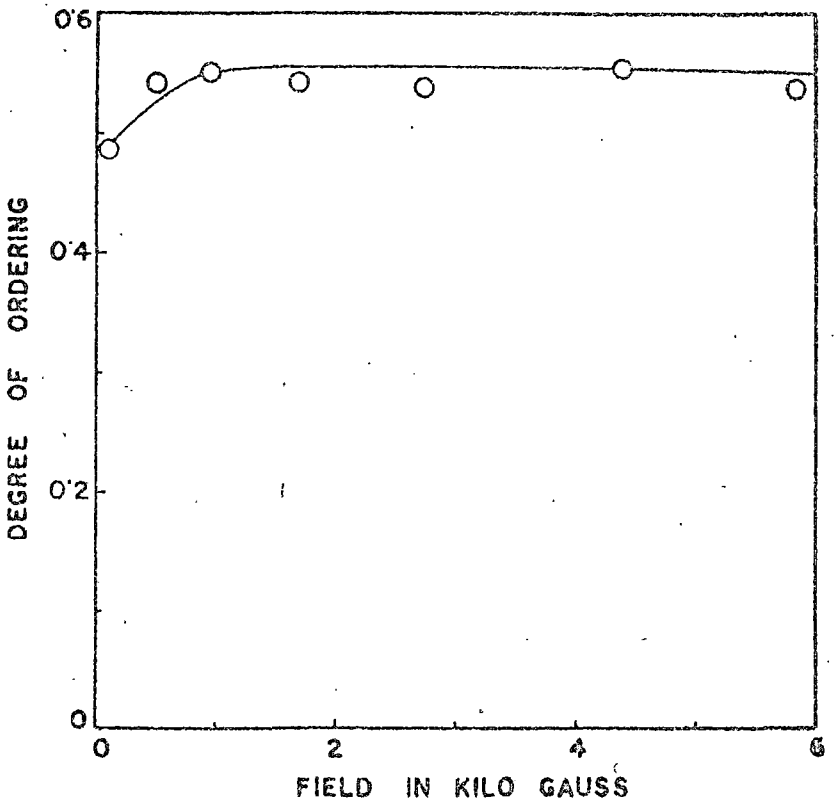

Fig. 7·4

a particular temperature D values decreases slightly with magnetic field. At lower magnetic fields the D value decreases and at about 0.9 K.Gauss attains a saturation value which is indicated by the graph 7.3. From the fig. 7.4 it is found that the ordering increases rapidly with increasing magnetic field H and reaches maximum value at the same field i.e. 0.9 K. Gauss. The sample as a whole consists of large number of domains, the molecule in each domain being ordered with the ordering characterized by the order parameter of the substance at the particular temperature concerned. But in absence of external field the director of domains themselves are randomly oriented. When an external field is applied the bulk sample becomes partially ordered with the increase in size of the domains. With the increase in field strength ordering increases and thus we get an idea about degree of ordering. For sufficiently strong magnetic field, we get monodomain sample i.e. the domain size becomes maximum extending throughout the sample, so that the average degree of ordering of the whole sample reaches a maximum value or saturation value, i.e. the order parameter of the substance at particular temperature.

Intensity Distribution, Orientational Distribution Function and order parameters:-

The O.D. obtained from angular scanning are converted to intensity values from the calibration curve (Fig. 2.3). Following the procedure mentioned in chapter 2, background correction for intensity has been done for each of the four

quadrant from the angle-intensity graph. At the maximum intensity position the angle is taken to be equal to zero, and then after 5° interval of θ , I (θ) was determined. The mean of the four intensity values for the four quadrants for each θ from (0° - 90°) was determined for each film. These θ versus I(θ) values at different temperatures at strong magnetic field (5.8 K.Gauss) are given in Table 7.21.

The calculated intensity values against θ are given in Table 7.22. A nearly perfect agreement is obtained between the experimental and calculated intensity values. The calculated intensity values are obtained from the least square fitting with eqn. 3.4 with the series truncated after eight terms.

The Table 7.23 gives the normalised distribution function $f(\beta)$ at angle β with respect to the director. The appearance of some negative $f(\beta)$ values are due to truncation errors. However, those negative values and 0 values are omitted with computer programme for the calculation of a_L values in eqn. 3.13. Using the a_L values we have obtained calculated $f(\beta)$ values. The calculated $f(\beta)$ values are also given in table 7.24. The coefficient a_L and the order parameter calculated with the distribution function are given in Table 7.25.

The percentage errors calculated for a_L values are given in chapter 3.

The normalised distribution function $f(\beta)$ Vs β at different temperatures are shown in fig. 7.5. As expected the distribution functions broadens at high temperatures.

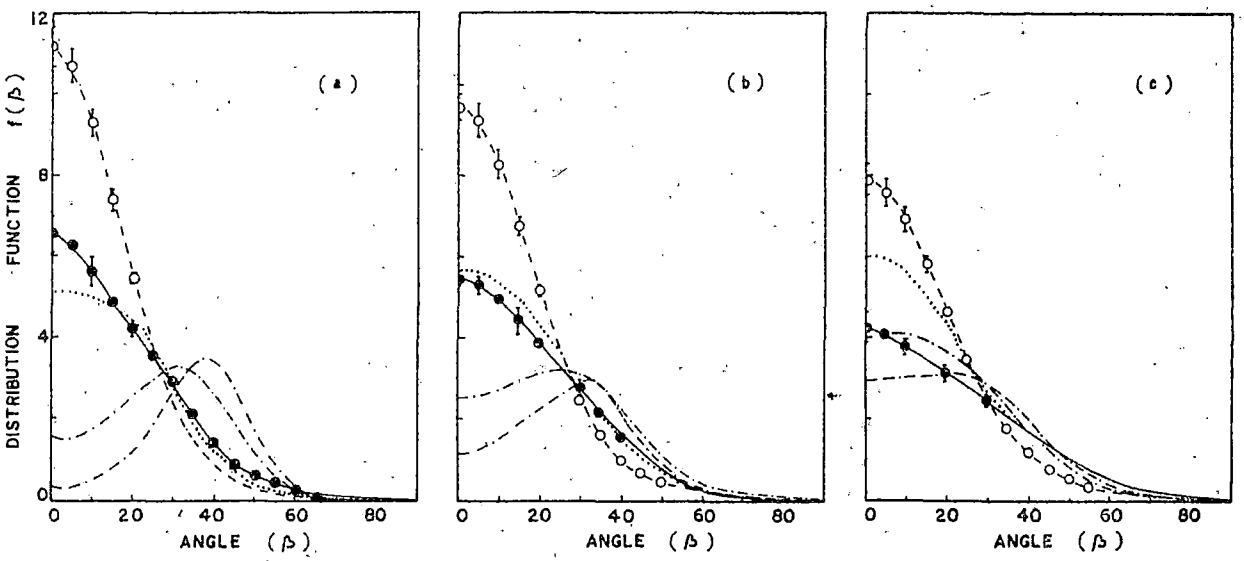

Fig. 7.5. Normalized orientational distribution function $f(\beta)$ against β, (*a*) at 39°C, (*b*) at 49°C, (*c*) at 55·5°C. —●—●—●— Calculated $f(\beta)$ from X-ray intensity data. —ϕ—ϕ—ϕ— Calculated $f(\beta)$ from the Maier–Saupe molecular field potential $\mathbf{V}(\beta)k^{-1} = -(2130 \pm 90)\bar{P}_2P_2(\cos\beta)$. Calculated $f(\beta)$ from a pseudo-potential containing the $P_4(\cos\beta)$ term for ..... $\mathbf{V}(\beta)k^{-1} = -(2130)\bar{P}_2P_2(\cos\beta) + (4070 + 2280)\bar{P}_4P_4(\cos\beta)$. —·—·—·—·— $\mathbf{V}(\beta)k^{-1} = -(2130)\bar{P}_2P_2(\cos\beta) + (4070)\bar{P}_4P_4(\cos\beta)$, – – – – $\mathbf{V}(\beta)k^{-1} = -(2130)\bar{P}_2P_2(\cos\beta) + (4070 - 2280)\bar{P}_4P_4(\cos\beta)$.

$\langle P_2 \rangle$ & $\bar{P}_2$ are equivalent, $\langle P_4 \rangle$ & $\bar{P}_4$ are equivalent.

The temperature dependence of order parameters $\langle P_2 \rangle$ and $\langle P_4 \rangle$ is shown in the fig. 7.6 together with the Maier-Saupe mean field predictions[7]. This fig. includes the order parameter values calculated by Vainshtein's approximation[6], i.e. $\langle P_2 \rangle_v$ and $\langle P_4 \rangle_v$ and also the $\langle P_2 \rangle$ values of OPHB from refractive index data as determined by Zeminder et al[9]. The mmk order parameter values are estimated to be accurate within $\pm$ 0.02. $\langle P_2 \rangle$ and $\langle P_4 \rangle$ values are always greater than the $\langle P_2 \rangle_v$ and $\langle P_4 \rangle_v$ values as predicted by Vainshtein. Although the Maier-Saupe predictions show the same qualitative behaviour as measured quantities there are significant quantitative descripancies. $\langle P_2 \rangle$ is found to be larger than that predicted by the M-S theory. Such differences were found by Leadbetters and Norris[6] for 4,4-di-n-heptyloxyazoxybenzene and 4,4'-di-n-octyloxyazoxy-benzene. Short range dipole-dipole interactions may increase the value of $\langle P_2 \rangle$. The $\langle P_4 \rangle$ value is significantly lower than the M-S predictions. Such behaviour of $\langle P_4 \rangle$ has already been observed in some liquid crystals[10,11]. In certain cases, values of $\langle P_4 \rangle$ are even found to be negative. The order parameter values at different temperatures are given in table 7.26.

Pseudopotential:-

The eqn. 3.14 is used for the calculation of pseudopotential.

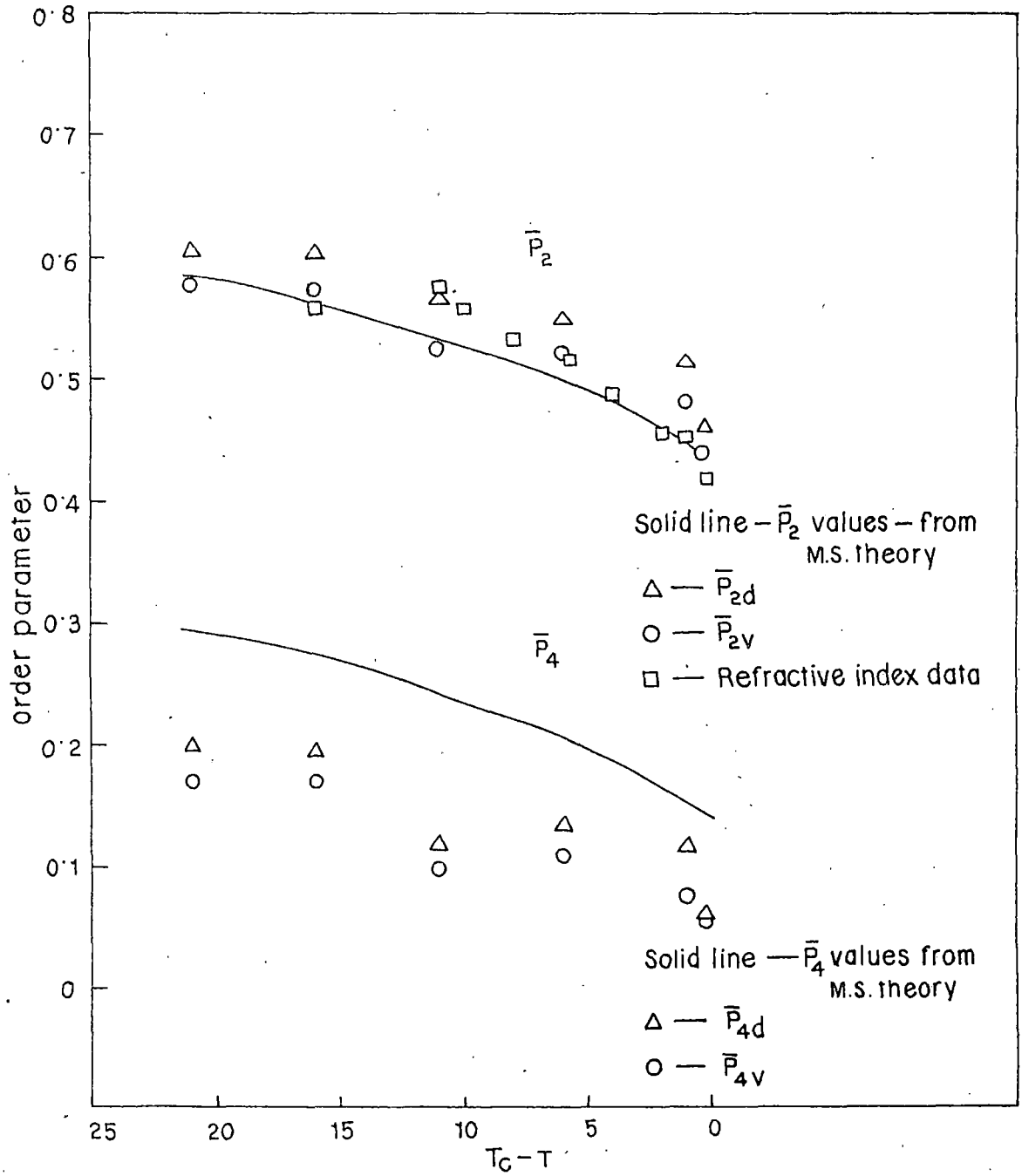

Fig. 7·6 $\langle P_2 \rangle$ and $\bar{P}_2$ are equivalent.
$\langle P_4 \rangle$ and $\bar{P}_4$ are equivalent.

The coefficients b_L can be calculated by using the relation ($b_L = -k\alpha_L T/\langle P_L \rangle$) as given in chapter 3 and we have done so for b_2 and b_4 (cf. the last two columns of the table 7.25). It is expected that b_L should be a function of the average intermolecular separation, which in turn depends upon temperature. Hence, since we are confined to a narrow range of temperature ($\sim 20°C$) and the cubic expna expansibility is expected to be small (except perhaps near the transition) we can treat the b_Ls as constants. Indeed the b_2 values are observed to be almost constant and show no systematic variation with temperature. On the other hand the b_4 values do show a systematic variation with temperature which is especially prominent near the transition temperature. We do not know why b_4 should show so large a temperature variation while b_2 is almost constant. This may be related to the pair potential between the CPMB molecules. These have large permanent dipole moments and so pair potential has a large contribution from permanent dipole-permanent dipole interaction.

This anomaly in the temperature dependence of b_2 and b_4 is quite unexpected, since according to theory[12] both these coefficients should vary directly with density, which in the narrow temperature range concerned is almost constant.

The xx temperature variation of b_4 shows quite clearly that the extension of the Maier-Saupe theory does not account for the behaviour of CPMB. This conclusion may be demonstrated in another way. If we neglect the temperature variation of b_4, and take the average over six temperatures, we can write the

angular part of the pseudopotential upto the $P_4(\cos\beta)$ term keeping the last one digit in round numbers) as

$$V(\beta)/k = -(2130 \pm 90)\langle P_2\rangle P_2(\cos\beta) + (4070 \pm 2280)\langle P_4\rangle P_4(\cos\beta) \quad \ldots(1)$$

The large standard deviation of b_4 is caused by its temperature variation. Since, the temperature variation of density is greater near the transition temperature we also tried to calculate the pseudopotential by taking an average over four temperature (neglecting the value of 54°C & 55.5°C). This gives

$$V(\beta)/k = -(2110 \pm 100)\langle P_2\rangle P_2(\cos\beta) + (2970 \pm 1240)\langle P_4\rangle P_4(\cos\beta)$$

The standard deviation of b_4 though reduced from the previous expression, is unreasonably large. In our paper on CPMB[13(a)] there are some errors in the a_L values and consequently $b_{L/k}$ and $V(\beta)/k$ values also included some errors. However, we have corrected those values in this chapter.

Normalised distribution function $f(\beta)$ value have also been calculated by using the pseudopotentials in eqn.1 as well as from same potential but neglecting the $P_4(\cos\beta)$ terms. Our results from three different temperatures 39°C, (312°K), 49°C (322°K) and 55.5°C (328.5°K) are shown in ~~figures~~ figure 7.5 (a, b, c). We find that by retaining only the $P_2(\cos\beta)$ term in the pseudopotential (Kaier-Saupek theory) the value of $f(\beta)$ calculated are in poor ~~agreement~~ agreement with the values determined

from the X-ray data. Including $P_4(\cos\beta)$ terms in the potential[13] improves the agreement, however, nothing definite can be said due to large uncertainty in b_4. The need to include the $P_4(\cos\beta)$ term may however, not stem from their presence in the pair potential, but from the failure of the molecular field approximation as applied in the Maier-Saupe theory[14].

In conclusion, the orientational distribution function obtained by us from the X-ray diffraction data do not agree well with the distribution function generated from the commonly accepted molecular field potential even after including the $P_4(\cos\beta)$ term. The descripancy may have various causes.

Firstly it may be due to the particular pseudopotential used, for example it has been shown by Humphries, James and Luckhurst[13] that under true cylindrical symmetry of the mesophase the pseudopotential will contain terms of the type $P_L\langle P_M\rangle$ ($L \neq M$) which are not generally included in the potential. Secondly, the permanent dipole-permanent dipole interaction potential may modify pseudopotential in this case. Chandrasekhar et al[15] have included the dipole-dipole interaction in the potential and it is clear that the form of the orientational distribution function will depend upon this potential. Thirdly the rigid cylindrical shape of the molecule assumed is obviously an over simplification. However, although an attempt has been made by Marcelja[16] to allow for the molecular flexibility the theory has not been used to evaluate the distribution function available from X-ray scattering experiment.

TABLE 7.1

Sample - CPHB, Mag.Field = Nil
Temperature 34°C.

L I N E A R S C A N N I N G

L in cm.	O.D.	L in cm.	O.D.
		2.5	0.465
OUTER HALO		2.4	0.47
		2.3	0.485
7.0	0.435	2.0	0.53
6.8	0.462	1.85	0.565
6.6	0.51	1.775	0.572
6.5	0.53	1.725	0.575
6.425	0.532	1.5	0.54
6.35	0.532	1.35	0.508
6.325	0.531	1.225	0.47
6.3	0.53		
6.15	0.512	INNER HALO	
6.0	0.498		
5.9	0.47	5.0	0.45
5.6	0.462	4.8	0.472
5.5	0.465	4.6	0.552
5.4	0.47	4.5	0.60
5.2	0.48	4.45	0.65
5.0	0.48	4.4	0.625
4.9	0.482	4.3	0.39
4.7	0.502	4.2	0.455
4.5	0.542	4.1	0.665
4.45	0.54	4.05	0.70
4.4	0.535	4.0	0.58
4.3	0.365	3.9	0.37
4.1	0.585	3.8	0.62
4.05	0.75	3.75	0.64
4.0	0.555	3.7	0.605
3.9	0.37	3.6	0.525
3.8	0.53	3.5	0.478
3.7	0.545	3.25	0.44
3.6	0.525	3.0	0.43
3.45	0.49	2.8	0.42
3.3	0.478		
3.2	0.472		
3.0	0.472		
3.1	0.472		
2.8	0.47		
2.6	0.468		

TABLE 7.2

Sample - CPHB, Mag.Field = Nil
Temperature 39°C.

L I N E A R S C A N N I N G

L in cm.	O.D.	L in cm.	O.D.
		2.95	0.472
OUTER HALO		2.85	0.472
		2.70	0.47
7.0	0.45	2.5	0.47
6.8	0.492	2.35	0.47
6.6	0.532	2.2	0.48
6.5	0.56	2.1	0.492
6.45	0.571	2.0	0.51
6.35	0.571	1.95	0.515
6.3	0.568	1.9	0.53
6.2	0.558	1.85	0.535
6.0	0.595	1.8	0.542
5.8	0.49	1.75	0.548
5.6	0.482	1.725	0.546
5.4	0.48	1.6	0.54
5.3	0.485	1.5	0.525
5.1	0.49	1.3	0.482
5.0	0.49	1.2	0.465
4.9	0.498		
4.7	0.505	INNER HALO	
4.5	0.555		
4.475	0.565	5.0	0.472
4.45	0.562	4.8	0.485
4.3	0.47	4.6	0.532
4.25	0.38	4.50	0.57
4.225	0.375	4.45	0.585
4.2	0.438	4.375	0.585
4.1	1.1	4.35	0.555
4.05	1.2	4.3	0.51
4.0	1.12	4.225	0.40
3.95	0.50	4.2	0.615
3.9	0.38	4.1	1.02
3.8	0.54	4.0	0.7
3.75	0.56	3.85	0.47
3.725	0.55	3.75	0.535
3.6	0.52	3.70	0.561
3.5	0.508	3.65	0.56
3.3	0.48	3.6	0.538
3.1	0.475	3.5	0.512
		3.4	0.492
		3.2	0.475
		3.0	0.475

TABLE 7.3

Sample - CPHB, Mag.Field = Nil
Temperature = 44°C

L I N E A R S C A N N I N G

L in cm.	O.D.	L in cm.	O.D.
		2.7	0.455
OUTER HALO		2.5	0.452
		2.3	0.455
7.0	0.445	2.2	0.47
6.8	0.482	2.1	0.482
6.7	0.51	1.95	0.505
6.5	0.56	1.85	0.520
6.45	0.561	1.75	0.535
6.4	0.562	1.725	0.532
6.35	0.562	1.70	0.53
6.325	0.561	1.50	0.505
6.25	0.552	1.30	0.46
6.1	0.52	1.20	0.435
5.9	0.492		
5.7	0.478	INNER HALO	
5.6	0.478		
5.5	0.48	5.0	0.475
5.4	0.478	4.7	0.50
5.2	0.485	4.6	0.522
5.0	0.49	4.5	0.54
4.9	0.492	4.45	0.552
4.8	0.51	4.4	0.554
4.6	0.552	4.375	0.548
4.5	0.572	4.35	0.545
4.475	0.572	4.20	0.36
4.40	0.570	4.15	0.45
4.35	0.455	4.05	0.665
4.2	0.485	4.0	0.615
4.1	0.58	3.95	0.37
4.0	0.43	3.9	0.44
3.9	0.375	3.8	0.56
3.8	0.55	3.75	0.60
3.6	0.562	3.7	0.67
3.5	0.498	3.5	0.54
3.3	0.482	3.3	0.50
3.2	0.47	3.0	0.49
3.1	0.47	2.8	0.48
3.0	0.468		
2.9	0.462		
2.8	0.46		
2.7	0.455		
2.5	0.452		

TABLE 7.4

Sample - CPHB, Mag.Field = Nil
Temperature = 50°C

L I N E A R S C A N N I N G

L in cm.	O.D.	L in cm.	O. D.
		2.1	0.55
OUTER HALO		2.0	0.569
		1.9	0.59
7.0	0.515	1.85	0.599
6.8	0.555	1.825	0.61
6.6	0.605	1.70	0.605
6.5	0.63	1.65	0.60
6.45	0.638	1.5	0.572
6.4	0.638	1.3	0.51
6.35	0.635	1.25	0.50
6.3	0.632		
6.2	0.618	INNER HALO	
6.1	0.60		
6.0	0.57	5.0	0.515
5.9	0.555	4.8	0.53
5.7	0.53	4.7	0.555
5.6	0.525	4.6	0.59
5.5	0.525	4.5	0.615
5.3	0.53	4.45	0.66
5.1	0.53	4.425	0.668
5.0	0.528	4.4	0.658
4.8	0.53	4.3	0.549
4.7	0.538	4.2	0.44
4.5	0.55	4.1	0.84
4.3	0.428	4.0	0.77
4.2	0.385	3.9	0.385
4.15	0.495	3.8	0.615
4.1	0.73	3.725	0.65
4.05	0.78	3.7	0.645
4.0	0.605	3.6	0.615
3.95	0.38	3.5	0.565
3.8	0.538	3.4	0.505
3.7	0.572	3.2	0.5
3.5	0.545	3.1	0.49
3.3	0.512	2.9	0.482
3.1	0.508		
3.0	0.51		
2.8	0.508		
2.7	0.501		
2.5	0.501		
2.4	0.505		
2.2	0.53		

TABLE 7.5

Sample - CPHB, Magnetic Field = Nil, Temperature = 54°C.

L I N E A R S C A N N I N G

L in cm.	O.D.	L in cm.	O.D.
	OUTER HALO	2.9	0.47
		2.7	0.465
		2.5	0.462
7.0	0.46	2.3	0.48
6.8	0.485	2.1	0.50
6.7	0.505	1.95	0.515
6.6	0.53	1.85	0.535
6.5	0.552	1.725	0.542
6.45	0.56	1.7	0.538
6.4	0.565	1.6	0.53
6.35	0.568	1.4	0.50
6.325	0.57	1.25	0.46
6.30	0.572		
6.25	0.565	INNER HALO	
6.2	0.555		
6.1	0.54	5.0	0.492
6.0	0.53	4.8	0.50
5.9	0.51	4.6	0.54
5.7	0.49	4.5	0.552
5.5	0.47	4.45	0.562
5.375	0.48	4.4	0.561
5.3	0.485	4.3	0.448
5.1	0.49	4.2	0.40
5.0	0.49	4.1	0.638
4.8	0.492	4.0	0.745
4.6	0.495	3.95	0.365
4.5	0.52	3.9	0.365
4.3	0.54	3.8	0.53
4.1	0.38	3.75	0.555
4.05	0.565	3.7	0.555
4.0	0.699	3.65	0.552
3.95	0.52	3.6	0.538
3.9	0.355	3.5	0.51
3.7	0.515	3.25	0.488
3.6	0.53	3.1	0.48
3.5	0.51	3.0	0.48
3.4	0.49		
3.2	0.48		
3.0	0.478		

TABLE 7.6

Sample: CPHB, Mag.Field 0.19 Killogauss, Temperature 50°C
Background Optical density = 0.325

66

LINEAR SCANNING				ANGULAR SCANNIN		
L in cm.	O.D.	L in cm.	O.D.	θ in degree	O.D.	Intensity
OUTER HALO						
7.0	0.42	2.35	0.44	350	0.055	6.5
6.9	0.438	2.3	0.455	0	0.055	6.5
6.8	0.445	2.2	0.46	10	0.06	7.0
6.7	0.462	2.1	0.482	20	0.067	7.75
6.6	0.485	2.0	0.505	30	0.075	9.0
6.5	0.50	1.9	0.512	40	0.10	12.0
6.4	0.51	1.85	0.518	50	0.12	15.0
6.35	0.515	1.7	0.505	60	0.145	18.0
6.3	0.495	1.5	0.472	70	0.17	21.25
6.25	0.486	1.2	0.422	80	0.185	23.0
6.2	0.48			84.5	0.186	23.2
6.1	0.465	INNER HALO		87	0.185	23.0
6.0	0.45			90	0.18	22.5
5.8	0.435	5.0	0.42	100	0.167	21.0
5.6	0.43	4.8	0.445	110	0.15	18.75
5.45	0.43	4.7	0.465	120	0.12	15.0
5.4	0.432	4.6	0.482	130	0.091	11.0
5.25	0.435	4.5	0.55	140	0.08	9.5
5.2	0.44	4.45	0.58	150	0.067	8.0
5.1	0.442	4.4	0.605	160	0.06	7.0
4.95	0.45	4.35	0.60	170	0.057	6.75
4.8	0.452	4.3	0.63	180	0.057	6.75
4.7	0.468	4.2	0.365	190	0.065	7.5
4.5	0.49	4.1	0.578	200	0.07	8.25
4.4	0.478	4.05	0.67	210	0.075	9.0
4.3	0.345	4.0	0.55	220	0.097	11.75
4.2	0.342	3.9	0.385	230	0.063	7.2
4.1	0.515	3.8	0.485	240	0.143	16.75
4.05	0.72	3.7	0.60	250	0.157	19.75
4.025	1.00	3.675	0.602	260	0.170	21.25
4.0	0.635	3.65	0.57	262	0.171	21.5
3.9	0.37	3.55	0.535	266	0.167	21.0
3.8	0.498	3.5	0.485	270	0.167	21.0
3.7	0.50	3.3	0.432	280	0.155	18.25
3.6	0.49	3.2	0.42	290	0.137	17.0
3.5	0.452	3.0	0.41	300	0.115	14.0
3.3	0.448			310	0.095	10.25
3.2	0.442			320	0.077	9.2
3.1	0.442			330	0.07	8.25
3.0	0.441			340	0.063	7.2
2.9	0.44			350	0.057	6.75
2.8	0.44					
2.7	0.432					
2.6	0.432					
2.4	0.434					

TABLE 7.7

Sample: CPHB, Mag. Field 0.5 K.Gauss, Temperature 50°C
Background Optical density = 0.315.

LINEAR SCANNING.				ANGULAR SCANNING		
L in cm.	O.D.	L in cm.	O.D.	θ in degree	O.D.	Intensity
OUTER HALO						
7.0	0.415	3.2	0.44	320	0.065	7.5
6.9	0.425	2.8	0.44	330	0.067	7.75
6.8	0.44	2.7	0.43	340	0.077	9.2
6.7	0.465	2.4	0.43	350	0.087	10.2
6.6	0.50	2.35	0.435	0	0.117	14.4
6.5	0.53	2.3	0.438	10	0.153	19.2
6.45	0.54	2.25	0.438	20	0.195	24.2
6.425	0.545	2.2	0.442	25	0.207	25.8
6.40	0.544	2.15	0.45	30	0.22	27.5
6.35	0.54	2.1	0.465	35	0.225	28.0
6.3	0.53	2.0	0.47	39	0.223	27.75
6.2	0.52	1.95	0.49	45	0.213	26.5
6.1	0.50	1.9	0.495	50	0.2	25.0
6.0	0.48	1.85	0.50	60	0.175	21.75
5.9	0.458	1.75	0.51	70	0.135	16.8
5.85	0.45	1.725	0.515	80	0.105	12.5
5.8	0.44	1.70	0.512	90	0.085	10.0
5.7	0.435	1.6	0.51	100	0.067	7.75
5.6	0.43	1.55	0.50	110	0.06	7.0
5.5	0.43	1.5	0.495	120	0.055	6.5
5.4	0.43	1.3	0.45	130	0.057	6.75
5.3	0.435	1.2	0.43	140	0.06	7.0
5.2	0.438			145	0.06	7.0
5.1	0.438	INNER HALO		150	0.06	7.0
5.05	0.435			160	0.07	8.25
5.0	0.43	5.0	0.4	170	0.077	9.2
4.7	0.43	4.8	0.42	180	0.10	12.0
4.6	0.44	4.6	0.485	190	0.13	16.0
4.5	0.448	4.5	0.52	200	0.16	20.0
4.4	0.448	4.45	0.572	210	0.185	23.0
4.3	0.415	4.4	0.58	215	0.205	25.5
4.25	0.34	4.375	0.562	219	0.21	26
4.2	0.34	4.3	0.505	222	0.205	25.5
4.15	0.538	4.2	0.385	225	0.2	25.0
4.1	0.99	4.1	0.745	230	0.195	24.2
4.05	1.22	4.05	0.78	240	0.163	20.0
4.0	0.60	4.0	0.70	250	0.127	15.3
3.95	0.36	3.9	0.35	260	0.1	12.0
3.9	0.365	3.8	0.385	270	0.085	10.0
3.8	0.44	3.75	0.525	280	0.075	9.0
3.7	0.445	3.725	0.55	290	0.065	7.5
3.6	0.44	3.70	0.53	300	0.6	7.0
3.5	0.44	3.6	0.475	310	0.055	6.5
3.3	0.435	3.5	0.455	320	0.07	8.25
3.25	0.435	3.4	0.42			

TABLE 7.8

Sample: CPMB, Mag.Field 0.91 K.Gauss, Temperature 50°C
Background optical density = 0.305.

LINEAR SCANNING				ANGULAR SCANNING		
L in cm.	O.D.	L in cm.	O.D.	θ in degree	O.D.	Intenesity
	OUTER HALO					
7.0	0.41	1.85	0.50	290	0.055	6.25
6.9	0.435	1.8	0.51	300	0.055	6.25
6.8	0.46	1.75	0.51	310	0.057	6.5
6.7	0.438	1.7	0.52	320	0.06	7.0
6.6	0.505	1.6	0.49	330	0.075	9.0
6.5	0.52	1.7	0.428	340	0.095	11.25
6.4	0.53	1.4	0.455	350	0.12	15.0
6.35	0.532	1.2	0.42	0	0.156	19.5
6.3	0.525			10	0.187	23.25
6.2	0.518	INNER HALO		20	0.21	26.0
6.1	0.492			25	0.22	27.5
5.9	0.455	5.0	0.4	29	0.22	27.5
5.8	0.44	4.7	0.432	30	0.223	27.75
5.7	0.435	4.6	0.53	35	0.22	27.5
5.5	0.43	4.55	0.57	40	0.203	25.25
5.4	0.435	4.525	0.60	50	0.17	21.25
5.3	0.44	4.5	0.61	60	0.133	16.25
5.2	0.44	4.45	0.60	70	0.105	12.5
5.0	0.43	4.4	0.5	80	0.085	10.0
4.8	0.43	4.3	0.345	90	0.073	8.5
4.7	0.44	4.2	0.635	100	0.065	7.5
4.6	0.45	4.15	0.73	110	0.06	7.0
4.5	0.46	4.05	0.58	120	0.06	7.0
4.4	0.47	4.0	0.48	130	0.06	7.0
4.3	0.44	3.95	0.435	140	0.07	8.25
4.2	0.355	3.9	0.53	150	0.085	10.0
4.1	0.712	3.8	0.615	160	0.105	12.5
4.0	0.382	3.75	0.61	170	0.13	16.0
3.9	0.325	3.7	0.53	180	0.155	19.25
3.8	0.398	3.5	0.428	190	0.185	23.0
3.7	0.46	3.25	0.39	200	0.193	24.0
3.6	0.46			210	0.193	24.0
3.5	0.44			215	0.185	23.0
3.4	0.435			220	0.165	20.5
3.3	0.43			230	0.145	18.0
2.9	0.43			240	0.055	5.25
2.8	0.425			250	0.085	10.0
2.7	0.42			260	0.07	8.0
2.5	0.42			270	0.063	7.25
2.35	0.428			280	0.063	7.25
2.3	0.435			290	0.055	6.25
2.25	0.44					
2.2	0.452					
2.0	0.475					
1.9	0.495					

TABLE 7.9

Sample: CPHB, Mag.Field 1.69 K.Gauss, Temperature 50°C
Background Optical density = 0.31.

LINEAR SCANNING				ANGULAR SCANNING		
L in cm.	O. D.	L in cm.	O. D.	Ø in degree	O.D.	Intensity
	OUTER HALO					
7.0	0.46	2.7	0.45	350	0.06	7.0
6.9	0.482	2.6	0.445	0	0.055	6.25
6.8	0.50	2.5	0.44	10	0.055	6.25
6.7	0.52	2.4	0.445	20	0.06	7.0
6.5	0.555	2.3	0.45	30	0.075	9.0
6.45	0.56	2.2	0.472	40	0.092	11.0
6.425	0.558	2.1	0.492	50	0.125	15.5
6.4	0.55	2.0	0.512	60	0.205	25.5
6.3	0.542	1.9	0.512	70	0.232	28.75
6.2	0.52	1.8	0.53	80	0.242	30.0
6.15	0.50	1.775	0.535	91	0.25	31.0
5.9	0.47	1.75	0.528	94	0.245	30.5
5.8	0.45	1.6	0.502	100	0.235	29.0
5.6	0.445	1.5	0.47	110	0.208	25.75
5.5	0.445	1.4	0.44	120	0.16	20.0
5.45	0.45	1.3	0.42	130	0.095	11.25
5.35	0.452	1.2	0.40	140	0.085	10.0
5.2	0.462			150	0.07	8.25
5.1	0.462	INNER HALO		160	0.06	7.0
5.0	0.461			170	0.055	6.5
4.9	0.46	5.0	0.405	180	0.055	6.5
4.8	0.46	4.9	0.41	190	0.06	7.0
4.7	0.462	4.8	0.428	200	0.072	8.5
4.5	0.478	4.7	0.45	220	0.092	11.0
4.4	0.48	4.6	0.47	230	0.118	14.5
4.375	0.475	4.5	0.52	240	0.19	23.7
4.325	0.45	4.45	0.59	250	0.208	26.0
4.3	0.425	4.35	0.635	260	0.21	26.0
4.2	0.325	4.3	0.66	262	0.212	26.5
4.15	0.335	4.25	0.625	264	0.22	27.5
4.1	0.425	4.2	0.56	271	0.22	27.5
4.015	0.56	4.15	0.375	275	0.22	27.5
4.0	0.385	4.1	0.382	280	0.225	28.0
3.9	0.36	4.05	0.42	284	0.22	27.5
3.85	0.49	4.025	0.53	290	0.20	25.0
3.8	0.52	4.0	0.50	300	0.16	20.5
3.7	0.515	3.95	0.45	310	0.125	15.5
3.65	0.505	3.9	0.36	320	0.092	11.0
3.6	0.419	3.8	0.51	330	0.078	9.25
3.4	0.47	3.7	0.62	340	0.038	8.25
3.3	0.46	3.65	0.655			
3.2	0.465	3.6	0.64			
2.95	0.465	3.55	0.605			
2.9	0.46	3.5	0.52			
2.8	0.452	3.4	0.465			

TABLE 7.10

Sample: CPHB, Mag. Field 2.74 K. Gauss, Temperature 50°C

O. D. (Background) = 0.32.

LINEAR SCANNING				ANGULAR SCANNING		
L in cm.	O.D.	L in cm.	O.D.	θ in degree	O. D.	Intensity
OUTER HALO						
7.0	0.445	2.7	0.462	270	0.05	5.75
6.9	0.465	2.5	0.462	280	0.05	5.75
6.8	0.49	2.4	0.465	290	0.052	6.0
6.7	0.515	2.3	0.472	300	0.055	6.5
6.6	0.53	2.2	0.49	310	0.062	7.25
6.5	0.54	2.05	0.515	320	0.078	9.25
6.45	0.542	2.0	0.54	330	0.10	12.0
6.3	0.522	1.9	0.56	340	0.138	17.0
6.15	0.495	1.75	0.568	350	0.17	21.25
6.05	0.472	1.7	0.565	0	0.208	26.0
6.0	0.47	1.6	0.552	10	0.218	27.25
5.95	0.46	1.5	0.52	12.5	0.218	27.25
5.9	0.452	1.4	0.49	15	0.212	26.5
5.8	0.45	1.3	0.47	20	0.21	26.0
5.7	0.44	1.25	0.455	30	0.192	24.0
5.5	0.448			40	0.16	20.0
5.4	0.45	INNER HALO		50	0.12	15.0
5.3	0.455			60	0.10	12.0
5.2	0.46	5.0	0.43	70	0.075	9.0
5.1	0.46	4.9	0.435	80	0.062	7.5
5.0	0.458	4.8	0.455	90	0.058	7.0
4.9	0.455	4.7	0.492	100	0.058	7.0
4.8	0.46	4.6	0.55	110	0.055	6.5
4.65	0.472	4.5	0.60	120	0.06	7.0
4.55	0.49	4.45	0.685	130	0.07	8.25
4.4	0.485	4.4	0.675	140	0.09	10.75
4.35	0.38	4.3	0.37	150	0.11	13.0
4.3	0.348	4.25	0.36	160	0.158	19.75
4.25	0.34	4.2	0.585	170	0.185	23.0
4.2	0.44	4.1	0.945	180	0.228	28.25
4.1	0.725	4.05	1.05	190	0.235	29.0
4.075	1.2	4.0	0.875	193	0.235	29.0
4.025	0.72	3.95	0.382	205	0.22	27.5
4.0	0.58	3.9	0.42	215	0.168	20.5
3.95	0.345	3.85	0.478	230	0.115	14.0
3.9	0.372	3.8	0.67	240	0.095	11.5
3.8	0.50	3.75	0.690	250	0.07	8.25
3.7	0.49	3.725	0.692	260	0.06	7.0
3.6	0.48	3.70	0.680	270	0.05	6.0
3.5	0.47	3.65	0.605			
3.3	0.465	3.6	0.52			
3.2	0.468	3.5	0.50			
3.1	0.47	3.4	0.460			
2.9	0.47	3.3	0.445			
2.8	0.465	3.0	0.42			

TABLE 7.11

Sample: CTHB, Mag.Field 4.38 K.Gauss, Temperature 50°C
Background optical density = 0.332

LINEAR SCANNING				ANGULAR SCANNING		
L in cm.	O.D.	L.in cm	O.D.	θ in degree	O.D.	Intensity
	OUTER HALO					
7.0	0.565	1.9	0.685	350	0.128	15.75
6.8	0.612	1.8	0.70	0	0.128	15.75
6.6	0.68	1.675	0.715	10	0.136	17.0
6.5	0.712	1.65	0.70	20	0.138	17.25
6.4	0.722	1.5	0.66	30	0.158	19.75
6.35	0.722	1.4	0.618	40	0.183	22.75
6.3	0.718	1.2	0.568	50	0.233	28.75
6.2	0.70			60	0.273	34.0
6.1	0.662	INNER HALO		70	0.323	42.0
6.0	0.64			80	0.366	49.0
5.9	0.605	5.0	0.49	85	0.378	51.25
5.8	0.585	4.8	0.52	90	0.38	51.5
5.6	0.555	4.7	0.56	93	0.378	51.25
5.4	0.552	4.5	0.702	100	0.358	47.75
5.3	0.55	4.45	0.8	110	0.308	39.5
5.1	0.552	4.4	0.798	120	0.253	31.25
4.9	0.54	4.35	0.78	130	0.118	14.5
4.7	0.54	4.3	0.535	140	0.166	21.0
4.65	0.55	4.2	0.56	150	0.146	18.2
4.5	0.572	4.15	0.85	160	0.138	17.25
4.4	0.59	4.1	0.83	170	0.128	15.75
4.3	0.592	4.0	0.675	180	0.127	15.7
4.2	0.535	3.9	0.4	190	0.131	16.2
4.15	0.395	3.8	0.76	200	0.136	16.7
4.05	0.435	3.75	0.795	210	0.14	17.5
4.0	0.665	3.725	0.80	220	0.17	21.0
3.95	0.58	3.7	0.73	230	0.213	26.5
3.9	0.402	3.6	0.61	240	0.263	32.5
3.8	0.42	3.5	0.58	250	0.313	40.5
3.7	0.565			260	0.358	47.75
3.35	0.582			267	0.378	51.25
3.5	0.572			269	0.386	52.6
3.4	0.55			270	0.388	53.0
3.2	0.54			275	0.383	52.0
3.1	0.548			282	0.356	47.5
2.9	0.735			290	0.303	38.5
2.8	0.56			300	0.25	31.0
2.7	0.545			310	0.203	25.25
2.6	0.542			320	0.173	21.5
2.5	0.545			330	0.158	19.5
2.4	0.555			340	0.146	18.2
2.3	0.57			350	0.138	17.0
2.2	0.58			0	0.130	16.0
2.1	0.61					
1.95	0.655					

TABLE 7.12

Sample: CPHB, Mag.Field 5.80 K.Gauss, Temperature 50°C
Background optical density = 0.33.

LINEAR SCANNING				ANGULAR SCANNING		
L in cm	O. D.	L in cm.	O. D.	θ in degree	O.D.	Intensity
	OUTER HALO					
7.0	0.45	2.2	0.475	350	0.052	6.2
6.9	0.468	2.1	0.505	0	0.051	6.1
6.8	0.48	2.0	0.534	10	0.055	6.5
6.7	0.572	1.85	0.565	20	0.058	6.75
6.6	0.54	1.8	0.572	30	0.078	9.25
6.5	0.555	1.7	0.572	40	0.088	10.25
6.4	0.57	1.65	0.562	50	0.112	13.5
6.35	0.568	1.5	0.538	60	0.15	18.7
6.2	0.54	1.3	0.482	70	0.195	24.25
6.1	0.52	1.2	0.472	80	0.225	28.0
6.0	0.50			85	0.23	28.5
5.9	0.485	INNER HALO		90	0.234	29.0
5.8	0.47			92.5	0.238	29.5
5.7	0.462	5.0	0.46	94	0.232	28.75
5.5	0.46	4.8	0.47	100	0.225	28.0
5.3	0.47	4.7	0.485	110	0.20	25.0
5.1	0.472	4.6	0.50	120	0.165	20.5
5.0	0.472	4.5	0.562	130	0.125	15.5
4.8	0.472	4.4	0.682	140	0.098	11.75
4.7	0.48	4.325	0.70	150	0.078	9.25
4.5	0.572	4.31	0.71	160	0.068	8.0
4.4	0.535	4.30	0.70	170	0.06	7.0
4.3	0.571	4.2	0.57	180	0.055	6.5
4.2	0.375	4.15	0.39	190	0.055	6.5
4.1	0.565	4.05	0.52	200	0.065	7.5
4.05	0.71	4.025	0.65	210	0.07	8.25
4.025	0.85	4.0	0.57	220	0.09	10.75
4.0	0.53	3.9	0.365	230	0.12	15.0
3.9	0.34	3.8	0.375	240	0.152	19.0
3.8	0.355	3.7	0.58	250	0.19	23.7
3.7	0.51	3.675	0.66	260	0.225	28.0
3.6	0.51	3.65	0.65	265	0.23	28.5
3.5	0.49	3.55	0.55	271	0.232	28.75
3.4	0.478	3.4	0.48	272	0.23	28.5
3.3	0.47	3.3	0.46	280	0.216	27.0
3.2	0.468	3.0	0.415	290	0.185	23.0
3.1	0.465			300	0.148	18.25
3.0	0.462			310	0.11	13.0
2.9	0.46			320	0.085	10.0
2.8	0.46			330	0.07	8.25
2.65	0.452			340	0.06	7.0
2.55	0.452			350	0.054	6.3
2.45	0.452			0	0.052	6.2
2.4	0.46					
2.3	0.462					

TABLE 7.13

Sample: CPHB, Mag. Field 5.80 K.Gauss, Temperature 34°C
Background optical density = 0.37.

LINEAR SCANNING				ANGULAR SCANNING		
L in cm.	O.D.	L in cm.	O. D.	θ in degree	O.D.	Intensity
	OUTER HALO					
7.0	0.518	2.0	0.565	350	0.050	6.0
6.8	0.55	1.85	0.60	0	0.040	4.9
6.6	0.60	1.80	0.612	10	0.045	5.2
6.4	0.625	1.75	0.612	20	0.048	5.5
6.35	0.62	1.70	0.605	30	0.06	7.0
6.2	0.59	1.60	0.595	40	0.062	7.2
6.1	0.57	1.40	0.545	50	0.10	12.0
6.0	0.548	1.20	0.492	60	0.142	17.75
5.9	0.522			70	0.195	24.25
5.8	0.50			80	0.25	31.0
5.7	0.485			87.5	0.258	32.0
5.6	0.482			90	0.259	32.2
5.5	0.488			94	0.25	31.0
5.4	0.485			105	0.22	27.5
5.3	0.49			110	0.20	25.0
5.2	0.492			120	0.14	17.5
5.1	0.492			130	0.092	11.0
5.0	0.490			140	0.07	8.25
4.9	0.485			150	0.055	6.5
4.8	0.480			160	0.045	5.2
4.6	0.490			170	0.042	4.80
4.5	0.51			180	0.045	5.2
4.4	0.53			190	0.042	4.8
4.2	0.515			200	0.05	6.0
4.1	0.39			210	0.052	6.2
4.05	0.44			220	0.062	7.2
3.90	0.44			230	0.09	10.7
3.80	0.475			240	0.115	14.0
3.70	0.552			250	0.165	20.5
3.60	0.535			260	0.21	26.0
3.50	0.505			265	0.242	30.0
3.40	0.485			270	0.26	32.2
3.00	0.490			280	0.258	32.0
2.9	0.495			290	0.21	26.2
2.85	0.492			300	0.155	19.5
2.8	0.492			310	0.11	13.0
2.7	0.492			320	0.072	8.5
2.6	0.488			330	0.058	6.75
2.5	0.488			340	0.05	6.0
2.4	0.495			350	0.05	6.0
2.3	0.50			360	0.04	4.9
2.2	0.512					
2.1	0.535					

TABLE 7.14

Sample: CPHB, Mag.Field 5.80 K.Gauss, Temperature 39°C
Background optical density = 0.42

LINEAR SCANNING				ANGULAR SCANNING		
L in cm	O. D.	L in cm	O. D.	θ in degree	O.D.	Intensity
OUTER HALO						
7.0	0.635	2.4	0.63	350	0.06	7.0
6.8	0.688	2.3	0.638	0	0.065	7.5
6.66	0.79	2.2	0.65	10	0.07	8.25
6.5	0.82	2.1	0.69	20	0.078	9.25
6.45	0.83	2.0	0.725	30	0.092	11.0
6.425	0.831	1.9	0.782	40	0.11	13.0
6.40	0.838	1.8	0.80	50	0.16	20.0
6.35	0.835	1.75	0.82	60	0.242	30.0
6.30	0.832	1.70	0.83	70	0.332	43.5
6.20	0.80	1.675	0.83	80	0.38	51.5
6.10	0.76	1.60	0.822	85	0.402	55.25
6.0	0.715	1.50	0.782	90	0.41	56.5
5.9	0.69	1.40	0.742	94	0.398	54.5
5.8	0.66	1.30	0.69	100	0.378	51.28
5.6	0.635	1.25	0.66	110	0.30	38.25
5.4	0.638	INNER HALO		120	0.205	25.5
5.2	0.65	5.0	0.545	130	0.155	19.5
5.0	0.64	4.8	0.572	140	0.110	13.0
4.8	0.63	4.65	0.62	150	0.090	10.5
4.75	0.638	4.6	0.672	160	0.08	9.5
4.7	0.65	4.5	0.72	170	0.08	9.5
4.5	0.85	4.45	0.85	180	0.07	8.25
4.4	0.16	4.4	0.905	190	0.075	9.0
4.35	0.69	4.35	0.990	205	0.08	9.5
4.2	0.46	4.3	0.935	210	0.088	10.25
4.1	0.81	4.25	0.895	220	0.140	17.5
4.05	0.79	4.2	0.51	230	0.20	25.0
4.0	0.63	4.15	0.47	240	0.275	34.25
3.95	0.435	4.1	0.68	250	0.325	42.25
3.9	0.435	4.025	0.91	260	0.38	51.5
3.85	0.50	4.0	0.97	267	0.388	52.75
3.8	0.59	3.95	0.75	270	0.378	51.25
3.7	0.70	3.9	0.63	280	0.33	43.25
3.6	0.685	3.85	0.475	290	0.255	31.5
3.5	0.670	3.80	0.51	300	0.168	21.0
3.4	0.64	3.75	0.625	310	0.13	16.0
3.3	0.622	3.70	0.88	320	0.09	10.75
3.2	0.622	3.675	0.98	330	0.07	8.25
3.1	0.622	3.65	0.985	340	0.065	7.5
3.0	0.63	3.60	0.84	350	0.06	7.0
2.9	0.63	3.50	0.735			
2.8	0.63	3.40	0.64			
2.7	0.628	3.30	0.58			
2.6	0.625	3.10	0.55			
2.5	0.62	3.00	0.535			

TABLE 7.15

Sample: CPHB, Mag. Field 5.80 K.Gauss, Temperature 44°C
Background optical density = 0.30.

LINEAR SCANNING				ANGULAR SCANNING		
L. in cm	O. D.	L in cm.	Φ. D.	Θ in degree	O.D.	Intensity
	OUTER HALO					
7.0	0.37	1.85	4.22	250	0.03	3.25
6.8	0.385	1.80	0.43	260	0.03	3.25
6.6	0.415	1.775	0.435	270	0.03	3.25
6.5	0.428	1.75	0.435	280	0.031	3.5
6.35	0.435	1.7	0.44	290	0.035	4.0
6.325	0.438	1.65	0.44	300	0.052	6.0
6.30	0.44	1.6	0.435	310	0.07	8.25
6.25	0.44	1.5	0.42	320	0.10	12.0
6.2	0.44	1.4	0.405	330	0.125	15.5
6.15	0.435	1.25	0.38	340	0.14	17.5
6.05	0.425			343	0.14	17.2
5.95	0.412	INNER HALO		344	0.139	17.2
5.85	0.398	5.0	0.375	347	0.138	17.2
5.75	0.38	4.8	0.398	0	0.125	15.5
5.5	0.375	4.7	0.412	10	0.1	12.0
5.4	0.37	4.6	0.438	20	0.07	8.25
5.325	0.375	4.55	0.47	30	0.48	5.5
5.2	0.378	4.45	0.52	40	0.038	4.25
5.05	0.38	4.4	0.56	50	0.03	3.25
4.9	0.384	4.35	0.558	60	0.028	3.0
4.7	0.392	4.3	0.44	70	0.025	2.5
4.55	0.41	4.2	0.332	80	0.025	2.5
4.4	0.44	4.15	0.625	90	0.03	3.25
4.3	0.448	4.05	0.80	100	0.032	3.6
4.2	0.398	4.0	0.655	110	0.038	4.25
4.1	0.325	3.9	0.32	120	0.05	5.75
4.05	0.40	3.8	0.515	130	0.072	8.5
4.025	0.90	3.7	0.53	140	0.098	11.7
4.0	0.90	3.725	0.50	150	0.12	15.0
3.95	0.795	3.60	0.47	156	0.13	16.0
3.8	0.34	3.30	0.37	160	0.132	16.2
3.6	0.428	3.20	0.36	175	0.115	14.0
3.5	0.41			180	0.10	12.0
3.4	0.398			190	0.085	10.0
3.3	0.38			200	0.068	8.0
2.8	0.372			210	0.05	5.75
2.7	0.37			220	0.04	4.9
2.6	0.37			230	0.03	3.25
2.5	0.368			240	0.028	3.0
2.35	0.37			250	0.03	3.25
2.25	0.375			260	0.03	3.25
2.15	0.39					
2.05	0.398					
1.95	0.41					

TABLE 7.16

Sample: CPHB, Mag. Field 5.80 K.Gauss, Temperature 49°C
Background optical density = 0.33.

LINEAR SCANNING				ANGULAR SCANNING		
L in cm	O.D.	L. in cm	O. D.	θ in degree	O.D.	Intensity
OUTER HALO						
7.0	0.455	1.85	0.582	350	0.05	6.0
6.8	0.49	1.7	0.587	0	0.05	6.0
6.6	0.535	1.65	0.590	10	0.058	6.75
6.45	0.562	1.55	0.585	20	0.055	6.5
6.4	0.578	1.3	0.495	30	0.07	8.25
6.35	0.585	1.25	0.48	40	0.088	10.5
6.3	0.585	INNER HALO		50	0.115	14.0
6.275	0.59			60	0.145	18.0
6.25	0.588	5.0	0.42	70	0.205	25.5
6.225	0.588	4.8	0.435	80	0.239	29.5
6.2	0.58	4.7	0.468	84	0.24	29.75
6.1	0.57	4.6	0.48	88	0.25	31.0
6.0	0.542	4.5	0.54	90	0.252	31.25
5.9	0.53	4.45	0.612	94	0.245	30.25
5.8	0.505	4.4	0.692	100	0.235	29.0
5.7	0.49	4.35	0.712	110	0.20	25.0
5.6	0.48	4.325	0.718	120	0.15	18.75
5.5	0.472	4.3	0.668	130	0.11	13.0
5.4	0.48	4.2	0.50	140	0.082	9.8
5.3	0.482	4.1	0.412	150	0.07	8.25
5.2	0.485	4.05	0.73	160	0.06	7.0
5.0	0.482	4.0	0.71	170	0.06	7.0
4.9	0.48	3.9	0.37	180	0.054	6.4
4.8	0.475	3.8	0.375	190	0.04	4.9
4.7	0.48	3.75	0.60	200	0.06	7.0
4.6	0.488	3.7	0.655	210	0.08	9.75
4.5	0.562	3.675	0.715	220	0.10	12.0
4.4	0.725	3.65	0.68	230	0.132	16.5
4.2	0.39	3.6	0.66	240	0.171	21.5
4.1	0.405	3.5	0.52	250	0.212	26.5
4.0	0.85			260	0.25	31.0
3.9	0.40			268	0.258	32.0
3.8	0.38			270	0.256	31.7
3.6	0.495			280	0.24	29.75
3.45	0.478			290	0.198	24.5
3.3	0.468			300	0.155	19.25
3.1	0.47			320	0.08	9.5
3.0	0.475			330	0.07	8.25
2.8	0.478			340	0.06	7.0
2.6	0.47			350	0.051	6.0
2.45	0.468					
2.3	0.49					
2.2	0.512					
2.0	0.55					
1.9	0.58					

TABLE 7.17

Sample: CPMB, Mag. Field 5.80 K.Gauss, Temperature 54°C
Background Optical density = 0.33

LINEAR SCANNING				ANGULAR SCANNING		
L in cm.	O.D.	L in cm	O. D.	θ in degree	O.D.	Intensity
	OUTER HALO					
7.0	0.45	2.4	0.448	350	0.082	9.75
6.9	0.46	2.3	0.45	0	0.075	9.00
6.7	0.512	2.1	0.462	10	0.085	10.00
6.4	0.518	2.0	0.475	20	0.095	11.30
6.35	0.522	1.9	0.492	30	0.10	12.00
6.25	0.52	1.85	0.50	40	0.11	13.0
6.2	0.518	1.80	0.502	50	0.12	14.5
6.15	0.512	1.75	0.505	60	0.14	17.5
6.1	0.51	1.70	0.50	70	0.162	20.2
6.05	0.502	1.60	0.48	80	0.18	22.5
6.0	0.50	1.3	0.44	85	0.195	24.2
5.85	0.48	1.25	0.435	87	0.195	24.2
5.7	0.465			88	0.192	23.7
5.5	0.462	INNER HALO		90	0.19	23.5
5.35	0.47			100	0.18	22.8
5.3	0.47	5.0	0.5	110	0.169	21.0
5.2	0.47	4.8	0.535	120	0.155	19.5
5.1	0.482	4.7	0.562	130	0.132	16.25
5.0	0.49	4.6	0.61	140	0.112	13.5
4.9	0.495	4.5	0.66	150	0.10	12.0
4.8	0.50	4.45	0.70	160	0.09	10.75
4.7	0.51	4.4	0.702	170	0.085	10.0
4.6	0.54	4.375	0.710	190	0.085	10.0
4.55	0.562	4.325	0.688	200	0.09	10.75
4.5	0.57	4.30	0.51	210	0.094	11.2
4.4	0.585	4.2	0.60	220	0.10	12.0
4.35	0.60	4.1	0.88	230	0.052	6.0
4.3	0.56	4.0	0.58	240	0.125	15.5
4.2	0.382	3.9	0.382	250	0.148	18.25
4.1	0.44	3.8	0.64	255	0.16	20.0
4.05	0.53	3.7	0.66	260	0.162	20.2
4.025	1.03	3.675	0.658	263	0.158	19.75
4.0	0.97	3.65	0.615	265	0.165	20.5
3.9	0.63	3.6	0.6	270	0.162	20.2
3.8	0.48	3.5	0.55	280	0.152	19.2
3.7	0.865	3.4	0.505	290	0.150	18.6
3.6	0.6	3.2	0.465	300	0.120	14.5
3.5	0.55	3.0	0.45	310	0.110	13.0
3.4	0.55			320	0.100	12.0
3.2	0.50			330	0.09	10.75
3.1	0.48			340	0.085	10.0
2.95	0.47			350	0.082	9.75
2.8	0.46					
2.65	0.445					
2.55	0.44					

TABLE 7.18

Sample: CPHB, Mag. Field 5.80 K.Gauss, Temperature 55.5°C
Background optical density = 0.335.

LINEAR SCANNING				ANGULAR SCANNING		
L in cm.	O. D.	L in cm	O. D.	θ in degree	O. D.	Intensity
	OUTER HALO					
7.0	0.492	2.2	0.512	0	0.103	12.25
6.9	0.51	2.1	0.532	10	0.104	12.5
6.7	0.54	2.0	0.555	20	0.11	13.0
6.6	0.575	1.85	0.588	30	0.117	14.7
6.5	0.598	1.80	0.608	40	0.135	16.5
6.35	0.602	1.75	0.608	50	0.155	19.25
6.325	0.605	1.65	0.592	60	0.186	23.2
6.30	0.60	1.5	0.57	70	0.227	28.0
6.20	0.588	1.3	0.575	80	0.25	31.0
6.10	0.562	1.25	0.50	90	0.269	33.3
6.00	0.54			100	0.265	32.75
5.9	0.525	INNER HALO		110	0.245	30.25
5.8	0.505			120	0.217	27.0
5.7	0.50	5.0	0.47	130	0.183	22.75
5.6	0.492	4.8	0.50	140	0.155	19.25
5.5	0.492	4.6	0.548	150	0.135	16.5
5.3	0.50	4.5	0.62	160	0.125	15.5
5.2	0.508	4.4	0.73	170	0.115	13.8
5.1	0.51	4.35	0.77	180	0.115	13.8
5.0	0.515	4.325	0.772	190	0.115	13.8
4.9	0.52	4.3	0.735	200	0.116	13.9
4.8	0.528	4.2	0.40	210	0.126	15.6
4.7	0.54	4.1	0.55	220	0.14	17.5
4.6	0.56	4.0	0.81	230	0.163	20.5
4.5	0.59	3.9	0.42	240	0.205	25.5
4.4	0.62	3.8	0.465	250	0.225	27.8
4.3	0.598	3.7	0.62	260	0.245	30.25
4.2	0.46	3.675	0.75	270	0.253	31.25
4.1	0.435	3.6	0.74	272.5	0.257	31.75
4.025	0.95	3.3	0.52	276	0.255	31.5
4.0	0.735	3.0	0.475	280	0.254	31.4
3.9	0.37			290	0.240	29.75
3.8	0.485			300	0.213	26.5
3.7	0.605			310	0.170	21.25
3.6	0.60			320	0.155	19.4
3.5	0.542			330	0.137	17.0
3.4	0.542			340	0.125	15.5
3.2	0.52			350	0.11	13.0
3.0	0.51					
2.85	0.50					
2.7	0.495					
2.6	0.495					
2.45	0.50					
2.35	0.512					

TABLE 7. 19.

Sample: CPHB.

Intermolecular distance 'D' and apparent length of the molecule 'ℓ' at different temperatures in presence and absence of magnetic field.

(Sample to film distance = 6.345 cm.)

Temp. °C.	Mag. field in K. Gauss	Outer halo			Inner halo		
		Dia. in cm.	Bragg angle (deg.)	'D' in Å	Dia. in cm.	Bragg angle (deg.)	'ℓ' in Å
34	0	4.675	10.112	4.91	0.7	1.579	27.99
34	5.8	4.725	10.211	4.86	0.675	1.522	29.02
39	0	4.675	10.112	4.91	0.7	1.579	27.99
39	5.8	4.725	10.211	4.86	0.7	1.579	27.99
44	0	4.65	10.062	4.93	0.675	1.522	29.02
44	5.8	4.65	10.062	4.93	0.675	1.522	29.02
49	0	4.625	10.012	4.96	0.725	1.635	27.02
49	5.8	4.625	10.012	4.96	0.7	1.579	27.99
54	0	4.575	9.913	5.0	0.725	1.635	27.02
54	5.8	4.6	9.963	4.98	0.7	1.579	27.99
55.5	0	4.575	9.913	5.0	-		
55.5	5.8	4.6	9.963	4.98	0.675	1.522	29.02

Table 7.20

Sample: OFHR.

Intermolecular distance and degree of ordering at different magnetic field at Temperature 50°C.

Temp. °C.	Magnetic field in (K.Gauss)	Outer halo			Degree of ordering (2nd.order)
		Dia. in cm.	Bragg angle (deg.)	'D' in Å	
	0	4.6	9.963	4.98	0
	0.19	4.625	10.012	4.96	0.49
	0.5	4.7	10.162	4.88	0.54
50	0.91	4.65	10.062	4.93	0.55
	1.69	4.675	10.112	4.91	0.54
	2.74	4.7	10.162	4.88	0.54
	4.38	4.7	10.162	4.88	0.56
	5.81	4.7	10.162	4.88	0.54

Table 7.21

Sample: CPNB.

Mean Intensity values at different temperatures.

θ (deg)	I (θ) at temperatures					
	34°C	39°C	44°C	49°C	54°C	55.5°C
0	28.13	46.63	14.75	25.25	13.25	19.67
5	27.00	44.08	14.13	24.75	12.75	19.17
10	25.00	41.69	13.19	23.850	12.06	18.33
15	22.06	37.56	12.00	21.31	10.75	17.33
20	18.94	32.88	10.50	18.75	9.44	15.75
25	15.94	28.44	8.63	16.38	8.44	14.42
30	12.44	22.06	6.94	13.38	7.13	12.33
35	9.31	15.63	5.44	10.50	5.94	10.42
40	7.00	11.75	4.06	8.31	4.75	8.58
45	9.94	8.50	3.13	6.38	4.00	7.17
50	3.44	5.75	2.38	4.94	4.25	5.75
55	2.44	3.69	1.69	3.33	2.38	4.42
60	1.63	2.44	1.25	2.50	1.75	3.08
65	1.19	1.69	0.88	1.44	1.19	1.75
70	0.75	1.13	0.68	0.93	0.88	1.58
75	0.38	0.81	0.40	0.56	0.50	1.08
80	0.20	0.63	0.19	0.25	0.13	0.63
85	0.11	0.38	0.06	0.06	0.00	0.38
90	0.00	0.25	0.06	0.00	0.00	0.13

Table 7.22.

Sample: CPMB.

Calculated Intensity values at different temperatures.

θ (deg)	Calculated I (θ) at temperatures °C					
	34°	39	44	49	54	55.5
0	27.97	46.35	14.593	25.28	13.235	19.605
5	27.16	45.08	14.250	24.77	12.855	19.252
10	25.00	41.82	13.309	23.37	11.905	18.354
15	22.10	37.61	11.962	21.34	10.751	17.204
20	18.95	33.02	10.384	18.91	9.591	15.899
25	15.75	27.89	8.690	16.21	8.381	14.313
30	12.54	22.13	6.982	13.361	7.080	12.395
35	9.45	16.31	5.403	10.628	5.847	10.378
40	6.86	11.457	4.092	8.266	4.8903	8.600
45	4.88	8.091	3.097	6.373	4.246	7.148
50	3.49	5.848	2.349	4.840	3.611	5.805
55	2.48	4.044	1.749	3.516	2.777	4.380
60	1.69	2.465	1.252	2.370	1.840	2.994
65	1.096	1.404	0.875	1.488	1.102	1.963
70	0.703	1.029	0.616	0.912	0.718	1.403
75	0.449	0.986	0.423	0.555	0.533	1.088
80	0.242	0.776	0.240	0.284	0.305	0.724
85	0.067	0.355	0.082	0.068	0.019	0.316
90	-0.06	0.129	0.016	-0.021	-0.119	0.129

Table 7.23.

Sample: CPHB.

Normalized distribution functions at different temperatures.

β (deg)	$f(\beta)$ values at different temperatures in °C.					
	34	39	44	49	54	55.5
0	6.914	6.508	6.028	5.382	5.556	4.267
5	6.634	6.228	5.845	5.237	5.274	4.119
10	5.918	5.553	5.361	4.857	4.602	3.775
15	5.034	4.809	4.719	4.358	3.892	3.428
20	4.194	4.184	4.031	3.820	3.341	3.158
25	3.444	3.605	3.335	3.254	2.885	2.885
30	2.733	2.922	2.635	2.653	2.380	2.503
35	2.039	2.135	1.971	2.054	1.841	2.035
40	1.419	1.417	1.414	1.532	1.419	1.609
45	0.949	0.923	1.009	1.137	1.199	1.308
50	0.642	0.644	0.736	0.851	1.079	1.086
55	0.442	0.455	0.536	0.620	0.894	0.846
60	0.295	0.276	0.372	0.416	0.607	0.571
65	0.183	0.133	0.245	0.251	0.335	0.339
70	0.109	0.071	0.163	0.143	0.185	0.221
75	0.068	0.070	0.111	0.084	0.136	0.162
80	0.037	0.063	0.065	0.044	0.089	0.113
85	0.011	0.029	0.022	0.012	0.016	0.048
90	0.011	0.008	0.003	0.002	0.023	0.015

TABLE 7.24.

Sample: CPHB.

Calculated $f(\beta)$ values at different temperatures

β (deg.)	$f(\beta)$ at temperatures in °C					
	34	39	44	49	54	55.5
0	7.154	6.605	6.647	5.558	5.590	4.393
5	6.738	6.285	6.132	5.322	5.304	4.193
10	5.786	5.537	5.056	4.768	4.625	3.741
15	4.816	4.739	4.145	4.178	3.884	3.304
20	4.070	4.087	3.651	3.693	3.273	3.014
25	3.475	3.534	3.389	3.263	2.793	2.826
30	2.850	2.930	2.994	2.764	2.363	2.591
35	2.125	2.216	2.270	2.160	1.935	2.199
40	1.430	1.505	1.461	1.559	1.530	1.707
45	0.915	0.951	0.889	1.091	1.203	1.263
50	0.602	0.596	0.597	0.785	0.968	0.952
55	0.424	0.388	0.481	0.591	0.791	0.753
60	0.308	0.260	0.430	0.440	0.617	0.599
65	0.209	0.171	0.348	0.291	0.419	0.435
70	0.120	0.104	0.207	0.157	0.232	0.264
75	0.058	0.058	0.086	0.071	0.108	0.134
80	0.027	0.032	0.030	0.031	0.049	0.065
85	0.015	0.021	0.013	0.016	0.027	0.037
90	0	0.018	0.009	0	0	0.030

Table 7.25

Sample: CPHB.

a_L, $\langle P_L \rangle$ and b_L (L = 2,4) values at different temperatures.

Temp. °C.	Temp. °K.	a_0	a_2	a_4	a_6	a_8	a_{10}	$\langle P_2 \rangle$	$\langle P_4 \rangle$	b_2/k	b_4/k
34	307	-1.328	4.001	-1.338	0.915	-0.743	0.460	0.605	0.201	-2030	2044
39	312	-1.306	3.901	-1.300	0.497	-0.449	0.337	0.603	0.196	-2023	1751
44	317	-1.197	3.808	-1.567	1.355	-1.369	0.861	0.564	0.12	-2140	4140
49	322	-1.170	3.803	-1.645	1.129	-0.808	0.405	0.547	0.135	-2338	3924
54	327	-0.926	3.309	-1.579	1.277	-0.693	0.333	0.511	0.116	-2118	4451
55.5	328.5	-0.826	3.088	-1.456	0.953	-0.712	0.432	0.460	0.059	-2205	8107

Table 7.26

Sample: CPHB

Order parameters at different temperatures.

Temp. °C	$\langle P_2 \rangle_V$	$\langle P_2 \rangle$	$\langle P_2 \rangle_{M.F}$	$\langle P_4 \rangle_V$	$\langle P_4 \rangle$	$\langle P_4 \rangle_{M.F}$
34	0.58	0.61	0.58	0.17	0.20	0.30
39	0.57	0.60	0.56	0.17	0.20	0.28
44	0.52	0.56	0.53	0.10	0.12	0.24
49	0.52	0.55	0.50	0.11	0.14	0.21
54	0.48	0.51	0.45	0.08	0.12	0.18
55.5	0.44	0.46	0.43	0.05	0.06	0.13

References

1. M/s. F. Hoffmann-La-Roche and Co., Basel, Switzerland, Cat. No. RO-CE 1540.
2. A. de Vries, A. Ekachi and N. Spielberg, J. Phys. Paris, 40, C147 (1979).
3. A. de Vries, S.D. Quadri, Liq. Crystals. Proc.Int.Conf. Bangalore, p. 179, Edited by S.Chandrasekhar (Heyden) (1979).
4. A.J.Leadbetter, R.M.Richardson and C.N.Colling, J. Phys. Paris, 36, C1-37 (1975).
5. J.E.Lydon and C.J.Cookley, J.Phys. Paris, 36, Get C1-45 (1975).
6. A.J.Leadbetter and E.K.Norris, Mole.Phys.38, 669 (1979).
7. P.J.Wojtowicz, Introduction to Liquid Crystals, Chapter 3 & 4, E.B. Priestley, Plenum Press (1974).
8. V.K.Vainshtein, Diffraction of Chain Molecules Elsevier (1966).
9. A. Zeminder, S.Paul and R.Paul, Mol.Cryst.Liq.Cryst.61,191(1980)
10. S.Jen, N.A.Clark, P.S.Pershan & E.B.Priestly, Phys. Rev. Lett. 31, 1552 (1973).
11. J.F.Kegen, J.Phys. Lett., Paris, 36 209 (1975).
12. M.Cotter., 1977, Mol.Cryst.Liq.Cryst.,39, 173. (1977)
13. R.L.Humphries, P.G.James and G.R.Luckhurst, J.Chem.Soc. Faraday Trans. II, 68, 1031 (1972).
13a. B.Bhattacharjee, S.Paul, & R.Paul, Mol.Phyat.~~Liq.Cryst.~~ 44, N06 (1982). P-1391
14. G.R.Luckhurst, P.Simpson and G.Zanoni, Chem.Phys.Lett.78 429 (1981).
15. N.V.Madhusudana and S.Chandrasekhar, Pramana, Suppl. 1, Ed. S. Chandrasekhar, Indian Academy of Science, p.57 (1981).
16. S. Marcelja, J. Chem. Phys. 60, 3599 (1974).

CHAPTER 8.

X-RAY DIFFRACTION STUDIES ON THE NEMATIC PHASE OF 4'-PENTYLOXY-4-CYANO BIPHENYL (5OCB IN SHORT) IN MAGNETIC FIELD.

CHAPTER 8.

X-RAY DIFFRACTION STUDIES ON THE NEMATIC PHASE OF 4'-PENTYLOXY-4-CYANOBIPHENYLS (5OCB IN SHORT) IN MAGNETIC FIELD.

1. Introduction

X-ray diffraction measurements on unoriented and oriented samples of two biphenyl compounds at different temperatures have been made. The compounds are two homologues of the series 4'-Alkoxy-4-cyanobiphenyl, namely pentyloxy cyanobiphenyl and octyloxycyanobiphenyl (5OCB and 8OCB in short). In this chapter we will discuss the results obtained from X-ray diffraction studies on 5OCB.

The transition temperature of 5OCB obtained from the literature[1] is given below -

$$\text{Solid} \xrightarrow{47.5^{\circ}C} \text{Nematic} \xrightarrow{67.5^{\circ}C} \text{Isotropic}$$

By X-ray diffraction and microscopic studies the phase transitions determined by us is as follows -

$$\text{Solid} \underset{\sim 31.5^{\circ}C}{\overset{47.5^{\circ}C}{\rightleftharpoons}} \text{Nematic} \overset{67.5^{\circ}C}{\rightleftharpoons} \text{Isotropic}$$

The orientational distribution function and order parameters for 5OCB by X-ray diffraction have not been reported so far.

Details of experimental method and theoretical background have been described in earlier chapters[2] (Chapt.2, 3, 4). The photographs of the unoriented samples and oriented samples

were taken in set up No. 1 and set up No.3 of Chapter 2 respectively.

2. Results and Discussions:-

(a) Intermolecular distance and apparent molecular length and degree of ordering.

Fig. 8.1 shows the photograph of the oriented sample of 500B at 39°C. The optical densities obtained for linear and angular scanning for different films at different temperatures and different magnetic fields are given in table 8.1 - 8.16. In case of angular scanning the corresponding intensity values are also presented in these tables.

Variation of 'D' and degree of ordering (2nd. order) calculated by Leadbetter's method with different magnetic field strength at 49°C are given in table 8.17. For the calculation of 'D', diameter of the outer halo/crescent and the corresponding Bragg angles are also given in the same table. Fig. 8.2 (b) and Fig. 8.2 (a), show the degree of ordering and variation of D with different field strength respectively. From Fig. 8.2 (b) it is found that at lower magnetic fields degree of ordering increases rapidly and at about 0.9 K.Gauss attains a saturation value. Variation of intermolecular distance with field indicates (in Fig. 8.2(a)) that the 'D' value decreases with increase in field strength. These are in good agreement with our previous experience with OPHB[2] as discussed in chapter 7.

Fig.8.3 gives the intermolecular distance of 500B at different temperature in absence of magnetic field and in

$\vec{H}$ ↑

Fig. 8.1. Photograph of the oriented sample of 50CB at 39°C (Supercooled nematic phase)

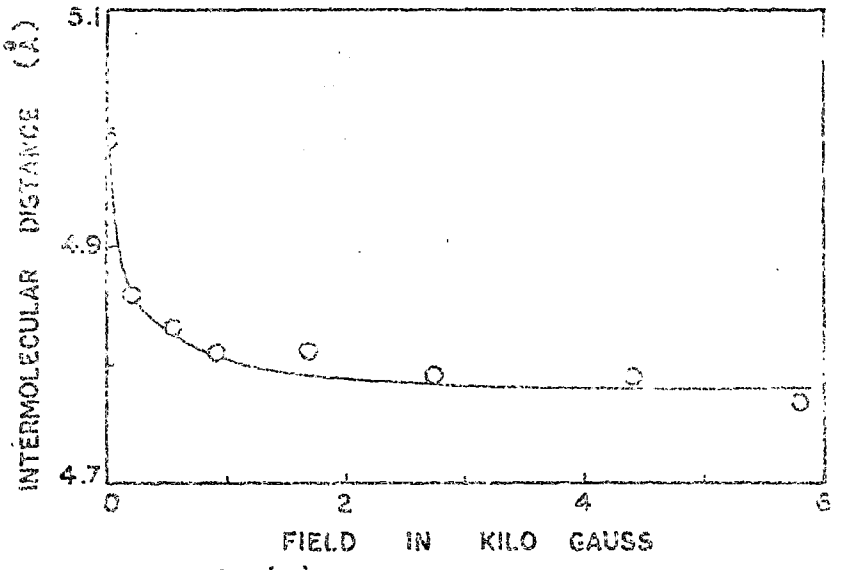

FIG. 6.2(a).

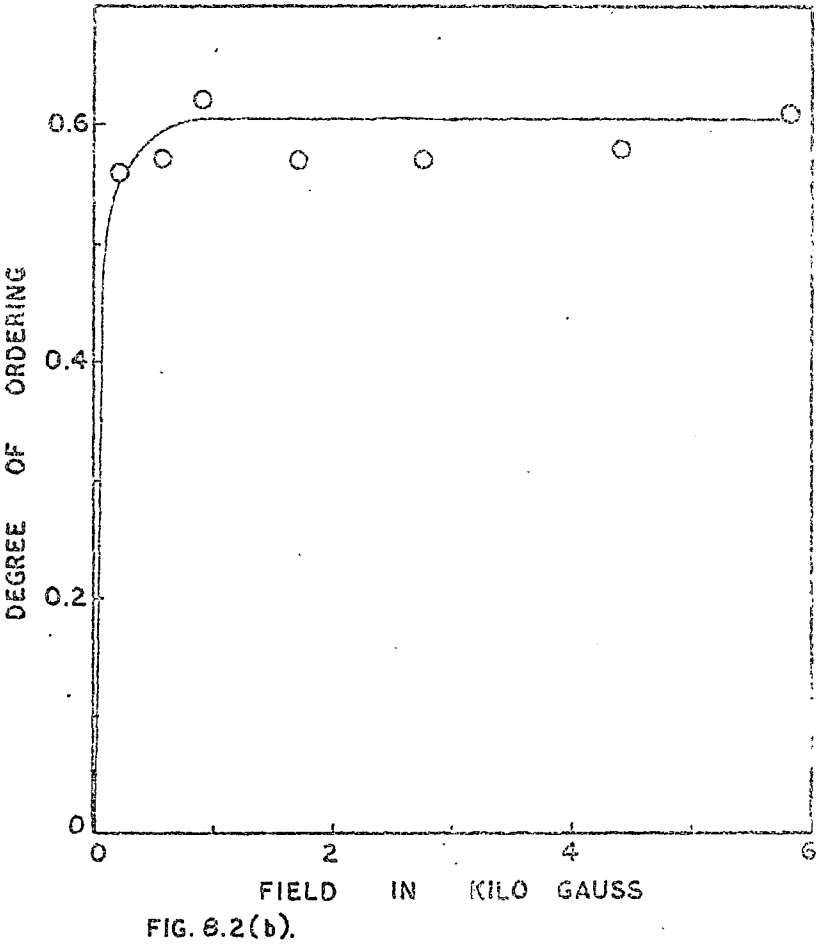

FIG. 6.2(b).

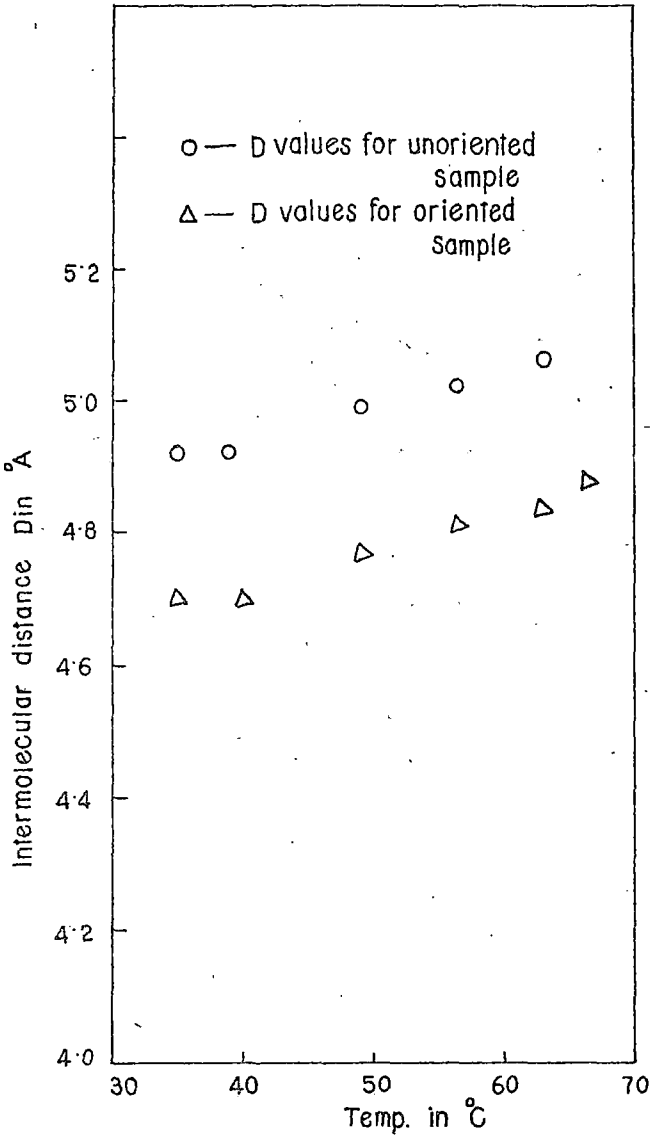

Fig. 8·3

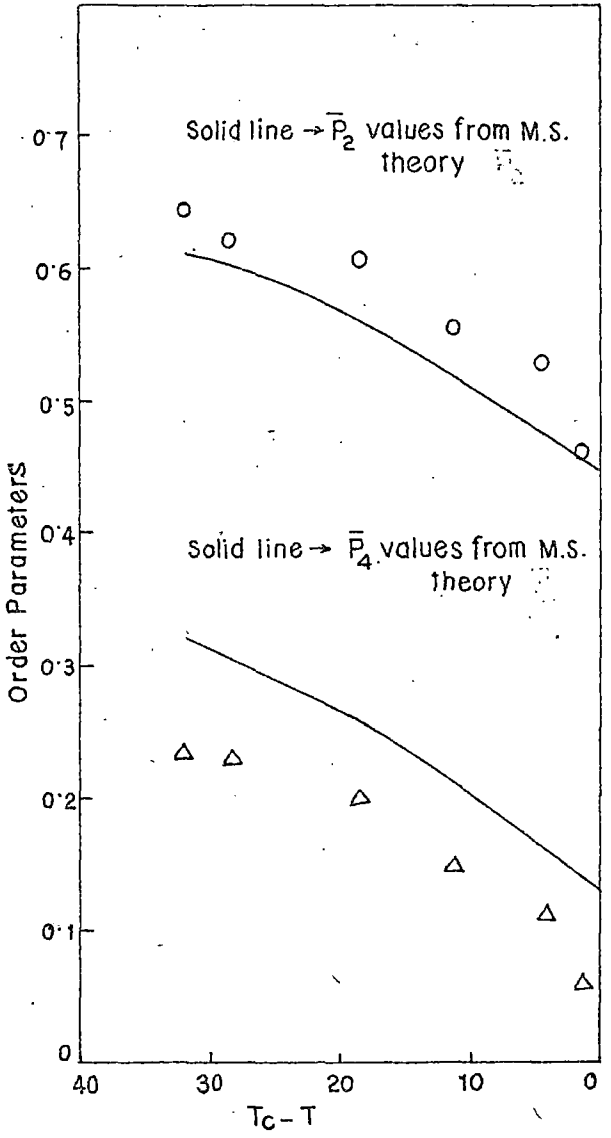

Fig. 8·5 $\langle P_2 \rangle$ & $\bar{P}_2$ are equivalent.
$\langle P_4 \rangle$ & $\bar{P}_4$ are equivalent.

presence of strong magnetic field 5.8 K.Gauss. The results are also given in tabular form in Table 8.18. In our paper on 50CB[2a] Fig. 2 represents the variation of 'D' for 50CB with temperature. There are slight errors in 'D' values for the last two temperatures i.e. for 63°C and 66°C. In this chapter the 'D' values are given in corrected form. All other quantities necessary for the calculation of 'D' are also given in the table. It is found from the fig. 8.3 that the application of magnetic field causes a decrease in the intermolecular distance. This is in accordance with our previous findings in CPHB[2]. 'D' also increases with increasing temperature and remains fairly constant in the supercooled region.

For the calculation of 'l' only for a few photographs, of unoriented samples we could measure the diameter of the inner halo properly and the measured diameter varies from 0.775 cm. to 0.8 cm. For the oriented photographs we failed to measure the diameter of the inner crescents. This is due to the fact that, inner ring is very small and practically it is obstructed by the lead stop. After calculation it was found that 'l' varies from 24.5 Å to 25.3 Å. This difference is within our experimental error. The length 'L' of 50CB molecule in its completely extended form is formed to be 17.5 Å with the help of a stereomodel unit. Thus l/L values is about 1.4 which is in accordance with some earlier work[2,3] on cyano compounds. The increase in apparent length may be due to the association in the nematic phase molecules having

large dipole moments. D & l values are calculated by following the usual procedure described in chapter 3, 4 and 7.

Intensity, Distribution Function and Order Parameter:

The mean of the four intensity values for the four quadrants for each θ (from 0° to 90°) i.e. I (θ) values for different θ values at different temperatures are given in Table 8.19 and the variation of $f(\beta)$ with β as obtained from I (θ) at different temperatures are presented in Tab.8.20. The fig. 8.4(a) represents the variation of $f(\beta)$ with β at 49°C. It can be observed from the fig. 8.4(b) (which shows the normalized distribution function at different temperature) that the orientational distribution function spreads out at higher temperatures as anticipated.

The order parameters $\langle P_2 \rangle$ and $\langle P_4 \rangle$ for 5OCB at different temperatures are shown in fig. 8.5. The order parameter values are also given in Table 8.21. The order parameter values are estimated to be accurate within $\pm$ 0.02. The $\langle P_2 \rangle$ values are found to be larger than $\langle P_2 \rangle$ M.F. (Maier-Saupe theoretical) ~~value~~ values. As explained in case of CPHB[2] (Chapter 7) this may be due to short range dipole dipole interactions. The experimental $\langle P_4 \rangle$ values are lower than the M.F. values. This discrepancy is in accordance with that observed in case of the Sample CPHB[2].

Pseudopotential:

In our earlier case (Chapt.7) we have calculated the pseudopotential or mean field potential for rigid cylind-

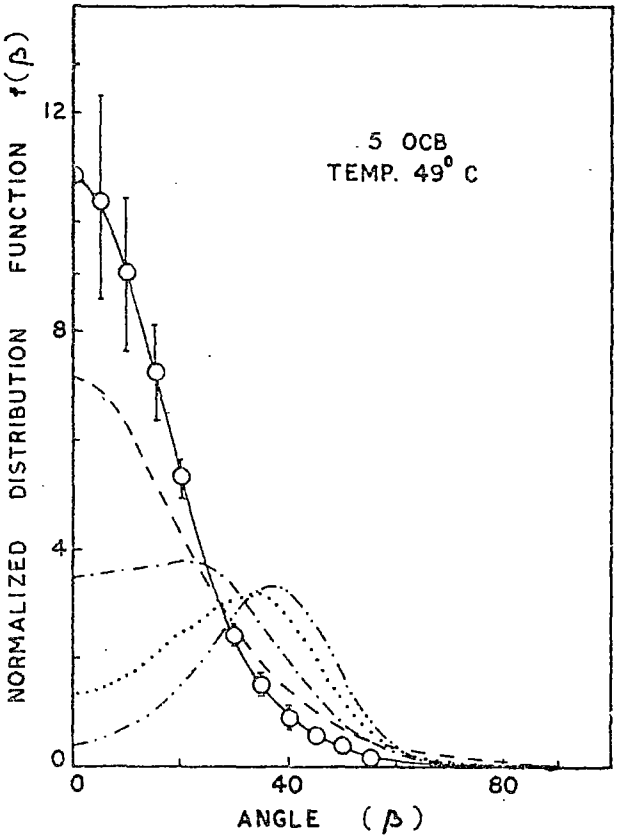

FIG. 8.4(a).

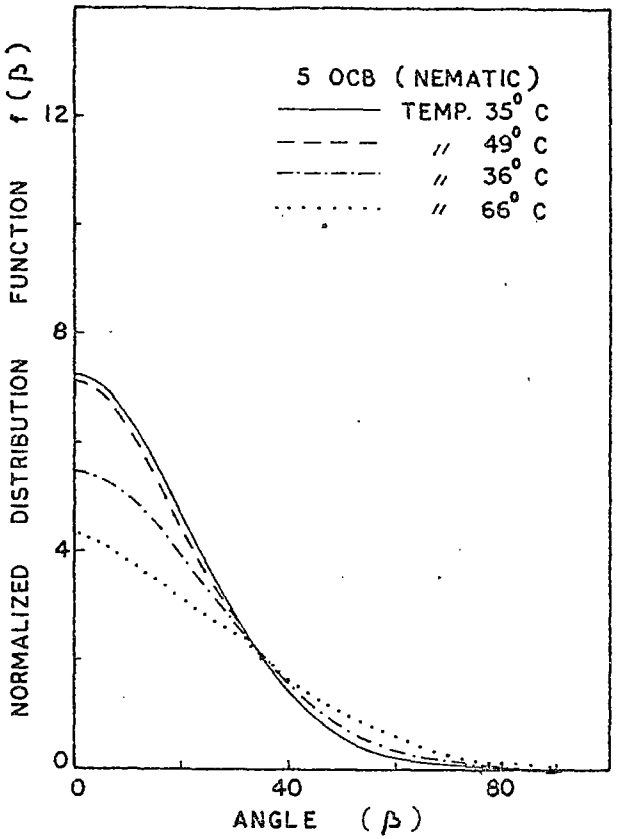

FIG. 8.4(b).

Variation of normalised orientational distribution function $f(\beta)$ with angle β at temperature 49°C for 5OCB.

- – – – – – Experimental data
- ——— Calculated value with pseudopotential $-(2460 \pm 350)\langle P_2\rangle P_2(\cos\beta)$
- —·—·—·— Calculated value with pseudopotential $-(2460)\langle P_2\rangle P_2(\cos\beta) + (3900 + 1500)\langle P_4\rangle P_4(\cos\beta)$
- . . . . . Calculated value with pseudopotential $-(2460)\langle P_2\rangle P_2(\cos\beta) + (3900)\langle P_4\rangle P_4(\cos\beta)$
- —··—··—··— Calculated value with pseudopotential $-(2460)\langle P_2\rangle P_2(\cos\beta) + (3900 - 1500)\langle P_4\rangle P_4(\cos\beta)$

rical molecule using the formula (equation 3.14)

$$V(\beta) = \sum_{L(even)} b_L \langle P_L \rangle P_L(\cos\beta) \qquad \ldots (1)$$

The coefficient b_L which are calculated from a_L values are assumed to be temperature independent in view of narrow temperature range concerned. a_L and b_L ($L = 2$ & 4) values are given in Table 8.22 against different temperatures. Taking six temperature data the angular part of the pseudopotential upto $P_4(\cos\beta)$ term (keeping the last two digits in round number) can be written as

$$V(\beta)/k = -(2460 \pm 350)\langle P_2 \rangle P_2(\cos\beta) + (3900 \pm 1500)\langle P_4 \rangle P_4(\cos\beta) \qquad \ldots (2)$$

Eq.(2) has the form proposed by Humphries et al[4]. It is seen that standard deviation for b_4 is quite large which suggests the breakdown in the assumption inherent in the mean field theory. In fig. 8.4(a)we have also shown the calculated normalized $f(\beta)$ values at 49°C as obtained from several pseudopotentials. It is indicated by the fig. 8.4(a) that the inclusion of the $P_4(\cos\beta)$ term in the pseudopotential results in worse agreement with the experimental. $f(\beta)$ values, this is contrary to our previous work[1], though nothing definite can be said in view of large uncertainty in b_4 values. Permanent dipole-permanent dipole interactions may modify the pseudopoantial to a form different from the form assumed by us (Eq. (1))[5].

TABLE 8.1

Sample: 50CB, Mag.Field = Nil
Temperature = 35°C.

LINEAR SCANNING

L in cm	O. D.	L in cm	O. D.
OUTER HALO		3.7	0.338
		3.65	0.335
		3.5	0.33
7.0	0.29	3.4	0.33
6.8	0.298	3.25	0.325
6.7	0.305	3.15	0.32
6.5	0.32	3.0	0.32
6.35	0.338	2.95	0.321
6.3	0.34	2.8	0.321
6.25	0.35	2.55	0.322
6.2	0.352	2.45	0.325
6.175	0.352	2.3	0.34
6.10	0.35	2.1	0.36
6.05	0.349	2.05	0.362
6.0	0.342	2.0	0.359
5.9	0.33	1.95	0.358
5.7	0.32	1.9	0.358
5.5	0.312	1.8	0.352
5.4	0.314	1.7	0.34
5.3	0.315	1.5	0.32
5.05	0.32	1.3	0.308
4.9	0.325	1.2	0.30
4.6	0.332		
4.4	0.315		
4.35	0.312		
4.25	0.29		
4.2	0.32		
4.15	0.475		
4.05	0.58		
4.0	0.45		
3.95	0.28		
3.9	0.29		
3.85	0.33		

TABLE 8.2

Sample: 50CB, Mag. Field = Nil
Temperature 39°C

LINEAR SCANNING

L in cm	O. D.	L in cm	O. D.
		4.15	1.09
OUTER HALO		4.1	1.105
		4.05	1.06
7.0	0.342	4.0	0.489
6.9	0.348	3.95	0.30
6.8	0.352	3.85	0.38
6.7	0.37	3.7	0.375
6.6	0.388	3.6	0.37
6.5	0.41	3.5	0.365
6.4	0.435	3.4	0.362
6.3	0.448	3.3	0.355
6.25	0.449	3.2	0.352
6.225	0.442	3.1	0.35
6.15	0.43	3.0	0.348
6.0	0.405	2.9	0.34
5.9	0.385	2.8	0.34
5.8	0.375	2.7	0.345
5.7	0.365	2.6	0.35
5.6	0.36	2.45	0.355
5.5	0.36	2.4	0.365
5.4	0.36	2.3	0.38
5.25	0.365	2.2	0.388
5.1	0.37	2.1	0.392
5.0	0.38	2.05	0.392
4.9	0.385	2.0	0.39
4.8	0.395	1.95	0.388
4.7	0.41	1.85	0.37
4.6	0.432	1.8	0.355
4.5	0.49	1.7	0.342
4.4	0.52	1.6	0.33
4.3	0.628	1.5	0.32
4.25	0.85	1.2	0.30
4.2	1.08		

TABLE 8.3

Sample: 50CB, Mag.Field = Nil
Temperature 49°C.

LINEAR SCANNING			
L in cm	O. D.	L in cm	O. D.
		3.95	0.45
OUTER HALO		3.9	0.36
		3.85	0.43
7.0	0.44	3.8	0.52
6.8	0.48	3.75	0.53
6.55	0.542	3.7	0.52
6.4	0.58	3.6	0.52
6.3	0.60	3.5	0.53
6.2	0.62	3.4	0.54
6.15	0.662	3.3	0.535
6.1	0.615	3.25	0.532
6.0	0.60	3.2	0.52
5.9	0.56	3.1	0.51
5.7	0.51	3.0	0.51
5.6	0.49	2.95	0.50
5.5	0.472	2.9	0.495
5.4	0.47	2.8	0.48
5.35	0.472	2.6	0.475
5.2	0.472	2.55	0.48
5.15	0.478	2.45	0.48
5.05	0.48	2.35	0.49
5.0	0.485	2.3	0.50
4.9	0.485	2.2	0.515
4.8	0.49	2.15	0.532
4.7	0.498	2.1	0.548
4.6	0.501	2.0	0.548
4.5	0.51	1.95	0.546
4.45	0.518	1.9	0.535
4.4	0.515	1.75	0.50
4.3	0.455	1.6	0.46
4.25	0.355	1.4	0.40
4.2	0.34	1.2	0.37
4.15	0.53		
4.1	1.24		
4.05	1.25		
4.0	1.12		

TABLE 8.4

Sample: 5 OCB, Mag. Field =Nil
Temperature 56°C.

LINEAR SCANNING			
L in cm.	O. D.	L in cm	O. D.
		4.1	0.98
OUTER HALO		4.05	1.03
		4.0	0.96
7.0	0.33	3.95	0.35
6.8	0.348	3.9	0.29
6.7	0.355	3.85	0.29
6.55	0.375	3.8	0.36
6.5	0.385	3.70	0.38
6.4	0.41	3.65	0.375
6.3	0.425	3.55	0.37
6.2	0.44	3.5	0.47
6.15	0.445	3.35	0.368
6.10	0.442	3.2	0.362
6.05	0.44	3.1	0.362
5.95	0.42	2.95	0.358
5.85	0.405	2.9	0.355
5.70	0.38	2.8	0.352
5.6	0.362	2.7	0.35
5.5	0.358	2.55	0.355
5.4	0.355	2.5	0.36
5.3	0.352	2.4	0.37
5.25	0.355	2.3	0.38
5.1	0.36	2.2	0.395
5.0	0.362	2.1	0.415
4.9	0.37	2.0	0.41
4.7	0.37	1.95	0.41
4.6	0.375	1.9	0.40
4.4	0.39	1.8	0.399
4.3	0.392	1.7	0.38
4.25	0.385	1.5	0.338
4.2	0.30	1.25	0.31
4.225	0.38		
4.15	0.53		

TABLE 8.5

Sample: 5 OCB, Mag. Field = Nil, Temperature = 63°C.

LINEAR SCANNING.

L in cm.	O. D.	L in cm.	O. D.
	OUTER HALO	4.0	0.875
		3.90	0.32
		3.80	0.38
7.0	0.31	3.7	0.41
6.8	0.33	3.6	0.402
6.7	0.34	3.5	0.40
6.5	0.36	3.4	0.40
6.35	0.385	3.3	0.398
6.3	0.39	3.2	0.392
6.25	0.40	3.1	0.388
6.2	0.41	3.0	0.39
6.15	0.412	2.9	0.385
6.05	0.415	2.8	0.382
6.025	0.41	2.7	0.39
5.95	0.405	2.6	0.40
5.8	0.382	2.5	0.41
5.6	0.368	2.4	0.42
5.5	0.36	2.25	0.448
5.3	0.365	2.2	0.465
5.1	0.372	2.1	0.472
5.0	0.378	2.0	0.482
4.9	0.382	1.975	0.48
4.7	0.39	1.90	0.47
4.55	0.40	1.80	0.45
4.5	0.41	1.75	0.46
4.4	0.418	1.6	0.42
4.3	0.39	1.45	0.39
4.25	0.32	1.3	0.36
4.2	0.55	1.2	0.352
4.15	0.67		
4.125	1.25		
4.1	1.2		
4.05	1.17		

TABLE 8.6

Sample: 50CB, Mag. Field = 0.19 K.Gauss, Temperature 49°C
Background optical density = 0.305.

LINEAR SCANNING				ANGULAR SCANNING		
L in cm	O. D.	L in cm.	O. D.	θ in degree.	O. D.	Intensity
OUTER HALO						
7.0	0.498	1.65	0.62	0.0	0.065	7.5
6.9	0.522	1.55	0.60	10	0.075	8.75
6.8	0.565	1.50	0.55	20	0.085	10.00
6.7	0.605	1.30	0.49	30	0.095	11.25
6.6	0.63	1.25	0.48	40	0.115	14.0
6.55	0.64			50	0.145	18.0
6.525	0.64	INNER HALO		60	0.203	25.25
6.5	0.638			70	0.257	31.75
6.4	0.615	5.0	0.44	80	0.31	39.8
6.25	0.565	4.9	0.455	85	0.333	43.6
6.20	0.542	4.8	0.48	90	0.33	43.2
6.0	0.495	4.70	0.505	100	0.31	39.8
5.9	0.478	4.60	0.53	111	0.265	32.75
5.7	0.465	4.50	0.555	120	0.195	24.25
5.55	0.46	4.475	0.538	130	0.137	17.0
5.5	0.465	4.45	0.5	140	0.107	13.00
5.4	0.468	4.35	0.37	150	0.087	10.2
5.2	0.47	4.25	0.312	160	0.083	9.75
5.05	0.465	4.2	0.37	170	0.07	8.2
5.0	0.46	4.10	0.82	180	0.067	7.75
4.9	0.46	4.0	0.665	190	0.07	8.20
4.65	0.77	3.90	0.45	200	0.077	9.2
4.2	0.35	3.85	0.555	210	0.083	9.75
4.1	0.89	3.8	0.578	220	0.105	12.5
4.0	0.70	3.725	0.598	230	0.145	18.0
3.9	0.328	3.70	0.588	240	0.197	24.5
3.8	0.472	3.6	0.542	250	0.255	31.5
3.7	0.492	3.5	0.512	256	0.28	35.0
3.5	0.472	3.35	0.49	261	0.305	39.0
3.3	0.46	3.1	0.442	266	0.325	42.5
3.15	0.462	3.0	0.455	269	0.333	43.6
3.0	0.465			270	0.33	43.2
2.8	0.462			280	0.303	38.5
2.6	0.46			290	0.265	32.7
2.5	0.46			300	0.21	26.2
2.35	0.472			310	0.157	19.75
2.2	0.51			320	0.125	15.5
2.0	0.56			330	0.103	12.25
1.9	0.60			340	0.09	10.7
1.85	0.628			350	0.083	9.75
1.725	0.625			0	0.075	8.75
1.70	0.625					

TABLE 8.7

Sample: 50CB, Mag. Field = 0.5 K.Gauss, Temperature 49°c
Background optical density = 0.32

LINEAR SCANNING				ANGULAR SCANNING		
L in cm.	O. D.	L in cm.	O. D.	θ in degree	O. D.	Intensity
OUTER HALO						
7.0	0.501	2.3	0.472	0	0.052	6.0
6.8	0.542	2.1	0.505	10	0.055	6.5
6.7	0.582	2.0	0.530	20	0.058	6.75
6.6	0.60	1.9	0.568	30	0.06	7.0
6.55	0.60	1.85	0.575	40	0.072	8.5
6.5	0.599	1.8	0.585	50	0.095	11.5
6.4	0.575	1.7	0.582	60	0.12	15.0
6.3	0.54	1.6	0.562	70	0.160	20.0
6.2	0.51	1.5	0.52	80	0.215	26.75
6.0	0.48	1.3	0.455	93	0.26	32.2
5.85	0.46	1.25	0.45	99	0.275	34.2
5.7	0.455			100	0.255	31.5
5.65	0.455			102	0.27	33.5
5.5	0.46			110	0.255	31.5
5.4	0.46			120	0.21	26.2
5.3	0.462			130	0.16	20.0
5.2	0.46			140	0.155	14.0
5.1	0.45			150	0.095	11.5
5.0	0.45			160	0.075	9.0
4.9	0.45			170	0.06	7.0
4.8	0.452			185	0.055	6.5
4.7	0.46			190	0.04	4.5
4.6	0.54			200	0.06	7.0
4.4	0.572			210	0.06	7.0
4.3	0.50			220	0.072	8.5
4.25	0.475			230	0.095	11.5
4.20	0.87			240	0.125	15.5
4.15	1.1			250	0.17	21.25
4.1	1.02			260	0.22	27.5
4.0	0.395			270	0.264	32.5
3.9	0.345			278	0.265	32.7
3.7	0.465			280	0.26	32.2
3.6	0.462			290	0.225	28.0
3.5	0.45			300	0.18	22.5
3.3	0.448			310	0.132	16.5
3.25	0.448			320	0.095	11.5
3.1	0.45			330	0.075	9.0
3.0	0.455			340	0.065	7.25
2.9	0.46			350	0.060	7.0
2.8	0.452			0	0.052	6.0
2.7	0.45					
2.5	0.452					

TABLE 6.8

Sample: 50CB, Mag. Field 0.91 K.Gauss, Temperature 49°C
Background optical density = 0.33.

LINEAR SCANNING				ANGULAR SCANNING		
L in cm	O. D.	L in cm	O. D.	Θ in degree	O. D.	Intensity
OUTER HALO						
7.0	0.53	2.6	0.522	0	0.075	9.0
6.8	0.59	2.45	0.525	10	0.075	9.0
6.6	0.705	2.35	0.53	20	0.085	10.0
6.5	0.748	2.2	0.552	30	0.10	12.0
6.4	0.752	2.1	0.582	40	0.13	13.2
6.375	0.75	2.05	0.61	50	0.185	23.0
6.3	0.74	2.0	0.622	60	0.262	32.5
6.2	0.702	1.95	0.63	70	0.34	45.0
6.1	0.64	1.925	0.635	80	0.40	55.0
6.0	0.615	1.85	0.68	88	0.422	58.6
5.9	0.59	1.8	0.70	91	0.421	58.4
5.8	0.56	1.75	0.735	100	0.39	53.25
5.7	0.54	1.7	0.74	110	0.32	41.5
5.6	0.538	1.65	0.76	120	0.225	28.0
5.5	0.535	1.575	0.77	130	0.17	21.25
5.4	0.54	1.55	0.76	140	0.125	15.5
5.3	0.542	1.5	0.748	150	0.105	12.5
5.2	0.55	1.3	0.67	160	0.095	11.5
5.1	0.55	1.2	0.60	170	0.09	10.7
5.0	0.54			180	0.088	10.2
4.9	0.53			190	0.088	10.2
4.75	0.532			200	0.095	11.5
4.7	0.54			210	0.13	16.0
4.6	0.552			225	0.17	21.2
4.5	0.57			230	0.21	26.2
4.4	0.568			240	0.282	35.2
4.3	0.37			250	0.36	48.0
4.2	0.335			260	0.418	58.0
4.15	0.39			265	0.428	59.75
4.1	0.36			268	0.426	59.25
4.0	0.37			270	0.420	58.2
3.8	0.32			280	0.37	50.0
3.7	0.585			290	0.285	35.7
3.6	0.55			300	0.21	26.2
3.5	0.532			310	0.145	18.0
3.4	0.522			320	0.11	13.0
3.3	0.525			330	0.085	10.0
3.2	0.528			340	0.08	9.5
3.1	0.532			350	0.075	9.0
2.95	0.535					
2.9	0.535					
2.7	0.530					

TABLE 8.9

Sample: 500B, Mag.Field = 1.69 K. Gauss, Temperature 49°C
Background optical density 0.28

LINEAR SCANNING				ANGULAR SCANNING		
L in cm	O. D.	L in cm.	O. D.	θ in degree	O. D.	Intensity
OUTER HALO						
7.0	0.480	3.35	0.46	350	0.07	8.0
6.9	0.515	3.3	0.46	0	0.062	7.2
6.8	0.55	3.2	0.47	10	0.068	8.0
6.7	0.59	3.1	0.475	20	0.071	8.3
6.6	0.62	3.0	0.48	30	0.085	9.0
6.5	0.632	2.9	0.48	40	0.112	13.5
6.45	0.632	2.8	0.475	50	0.155	19.0
6.425	0.625	2.7	0.47	60	0.219	27.2
6.4	0.618	2.6	0.47	70	0.29	36.5
6.3	0.60	2.5	0.475	80	0.33	43.25
6.2	0.565	2.35	0.49	87	0.352	47.0
6.1	0.53	2.2	0.52	90	0.352	47.0
6.0	0.505	2.0	0.60	92	0.349	46.25
5.9	0.482	1.8	0.645	100	0.32	41.5
5.8	0.475	1.7	0.60	110	0.26	32.25
5.6	0.47	1.6	0.622	120	0.195	24.25
5.55	0.47	1.5	0.575	130	0.14	17.5
5.5	0.478	1.4	0.53	140	0.11	13.25
5.4	0.48	1.2	0.475	150	0.092	10.7
5.3	0.485	INNER HALO		160	0.082	9.75
5.2	0.48			170	0.075	9.0
5.15	0.475	5.0	0.42	180	0.072	8.5
5.1	0.47	4.8	0.47	190	0.08	9.5
5.0	0.458	4.7	0.505	200	0.09	10.5
4.9	0.45	4.65	0.51	210	0.10	12.0
4.8	0.45	4.6	0.55	224	0.15	18.7
4.75	0.452	4.55	0.53	230	0.19	24.2
4.6	0.478	4.5	0.59	240	0.252	31.2
4.5	0.49	4.45	0.55	250	0.32	42.0
4.4	0.50	4.3	0.29	255	0.338	44.75
4.3	0.42	4.25	0.32	260	0.355	47.25
4.25	0.38	4.20	0.49	264	0.358	47.75
4.2	0.72	4.25	0.65	267	0.35	46.5
4.15	1.0	4.10	0.92	270	0.345	45.5
4.125	1.25	4.05	0.93	280	0.31	40.0
4.1	0.87	4.0	0.89	290	0.252	31.2
4.05	0.62	3.95	0.37	300	0.19	23.5
4.0	0.485	3.80	0.46	310	0.135	16.5
3.95	0.29	3.7	0.53	320	0.105	12.5
3.85	0.30	3.65	0.53	330	0.08	9.5
3.75	0.46	3.6	0.51	340	0.075	9.0
3.6	0.46	3.5	0.50	350	0.07	8.0
3.5	0.46	3.4	0.48			
3.45	0.455	3.2	0.43			
3.4	0.455	3.0	0.415			

TABLE 8.10

Sample: 50CB, Mag. Field 2.74 K.Gauss, Temperature 49°C
Background optical density = 0.265.

LINEAR SCANNING				ANGULAR SCANNING		
L in cm	O. D.	L in cm	O. D.	θ in degree	O. D.	Intensit
OUTER HALO						
7.0	0.378	2.1	0.41	350	0.047	5.4
6.8	0.40	2.0	0.42	0	0.035	3.8
6.7	0.435	1.95	0.438	10	0.047	5.4
6.6	0.45	1.8	0.468	20	0;05	6.0
6.5	0.462	1.7	0.475	30	0.057	6.75
6.45	0.462	1.65	0.475	40	0.07	8.25
6.4	0.655	1.5	0.448	50	0.093	11.0
6.3	0.448	1.3	0.392	60	0.123	15.0
6.2	0.428	1.25	0.375	70	0.157	21.25
6.1	0.40			80	0.19	23.6
6.0	0.355	INNER HALO		88	0.197	24.5
5.9	0.375			92	0.197	24.5
5.8	0.370	5.0	0.36	95	0.197	24.5
5.6	0.368	4.8	0.388	100	0.185	23.0
5.5	0.368	4.7	0.41	110	0.155	18.25
5.4	0.37	4.55	0.46	120	0.117	14.5
5.3	0.372	4.5	0.42	130	0.087	10.25
5.2	0.37	4.45	0.452	140	0.07	8.25
5.0	0.365	4.4	0.40	150	0.055	6.5
4.9	0.362	4.25	0.30	160	0.047	5.40
4.7	0.368	4.2	0.71	170	0.043	5.0
4.6	0.38	4.10	1.2	180	0.043	5.0
4.4	0.36	4.05	0.94	190	0.045	5.2
4.3	0.28	4.0	0.74	200	0.047	5.4
4.2	0.28	3.95	0.29	210	0.055	6.5
4.1	0.78	3.9	0.30	220	0.07	8.25
4.05	1.26	3.85	0.38	230	0.095	11.5
4.0	0.89	3.8	0.41	240	0.125	15.5
3.9	0.375	3.75	0.43	250	0.163	20.5
3.8	0.38	3.7	0.428	260	0.193	24.0
3.6	0.37	3.65	0.422	267	0.203	25.25
3.5	0.365	3.6	0.405	276	0.205	25.5
3.35	0.365	3.5	0.40	278	0.203	25.25
3.3	0.37	3.3	0.36	285	0.185	23.0
3.1	0.37	3.0	0.335	290	0.165	20.75
3.0	0.372			300	0.135	16.7
2.9	0.375			310	0.103	12.8
2.75	0.372			320	0.083	9.8
2.6	0.37			330	0.065	7.5
2.45	0.372			340	0.055	6.5
2.35	0.382			350	0.05	6.0
2.2	0.39			0	0.035	3.8

TABLE 8.11

Sample: 500B, Mag.Field 4.3 K.Gauss, Temperature 49°C

Background optical density = 0.30

LINEAR SCANNING				ANGULAR SCANNING		
L in cm	O. D.	L in cm	O. D.	θ in degree	O. D.	Intensity
OUTER HALO						
7.0	0.455	2.7	0.48	0	0.07	8.2
6.9	0.49	2.6	0.48	10	0.05	5.75
6.76	0.565	2.5	0.455	20	0.08	9.50
6.6	0.605	2.35	0.478	30	0.09	10.5
6.5	0.65	2.30	0.48	40	0.108	12.75
6.4	0.665	2.35	0.49	50	0.14	17.5
6.375	0.67	2.2	0.51	60	0.19	23.5
6.3	0.668	2.0	0.552	70	0.262	32.5
6.2	0.635	1.9	0.60	81	0.33	43.0
6.0	0.568	1.75	0.65	91	0.38	51.5
5.9	0.525	1.65	0.675	95	0.39	53.25
5.7	0.49	1.575	0.685	97	0.38	51.5
5.6	0.48	1.55	0.68	100	0.375	50.75
5.45	0.475	1.5	0.678	110	0.34	45.0
5.4	0.48	1.4	0.635	120	0.265	32.75
5.3	0.48	1.3	0.58	130	0.19	23.75
5.2	0.485	1.2	0.52	140	0.135	16.5
5.1	0.485			150	0.10	12.0
5.0	0.485			160	0.075	8.75
4.95	0.48			170	0.07	8.25
4.85	0.47			180	0.06	7.0
4.7	0.475			190	0.058	6.75
4.6	0.49			200	0.065	7.5
4.45	0.51			210	0.078	9.25
4.35	0.51			220	0.088	10.25
4.3	0.425			230	0.122	15.0
4.2	0.33			240	0.175	21.75
4.15	0.49			250	0.232	28.75
4.10	0.47			260	0.312	40.25
4.05	1.15			270	0.362	48.2
4.0	1.16			275	0.37	50.0
3.95	0.80			280	0.37	50.0
3.9	0.31			285	0.365	49.0
3.8	0.305			290	0.36	48.0
3.7	0.48			291	0.325	42.5
3.6	0.50			300	0.275	34.0
3.5	0.48			310	0.205	25.5
3.4	0.47			320	0.15	18.7
3.3	0.465			330	0.112	13.2
3.2	0.475			340	0.09	10.5
3.0	0.485			350	0.08	9.5
2.9	0.485			0	0.072	8.25

TABLE 8.12

Sample: 50CB. Mag.Field 5.80 K.Gauss, Temperature 49°C,
Background Optical Density 0.31

LINEAR SCANNING				ANGULAR SCANNING		
L in cm.	O. D.	L in cm.	O. D.	θ in (deg)	O. D.	Intensity
	OUTER HALO					
7.0	0.595	2.7	0.535	0	0.078	9.2
6.9	0.645	2.6	0.522	10	0.08	9.5
6.8	0.68	2.45	0.525	20	0.09	10.7
6.7	0.73	2.35	0.54	30	0.10	12.0
6.6	0.76	2.2	0.57	40	0.12	15.5
6.575	0.762	2.1	0.582	50	0.165	20.5
6.525	0.765	2.05	0.64	60	0.238	29.5
6.5	0.755	2.0	0.65	70	0.315	40.5
6.4	0.745	1.95	0.67	80	0.39	53.2
6.2	0.65	1.925	0.675	91	0.45	63.7
6.0	0.54	1.85	0.72	93	0.448	63.2
5.8	0.54	1.8	0.73	100	0.43	60.0
5.6	0.54	1.75	0.745	110	0.37	50.0
5.5	0.54	1.7	0.755	121	0.27	33.5
5.4	0.545	1.65	0.75	130	0.20	25.0
5.3	0.548	1.6	0.735	140	0.15	18.7
5.2	0.55	1.575	0.73	150	0.12	15.0
5.1	0.54	1.55	0.72	160	0.10	12.0
5.0	0.53	1.5	0.69	170	0.09	10.7
4.9	0.53	1.3	0.60	180	0.045	5.2
4.75	0.532	1.2	0.54	192	0.088	10.2
4.7	0.545			200	0.09	10.7
4.5	0.565			210	0.11	13.0
4.45	0.57			220	0.14	17.5
4.35	0.585			232	0.195	24.2
4.25	0.48			240	0.25	31.0
4.2	0.575			250	0.325	42.2
4.1	1.07			260	0.39	53.2
4.075	1.36			265	0.405	55.5
4.0	0.89			269	0.41	56.5
3.95	0.36			270	0.408	55.2
3.85	0.38			280	0.37	50.0
3.8	0.50			290	0.30	38.2
3.7	0.57			300	0.22	27.5
3.6	0.55			310	0.16	20.0
3.5	0.54			320	0.118	14.5
3.4	0.52			330	0.095	11.5
3.3	0.522			340	0.082	9.7
3.2	0.525			350	0.078	9.2
3.1	0.532			0	0.078	9.2
2.95	0.535					
2.9	0.545					

TABLE 8.13

Sample: 500B. Mag.Field 5.80 K.Gauss, Temperature 35°C
Background Optical Density = 0.31.

LINEAR SCANNING				ANGULAR SCANNING		
L in cm.	O. D.	L in cm.	O. D.	θ in (deg.)	O. D.	Intensity.
		3.5	0.39	355	0.025	2.5
OUTER HALO		3.4	0.388	5	0.025	2.5
		3.3	0.382	15	0.028	3.0
7.0	0.39	3.2	0.388	20	0.03	3.25
6.9	0.40	3.1	0.39	30	0.032	3.5
6.8	0.425	3.0	0.399	40	0.032	3.5
6.7	0.448	2.9	0.399	50	0.046	5.5
6.6	0.466	2.75	0.399	60	0.07	8.5
6.5	0.482	2.65	0.39	70	0.104	12.5
6.45	0.484	2.55	0.39	75	0.13	16.0
6.4	0.48	2.4	0.39	80	0.142	17.7
6.3	0.46	2.3	0.39	84	0.152	19.0
6.2	0.44	2.15	0.395	88	0.16	20.0
6.05	0.418	2.1	0.405	92	0.165	20.5
6.0	0.41	2.05	0.412	95	0.161	20.2
5.9	0.40	1.9	0.429	100	0.155	19.25
5.75	0.392	1.8	0.452	110	0.125	15.5
5.65	0.391	1.75	0.47	120	0.085	10.0
5.5	0.392	1.65	0.475	130	0.055	6.5
5.4	0.398	1.55	0.482	140	0.035	4.0
5.3	0.396	1.525	0.48	150	0.03	3.25
5.2	0.398	1.5	0.472	160	0.02	2.0
5.1	0.399	1.4	0.45	170	0.019	1.8
5.0	0.395	1.3	0.432	185	0.02	2.0
4.9	0.388	1.2	0.41	190	0.018	1.75
4.8	0.388			200	0.018	1.75
4.7	0.389			210	0.02	2.0
4.6	0.395			220	0.03	3.25
4.5	0.40			230	0.042	4.75
4.35	0.395			240	0.062	7.2
4.3	0.392			250	0.095	11.25
4.25	0.35			260	0.132	16.25
4.2	0.332			265	0.145	18.0
4.1	0.405			270	0.155	19.25
4.05	0.59			272	0.158	19.8
4.0	0.425			275	0.16	20.0
3.9	0.32			278	0.155	19.25
3.85	0.33			285	0.142	17.7
3.8	0.38			290	0.13	16.0
3.75	0.40			300	0.91	11.0
3.65	0.40			310	0.062	7.25
3.6	0.399			320	0.048	5.5
				330	0.042	4.75
				340	0.042	4.75

TABLE 8.14

Sample: 5003, Mag. Field 5.80 K.Gauss, Temperature 56°C
Background optical density = 0.31.

LINEAR SCANNING				ANGULAR SCANNING		
L in cm.	O. D.	L in cm.	O. D.	θ in degree	O. D.	Intensity
		3.35	0.39	350	0.02	2.0
OUTER HALO		3.2	0.39	0	0.022	2.25
		3.1	0.392	10	0.02	2.0
7.0	0.398	2.95	0.39	20	0.025	2.5
6.8	0.42	2.8	0.388	30	0.028	3.6
6.65	0.45	2.7	0.385	40	0.035	4.0
6.55	0.458	2.6	0.382	50	0.042	4.75
6.5	0.458	2.45	0.38	60	0.062	7.2
6.45	0.45	2.3	0.385	70	0.082	9.75
6.4	0.442	2.15	0.395	80	0.112	13.5
6.3	0.432	2.1	0.408	90	0.132	15.2
6.2	0.42	2.05	0.412	96	0.142	17.175
6.1	0.401	1.9	0.425	99	0.14	17.2
6.0	0.392	1.8	0.44	107	0.13	16.0
5.9	0.39	1.775	0.448	115	0.115	14.0
5.8	0.39	1.75	0.442	120	0.108	13.0
5.7	0.388	1.65	0.441	130	0.082	9.75
5.6	0.39	1.5	0.432	140	0.06	7.0
5.5	0.39	1.4	0.412	150	0.048	5.5
5.4	0.39	1.3	0.392	160	0.038	4.2
5.3	0.392	1.2	0.38	170	0.03	3.2
5.2	0.392			180	0.028	3.0
5.1	0.392			190	0.025	2.6
5.0	0.39			200	0.03	3.2
4.9	0.39			210	0.032	3.5
4.8	0.39			220	0.040	4.5
4.7	0.399			230	0.045	5.2
4.6	0.425			240	0.060	7.0
4.5	0.84			250	0.091	10.6
4.45	0.92			260	0.11	13.0
4.4	0.568			270	0.122	15.0
4.35	0.44			275	0.128	15.75
4.3	0.425			277	0.129	15.9
4.25	0.382			279	0.129	15.9
4.2	0.365			282	0.125	15.5
4.15	0.553			290	0.11	13.0
4.1	0.82			300	0.092	10.75
4.05	0.82			310	0.062	7.25
4.0	0.54			320	0.045	5.25
3.95	0.33			330	0.030	3.25
3.9	0.34			340	0.025	2.5
3.8	0.41			350	0.022	2.25
3.7	0.41					
3.6	0.40					
3.5	0.39					

TABLE A.15

Sample: 500B, Mag.Field 5.80 K.Gauss, Temperature 63°C
Background optical density 0.30

LINEAR SCANNING				ANGULAR SCANNING		
L in cm	O. D.	L in cm.	O. D.	θ in degree	O. D.	Intensity
OUTER HALO		3.5	0.412	350	0.05	5.75
		3.4	0.408	0	0.048	5.5
		3.3	0.41	10	0.052	6.0
7.0	0.41	3.2	0.41	20	0.055	6.25
6.8	0.462	3.1	0.41	30	0.07	8.25
6.6	0.49	3.0	0.408	40	0.09	10.6
6.55	0.495	2.85	0.401	50	0.11	13.25
6.525	0.498	2.8	0.401	60	0.139	17.5
6.475	0.495	2.6	0.401	70	0.17	20.2
6.425	0.492	2.55	0.399	80	0.19	23.5
6.35	0.482	2.5	0.399	86	0.20	25.0
6.25	0.462	2.3	0.402	8.75	0.20	25.0
6.2	0.46	2.25	0.415	91	0.197	24.5
6.1	0.44	2.15	0.422	100	0.18	22.4
6.0	0.422	2.1	0.43	110	0.15	18.7
5.9	0.415	2.0	0.442	120	0.13	16.0
5.8	0.41	1.9	0.451	130	0.105	12.5
5.7	0.40	1.85	0.468	140	0.08	9.5
5.6	0.40	1.75	0.472	150	0.065	7.5
5.5	0.40	1.70	0.472	160	0.06	7.0
5.4	0.402	1.65	0.47	175	0.038	4.35
5.3	0.405	1.6	0.468	185	0.055	6.5
5.15	0.408	1.5	0.458	195	0.065	7.75
5.05	0.408	1.4	0.43	205	0.07	8.25
4.95	0.409	1.3	0.40	210	0.075	9.0
4.8	0.41	1.25	0.38	220	0.095	11.5
4.6	0.415	1.2	0.38	230	0.12	14.75
4.45	0.468			242	0.15	18.6
4.4	0.48			250	0.17	21.25
4.35	0.462			257	0.173	21.6
4.3	0.348			260	0.173	21.6
4.2	0.321			265	0.173	21.6
4.15	0.435			267	0.172	21.5
4.10	0.73			270	0.17	21.25
4.05	0.86			280	0.15	18.6
4.0	0.54			290	0.128	15.75
3.95	0.34			300	0.098	11.75
3.9	0.32			310	0.075	9.0
3.85	0.37			320	0.064	7.5
3.75	0.44			330	0.055	6.5
3.7	0.432			340	0.05	5.75
3.65	0.425					

TABLE 8.16

Sample: 500B, Mag. Field 5.80 K.Gauss, Temperature 66°C
Background optical density = 0.305.

LINEAR SCANNING				ANGULAR SCANNING		
L in cm	O. D.	L in cm.	O. D.	θ in degree	O. D.	Intensity
OUTER HALO						
7.0	0.4	1.95	0.465	0	0.095	11.25
6.9	0.425	1.9	0.47	10	0.085	10.0
6.7	0.46	1.85	0.475	20	0.095	11.25
6.5	0.499	1.65	0.488	30	0.10	12.0
6.45	0.5	1.6	0.485	40	0.115	14.0
6.35	0.5	1.55	0.48	50	0.13	16.0
6.3	0.495	1.5	0.465	60	0.145	18.0
6.2	0.48	1.3	0.442	70	0.165	20.5
6.1	0.468	1.2	0.418	80	0.175	21.75
6.0	0.455			90	0.185	23.0
5.9	0.445			97	0.195	24.2
5.7	0.445			102	0.193	24.0
5.5	0.45			110	0.19	23.5
5.35	0.462			120	0.175	21.75
5.15	0.485			130	0.16	20.0
5.0	0.492			140	0.145	18.0
4.8	0.518			150	0.133	16.5
4.7	0.51			160	0.123	15.2
4.6	0.50			170	0.115	14.0
4.45	0.501			180	0.11	13.2
4.35	0.498			190	0.113	13.5
4.2	0.39			200	0.115	14.0
4.15	0.71			210	0.12	15.0
4.05	0.95			220	0.135	16.5
4.0	0.58			230	0.143	17.75
3.95	0.355			240	0.15	18.65
3.9	0.37			250	0.163	20.25
3.8	0.465			260	0.175	22.0
3.7	0.475			268	0.177	22.2
3.6	0.462			272	0.175	22.0
3.45	0.45			275	0.17	21.25
3.2	0.44			285	0.17	21.25
3.1	0.435			290	0.113	13.5
3.0	0.435			300	0.143	17.5
2.9	0.43			310	0.116	14.1
2.75	0.425			320	0.105	12.5
2.5	0.422			330	0.105	12.5
2.3	0.43			340	0.1	12.0
2.15	0.44			350	0.095	11.2
2.05	0.45			0	0.095	11.2

Table 8.17

Sample: 500B.

Variation of 'D' and degree of ordering with magnetic field at 49°C.

Field in K.Gauss.	Distance of the sample from the film in cm.	Outer halo			Degree of ordering (2nd.order)
		Diameter in cm.	Bragg angle (deg.)	'D' in Å	
0	5.655	4.1	9.963	4.98	0
0.19	6.345	4.725	10.211	4.86	0.56
0.55	6.345	4.75	10.261	4.83	0.57
0.91	6.345	4.775	10.31	4.81	0.62
1.69	6.345	4.775	10.31	4.81	0.57
2.74	6.345	4.8	10.36	4.79	0.57
4.38	6.345	4.8	10.36	4.79	0.58
5.80	6.345	4.825	10.41	4.77	0.61

Table 8.18

Sample: 500B.

Intermolecular distance 'D' at different temperatures in absence and presence of magnetic field.

Temp. °C.	Field in (K.Gauss)	Distance of the sample from the film(cm.)	Outer halo		
			Diam. (cm)	Bragg angle (degree)	'D' in Å
35	0	5.655	4.15	10.075	4.92
35	5.8	6.345	4.9	10.556	4.7
39	0	5.655	4.125	10.0	4.92
39	5.8	6.345	4.9	10.556	4.7
49	0	5.655	4.1	9.963	4.98
49	5.8	6.345	4.825	10.408	4.75
56	0	5.655	4.05	9.851	5.03
56	5.8	6.345	4.775	10.310	4.81
63	0	5.655	4.025	9.795	5.06
63	5.8	6.345	4.75	10.261	4.84
66	5.8	6.345	4.7	10.162	4.88

Table 8.19

Sample: 50CB.

Mean Intensity at different temperatures.

θ (deg)	I(θ) for temperatures °C					
	35	39	49	56	63	66
0	21.75	18.25	49.63	29.25	17.5	11.5
5	21.38	17.6	47.25	28.69	17.063	11.15
10	19.44	16.13	43.56	26.91	15.9	10.69
15	17.31	14.31	38.63	24.63	14.44	9.85
20	14.50	11.78	32.13	21.5	13.06	9.31
25	11.81	9.01	26.19	18.25	11.53	8.313
30	9.06	7.15	20.69	15.06	9.81	7.34
35	6.63	5.31	16.13	12.13	8.11	6.29
40	4.75	3.99	12.38	9.31	6.43	5.11
45	3.19	2.93	9.0	6.88	5.01	4.175
50	1.88	2.3	6.63	4.75	3.75	3.44
55	1.25	1.54	4.38	3.38	2.56	2.63
60	0.80	1.0	2.94	2.25	1.74	2.06
65	0.50	0.6	1.81	1.625	1.23	1.43
70	0.19	0.4	0.75	1.063	0.75	0.89
75	0.06	0.3	0.38	1.38	0.40	0.60
80	0	0.188	0.19	0.45	0.175	0.36
85	0	0.075	0	0.25	0	0.125
90	0	0	0	0.063	0	0

Table 8.20

Sample: 500B.

Normalised distribution function at different temperatures.

β (deg)	$f(\beta)$ at temperatures in °C					
	35°C	39°C	49°C	56°C	63°C	66°C
0	7.246	7.313	7.137	5.468	5.404	4.326
5	7.023	7.102	6.884	5.366	5.184	4.154
10	6.410	6.502	6.196	5.022	4.634	3.747
15	5.542	5.602	5.254	4.510	3.997	3.324
20	4.576	4.536	4.251	3.899	3.453	3.018
25	3.636	3.493	3.327	3.256	3.017	2.779
30	2.783	2.494	2.543	2.634	2.602	2.483
35	2.037	1.751	1.906	2.073	2.148	2.085
40	1.406	1.242	1.402	1.584	1.682	1.657
45	0.905	0.910	1.013	1.163	1.266	1.300
50	0.548	0.669	0.717	0.803	0.929	1.037
55	0.325	0.464	0.490	0.511	0.658	0.823
60	0.198	0.288	0.314	0.308	0.436	0.615
65	0.119	0.164	0.183	0.198	0.267	0.422
70	0.061	0.098	0.093	0.153	0.159	0.273
75	0.020	0.066	0.039	0.125	0.095	0.169
80	0.001	0.041	0.013	0.080	0.048	0.091
85	-0.001	0.015	0.003	0.029	0.009	0.030
90	0	0.003	0	00.005	0.007	0.006

Table 8.21

Sample: 500B

Variation of $\langle P_L \rangle$ values with temperatures L = 2 and 4.

Temp. °C.	$\langle P_2 \rangle_V$	$\langle P_2 \rangle$	$\langle P_2 \rangle_{M.F}$	$\langle P_4 \rangle_V$	$\langle P_4 \rangle$	$\langle P_4 \rangle_{M.F.}$
35	0.63	0.64	0.62	0.21	0.23	0.32
39	0.57	0.62	0.60	0.18	0.23	0.30
49	0.58	0.61	0.56	0.16	0.20	0.26
56	0.52	0.56	0.52	0.13	0.15	0.21
63	0.51	0.53	0.48	0.09	0.11	0.17
66	0.44	0.46	0.45	0.04	0.06	0.14

Table 8.22

Sample: 500B.

a_L and b_L (L = 2 and 4) at different temperatures.

Temp. °C.	Temp. °K	a_0	a_2	a_4	a_6	a_8	a_{10}	b_2/k	b_4/k
35	308	-2.488	6.459	-3.723	2.939	-2.44	1.327	-3094	5003
39	312	-1.414	4.156	-1.478	1.248	-0.981	0.533	-2105	2023
49	322	-1.659	4.784	-2.296	1.797	-1.233	0.632	-2546	3696
58	329	-1.136	3.663	-1.368	0.895	-1.000	0.760	-2171	3041
63	336	-1.152	3.808	-1.850	1.248	-0.922	0.61	-2428	5809
66	339	-0.893	3.272	-1.83	1.44	-1.296	0.844	-2426	10696

References:-

1. M/s. F. Hoffmann-La-Roche and Co., Basel, Switzerland, Catalogue.

2. B. Bhattacharjee, S. Paul and R. Paul, Mol. Phys. 44, 1391 (1981).

2a. Basana Bhattacharjee, Sukla Paul and Ranjit Paul, Mol.Cryst.Liq.Cryst. 89, pp. 181-192 (1982).

3. A. J. Leadbetter, R.M. Richardson and C.N. Colling J. Phys. (Paris) 36, 1-37 (1975).

4. R.L.Humphries, P.G. James and G.R.Luckhurst, Jour. Chem. Soc. Faraday, Trans. II. 68, 1031 (1972).

5. N.V.Madhusudan and S. Chandrasekhar in Pramana, Suppl. 1, p. 57-68, Editor S.Chandrasekhar, Indian Academy of Science, Bangalore (1975).

CHAPTER 9.

X-RAY DIFFRACTION STUDIES ON THE MESOPHASES OF 4'-OCTYLOXY-4-CYANO BIPHENYL (8OCB IN SHORT) IN MAGNETIC FIELD.

CHAPTER 9

X-RAY DIFFRACTION STUDIES ON THE MESOPHASES OF 4'-OCTYLOXY-4-CYANOBIPHENYL (8OCB IN SHORT) IN MAGNETIC FIELD.

1. Introduction

The structural formula of 8 OCB has been given in chapter 2. The transition temperature of the sample obtained from literature[1] is given as

$$\text{Solid} \xrightleftharpoons{54.5^\circ C} \text{Smectic} \xrightleftharpoons{79^\circ C} \text{Isotropic}$$

But our X-ray and texture studies show the phase transitions as

$$\text{Solid} \underset{\sim 35^\circ C}{\overset{54.5^\circ C}{\rightleftharpoons}} \text{Smectic} \underset{}{\overset{67^\circ C}{\rightleftharpoons}} \text{Nematic} \underset{}{\overset{79.5^\circ C}{\rightleftharpoons}} \text{Isotropic}$$

Leadbetter et al[2] have determined the smectic layer thickness and Als-niels et al[3] have reported by X-ray critical scattering at the nematic-smectic A transition. But uptil now values of order parameters and distribution function of 8OCB have not been reported.

Experimental technique and theoretical background are described in previous chapters[4,5].

The sample in the nematic phase was aligned by heating it to the desired temperature in the presence of magnetic field of 5.8 Kilo gauss and the sample in the smectic phase was aligned by heating it to the nematic phase and then cooling down to the desired temperature in presence of magnetic field.

2. Results and Discussions:-

From polarizing microscopic study (as described in chapter 2) it is found that the sample possesses focal conic and fan texture of S_A phase. Having two different phases, the ~~xkx~~ photographs of 800B in the presence of magnetic field, show two different patterns. Two photographs of oriented sample one at S_A phase (at 40°C) and the other at nematic phase (at 74 °C) are given in fig. 9.1 & 9.2 respectively.

The photographs in the nematic phase are similar in nature to those obtained from 500B (chapter 8) and the smectic phase photographs consist of two diffuse outer maxima (showing disordered structure within the layer) and two sharp spots (001) reflection. The line joining the inner spots is perpendicular to the line joining the outer maxima indicating that the mesophase concerned is of S_A type (Fig. 9.1). The data obtained from linear and angular scanning of films at different temperatures are given in table ~~9.1~~ 9.1 to 9.15.

Intermolecular distance (D), apparent length of the molecule for nematic phase (l) and layer thickness (d) in case of smectic phase.

The intermolecular distance, apparent length of the molecule or layer thickness for unoriented and oriented samples are calculated by the procedure described in earlier chapters(3,7). The values are given in table 9.16. Variation of D with magnetic field are shown in the fig. 9.3. In accordance with our previous finding in 500B (chapter 8) it is found that the application of magnetic field causes a decrease

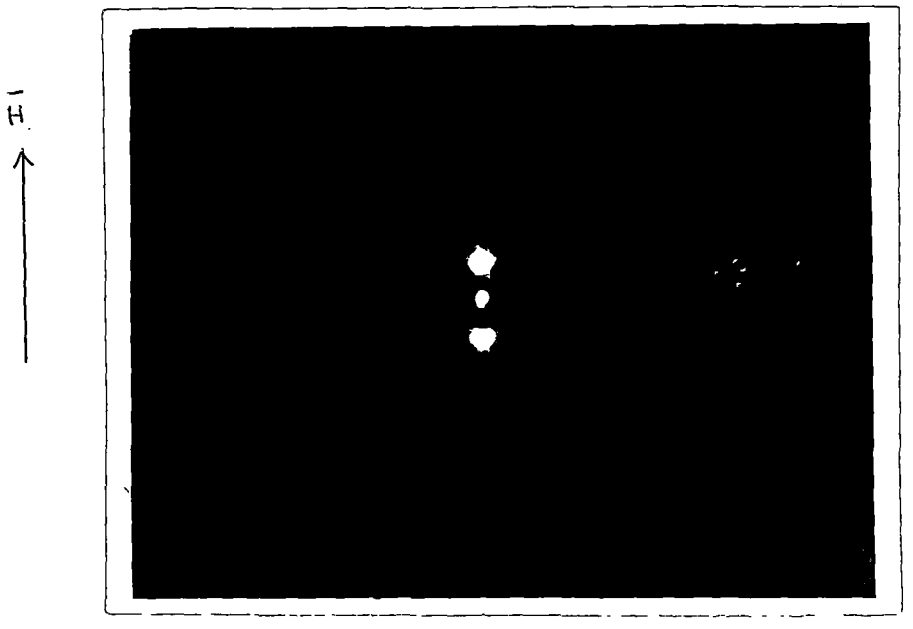

Fig. 9.1. Photograph of oriented S_A phase of 8OCB at 40°C.

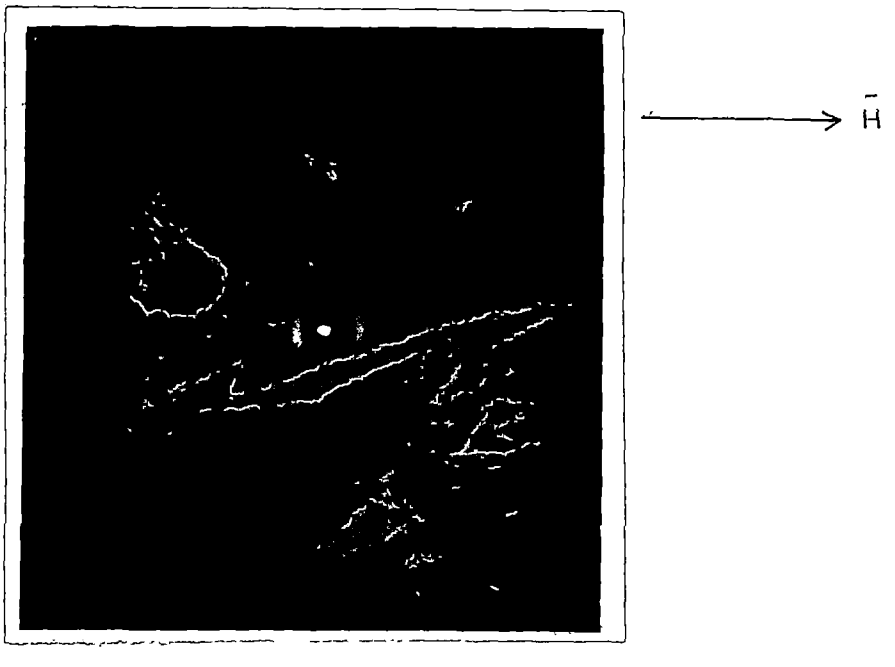

Fig. 9.2. Photograph of oriented nematic phase of 8OCB at 74°C.

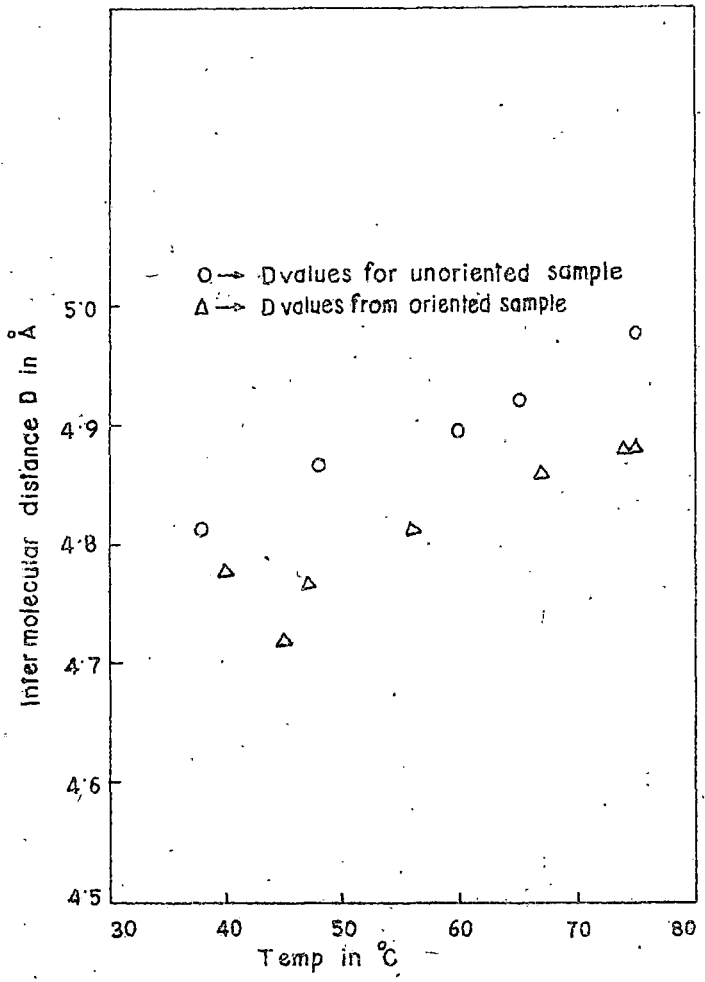

Fig. 9·3

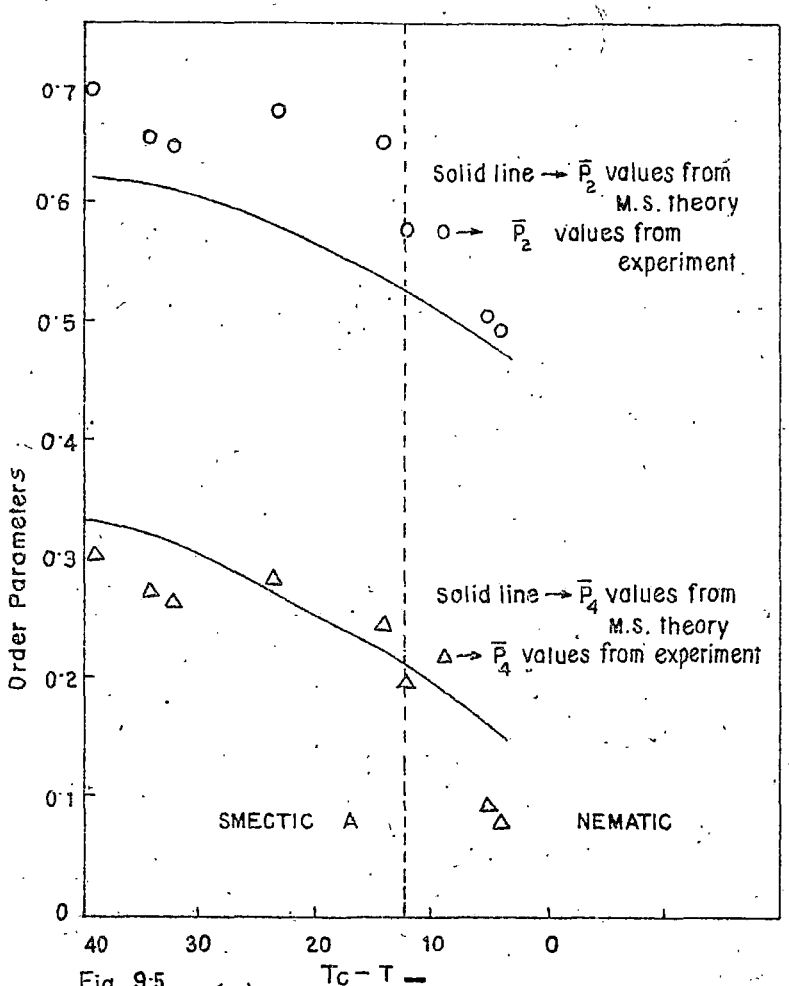

Fig. 9·5

$\langle P_2 \rangle$ & $\bar{P}_2$ are equivalent.

$\langle P_4 \rangle$ & $\bar{P}_4$ are equivalent.

in the intermolecular distance and D values increases with increase in temperature. There is no observable change in 'D' values at the Smectic A - Nematic phase transition.

The variation of the layer thickness 'd' in smectic phase of 8OCB is very slight. The mean value is 32.0 ± 1 Å. The length L of the molecule of 8OCB in its fully extended form is 23.5 Å.

Recently, Leadbetter et al[6] and de Vries et al[7,8] have pointed out the necessity of correction for orientational disorder in the calculation of the layer thickness in Smectic A phase. We have tried to take into account the orientational disorder in the following manner. The local thickness of a smectic layer (smectic A) is $L\,Cos\,\theta$ where, L is the molecular length (or the length of the dimer, if dimers produce the smectic layer) and θ is the angle made by the molecular long axis with the director. On averaging the effective layer thickness is $\left[L \langle Cos\,\theta \rangle\right]$, where,

$$\langle Cos\,\theta \rangle = \int_0^{\pi/2} Cos\,\theta\, f(\theta)\, Sin\,\theta\, d\theta$$

$$= \frac{1}{2}\int_0^{\pi/2} Sin\,2\theta\, f(\theta)\, d\theta \qquad \ldots (1)$$

$f(\theta)$ being the normalised orientational distribution function.

Since, we have already determined the normalized orientational distribution function $f(\theta)$ from the X-ray diffraction intensities for aligned sample of 8OCB (values are given in Table 9.19), we can easily evaluated $\langle cos\theta \rangle$ from

equation (1). We can reasonably assume that the measurement of the inner ring in the X-ray pattern gives the effective layer thickness value, i.e. $d = L \langle \cos\theta \rangle$. Hence, $[d/\langle \cos\theta \rangle]$ gives the length of the molecule (monomer or dimer) forming the smectic layer. In table 9.17 we have given the values of d, $\langle \cos\theta \rangle$ and $[d/\langle \cos\theta \rangle]$ at different temperatures for 80CB. The mean value of $[d/\langle \cos\theta \rangle]$ is 36.9 ± 1.1 Å where as molecular length from the model is 23.5 Å. Evidently the molecules of 80CB form dimers with partial overlap of their rigid parts.

However, the ratio of the dimer length to the monomer length is about 1.57 instead of 1.36 obtained without correction for orientational disorder.

In the nematic phase the value of 'l' is found to be 31.34 Å to 31.75 Å. The reason for the difference between the measured and apparent length of the molecule is same as for 50OB (Chapter 8).

Intensity, Distribution Function and Order Parameter.

θ - $I(\theta)$ (i.e. the mean intensity for four quadrants) values at different temperatures in the supercooled smectic A, smectic A and nematic phases are given

in table 9.18 and the variation of $f(\beta)$ with β as obtained from $I(\theta)$ values at different temperatures are presented in table 9.19. The fig. 9.4 (a) represents the variation of $f(\beta)$ with β in the nematic phase at 67°C.

In our paper for 80OB[3a] the fig. 5 represents the $f(\beta)$ values against β at 74°C but actually the temperature ~~will~~ should be 67°C.

In accordance with other nematic samples such as OPHB and 50OB, it is found from the fig. 9.4 (b) and 9.4 (c) that the orientational distribution function spreads out at higher temperatures.

The order parameter values against different temperature are plotted in fig. 9.5. The values of $\langle P_2 \rangle$ and $\langle P_4 \rangle$ at different temperatures in the smectic A phase and nematic phase are given in table 9.20.

The order parameter values are estimated to be accurate within $\pm$ 0.02 except in the case of supercooled 80OB where the uncertainty is somewhat greater. The first order S_A- Nematic phase transition in 80OB is observed at 67°C which is clearly indicated by discontinuities in $\langle P_2 \rangle$ and $\langle P_4 \rangle$ values. Experimental values of $\langle P_2 \rangle$ are found to be larger than Maier-Saupe (MS) theoretical values. As explained earlier this may be due to short range dipole-dipole interactions. In the nematic phase $\langle P_4 \rangle$ values are found to be lower than the M.S. values. This discrepancy in $\langle P_4 \rangle$ values is not

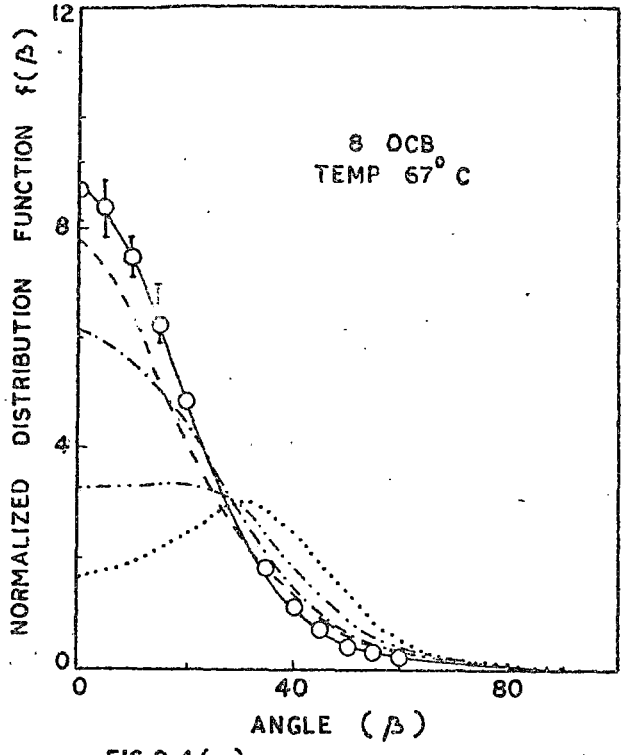

FIG.9.4(a).

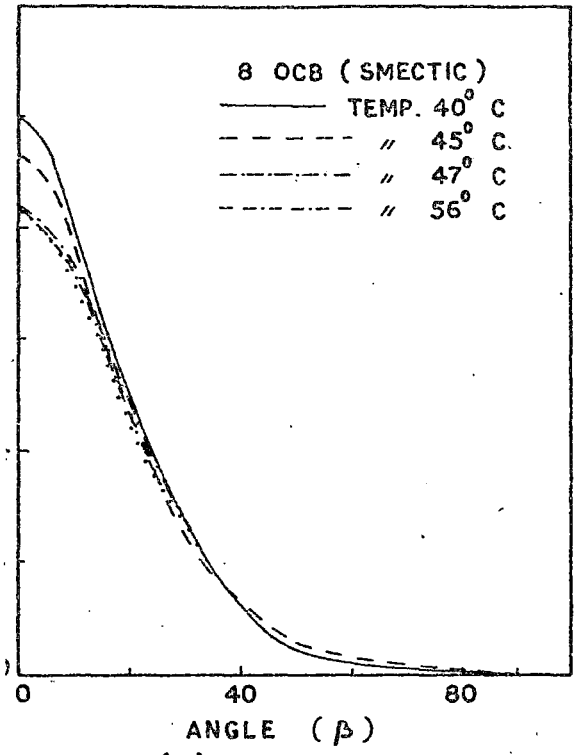

FIG. 9.4(b).

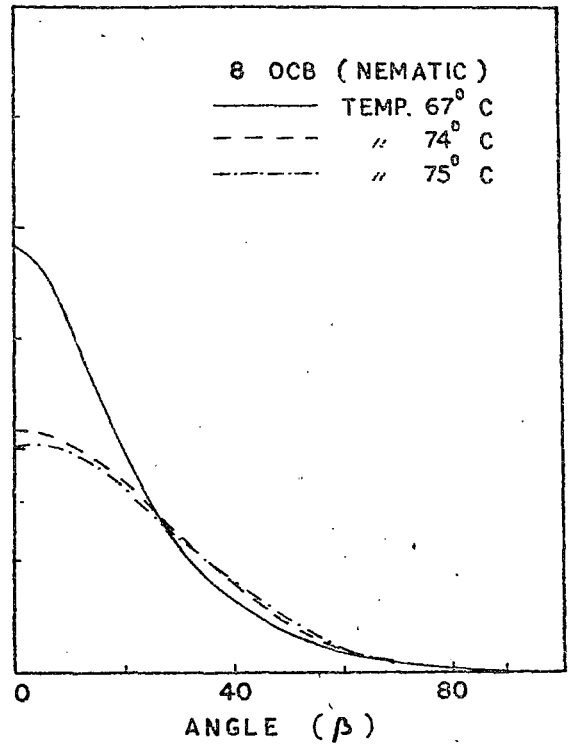

FIG. 9.4(c).

Variation of normalised orientational distribution function $f(\beta)$ with angle β at 67°C for 8OCB.

- – – – – – Experimental data
- ——— Calculated value with pseudopotential $-(2300 \pm 130)\ \langle P_2 \rangle\ P_2(\cos\beta)$.
- —·—·—·— Calculated value with pseudopotential $-(2300)\ \langle P_2 \rangle\ P_2(\cos\beta) + (4400 + 2700)\ \langle P_4 \rangle\ P_4(\cos\beta)$
- —··—··—·· Calculated value with pseudopotential $-(2300)\ \langle P_2 \rangle\ P_2(\cos\beta) + (4400)\ \langle P_4 \rangle\ P_4(\cos\beta)$
- . . . . . Calculated value with pseudopotential $-(2300)\ \langle P_2 \rangle\ P_2(\cos\beta) + (4400 - 2700)\ \langle P_4 \rangle\ P_4(\cos\beta)$.

unusual. In the smectic phase experimental $\langle P_4 \rangle$ values seem to agree with MS values within experimental uncertainity.

Pseudopotential:-

As in other samples, the pseudopotential can be calculated by using the relation 3.14. a_L values and b_L/K (for L =2, and 4) are given in table 9.21 for different temperatures in the smectic and nematic regions. From the data for the five temperatures in smectic phase and two temperatures in the nematic phase omitting the last temperature from table 9.21 the mean of the coefficients b_2/k and b_4/k and the standard deviations of the coefficients have been written in table 9.22. In the nematic phase we have only two diffraction photograph in the narrow temperature range of 12.5°C. The angular part of the pseudopotential in the nematic phase is given by

$$V(\beta)/k = -(2300 \pm 130) \langle P_2 \rangle P_2(\cos\beta) + (4400 \pm 2700) \langle P_4 \rangle P_4(\cos\beta).$$

In fig. 9.4(a) we have included the calculated $f(\beta)$ values at 67°C obtained from several pseudopotentials. A similar case is observed here as in 5OCB i.e. the inclusion of the $P_4(\cos\beta)$ term in the pseudopotential results in worse agreement with the experimental $f(\beta)$ values.

TABLE 9.1

Sample: 800B, Mag.Field = Nil, Temperature 38°C.

LINEAR SCANNING

L in cm.	O. D.	L in cm.	O. D.	L in cm	O. D.
		4.1	1.225	1.5	0.37
OUTER HALO		4.075	1.3	1.3	0.352
7.0	0.38	4.05	0.64	1.25	0.35
6.9	0.39	4.0	0.47		
6.8	0.41	3.95	0.54	INNER HALO	
6.7	0.428	3.9	0.59	5.0	0.435
6.6	0.45	3.875	0.60	4.9	0.44
6.5	0.48	3.85	0.56	4.8	0.45
6.45	0.49	3.8	0.53	4.75	0.46
6.4	0.51	3.75	0.505	4.7	0.465
6.35	0.52	3.7	0.488	4.65	0.47
6.3	0.528	3.6	0.46	4.6	0.498
6.25	0.525	3.5	0.452	4.55	0.505
6.2	0.52	3.4	0.44	4.5	0.528
6.15	0.50	3.3	0.43	4.45	0.585
6.1	0.49	3.2	0.42	4.40	0.62
6.0	0.47	3.15	0.42	4.35	0.69
5.9	0.45	3.1	0.42	4.3	0.66
5.8	0.435	3.0	0.415	4.25	0.615
5.7	0.42	2.9	0.41	4.2	0.545
5.6	0.415	2.7	0.402	4.15	0.77
5.5	0.41	2.65	0.405	4.1	1.1
5.45	0.412	2.55	0.410	4.05	1.04
5.4	0.412	2.5	0.410	4.0	0.73
5.35	0.415	2.45	0.415	3.95	0.355
5.2	0.42	2.4	0.420	3.9	0.425
5.1	0.425	2.3	0.425	3.85	0.62
5.0	0.43	2.25	0.435	3.8	0.70
4.9	0.435	2.2	0.44	3.775	0.69
4.8	0.445	2.15	0.452	3.75	0.56
4.7	0.46	2.1	0.46	3.7	0.50
4.6	0.47	2.05	0.465	3.65	0.485
4.55	0.50	2.025	0.46	3.6	0.46
4.5	0.525	2.0	0.46	3.5	0.45
4.45	0.57	1.95	0.455	3.4	0.44
4.4	0.56	1.9	0.44	3.2	0.42
4.35	0.545	1.8	0.41		
4.3	0.40	1.7	0.39		
4.2	0.955	1.6	0.38		

TABLE 9.2

Sample: 80CB, Mag. Field = Nil, Temperature 48°C

LINEAR SCANNING

L in cm.	O. D.	L in cm.	O. D.	L in cm.	O. D.
OUTER HALO		4.3	0.345	INNER HALO	
7.0	0.35	4.275	0.365	5.0	0.46
6.9	0.35	4.2	0.745	4.9	0.465
6.8	0.36	4.15	0.94	4.8	0.475
6.7	0.375	4.125	0.70	4.75	0.49
6.6	0.385	4.1	0.76	4.7	0.50
6.5	0.40	4.05	1.1	4.65	0.525
6.45	0.405	4.025	1.09	4.6	0.555
6.4	0.42	4.0	1.08	4.5	0.72
6.375	0.425	3.95	0.92	4.45	0.87
6.35	0.43	3.9	0.835	4.425	0.905
6.33	0.445	3.85	0.665	4.4	0.895
6.25	0.45	3.8	0.66	4.395	0.695
6.2	0.452	3.7	0.57	4.3	0.55
6.15	0.46	3.6	0.525	4.25	0.59
6.1	0.455	3.5	0.51	4.2	1.07
6.05	0.45	3.4	0.498	4.15	1.2
5.975	0.44	3.35	0.485	4.1	0.13
5.95	0.438	3.2	0.475	4.05	0.89
5.85	0.43	3.1	0.465	4.0	0.62
5.7	0.42	3.0	0.46	3.95	0.44
5.6	0.415	2.95	0.455	3.9	0.49
5.55	0.412	2.85	0.45	3.85	0.89
5.5	0.415	2.75	0.452	3.8	0.83
5.3	0.418	2.65	0.455	3.75	0.77
5.2	0.425	2.6	0.465	3.7	0.59
5.2	0.428	2.5	0.47	3.65	0.55
5.15	0.435	2.45	0.49	3.6	0.51
5.1	0.44	2.35	0.50	3.5	0.48
5.05	0.442	2.25	0.525		
4.9	0.45	2.15	0.575		
4.8	0.462	2.1	0.60		
4.7	0.48	1.95	0.615		
4.6	0.505	1.9	0.612		
4.5	0.56	1.85	0.61		
4.45	0.55	1.75	0.575		
4.4	0.48	1.65	0.535		
4.35	0.37	1.5	0.49		
		1.25	0.44		

TABLE 9.3

Sample: 800B, Mag. Field = Nil, Temperature 55°C.

LINEAR SCANNING

L in cm	O. D.	L in cm	O. D.	L in cm	O. D.
OUTER HALO		4.2	0.70	1.5	0.43
		4.15	1.00	1.35	0.395
7.0	0.47	4.125	1.0	1.2	0.38
6.9	0.495	4.1	0.99		
6.85	0.505	4.05	1.02	INNER HALO	
6.8	0.52	4.025	1.11	5.0	0.58
6.7	0.555	4.0	0.96	4.8	0.60
6.6	0.59	3.95	0.39	4.7	0.638
6.5	0.635	3.9	0.42	4.6	0.688
6.4	0.71	3.85	0.89	4.55	0.625
6.35	0.73	3.775	1.01	4.325	0.905
6.3	0.76	3.75	0.93	4.5	0.94
6.25	0.765	3.7	0.73	4.475	0.955
6.2	0.788	3.6	0.63	4.45	0.945
6.15	0.762	3.5	0.615	4.425	0.945
6.1	0.74	3.45	0.58	4.4	0.725
6.05	0.705	3.375	0.57	4.35	0.42
6.0	0.695	3.3	0.55	4.3	0.38
5.9	0.65	3.25	0.535	4.275	0.41
5.8	0.622	3.175	0.525	4.25	0.83
5.7	0.59	3.1	0.515	4.2	1.0
5.6	0.57	3.0	0.51	4.15	0.725
5.5	0.555	2.95	0.505	4.1	1.29
5.45	0.552	2.85	0.50	4.05	1.3
5.4	0.55	2.75	0.49	4.025	1.1
5.3	0.56	2.7	0.49	4.0	0.725
5.25	0.565	2.625	0.49	3.95	0.83
5.2	0.562	2.5	0.492	3.9	1.01
5.1	0.57	2.4	0.502	3.875	1.1
5.0	0.575	2.35	0.51	3.85	1.13
4.9	0.59	2.25	0.52	3.825	1.07
4.8	0.61	2.225	0.528	3.8	1.01
4.75	0.61	2.175	0.535	3.7	0.78
4.6	0.645	2.1	0.538	3.6	0.71
4.5	0.72	2.05	0.535	3.5	0.66
4.4	0.95	2.0	0.532	3.4	0.63
4.35	1.02	1.9	0.515		
4.3	0.905	1.8	0.475		
4.25	0.59	1.65	0.44		

TABLE 9.4

Sample: 800B, Mag. Field = Nil, Temperature 60°C

LINEAR SCANNING

L in cm	O. D.	L in cm.	O. D.	L in cm.	O. D.
		4.15	0.69	4.8	0.505
OUTER HALO		4.1	0.89	4.7	0.535
7.0	0.46	4.05	0.75	4.6	0.568
6.9	0.475	4.0	0.64	4.55	0.58
6.8	0.50	3.95	0.58	4.45	0.68
6.7	0.53	3.9	0.675	4.4	0.73
6.6	0.565	3.8	0.775	4.35	0.98
6.5	0.61	3.7	0.635	4.3	1.03
6.4	0.65	3.6	0.615	4.275	1.01
6.3	0.672	3.55	0.62	4.25	0.875
6.25	0.685	3.5	0.63	4.2	0.42
6.2	0.68	3.4	0.638	4.15	0.46
6.1	0.66	3.3	0.615	4.1	0.86
6.0	0.62	3.2	0.585	4.05	0.98
5.9	0.58	3.1	0.57	4.025	0.99
5.8	0.55	3.0	0.54	4.0	0.84
5.7	0.52	2.9	0.51	3.95	0.50
5.6	0.505	2.8	0.498	3.9	0.405
5.5	0.50	2.7	0.49	3.85	0.635
5.4	0.50	2.6	0.48	3.8	0.765
5.3	0.50	2.5	0.478	3.75	0.95
5.25	0.501	2.45	0.48	3.725	1.15
5.2	0.502	2.35	0.49	3.7	0.88
5.15	0.505	2.3	0.50	3.65	0.80
5.1	0.51	2.2	0.51	3.60	0.61
5.05	0.515	2.15	0.525	3.50	0.58
5.0	0.52	2.1	0.53	3.40	0.54
4.95	0.525	2.05	0.53	3.3	0.51
4.85	0.53	2.0	0.525	3.2	0.49
4.75	0.54	1.9	0.505	3.0	0.48
4.65	0.56	1.75	0.465		
4.55	0.595	1.7	0.435		
4.5	0.635	1.5	0.41		
4.4	0.67	1.3	0.385		
4.35	0.61	[illegible]			
4.3	0.40	INNER HALO			
4.25	0.36				
4.225	0.37	5.0	0.48		
4.2	0.51	4.9	0.49		

TABLE 9.5

Sample: 80CB, Mag. Field = Nil, Temperature 65°C

LINEAR SCANNING

L in cm	O. D.	L in cm.	O. D.	L in cm.	O. D.
OUTER HALO					
7.0	0.43	4.3	0.735	1.8	0.455
6.9	0.445	4.25	0.595	1.7	0.448
6.8	0.478	4.2	0.52	1.6	0.42
6.6	0.51	4.15	0.77	1.5	0.40
6.5	0.54	4.1	1.03	1.3	0.385
6.45	0.56	4.05	1.24		
6.4	0.575	4.0	0.99	**INNER HALO**	
6.35	0.59	3.95	0.372		
6.3	0.60	3.85	0.598	5.0	0.475
6.25	0.61	3.8	0.645	4.9	0.485
6.2	0.61	3.75	0.68	4.8	0.498
6.15	0.608	3.725	0.695	4.7	0.515
6.1	0.605	3.70	0.605	4.65	0.53
6.05	0.59	3.65	0.565	4.6	0.55
6.0	0.575	3.6	0.538	4.5	0.57
5.9	0.55	3.55	0.52	4.45	0.59
5.8	0.52	3.5	0.515	4.4	0.79
5.7	0.50	3.4	0.49	4.35	0.79
5.6	0.48	3.3	0.48	4.325	0.78
5.5	0.475	3.2	0.47	4.3	0.57
5.4	0.47	3.1	0.475	4.2	0.405
5.3	0.472	3.0	0.47	4.1	0.74
5.25	0.472	2.9	0.465	4.05	1.3
5.15	0.475	2.8	0.46	4.0	1.2
5.1	0.48	2.6	0.46	3.9	0.46
5.0	0.485	2.5	0.465	3.85	0.56
4.95	0.49	2.45	0.47	3.825	0.95
4.85	0.49	2.4	0.48	3.8	0.82
4.8	0.50	2.3	0.498	3.75	0.745
4.7	0.515	2.25	0.50	3.65	0.6
4.6	0.55	2.2	0.525	3.6	0.59
4.5	0.568	2.15	0.52	3.5	0.54
4.45	0.615	2.1	0.52	3.4	0.52
4.4	0.645	2.05	0.525	3.3	0.51
4.35	0.768	2.0	0.520	3.0	0.49
4.325	0.78	1.95	0.50		

TABLE 9.6

Sample: 800B, Neg. Field = Nil, Temperature 75°C.

LINEAR SCANNING

L in cm.	O. D.	L in cm.	O. D.	L in cm.	O. D.
OUTER HALO		4.35	0.598		
		4.3	0.41	INNER HALO	
7.0	0.405	4.2	0.735		
6.9	0.425	4.15	1.05	5.0	0.46
6.8	0.45	4.1	1.41	4.9	0.47
6.7	0.47	4.0	1.05	4.8	0.48
6.6	0.49	3.95	0.44	4.7	0.51
6.5	0.525	3.9	0.50	4.65	0.515
6.4	0.55	3.8	0.62	4.6	0.54
6.35	0.56	3.7	0.58	4.525	0.562
6.3	0.58	3.6	0.565	4.5	0.575
6.25	0.582	3.5	0.54	4.45	0.665
6.225	0.585	3.4	0.552	4.4	0.695
6.2	0.588	3.3	0.54	4.35	0.72
6.15	0.58	3.2	0.515	4.325	0.76
6.1	0.57	3.1	0.505	4.3	0.61
6.05	0.562	3.0	0.50	4.2	0.45
6.0	0.55	2.9	0.48	4.15	0.73
5.9	0.52	2.8	0.47	4.1	1.02
5.8	0.508	2.7	0.468	4.05	1.34
5.7	0.49	2.6	0.465	4.0	1.15
5.65	0.48	2.5	0.47	3.9	0.39
5.6	0.472	2.4	0.48	3.8	0.53
5.5	0.465	2.3	0.505	3.775	0.7
5.4	0.46	2.2	0.51	3.7	0.635
5.3	0.465	2.1	0.522	3.6	0.525
5.25	0.468	2.075	0.522	3.5	0.515
5.2	0.47	2.05	0.52	3.4	0.50
5.1	0.478	2.0	0.515	3.3	0.49
5.0	0.482	1.9	0.485	3.2	0.48
4.9	0.49	1.8	0.455	3.1	0.465
4.8	0.50	1.5	0.4	3.0	0.45
4.7	0.518	1.25	0.37		
4.6	0.55				
4.5	0.57				
4.4	0.605				

TABLE 9.7

Sample: 80CB, Mag. Field, Nil, Temperature 77°C.

LINEAR SCANNING

L in cm.	O. D.	L in cm.	O. D.	L in cm.	O. D.
		4.4	0.562	2.2	0.42
OUTER HALO		4.35	0.61	2.15	0.43
7.0	0.39	4.3	0.61	2.1	0.43
6.9	0.40	4.25	0.59	2.05	0.432
6.8	0.415	4.2	0.40	2.0	0.43
6.7	0.435	4.15	0.45	1.95	0.425
6.6	0.44	4.10	0.98	1.9	0.415
6.5	0.468	4.05	1.05	1.8	0.315
6.45	0.48	4.0	1.02	1.6	0.375
6.4	0.49	3.95	0.365	1.5	0.36
6.35	0.50	3.9	0.35	1.3	0.34
6.25	0.515	3.85	0.515		
6.2	0.515	3.8	0.54	INNER HALO	
6.15	0.518	3.75	0.55		
6.1	0.512	3.7	0.535	5.0	0.44
6.05	0.50	3.65	0.525	4.9	0.44
6.0	0.50	3.6	0.48	4.8	0.45
5.95	0.49	3.55	0.478	4.7	0.455
5.9	0.48	3.5	0.47	4.6	0.48
5.85	0.47	3.4	0.47	4.55	0.50
5.8	0.46	3.35	0.46	4.5	0.515
5.75	0.452	3.3	0.46	4.45	0.55
5.7	0.45	3.25	0.45	4.4	0.565
5.65	0.44	3.2	0.448	4.35	0.615
5.6	0.438	3.15	0.44	4.3	0.625
5.55	0.438	3.1	0.432	4.25	0.61
5.5	0.43	3.05	0.43	4.2	0.4
5.4	0.43	2.95	0.42	4.15	0.52
5.3	0.428	2.9	0.425	4.1	1.05
5.2	0.43	2.85	0.415	4.05	1.1
5.1	0.435	2.8	0.41	4.0	1.05
5.0	0.442	2.7	0.41	3.95	0.35
4.9	0.448	2.6	0.41	3.9	0.335
4.8	0.452	2.5	0.41	3.85	0.34
4.7	0.47	2.45	0.412	3.8	0.515
4.6	0.49	2.4	0.415	3.7	0.535
4.55	0.50	2.35	0.415	3.7	0.53
4.5	0.51	2.3	0.42	3.55	0.465
4.45	0.552	2.25	0.425	3.10	0.415

TABLE 9.8

Sample: 60CB, Mag. Field 5.81 K.Gauss, Temperature 40°C,
Background Optical Density = 0.43.

LINEAR SCANNING				ANGULAR SCANNING		
L in cm	O. D.	L in cm.	O. D.	θ in degree	O. D.	Intensity
		3.0	0.65	70	0.085	10.0
OUTER HALO		2.95	0.635	80	0.085	10.0
		2.8	0.65	90	0.09	10.75
7.0	0.69	2.75	0.642	100	0.092	11.0
6.8	0.76	2.55	0.64	110	0.112	13.75
6.7	0.805	2.4	0.64	120	0.145	18.0
6.6	0.855	2.15	0.675	130	0.225	28.0
6.55	0.86	2.1	0.70	140	0.31	39.75
6.5	0.87	2.0	0.715	150	0.375	50.75
6.45	0.865	1.9	0.75	160	0.43	60.0
6.4	0.845	1.8	0.80	163	0.430	60.0
6.3	0.825	1.75	0.82	164	0.425	59.0
6.2	0.79	1.65	0.82	170	0.38	51.75
6.1	0.745	1.625	0.818	180	0.310	39.75
6.0	0.692	1.6	0.81	190	0.218	26.75
5.9	0.68	1.5	0.775	200	0.155	19.5
5.8	0.66	1.4	0.715	210	0.120	15.0
5.7	0.65	1.3	0.675	220	0.105	12.5
5.6	0.65	1.2	0.64	230	0.115	14.0
5.5	0.65			240	0.125	15.5
5.4	0.655	INNER HALO		250	0.142	17.75
5.3	0.665			260	0.145	18.0
5.2	0.67	5.0	0.6	270	0.145	18.0
5.1	0.67	4.8	0.65	280	0.130	16.25
5.0	0.672	4.6	0.7	290	0.14	17.5
4.9	0.685	4.5	0.85	300	0.18	22.5
4.75	0.71	4.45	1.035	312	0.27	33.5
4.65	0.75	4.4	1.52	320	0.33	43.25
4.55	0.81	4.35	1.67	330	0.405	55.75
4.35	0.875	4.325	1.785	334	0.41	56.5
4.325	0.83	4.3	1.685	335	0.41	56.5
4.2	0.55	4.2	1.442	337	0.408	56.25
4.15		4.15	0.55	338	0.402	55.5
4.1	0.88	4.05	0.60	340	0.39	53.5
4.05	1.2	4.025	1.09	350	0.345	45.75
4.0	0.82	4.0	1.75	0	0.278	34.75
3.95	0.60	3.9	0.7	10	0.20	25.0
3.9	0.885	3.8	0.68	20	0.15	18.75
3.8	0.95	3.7	1.72	30	0.12	15.0
3.7	0.835	3.675	1.7	40	0.105	12.5
3.6	0.78	3.65	1.59	50	0.10	12.25
3.55	0.745	3.6	1.535	60	0.095	11.5
3.5	0.735	3.5	0.915	68	0.09	10.75
3.35	0.69	3.4	0.755	70	0.10	12.25
3.25	0.668	3.0	0.625			

TABLE 9.9

Sample: 80CB, Mag. Field= 5.81 K.Gauss, Temperature 45°C
Background Optical Density = 0.37

LINEAR SCANNING				ANGULAR SCANNING		
L in cm.	O. D.	L in cm.	O. D.	θ in degree	O. D.	Intensity
OUTER HALO		3.4	0.489	0	0.04	4.95
		3.3	0.48	10	0.04	4.95
		3.2	0.47	20	0.045	5.25
7.0	0.47	3.1	0.48	30	0.045	5.25
6.9	0.46	2.9	0.48	40	0.05	6.0
6.8	0.50	2.8	0.48	50	0.06	7.25
6.7	0.52	2.65	0.475	60	0.08	9.75
6.6	0.55	2.6	0.475	70	0.12	15.0
6.5	0.57	2.5	0.47	80	0.170	21.25
6.475	0.572	2.3	0.48	90	0.190	23.75
6.45	0.57	2.1	0.49	93	0.192	24.0
6.4	0.57	1.9	0.52	100	0.185	23.0
6.3	0.54	1.75	0.568	110	0.135	16.75
6.2	0.535	1.65	0.575	120	0.1	12.25
6.1	0.51	1.6	0.58	130	0.068	8.0
6.0	0.50	1.55	0.58	140	0.052	6.25
5.9	0.485	1.525	0.578	150	0.03	3.25
5.8	0.48	1.5	0.568	160	0.028	3.0
5.7	0.47	1.4	0.555	170	0.025	2.75
5.6	0.465	1.15	0.49	180	0.03	3.25
5.5	0.465	INNER HALO		190	0.032	3.5
5.4	0.468	5.0	0.44	200	0.03	3.25
5.35	0.47	4.8	0.465	210	0.03	3.25
5.25	0.47	4.6	0.51	220	0.04	4.95
5.1	0.47	4.45	1.12	230	0.02	2.0
5.0	0.47	4.4	1.541	240	0.08	9.75
4.9	0.46	4.375	1.54	250	0.11	13.5
4.8	0.465	4.35	1.5	260	0.16	20.0
4.7	0.47	4.3	1.35	270	0.19	23.75
4.6	0.475	4.2	0.49	271	0.192	24.0
4.5	0.49	4.1	0.63	272	0.192	24.0
4.45	0.50	4.05	0.65	274	0.191	23.75
4.3	0.495	4.25	0.69	275	0.19	23.75
4.2	0.435	4.0	0.725	280	0.17	21.25
4.15	0.41	3.95	0.56	290	0.12	15.0
4.1	0.42	3.9	0.48	300	0.035	4.0
4.05	0.515	3.8	0.482	310	0.065	7.75
4.0	0.88	3.75	1.29	320	0.05	6.0
3.95	0.76	3.7	1.355	330	0.048	5.75
3.9	0.59	3.675	1.285	340	0.055	6.5
3.8	0.41	3.65	1.2	350	0.052	6.25
3.75	0.50	3.6	0.605	0	0.045	5.25
3.7	0.51	3.55	0.53			
3.6	0.51	3.5	0.472			
3.5	0.49	3.2	0.435			
		3.0	0.425			

TABLE 9.10

Sample: 800B, Mag. Field = 5.81 K.Gauss, Temperature 47°C
Background Optical Density = 0.46.

LINEAR SCANNING				ANGULAR SCANNING		
L in cm.	O. D.	L in cm	O. D.	θ in degree	O. D.	Intensity
		2.8	0.59	0	0.052	6.25
OUTER HALO		2.6	0.58	10	0.052	6.25
		2.4	0.575	20	0.045	5.25
7.0	0.58	2.3	0.582	30	0.055	6.5
6.9	0.598	2.2	0.59	40	0.055	6.5
6.8	0.615	2.0	0.625	50	0.065	7.75
6.7	0.64	1.9	0.642	60	0.08	9.75
6.6	0.665	1.8	0.67	70	0.12	15
6.5	0.685	1.7	0.70	80	0.16	20
6.48	0.685	1.65	0.702	90	0.20	25
6.45	0.685	1.55	0.698	95	0.21	26.25
6.4	0.68	1.5	0.682	97	0.215	26.75
6.2	0.64	1.4	0.66	98	0.214	26.75
6.1	0.615	1.15	0.59	100	0.212	26.5
6.0	0.605			105	0.202	25.25
5.9	0.585	INNER HALO		110	0.18	22.5
5.8	0.57			120	0.14	17.5
5.7	0.57	5.0	0.58	130	0.10	12.25
5.6	0.57	4.9	0.59	140	0.07	8.25
5.5	0.550	4.8	0.61	150	0.052	6.25
5.4	0.575	4.7	0.63	160	0.055	6.5
5.2	0.585	4.6	0.682	170	0.052	6.25
5.1	0.585	4.5	0.92	180	0.055	6.5
5.0	0.595	4.4	0.615	190	0.058	7.0
4.9	0.605	4.395	0.585	200	0.055	6.5
4.8	0.615	4.3	0.88	215	0.062	7.5
4.7	0.62	4.2	0.535	220	0.075	9.0
4.6	0.64	4.1	0.795	230	0.08	9.75
4.5	0.68	4.05	1.0	240	0.105	12.75
4.4	0.72	4.0	1.0	250	0.14	17.5
4.3	0.70	3.95	0.875	260	0.19	23.75
4.2	0.57	3.9	0.512	270	0.23	28.5
4.1	0.52	3.85	0.56	275	0.235	29.25
4.0	1.05	3.8	1.45	278	0.235	29.25
3.95	0.885	3.75	1.6	280	0.230	28.5
3.9	0.485	3.70	1.44	290	0.20	25.0
3.8	0.48	3.65	1.0	300	0.14	17.5
3.6	0.7	3.60	0.89	310	0.102	12.5
3.5	0.66	3.5	0.69	320	0.075	9.0
3.4	0.635	3.4	0.64	330	0.075	9.0
3.2	0.60	3.1	0.582	340	0.085	10.0
3.0	0.595	3.0	0.57	350	0.065	7.75
2.95	0.59			0	0.062	7.5

TABLE 9.11

Sample: 800B, Mag. Field 5.81 K.Gauss, Temperature 56°C
Background Optical Density = 0.515

LINEAR SCANNING				ANGULAR SCANNING		
L in cm.	O. D.	L in cm.	O. D.	θ in degree	O. D.	Intensity
		2.25	0.586	0	0.025	2.75
OUTER HALO		2.15	0.598	10	0.027	3.0
		2.0	0.622	20	0.027	3.0
7.0	0.6	1.9	0.65	30	0.03	3.25
6.75	0.642	1.8	0.66	40	0.03	3.25
6.6	0.67	1.775	0.67	50	0.037	4.25
6.5	0.69	1.7	0.68	60	0.050	6.0
6.45	0.69	1.675	0.68	71	0.085	10.0
6.425	0.688	1.65	0.675	80	0.115	14.0
6.4	0.686	1.55	0.668	84	0.145	18.25
6.3	0.67	1.5	0.652	90	0.155	19.5
6.0	0.618	1.4	0.632	94	0.167	21.0
5.8	0.6	1.2	0.602	95	0.167	21.0
5.7	0.598			99	0.17	21.25
5.6	0.60	INNER HALO		100	0.17	21.25
5.5	0.60			102	0.166	20.75
5.2	0.618	5.0	0.59	110	0.15	18.75
5.1	0.628	4.85	0.6	120	0.11	13.5
5.0	0.632	4.7	0.612	130	0.08	9.75
4.9	0.625	4.6	0.64	140	0.057	6.75
4.85	0.628	4.5	0.69	150	0.04	4.95
4.7	0.655	4.45	0.71	160	0.035	4.0
4.5	0.685	4.4	0.742	170	0.035	4.0
4.4	0.71	4.35	0.965	180	0.035	4.0
4.3	0.61	4.3	1.07	190	0.033	3.75
4.2	0.52	4.275	1.32	200	0.04	4.95
4.1	0.59	4.26	1.36	210	0.035	4.0
4.05	0.80	4.25	1.34	220	0.03	3.25
4.0	0.7	4.2	1.21	230	0.035	4.0
3.95	0.64	4.15	0.775	240	0.055	6.5
3.9	0.52	4.1	0.53	250	0.085	10.0
3.85	0.55	4.05	0.525	260	0.125	15.5
3.8	0.705	4.0	0.798	271	0.155	19.5
3.75	0.732	3.95	0.92	276	0.160	20.0
3.7	0.72	3.9	0.798	279	0.162	20.5
3.65	0.715	3.8	0.552	280	0.160	20.0
3.5	0.665	3.725	1.01	284	0.155	19.5
3.4	0.64	3.7	1.17	293	0.125	15.5
3.2	0.62	3.675	1.56	300	0.093	11.25
3.1	0.61	3.65	1.54	310	0.06	7.25
3.0	0.608	3.5	0.825	320	0.04	4.95
2.9	0.602	3.4	0.675	330	0.035	4.0
2.75	0.60	3.2	0.635	340	0.033	3.75
2.6	0.59	3.1	0.605	350	0.030	3.25
2.4	0.585	3.0	0.595	0	0.031	3.5

TABLE 9.12

Sample: SOOB, Mag.Field = 5.81 K.Gauss, Temperature 65°C
Background Optical Density = 0.45.

LINEAR SCANNING				ANGULAR SCANNING		
L in cm.	O. D.	L in cm.	O. D.	θ in degree	O. D.	Intensity
		2.5	0.58	340	0.07	8.25
OUTER HALO		2.35	0.578	350	0.065	7.75
		2.25	0.58	0	0.062	7.5
7.0	0.59	2.0	0.61	10	0.058	7.0
6.8	0.62	1.8	0.68	20	0.07	8.25
6.5	0.71	1.65	0.72	30	0.08	9.75
6.4	0.74	1.55	0.738	40	0.10	12.25
6.375	0.741	1.525	0.735	50	0.14	17.5
6.35	0.741	1.50	0.725	60	0.192	24.0
6.325	0.739	1.4	0.692	70	0.265	33.0
6.3	0.73	1.15	0.615	77	0.284	35.5
6.15	0.69			78	0.285	35.75
6.0	0.64	INNER HALO		79	0.278	34.75
5.8	0.598			80	0.265	33.0
5.7	0.59	5.0	0.565	85	0.278	34.75
5.6	0.58	4.9	0.582	90	0.265	33.0
5.5	0.58	4.7	0.64	100	0.205	25.5
5.4	0.578	4.6	0.685	110	0.152	19.0
5.3	0.58	4.6	0.712	120	0.112	13.5
5.2	0.582	4.525	1.0	130	0.085	10.0
5.1	0.588	4.5	1.05	140	0.072	8.5
5.0	0.595	4.45	1.45	150	0.065	7.75
4.8	0.595	4.425	1.655	160	0.072	8.5
4.5	0.665	4.4	1.66	170	0.07	8.25
4.4	0.69	4.38	1.61	180	0.07	8.25
4.35	0.685	4.35	1.36	190	0.07	8.25
4.25	0.528	4.325	0.772	200	0.075	9.0
4.15	0.46	4.2	0.5	210	0.088	10.5
4.1	0.47	4.175	0.495	225	0.115	14.0
4.25	1.65	4.45	0.76	240	0.20	25.0
4.0	1.105	4.1	0.95	250	0.26	32.25
3.25	1.1	4.06	1.06	260	0.292	37.0
3.9	0.545	4.05	0.95	262	0.29	36.75
3.8	0.492	4.0	0.78	270	0.27	33.5
3.75	0.725	3.95	0.605	280	0.215	26.75
3.65	0.765	3.9	0.55	290	0.165	20.75
3.55	0.735	3.8	1.24	300	0.12	15.0
3.5	0.718	3.75	1.51	310	0.09	10.75
3.45	0.68	3.725	1.50	320	0.072	8.5
3.4	0.672	3.6	0.92	330	0.075	9.0
3.3	0.64	3.50	0.68	340	0.075	9.0
3.1	0.615	3.25	0.60	350	0.065	7.75
2.95	0.608	3.1	0.575			
2.8	0.60	3.0	0.56			
2.7	0.59	2.85	0.5			

TABLE 9.13

Sample: 800B, Mag. Field = 5.81 K.Gauss, Temperature 67°C
Background Optical Density = 0.44.

LINEAR SCANNING				ANGULAR SCANNING		
L in cm.	O. D.	L in cm.	O. D.	Θ in degrees	O. D.	Intensity
		2.9	0.585	350	0.06	7.25
OUTER HALO		2.75	0.582	0	0.06	7.25
		2.6	0.58	10	0.06	7.25
7.0	0.57	2.5	0.575	20	0.062	7.5
6.9	0.58	2.4	0.572	30	0.072	8.5
6.7	0.64	2.3	0.575	40	0.085	10.0
6.5	0.70	2.2	0.585	52	0.122	15.25
6.4	0.72	2.1	0.595	61	0.162	20.5
		2.0	0.62	70	0.21	21.25
6.375	0.722	1.8	0.67	80	0.26	32.25
6.35	0.722	1.7	0.695	87	0.28	35.0
6.3	0.718	1.625	0.702	90	0.285	35.75
6.2	0.692	1.6	0.70	92	0.282	35.25
6.1	0.675	1.55	0.695	95	0.278	34.75
6.0	0.642	1.5	0.69	100	0.27	33.5
5.8	0.60	1.4	0.66	110	0.24	30.0
5.7	0.585	1.15	0.57	120	0.195	24.25
5.6	0.575			130	0.15	17.25
5.5	0.57	INNER HALO		140	0.12	15.0
5.4	0.57			150	0.09	10.75
5.3	0.575	5.0	0.525	160	0.092	11.0
5.2	0.575	4.9	0.53	170	0.075	9.0
5.1	0.58	4.8	0.54	180	0.065	7.75
5.0	0.58	4.7	0.55	190	0.072	8.5
4.8	0.57	4.6	0.575	200	0.08	9.75
4.7	0.565	4.5	0.64	210	0.10	12.25
4.6	0.57	4.4	1.055	220	0.115	14.0
4.5	0.57	4.3	1.2	230	0.132	16.5
4.4	0.59	4.28	1.05	240	0.165	20.75
4.3	0.602	4.25	0.59	250	0.2	25.0
4.2	0.53	4.15	0.49	260	0.232	29.0
4.1	0.45	4.07	0.57	270	0.255	31.5
4.0	0.5	4.05	0.595	277	0.256	31.75
3.98	0.75	4.00	0.82	279	0.257	32.0
3.95	0.67	3.95	0.78	280	0.25	31.0
3.9	0.605	3.9	0.512	290	0.215	26.75
3.8	0.46	3.8	0.59	300	0.16	20.0
3.7	0.59	3.75	0.23	310	0.11	13.5
3.6	0.59	3.7	0.275	320	0.10	12.25
3.5	0.59	3.675	0.26	330	0.088	10.50
3.4	0.575	3.65	1.02	340	0.08	9.75
3.3	0.57	3.6	0.84	350	0.07	8.25
3.2	0.57	3.5	0.61			
3.1	0.58	3.25	0.55			
3.0	0.58	3.0	0.532			

TABLE 9.14.

Sample: 800B, Mag. Field 5.81 K.Gauss, Temperature 74°C
Background Optical Density = 0.395

LINEAR SCANNING				ANGULAR SCANNING		
L in cm.	O. D.	L in cm.	O. D.	θ in degree	O. D.	Intensity
		3.0	0.57	0	0.095	12.0
OUTER HALO		2.9	0.56	10	0.097	11.5
		2.7	0.55	20	0.105	12.75
7.0	0.52	2.5	0.542	31	0.117	14.25
6.9	0.53	2.4	0.542	43	0.15	17.25
6.8	0.55	2.3	0.548	50	0.17	21.25
6.6	0.59	2.2	0.56	60	0.197	24.5
6.4	0.632	2.0	0.582	70	0.22	27.5
6.35	0.635	1.85	0.605	82	0.225	28.0
6.325	0.635	1.75	0.625	84	0.225	28.0
6.3	0.632	1.625	0.635	85	0.223	27.75
6.2	0.62	1.5	0.625	90	0.217	27.0
6.1	0.61	1.4	0.6	100	0.205	25.75
6.0	0.59	1.25	0.572	110	0.175	22.0
5.9	0.57	1.125	0.538	120	0.147	18.25
5.8	0.553			130	0.125	15.5
5.7	0.543	INNER HALO		140	0.105	12.75
5.5	0.54			150	0.095	12.0
5.4	0.54	5.0	0.555	160	0.09	10.75
5.2	0.55	4.8	0.58	170	0.085	10.0
4.95	0.56	4.6	0.65	180	0.085	10.0
4.75	0.59	4.4	0.792	190	0.09	10.75
4.6	0.608	4.35	0.925	200	0.1	12.25
4.5	0.638	4.3	0.935	210	0.105	12.75
4.45	0.668	4.275	0.925	220	0.133	16.75
4.35	0.688	4.25	0.81	230	0.157	19.75
4.25	0.69	4.2	0.52	240	0.195	24.25
4.225	0.685	4.125	0.442	250	0.225	28.0
4.2	0.57	4.1	0.50	260	0.235	29.25
4.1	0.43	4.05	0.625	263	0.235	29.25
4.0	0.69	4.0	0.675	265	0.236	29.5
3.975	1.2	3.975	0.745	266	0.235	29.25
3.95	1.15	3.95	0.698	270	0.233	29.0
3.9	0.7	3.85	0.55	273	0.225	28.0
3.85	0.49	3.825	0.45	280	0.215	26.75
3.825	0.435	3.8	0.51	290	0.185	23.0
3.75	0.50	3.75	0.595	300	0.16	20.0
3.7	0.732	3.7	0.92	310	0.14	17.5
3.6	0.735	3.625	0.925	320	0.123	15.5
3.575	0.72	3.6	0.92	330	0.108	13.0
3.5	0.69	3.5	0.745	340	0.108	13.0
3.45	0.66	3.4	0.65	350	0.105	12.75
3.35	0.63	3.2	0.58	0	0.106	12.75
3.25	0.608	3.1	0.54			
3.2	0.59					

TABLE 9.15

Sample: 800B, Mag. Field = 5.81 K. Gauss, Temperature 75°C
Background Optical Density = 0.47

LINEAR SCANNING				ANGULAR SCANNING		
L in cm.	O. D.	L in cm.	O. D.	θ in degrees	O. D.	Intensity
OUTER HALO		2.9	0.55	270	0.06	7.25
		2.8	0.549	280	0.06	7.25
		2.7	0.55	290	0.055	6.5
7.0	0.53	2.6	0.548	300	0.052	6.25
6.9	0.542	2.5	0.55	310	0.06	7.25
6.8	0.558	2.4	0.552	320	0.06	7.25
6.7	0.575	2.25	0.555	330	0.072	8.5
6.6	0.59	2.1	0.57	340	0.092	11.0
6.5	0.60	2.0	0.58	355	0.105	12.75
6.45	0.601	1.9	0.592	0	0.115	14.0
6.425	0.6	1.75	0.62	9	0.122	15.25
6.35	0.598	1.55	0.625	11	0.122	15.25
6.3	0.598	1.5	0.622	16	0.125	15.5
6.2	0.58	1.45	0.618	20	0.121	15.0
6.1	0.565	1.4	0.612	30	0.118	14.5
6.0	0.60	1.2	0.57	40	0.105	12.75
5.9	0.548			50	0.092	11.0
5.8	0.54	INNER HALO		60	0.09	10.75
5.7	0.535			70	0.08	9.75
5.6	0.538	5.0	0.535	80	0.07	8.25
5.5	0.54	4.9	0.545	90	0.062	7.50
5.4	0.54	4.7	0.57	100	0.06	7.25
5.3	0.542	4.6	0.58	110	0.06	7.25
5.2	0.545	4.5	0.618	120	0.06	7.25
5.1	0.545	4.45	0.688	130	0.07	8.25
5.0	0.55	4.4	0.712	140	0.08	9.75
4.8	0.552	4.375	0.708	150	0.09	10.75
4.7	0.55	4.3	0.572	160	0.105	12.75
4.6	0.555	4.25	0.49	170	0.12	15.0
4.5	0.56	4.2	0.50	185	0.142	17.75
4.4	0.565	4.1	0.601	189	0.15	17.25
4.3	0.565	4.05	0.85	190	0.149	18.5
4.2	0.54	4.0	0.61	200	0.145	18.0
4.1	0.49	3.95	0.49	210	0.14	17.5
4.05	0.488	3.9	0.499	220	0.128	16.0
4.0	0.75	3.8	0.62	230	0.112	13.75
3.85	0.488	3.725	0.69	240	0.105	12.75
3.8	0.485	3.7	0.68	250	0.08	9.75
3.75	0.54	3.65	0.64	260	0.07	8.25
3.6	0.575	3.6	0.61	270	0.06	7.25
3.5	0.575	3.4	0.56			
3.4	0.57	3.2	0.55			
3.3	0.565	3.0	0.54			
3.1	0.555					
3.0	0.552					

TABLE 9.16

Sample: 80CB.

D and ℓ or d values for 80CB at different temperatures.

Temp. °C.	Sample to film distance cm. *	Outer halo			Inner halo/ring		
		Dia.cm.	Bragg angle (deg.)	'D' Å	Dia.cm.	Bragg angle (deg.)	'd'/ℓ Å
38	5.655	4.25	10.297	4.818	0.55	1.392	31.75
40	6.345	4.8	10.359	4.789	0.6	1.354	32.64
45	6.345	4.875	10.507	4.722	0.6	1.354	32.64
47	6.345	4.825	10.411	4.766	-	-	-
48	5.655	4.2	10.186	4.87	0.575	1.455	30.36
56	6.345	4.775	10.310	4.812	0.6	1.354	32.64
60	5.655	4.175	10.131	4.89	0.575	1.455	30.36
65	5.655	4.15	10.075	4.92	0.575	1.455	30.36
67	6.345	4.725	10.211	4.858	0.6	1.354	32.64
74	6.345	4.7	10.162	4.881	0.625	1.409	32.34
75	5.655	4.1	9.963	4.978	0.55	1.392	31.75
75	6.345	4.7	10.162	4.881	0.625	1.409	31.34

* For a unoriented sample the sample to film distance is 5.655 cm. for oriented sample - the sample to film distance is 6.345 cm.

TABLE 9.17

'd', $\langle \cos\theta \rangle$ and $[d/\langle \cos\theta \rangle]$ values at different temperatures.

Temp. °C.	'd' Å	$\langle \cos\theta \rangle$	$[d/\langle \cos\theta \rangle]$
38	31.75	0.872	36.41
45	32.64	0.866	37.69
48	30.36	0.863	35.18
56	32.64	0.87	37.52
65	32.64	0.864	37.78

Mean d = 32.0 ± 1 Å

Mean $d/\langle \cos\theta \rangle$ = 36.9 ± 1 Å

TABLE 9.18.

Sample: 80CB.

Mean Intensity values at different temperatures.

θ (deg.)	I(θ) values at temperatures.							
	40°C	45°C	47°C	56°C	65°C	67°C	74°C	75°C
0	45.75	20.45	22.0	17.65	28.75	26.58	18.0	10.13
5	43.88	19.38	21.06	16.94	27.41	25.56	17.84	10.11
10	38.06	17.37	18.96	15.96	25.0	23.63	17.15	9.81
15	32.38	14.56	16.50	13.64	21.31	19.0	15.8	9.00
20	26.06	11.30	13.68	10.58	17.61	16.85	14.26	8.14
25	20.44	8.06	10.73	8.39	14.26	13.5	12.58	7.15
30	15.00	6.87	7.91	6.05	11.11	10.75	10.7	6.24
35	10.31	4.86	5.56	4.51	8.20	8.44	8.80	5.26
40	6.75	3.00	3.81	3.00	5.88	6.63	7.19	4.34
45	4.25	2.75	2.50	1.79	4.05	5.19	5.78	3.68
50	2.56	1.87	1.71	1.19	2.58	3.81	4.46	2.75
55	1.75	1.02	1.56	0.81	1.64	3.06	3.30	2.03
60	0.59	0.63	0.94	0.43	0.84	2.31	2.31	1.46
65	0.06	0.39	0.64	0.24	0.43	1.56	1.59	1.00
70	0	0.30	0.47	0.05	0.13	1.00	1.06	0.53
75	0	0.14	0.36	0	0	0.63	0.65	0.23
80	0	0.11	0.19	0	0	0.25	0.29	0.06
85	0	0.03	0.06	0	0	0	0.05	0
90	0	0	0	0	0	0	0	0

TABLE 9.19

Sample: 80CB.

Normalized distribution function at different temperatures.

β (deg)	$f(\beta)$ at different temperatures.							
	40°C	45°C	47°C	56°C	65°C	67°C	74°C	75°C
0	10.11	9.337	8.364	8.301	8.350	7.722	4.456	4.156
5	9.42	8.809	7.981	8.063	7.957	7.333	4.393	4.146
10	7.945	7.700	7.005	7.365	6.939	6.333	4.206	4.067
15	6.233	6.138	5.809	6.281	5.666	5.102	3.902	3.826
20	4.785	4.594	4.680	4.983	4.468	3.978	3.495	3.406
25	3.685	3.316	3.676	3.705	3.482	3.091	3.017	2.898
30	2.758	2.370	2.735	2.636	2.671	2.394	2.514	2.421
35	1.891	1.704	1.854	1.830	1.971	1.811	2.048	2.029
40	1.157	1.233	1.139	1.235	1.373	1.325	1.627	1.691
45	0.672	0.880	0.682	0.781	0.909	0.960	1.280	1.362
50	0.423	0.598	0.456	0.451	0.584	0.714	0.981	1.042
55	0.280	0.367	0.340	0.250	0.364	0.543	0.718	0.766
60	0.146	0.195	0.241	0.152	0.206	0.482	0.495	0.548
65	0.030	0.093	0.149	0.100	0.094	0.277	0.325	0.372
70	-0.010	0.054	0.092	0.049	0.030	0.176	0.200	0.217
75	-0.006	0.044	0.068	0.002	0.006	0.102	0.126	0.094
80	0.011	0.034	0.045	-0.015	0.001	0.048	0.062	0.023
85	0.004	0.008	0.015	-0.003	-0	0.010	0.015	0.002
90	-0.006	-0.003	-0.001	0.007	-0.001	-0.005	-0.003	0

TABLE 9.20

Sample: 80OB.

Order parameters values at different temperature.

Temp. °C.	Temp. °K.	$\langle P_2 \rangle_V$	$\langle P_2 \rangle$	$\langle P_2 \rangle_{M.F.}$	$\langle P_4 \rangle_V$	$\langle P_4 \rangle$	$\langle P_4 \rangle_{M.F.}$	Phase
40	313	0.68	0.70	0.62	0.27	0.30	0.33	
45	318	0.62	0.66	0.62	0.22	0.27	0.32	
47	320	0.61	0.65	0.62	0.22	0.27	0.32	Smectic
56	329	0.66	0.68	0.58	0.25	0.28	0.27	
65	338	0.63	0.65	0.54	0.21	0.24	0.23	
67	340	0.52	0.58	0.52	0.13	0.20	0.21	
74	347	0.48	0.50	0.49	0.07	0.09	0.17	Nematic
75	348	0.48	0.49	0.47	0.06	0.07	0.16	

TABLE 9.21

Sample: 80OB.

a_L & b_L (L = 2 & 4) values at different temperatures.

Temp. °K.	a_0	a_2	a_4	a_6	a_8	a_{10}	b_2/k	b_4/k
313	-4.659	11.082	-7.685	5.605	-3.147	1.141	-4983	7965
318	-1.589	4.359	-1.161	0.692	-0.188	0.161	-2112	1352
320	-1.384	3.903	-0.766	0.682	-0.684	0.386	-1931	920
329	-3.025	7.585	-4.533	3.642	-2.701	1.273	-3675	5289
338	-2.841	7.330	-4.605	3.609	-2.679	1.452	-3806	6432
340	-1.184	3.753	-1.459	1.433	-1.086	0.652	-2212	2505
347	-0.989	3.456	-1.651	1.157	-0.895	0.472	-2389	6296
348	-1.527	4.786	-3.507	3.061	-2.854	1.688	-3378	16492

TABLE 9.22

Sample: BOOB.

Coefficients of Pseudopotential.

Coefficients	Smectic phase		Nematic phase	
	Mean	Standard deviation	Mean	Standard deviation
b_2/k	− 3300	1280	− 2300	130
b_4/k	4400	3100	4400	2680

References:

1. M/s. F. Hoffmann-La-Roche & Co. Basel, Switzerland Cat.
2. A.J.Leadbetter & J.C. Frost and J.P.Gaughan, J.Phys. 40, 375 (1979).
3. J. Alaniels, R.J. Birgeneu, N.Kaplan, J.D. Litster and C.R.Safinya. Bull. Am. Phys. Soc. 23, 352 (1978).
3a. D.Bhattacharjee, S.Paul and R. Paul, Mol.~~Phys~~ Cryst. ~~Liq~~ & Liq.Cryst. 89 , 181 P, (1982).
4. D.Bhattacharjee, S. Paul and R. Paul, Molec. Phys. 44, 1391 (1981).
5. D.Bhattacharjee, R. Paul & S. Paul, Mol.Cryst.Liq.Cryst. 88 245 (1982).
6. A. J. Leadbetter and R.M.Richardson, Mol.Phys. 35, 1191 (1978).
7. A.E. de Vries, A. Ekachai and N. Spielberg, Mol.Cryst. Liq. Cryst. Letters 49 143 (1979).
8. A.E. de Vries, Ninth International Conference on Liquid Crystals, abstract No. B8.

CHAPTER 10.

X-RAY DIFFRACTION STUDIES ON SMECTIC PHASE OF 4'-(n-(p-PENTYLOXY CARBONYLOXY BENZYLIDENE) AMINO) VALEROPHENONE (PCBAV IN SHORT) IN MAGNETIC FIELD.

CHAPTER 10.

X-RAY DIFFRACTION STUDIES ON SMECTIC PHASE OF 4'-(n-(p-PENTYLOXY CARBONYLOXY-BENZYLIDENE) AMINO) VALEROPHENONE (PCBAV IN SHORT) IN MAGNETIC FIELD.

1. Introduction

The structure of PCBAV is given in chapter 2.

The compound PCBAV has got a smectic phase over a fairly wide range of temperature. The transition temperatures obtained from Eastman Data Service Catalogue (No. 11441) are -

$$\text{Crystal} \xrightarrow{77^\circ C} \text{Smectic} \xrightarrow{115^\circ C} \text{Isotropic}$$

The phase transition as determined by us from the X-ray diffraction and texture studies are

$$C \underset{\sim 60^\circ C}{\overset{77^\circ C}{\rightleftharpoons}} S_A \overset{115^\circ C}{\rightleftharpoons} I$$

This chapter includes the results obtained from X-ray diffraction studies of the sample PCBAV both in presence and absence of magnetic field. The theoretical background and the method of data analysis are described in earlier chapters. Orientational distribution functions and order parameters for both nematic and smectic phase of some mesomorphic compounds have been determined by Leadbetter et al[1,2]. They have also calculated the translational order parameter of S_A phase. For this sample an attempt has also been made by us to calculate the approximate value for the translational order parameter τ_1 and average value of the root mean square displacement $\langle z^2 \rangle^{1/2}$, in addition to the orientational distribution function and order parameters $\langle P_2 \rangle$ & $\langle P_4 \rangle$.

2. Experimental results and discussions:-

Texture and DSC Studies.

The texture of the sample was observed under polarizing microscope. During heating focal conic texture of S_A was observed and during cooling both focal conic and ~~as~~ fan texture of S_A were observed[3]. We had not been successful with our conoscopic observations, so it cannot be said definitely whether the phase is unaxial or ~~as~~ biaxial. But from the texture studies it is found that the smectic phase is of A type. A DSC (Differential Scanning Calorimetry) was done for the substance, phase changes were observed at the same temperatures as mentioned above.

X-ray diffraction studies:-

The X-ray diffraction photographs of the unoriented sample were taken at different temperatures in the set up No.1 (Fig. 2.1) of chapter 2 and the photographs of oriented samples at different temperatures were taken in the set up No. 2 (Fig.2.2) of chapter 2. The sample was heated upto isotropic phase in presence of magnetic field 5.81 K.gauss and then cooled down to desired temperatures in presence of the same field and flat plate photographs were taken with an exposure time 2 - 3 hours. The X-ray diffraction photograph of the unoriented sample, i.e. without application of magnetic field at 95°C is shown in the fig. 10.1 and the photograph of the oriented sample in presence of magnetic field 5.81 K.gauss at 69°C is shown in the fig.10.2.

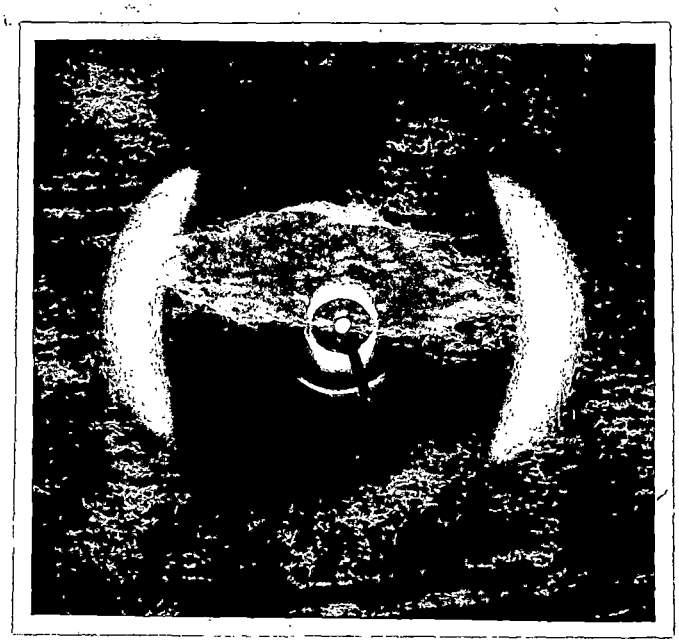

Fig. 10.1. Photograph of unoriented S_A phase of FCBAV at 95°C

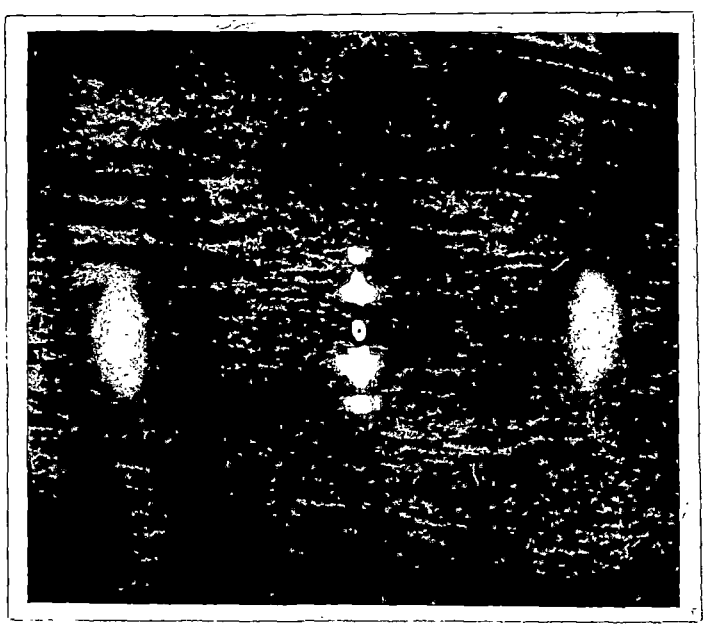

Fig. 10.2. Photograph of oriented S_A phase of FCBAV at 69°C

The orientation is in the $\overline{H}$ direction i.e. the direction of the magnetic field as shown in the fig. 10.2. This was found to be sufficiently strong to produce a monodomain sample as seen from the sharpness of the inner spot of the photograph (Fig. 10.2). The photograph taken with a higher magnetic field of 6.5 K.Gauss gave substantially the same ~~xx~~ pattern. Further experimental details have been discussed in earlier chapters[4].

The photograph of unoriented sample i.e. Fig. 10.1 shows a sharp inner ring with its second order and a diffuse outer ring, typical of S_A or S_C type. The pattern of the oriented sample consists of two diffuse outer maxima, which shows that the structure within the layer is undoubtedly disordered. ~~x~~ The (001) and (002) diffraction spots are sharp. From the diffraction pattern of oriented sample it is obvious that the smectic phase is of A type. The line joining the outer maxima is perpendicular to the line joining (001) maxima, which shows that the molecules are perpendicular to the smectic ~~xxxxx~~ planes.

The data obtained from the linear and angular scanning for oriented and unoriented films at different temperatures are given in table 10.1 - 10.9.

Average Intermolecular distance 'D' and smectic layer thickness 'd'

Average distance between the neighbouring molecules 'D' and the layer spacings 'd' are calculated from X-ray diffraction photographs following the procedure discussed in

chapter 3,4,7 etc. 'D' and 'd' values along with the diameter for the outer and inner maxima or halo and the corresponding Bragg ~~xxxx~~ angle are given in table 10.10. The table also contains the actual distance between the sample and the film for the different set up. The temperature dependence of D and 'd' have been discussed by de Vries[5,6]. The variation of lateral spacings 'D' with temperature is shown in the fig. 10.3. It is seen that the application of magnetic field causes a decrease in the intermolecular distance. We are unable to explain the cause of this decrease in intermolecular distance, however, ~~some~~ effect has been observed in other samples as well. The 'D' value increases with the rising temperature. With the help of a stereo model unit (Prentice Hall, Inc, West Nyack), N.Y. 10984) we have measured the ~~xxxx~~ molecular length L in their completely extended form and found the value to be 26 Å. The experimental 'd' values are observed from the unoriented sample varies from 27.3 Å to 25.6 Å i.e. d values decreases with increasing temperature. It seems that, as the temperatures rises the thermal vibration of the molecules causes a decrease in the layer thickness. As discussed in chapter 9 we have tried to take into account the orientational disorder in the calculation of layer thickness in Smectic A phase. The values of d, $\langle \cos\theta \rangle$ and $\left[d / \langle \cos\theta \rangle \right]$ (calculated by the process described in chapter 9) at different temperatures are given in table 10.10.

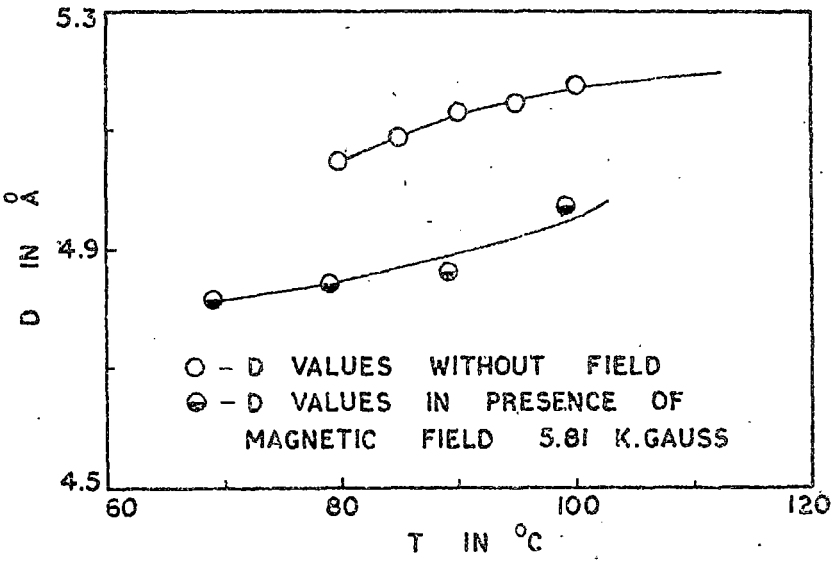

FIG. 10.3.

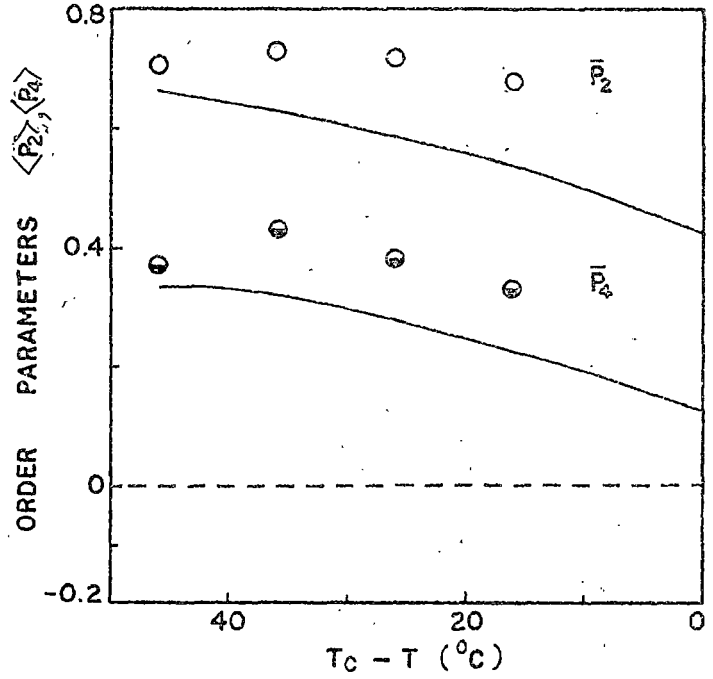

FIG. 10.5. Solid lines — $\langle P_2 \rangle_{M.F.}$ and $\langle P_4 \rangle_{M.F.}$ Values

$\langle P_2 \rangle$ & $\bar{P}_2$ are equivalent, $\langle P_4 \rangle$ & $\bar{P}_4$ are equivalent.

The mean value of $d/\langle\cos\theta\rangle$ is 30.1 ± 0.3 Å. The ratios of the d and L values and $d/\langle\cos\theta\rangle$ and L values are 1.03 and 1.2 respectively. However we are unable to explain why the corrected layer thickness is larger than the molecular length since there seems to be little probability of forming dimers of the molecules of PCBAV. For 'd' measurements our experimental error is ± 1.2 Å near 25 Å.

Intensity, Normalized distribution function, orientational order parameters.

θ Versus $I(\theta)$ (i.e. the mean of four intensity values for the four quadrants for each θ from 0° - 90°) values at different temperatures are given in table 10.11. The normalized distribution function $f(\beta)$ as a function of β for different temperatures, as obtained from experimental intensity values, are also given in the same table.

The fig. 10.4 shows graphically the variation of $f(\beta)$ with β at different temperatures. We expect as temperature decreases, the function s to become more peaked at $\beta=0°$. Our $f(\beta)$ curves generally conform to this idea except that the curve at 69° is less than that at 79°C. Since, DSC, X-ray and texture studies do not show any phase transition between 79°C and 69°C while cooling PCBAV at 69°C is in S_A phase. However, we are unable to explain the cause of this anomally.

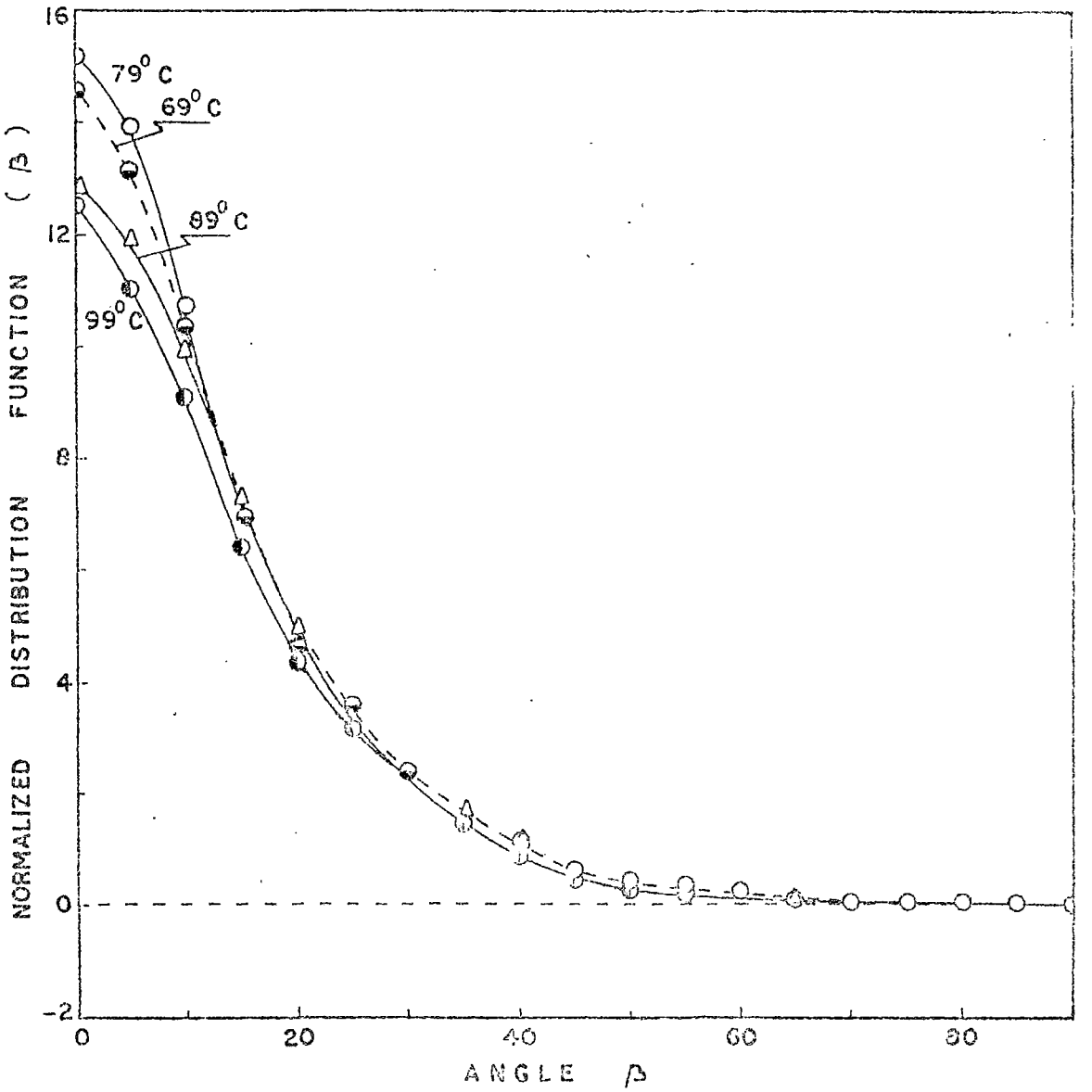
79° C
69° C
89° C
99° C
NORMALIZED DISTRIBUTION FUNCTION (β)
ANGLE β
16
12
8
4
0
-2
0
20
40
60
80

FIG. 10.4.

Orientational order parameters $\langle P_2 \rangle$ & $\langle P_4 \rangle$ at different temperatures are given in table 10.12. The table also includes the Maier-Saupe theoretical mean field values and also the values of $\langle P_2 \rangle_V$ and $\langle P_4 \rangle_V$ i.e. order parameters, calculated by Vainshtein's approximation[7]. Fig. 10.5 represents the order parameter values against $T_c - T$. Both $\langle P_2 \rangle$ and $\langle P_4 \rangle$ values are found to be larger than MS theoretical values. Anomalus nature of $f(\beta)$ at 69°C is reflected in the values of $\langle P_2 \rangle$ and $\langle P_4 \rangle$ at that temperature. The experimental order parameters values are estimated to be accurate within $\pm$ 0.02. Leadbetter and Wrighton[2] have calculated $\langle P_2 \rangle$ values in the S_A phase of TBBA and 40S from X-ray diffraction data. Contrary to our observations, they found that the experimental $\langle P_2 \rangle$ values are lower than the MS theoretical values. According to them the simple mean field theory does not predict correctly the magnitude and temperature dependence of $\langle P_2 \rangle$ for smectic phase.

Translational order parameter for S_A phase.

SmecticA, a liquid crystalline phase possess both orientational and translational orders as described in chapter 1. Theory of S_A order parameters have been proposed by a number of investigators. It was pointed out by McMillan[8] that the smectic layer distribution functions are directly related to the intensity of the layer reflections. The distribution functions normal to the layers may be written

$$f(z) = \frac{1}{d}\left[1 + \sum_{l=1}^{\infty} \tau_l \cos(2\pi l z/d)\right] \qquad \ldots (1)$$

with

$$\tau_l = \langle \cos(2\pi l z/d) \rangle$$

where, d is the layer spacings, Z is the displacement of the molecular centre in the direction perpendicular to the layer plane, and τ_l is the translational order parameter. The intensity of the (00 l) layer reflection is

$$I(00\,l) = C\,\tau_l^2 \langle F(00l) \rangle^2 \qquad \ldots (2)$$

where, F(00 l) is the structure factor for a perfect layer and C is a constant.

For a Gaussian distribution -

$$F(z) = \left[2\pi \langle z^2 \rangle\right]^{-1/2} \exp\left[-\frac{z^2}{2\langle z^2 \rangle}\right] \qquad \ldots (3)$$

$$\tau_l = \langle \cos(2\pi l z/d) \rangle$$

$$= \exp\left[-2\pi^2 l^2 \langle z^2 \rangle / d^2\right] = \tau_1^{l^2}$$

Equation 2 shows that the intensity of the 1st. order layer reflection is proportional to smectic order parameter τ_1^2 If two or more ℓ reflection are observed then assumption of a constant value of $\langle F(00l) \rangle$ and a Gaussian form for $f(z)$ enables us to obtain τ_1 and $\langle z^2 \rangle^{1/2}$

In the S_A phase of PCHAV two layer reflections are observed as shown in the fig. 10.1 and 10.2. The inner ring is very close to the atop. We could not get an accurate value of the translational order parameter due to the inaccuracy in the measurement of intensity of the inner ring.

However, we measured I (002) and I (001) at 69°C

I(002) = 0.41, I(001) = 1.33.

Intensity values were then corrected for Lorentz and polarization factors

$$\left[I(001)/LP_1 = 1.33/31.7 \quad \text{and} \quad I(002)/LP_2 = \frac{0.41}{5.78} \right]$$

$$\frac{I(002)/LP_2}{I(001)/LP_1} = 0.6193 = \frac{\tau_2^2}{\tau_1^2}.$$

i.e. $\frac{\tau_2}{\tau_1} = 0.7870.$

or $\tau_1^3 = 0.7870$, i.e. $\tau_1 = 0.9233.$

From relation -

$$\tau_1 = \exp. 2\pi^2 \langle z^2 \rangle / d^2 = 0.9233$$

or $\langle z^2 \rangle = 2.43$ Å

$\langle z^2 \rangle^{1/2} = 1.56$ Å

Thus $\tau_1 = 0.923$ and $\langle z^2 \rangle^{1/2} = 1.56$ Å.

Pseudopotential:-

We have calculated the angular part of the pseudopotential in the form -

$$V(\beta)/_k = \sum_{L(even)} b_L \langle P_L \rangle P_L (\cos\beta)$$

from least square fitting of $\ln f(\beta)$ values (as described in chapters 3, 7).

The coefficients b_L values calculated from a_L values are assumed to be temperature independent in view of small temperature range only of 30°C. a_L values and b_L values (L = 2 and 4) are given in table 10.13.

Taking all four temperature data, the pseudopotential can be written (upto $P_4(\cos\beta)$ term keeping the last digit in round number) as

$$V(\beta)/_k = -(2450 \pm 200) \langle P_2 \rangle P_2 \cos\beta + (1050 \pm 700) \langle P_4 \rangle P_4 \cos\beta .$$

So it is seen that the standard deviation for b_2 is reasonable while that of b_4 is large, suggesting the breakdown of the idea of the Legendre polynomial expansion of the pseudopotential. This is in accordance with our earlier results on nematics[4,4a] (chapter 7 and 8) and also smectics[4a] (chapter 9). As the sample possesses only S_A phase, and the validity of simple Mean field theory (Maier-Saupe) is somewhat less in case of S_A phase[2], the comparison between the experimentally obtained $f(\beta)$ values with those obtained from Maier-Saupe Mean Field potential is not done here.

Table 10.1.

Sample: PCBAV, Mag.Field Nil
Temp. 80°C

LINEAR SCANNING			
L in cm.	O. D.	L in cm.	O. D.
		3.0	0.44
OUTER HALO		2.9	0.50
		2.8	0.57
7.0	0.525	2.7	0.64
6.9	0.575	2.6	0.69
6.8	0.61	2.5	0.77
6.6	0.75	2.4	0.86
6.4	0.91	2.3	0.99
6.35	0.935	2.2	1.095
6.3	0.95	2.17	1.10
6.28	0.96	2.15	1.95
6.25	0.935	2.1	1.08
6.20	0.90	2.0	1.0
6.1	0.82	1.9	0.9
6.0	0.69	1.8	0.08
5.9	0.66	1.6	0.65
5.8	0.60	1.4	0.57
5.7	0.58	1.3	0.55
5.6	0.57		
5.5	0.57	INNER HALO	
5.4	0.58		
5.3	0.59	5.0	0.66
5.2	0.60	4.95	0.82
5.1	0.61	4.92	0.89
5.0	0.625	4.9	0.80
4.9	0.63	4.8	0.57
4.8	0.62	4.7	0.81
4.715	0.61	4.68	1.01
4.7	0.72	4.65	1.25
4.6	0.79	4.60	1.7
4.55	0.84	4.58	1.88
4.5	0.77	4.575	1.882
4.4	0.50	4.52	0.56
4.35	0.39	4.15	0.44
4.25	0.60	4.0	1.5
4.0	0.42	3.95	2.06
3.9	0.67	3.92	2.09
3.88	0.69	3.90	1.75
3.8	0.51	3.85	1.12
3.7	0.43	3.75	0.69
3.6	0.39	3.70	0.66
3.5	0.38	3.65	0.80
3.3	0.38	3.60	0.86
3.2	0.39	3.55	0.74
3.1	0.40	3.5	0.68

Table 10.2

Sample: PCBAV, Mag.Field Nil
Temp. 85°C

LINEAR SCANNING			
L in cm.	O. D.	L in cm.	O. D
		3.0	0.50
OUTER HALO		2.9	0.50
		2.8	0.48
7.0	0.49	2.7	0.49
6.9	0.51	2.5	0.52
6.8	0.54	2.4	0.55
6.7	0.58	2.2	0.64
6.6	0.64	2.1	0.67
6.5	0.71	2.08	0.675
6.4	0.79	2.02	0.67
6.3	0.87	2.0	0.67
6.25	0.91	1.9	0.64
6.2	0.94	1.8	0.58
6.15	0.925	1.6	0.50
6.1	0.90	1.4	0.45
6.0	0.80	1.3	0.44
5.9	0.70		
5.8	0.63		
5.6	0.58	INNER HALO.	
5.5	0.56		
5.4	0.57	5.0	0.57
5.3	0.58	4.9	0.59
5.2	0.59	4.8	0.60
5.1	0.59	4.75	0.62
5.0	0.59	4.72	0.60
4.9	0.59	4.7	0.59
4.8	0.59	4.65	0.575
4.6	0.60	4.6	0.59
4.55	0.61	4.55	0.65
4.5	0.55	4.5	1.025
4.4	0.32	4.48	1.05
4.3	0.39	4.45	1.04
4.2	1.02	4.4	0.59
4.14	0.98	4.3	0.35
4.1	0.61	3.95	0.39
4.0	0.39	3.85	1.15
3.9	0.64	3.82	1.57
3.84	0.73	3.8	1.54
3.8	0.70	3.7	0.69
3.75	0.64	3.60	0.60
3.7	0.61	3.5	0.65
3.6	0.57	3.4	0.62
3.5	0.57	3.3	0.59
3.4	0.56	3.2	0.58
3.3	0.56	3.1	0.56
3.2	0.54		

TABLE 10.3

Sample: PCBAV.

Mag.Field = Nil, Temp.90°C

LINEAR SCANNING			
L in cm.	O. D.	L in cm.	O. D.
		2.6	0.63
Outer halo		2.5	0.72
		2.4	0.82
7.0	0.51	2.3	0.92
6.8	0.61	2.25	0.98
6.6	0.76	2.2	1.1
6.5	0.85	2.175	1.15
6.4	9.4	2.15	1.2
6.3	1.3	2.125	1.15
6.25	1.4	2.0	1.1
6.22	1.5	1.9	0.88
6.2	1.455	1.8	0.78
6.1	0.99	1.7	0.69
6.0	0.85	1.6	0.63
5.9	0.74	1.5	0.58
5.8	0.67	1.4	0.55
5.6	0.58	1.3	0.52
5.5	0.57		
5.4	0.58	INNER HALO	
5.3	0.60		
5.2	0.61	5.0	0.56
5.1	0.62	4.9	0.65
5.0	0.63	4.85	0.69
4.9	0.63	4.8	0.59
4.8	0.66	4.75	0.58
4.7	0.61	4.7	0.62
4.6	0.66	4.6	1.07
4.5	1.05	4.58	1.25
4.48	1.06	4.54	1.55
4.46	1.05	4.52	1.46
4.0	0.54	4.4	0.45
3.9	0.5	4.0	0.34
3.83	1.14	3.9	0.88
3.8	1.0	3.88	1.06
3.7	0.6	3.87	1.07
3.6	0.59	3.85	1.02
3.5	0.66	3.8	0.78
3.4	0.62	3.7	0.59
3.3	0.62	3.6	0.68
3.2	0.61	3.55	0.80
3.1	0.60	3.5	0.67
3.0	0.60	3.4	0.58
2.9	0.58	3.3	0.54
2.8	0.58	3.2	0.52
2.7	0.60	3.1	0.50

TABLE 10.4

Sample: PCBAV.

Mag. Field = Nil, Temp. 95°C.

LINEAR SCANNING			
L in cm.	O. D.	L in cm.	O. D.
		2.7	0.53
Outer halo		2.6	0.57
7.0	0.45	2.5	0.59
6.9	0.49	2.4	0.66
6.8	0.50	2.3	0.77
6.7	0.55	2.25	0.83
6.6	0.60	2.2	0.86
6.5	0.68	2.18	0.89
6.4	0.73	2.15	0.9
6.3	0.85	2.1	0.905
6.2	0.95	2.08	0.9
6.16	0.955	2.0	0.89
6.1	0.94	1.9	0.8
6.0	0.84	1.7	0.65
5.9	0.74	1.6	0.57
5.8	0.65	1.4	0.5
5.7	0.59		
5.6	0.55	INNER HALO	
5.4	0.54		
5.3	0.55	5.0	0.48
5.2	0.56	4.9	0.60
5.1	0.57	4.8	0.52
5.0	0.58	4.7	0.55
4.9	0.58	4.65	0.66
4.8	0.575	4.6	0.88
4.7	0.57	4.55	1.14
4.6	0.58	4.53	1.22
4.5	0.68	4.5	1.02
4.35	0.29	4.4	0.3
4.3	0.32	4.0	0.3
4.2	0.98	3.95	0.36
4.18	1.15	3.9	1.47
4.0	0.31	3.86	1.48
3.9	0.45	3.82	1.22
3.85	0.66	3.8	0.98
3.8	0.66	3.75	0.70
3.7	0.57	3.7	0.60
3.6	0.56	3.62	0.52
3.5	0.56	3.6	0.53
3.4	0.57	3.58	0.55
3.2	0.56	3.52	0.58
3.1	0.52	3.5	0.57
3.0	0.53	3.4	0.52
2.9	0.53	3.2	0.46
2.8	0.52	3.0	0.43

Table 10.5(a)

Sample: PCBAV, Mag.Field = Nil
Temperature 100°C

LINEAR SCANNING			
L in cm.	O. D.	L in cm.	O. D.
		3.0	0.42
	Outer halo	2.9	0.405
		2.7	0.40
7.0	0.34	2.5	0.43
6.9	0.41	2.4	0.46
6.7	0.47	2.3	0.49
6.4	0.52	2.2	0.52
6.35	0.55	2.175	0.525
6.3	0.58	2.15	0.53
6.25	0.62	2.12	0.535
6.2	0.63	2.1	0.53
6.175	0.635	2.0	0.51
6.15	0.64	1.9	0.47
6.125	0.635	1.8	0.44
6.0	0.57	1.7	0.40
5.8	0.49	1.6	0.39
5.7	0.47	1.4	0.34
5.6	0.45		
5.5	0.43	INNER HALO	
5.45	0.42		
5.4	0.43	5.0	0.46
5.3	0.45	4.9	0.50
5.2	0.45	4.85	0.52
5.0	0.48	4.8	0.53
4.8	0.53	4.75	0.52
4.7	0.50	4.7	0.50
4.6	0.59	4.6	0.59
4.5	0.92	4.55	0.77
4.4	0.33	4.525	0.92
4.35	0.28	4.5	0.97
4.3	0.30	4.475	0.85
4.2	0.52	4.45	0.65
4.15	0.70	4.4	0.33
4.1	0.62	4.0	0.34
4.05	0.46	3.95	0.40
4.0	0.34	3.9	0.66
3.9	0.66	3.82	1.35
3.85	1.125	3.8	1.12
3.8	1.11	3.75	0.75
3.7	0.50	3.7	0.56
3.65	0.50	3.65	0.50
3.6	0.51	3.6	0.51
3.5	0.54	3.525	0.53
3.4	0.48	3.5	0.54
3.3	0.45	3.4	0.48

Table 10.5 (b)

Sample: PCBAV, Mag.Field = Nil
Temperature 110°C

LINEAR SCANNING			
L in cm.	O. D.	L in cm.	O. D.
		3.0	0.44
	Outer halo	2.9	0.43
		2.8	0.43
7.0	0.38	2.6	0.44
6.9	0.39	2.5	0.46
6.7	0.43	2.4	0.49
6.6	0.46	2.3	0.52
6.5	0.50	2.2	0.56
6.4	0.55	2.175	0.56
6.3	0.60	2.15	0.57
6.28	0.61	2.1	0.56
6.25	0.62	2.05	0.555
6.2	0.63	2.025	0.555
6.15	0.62	2.0	0.55
6.1	0.60	1.9	0.52
6.0	0.56	1.8	0.48
5.9	0.51	1.6	0.42
5.8	0.48	1.4	0.38
5.7	0.46		
5.6	0.45	INNER HALO	
5.55	0.44		
5.5	0.445	4.9	0.49
5.4	0.45	4.8	0.50
5.1	0.49	4.7	0.51
5.0	0.495	4.675	0.54
4.9	0.51	4.65	0.54
4.8	0.52	4.625	0.545
4.7	0.53	4.6	0.545
4.68	0.525	4.575	0.45
4.65	0.525	4.55	0.40
4.6	0.52	4.5	0.31
4.58	0.51	4.45	0.27
4.45	0.30	4.4	0.30
4.1	0.42	4.15	0.40
4.05	0.36	4.1	0.33
4.0	0.42	4.05	0.36
3.9	0.63	4.0	0.46
3.85	0.59	3.95	0.50
3.8	0.55	3.925	0.53
3.7	0.52	3.9	0.55
3.6	0.50	3.875	0.54
3.5	0.49	3.825	0.515
3.4	0.48	3.8	0.50
3.3	0.47	3.7	0.48
3.2	0.46	3.6	0.47
		3.5	0.46

TABLE 10.6

Sample: PCBAV, Mag.Field = 5.81 K.Gauss, Temperature 69°C
Background Optical Density = 0.38

LINEAR SCANNING						ANGULAR SCANNING		
L in cm	O. D.	L in cm.	O. D.	L in cm.	O. D.	θ in degree	O.D.	Intensity
		3.8	0.38	4.8	0.93	350	0.06	7.0
OUTER HALO		3.7	0.505	4.75	0.701	0	0.058	6.75
		3.6	0.505	4.7	0.63	10	0.06	7.0
7.0	0.5	3.5	0.51	4.6	0.74	20	0.065	7.5
6.9	0.535	3.4	0.495	4.35	1.46	30	0.082	9.75
6.8	0.56	3.3	0.49	4.475	1.85	40	0.095	11.5
6.7	0.61	3.2	0.49	4.46	1.915	57	0.168	21.0
6.55	0.692	3.05	0.501	4.45	1.915	60	0.189	23.6
6.5	0.735	2.9	0.51	4.425	1.63	70	0.29	36.5
6.45	0.74	2.75	0.512	4.375	1.31	80	0.36	48.0
6.4	0.76	2.6	0.505	4.35	0.92	84	0.375	50.75
6.38	0.759	2.5	0.505	4.3	0.43	85	0.376	51.0
6.35	0.756	2.45	0.50	4.225	0.385	87	0.372	50.25
6.25	0.702	2.35	0.50	4.2	0.41	90	0.35	46.5
6.2	0.682	2.15	0.515	4.1	0.86	100	0.23	28.5
6.1	0.62	2.0	0.58	4.075	0.95	110	0.12	14.75
6.0	0.568	1.9	0.63	4.05	0.82	120	0.07	8.5
5.9	0.548	1.85	0.655	3.95	0.725	130	0.052	6.25
5.8	0.52	1.8	0.67	3.9	0.53	140	0.04	4.5
5.7	0.505	1.75	0.725	3.85	0.88	150	0.03	3.25
5.6	0.50	1.65	0.748	3.825	1.055	160	0.03	3.25
5.5	0.505	1.625	0.742	3.8	1.25	170	0.025	2.5
5.4	0.52	1.6	0.74	3.75	1.855	180	0.025	2.5
5.3	0.53	1.5	0.68	3.7	2.09	190	0.03	3.25
5.25	0.525	1.4	0.622	3.65	2.182	200	0.035	4.0
5.2	0.53	1.3	0.568	3.625	2.165	215	0.05	6.0
5.1	0.53	1.2	0.52	3.6	1.52	230	0.085	10.0
5.0	0.518	1.15	0.505	3.475	0.76	240	0.14	17.5
4.9	0.502			3.4	0.682	250	0.23	28.75
4.8	0.50	INNER HALO		3.375	0.665	260	0.348	46.0
4.7	0.495			3.35	0.895	263	0.36	48.0
4.6	0.50	5.5	0.39	3.3	0.985	265	0.358	47.75
4.5	0.51	5.4	0.392	3.25	1.01	270	0.338	44.5
4.4	0.552	5.3	0.41	3.225	1.02	280	0.21	26.25
4.35	0.565	5.2	0.425	3.215	0.93	290	0.12	14.75
4.3	0.552	5.1	0.442	3.2	0.86	300	0.8	9.5
4.2	0.53	5.0	0.472	3.1	0.525	310	0.065	7.5
4.15	0.425	4.95	0.60	3.0	0.501	320	0.06	7.0
4.1	0.478	4.9	0.665	2.95	0.475	330	0.055	6.5
4.0	0.92	4.875	0.95	2.8	0.45	340	0.06	7.0
3.95	0.895	4.85	0.988	2.7	0.44	350	0.065	7.5
3.9	0.385	4.825	0.98			3	0.062	7.2

TABLE 10.7

Sample: PCBAV, Mag.Field = 5.81 K.Gauss, Temperature 79°C
Background Optical Density = 0.355.

LINEAR SCANNING						ANGULAR SCANNING		
L in cm.	O.D.	L in cm	O. D.	L in cm	O. D.	θ in degree	O.D.	Intensi
OUTER HALO								
7.0	0.49	2.7	0.51	4.05	0.93	350	0.085	10.0
6.9	0.515	2.7	0.50	4.0	1.15	0	0.085	10.0
6.8	0.555	2.3	0.501	3.95	1.02	10	0.085	10.0
6.7	0.58	2.2	0.52	3.9	0.70	20	0.09	10.70
6.6	0.635	2.1	0.54	3.85	0.49	30	0.09	11.70
6.45	0.71	1.975	0.58	3.825	0.40	40	0.097	11.75
6.4	0.72	1.85	0.65	3.8	0.46	50	0.12	15.0
6.375	0.732	1.70	0.71	3.725	0.68	60	0.155	19.5
6.35	0.735	1.6	0.715	3.7	1.27	70	0.235	29.0
6.3	0.73	1.575	0.71	3.675	1.65	78	0.315	40.75
6.2	0.688	1.5	0.665	3.65	1.71	83	0.355	47.25
6.1	0.625	1.3	0.56	3.6	1.715	85	0.365	49.0
6.0	0.57	1.1	0.50	3.55	1.65	88	0.363	48.5
5.8	0.51			3.5	1.0	92	0.353	47.0
5.7	0.505	INNER HALO		3.49	0.86	100	0.295	37.5
5.5	0.51			3.45	0.59	110	0.22	27.5
5.4	0.51	5.5	0.408	3.35	0.51	120	0.165	20.5
5.2	0.53	5.4	0.402	3.325	0.512	130	0.135	16.5
5.0	0.52	5.3	0.41	3.3	0.65	140	0.125	15.5
4.8	0.49	5.2	0.42	3.25	0.75	150	0.117	14.3
4.6	0.48	5.1	0.425	3.225	0.74	160	0.11	12.25
4.5	0.485	5.0	0.438	3.21	0.749	170	0.115	14.0
4.4	0.50	4.9	0.46	3.2	0.75	180	0.117	14.3
4.35	0.51	4.85	0.58	3.15	0.535	190	0.109	13.0
4.275	0.50	4.8	0.73	3.1	0.48	200	0.107	12.75
4.2	0.435	4.775	0.82	3.0	0.45	210	0.107	12.75
4.15	0.38	4.75	0.81	2.85	0.43	220	0.107	14.3
4.1	0.382	4.7	0.647	2.7	0.42	230	0.115	14.0
4.05	0.495	4.65	0.50	2.4	0.42	240	0.155	18.4
4.0	0.52	4.60	0.56	2.2	0.425	250	0.215	26.75
3.975	0.62	4.55	0.655			258	0.285	35.75
3.9	0.49	4.5	0.712			264	0.337	44.5
3.8	0.40	4.475	1.385			265	0.345	45.5
3.7	0.48	4.45	1.835			270	0.343	44.25
3.6	0.525	4.425	1.96			280	0.285	35.75
3.5	0.50	4.35	2.17			290	0.215	26.75
3.4	0.49	4.340	2.172			300	0.14	17.5
3.3	0.482	4.325	2.1			310	0.115	14.0
3.2	0.485	4.25	1.325			320	0.1	12.5
3.1	0.488	4.2	0.92			330	0.097	11.75
3.0	0.505	4.10	0.39			340	0.095	11.5
2.9	0.52	4.08	0.4			350	0.1	12.5

TABLE 10.8

Sample: PCBAV, Mag.Field = 5.81 K.Gauss, Temperature 89°C
Background Optical Density 0.36.

LINEAR SCANNING						ANGULAR SCANNING		
L in cm.	O.D.	L in cm	O.D.	L in cm	O.D.	θ in degree	O. D.	Intensity
OUTER HALO		3.7	0.61	4.55	1.57	0	0.162	20.25
		3.6	0.58	4.5	1.815	10	0.165	20.5
		3.4	0.55	4.475	1.92	20	0.172	21.5
7.0	0.55	3.25	0.548	4.45	1.66	30	0.182	22.7
6.9	0.582	3.2	0.55	4.4	1.31	40	0.182	22.7
6.8	0.612	2.9	0.555	4.325	0.51	50	0.198	24.6
6.65	0.70	2.8	0.555	4.225	0.43	60	0.23	28.0
6.55	0.74	2.65	0.54	4.2	0.82	70	0.272	34.0
6.5	0.77	2.5	0.538	4.1	1.02	80	0.355	47.25
6.45	0.772	2.4	0.534	4.075	1.03	90	0.42	58.25
6.425	0.781	2.25	0.55	4.05	0.76	94	0.432	60.4
6.4	0.79	2.2	0.562	4.0	0.648	96.5	0.442	62.25
6.375	0.785	2.1	0.60	3.95	0.45	98	0.441	62.1
6.35	0.78	2.0	0.605	3.90	0.538	105	0.405	55.6
6.25	0.74	1.9	0.608	3.85	0.98	110	0.36	48.0
6.15	0.71	1.8	0.73	3.825	1.73	120	0.28	35.0
6.1	0.67	1.75	0.76	3.75	2.125	130	0.23	28.0
6.0	0.622	1.675	0.761	3.725	2.19	140	0.21	26.25
5.9	0.595	1.65	0.76	3.70	2.1	150	0.195	24.25
5.8	0.57	1.6	0.73	3.65	1.35	160	0.192	23.75
5.7	0.55	1.5	0.715	3.6	1.195	170	0.182	22.7
5.6	0.55	1.4	0.648	3.55	0.76	180	0.182	22.7
5.5	0.55	1.25	0.598	3.45	0.65	190	0.18	22.5
5.4	0.56	1.2	0.54	3.35	0.788	200	0.175	22.0
5.3	0.56			3.325	0.788	220	0.185	23.0
5.125	0.57	INNER HALO		3.3	0.70	230	0.192	24.0
5.0	0.56			3.2	0.58	240	0.19	23.5
4.85	0.56	5.5	0.475	3.0	0.515	250	0.28	35.0
4.65	0.565	5.4	0.478	2.9	0.51	260	0.37	50.0
4.6	0.58	5.3	0.482	2.75	0.50	270	0.41	56.0
4.45	0.61	5.2	0.488	2.5	0.49	275	0.412	56.7
4.35	0.55	5.05	0.528	2.3	0.495	280	0.415	57.25
4.25	0.43	4.95	0.595			290	0.31	40.0
4.2	0.40	4.9	0.668			300	0.242	30.0
4.1	0.492	4.875	0.70			310	0.205	25.5
4.05	0.99	4.85	0.68			320	0.182	22.7
4.0	0.915	4.8	0.63			330	0.17	21.25
3.95	0.82	4.75	0.61			340	0.17	21.25
3.9	0.42	4.675	0.658			350	0.162	20.25
3.8	0.58	4.6	0.83			0	0.162	20.25

TABLE 10.9

Sample: POBAV, Mag.Field = 5.81 K.Gauss, Temperature 99°C
Background Optical Density = 0.32.

LINEAR SCANNING						ANGULAR SCANNING		
L in cm.	O. D.	L in cm	O. D.	L in cm.	O. D.	θ in degree	O. D.	Intensity
OUTER HALO								
7.0	0.605	3.2	0.63	4.15	0.75	0	0.255	31.7
6.9	0.62	3.0	0.65	4.1	0.82	10	0.252	31.25
6.8	0.65	2.9	0.66	4.075	1.31	20	0.255	31.7
6.7	0.692	2.55	0.649	4.05	1.3	30	0.255	31.7
6.5	0.76	2.45	0.64	4.25	1.07	40	0.26	32.25
6.45	0.79	2.3	0.652	4.0	0.99	50	0.27	33.0
6.4	0.795	2.0	0.735	3.95	0.41	60	0.28	35.0
6.375	0.80	1.85	0.85	3.85	0.41	70	0.315	40.75
6.35	0.801	1.75	0.852	3.8	1.05	80	0.37	50.0
6.3	0.80	1.725	0.85	3.725	1.72	90	0.45	64.0
6.2	0.77	1.7	0.849	3.72	1.80	95	0.46	66.0
6.1	0.72	1.5	0.782	3.7	2.02	98	0.47	68.0
6.0	0.692	1.3	0.68	3.675	1.73	101	0.478	69.5
5.9	0.66	1.15	0.63	3.6	1.41	103	0.47	68.0
5.7	0.62			3.55	0.75	110	0.44	62.0
5.6	0.612	INNER HALO				120	0.372	52.25
5.5	0.612					130	0,32	41.5
5.4	0.625	5.5	0.41			140	0.29	36.5
5.3	0.635	5.4	0.42			150	0.285	35.5
5.1	0.642	5.2	0.44			160	0.28	35.0
5.0	0.632	5.1	0.45			170	0.281	35.2
4.9	0.625	5.0	0.482			180	0.281	35.2
4.8	0.625	4.85	0.732			200	0.28	35.0
4.7	0.625	4.825	0.78			212	0.282	35.25
4.6	0.632	4.8	0.8			230	0.305	39.0
4.5	0.64	4.78	0.785			240	0.33	43.25
4.4	0.54	4.7	0.58			250	0.385	52.5
4.3	0.475	4.675	0.582			260	0.462	56.5
4.2	0.47	4.6	0.71			270	0.53	82.25
4.1	0.675	4.575	1.0			280	0.52	79.75
4.05	0.99	4.55	1.13			290	0.455	65.5
4.025	1.45	4.5	1.38			300	0.39	54.0
4.0	1.4	4.46	2.2			310	0.34	45.0
3.975	1.15	4.45	2.12			320	0.30	38.25
3.9	0.6	4.4	1.96			330	0.29	36.5
3.75	0.73	4.35	1.79			340	0.275	34.25
3.6	0.69	4.325	0.91			350	0.27	33.5
3.5	0.67	4.25	0.662			0	0.26	32.25
3.4	0.64	4.2	0.425					

TABLE 10.10

Sample: PCBAV.

Intermolecular distance (D) and layer spacing (d) in presence and absence of magnetic field.

Temp. °C.	Sample to film distance (cm.)	Outer halo			Inner halo			$\langle \cos\theta \rangle$	$d/\langle \cos\theta \rangle$
		Dia. (cm.)	Bragg angle (deg.)	D in Å	Dia.in cm(cm.)	Bragg angle (deg.)	d in Å		
69_a	6.345	4.775	10.31	4.81	-	-	-	0.89	-
79_a	6.345	4.75	10.26	4.84	-	-	-	0.889	-
80	5.801	4.11	9.819	5.05	0.655	1.612	27.35	-	30.42
85	5.801	4.12	9.775	5.09	0.66	1.628	27.15		
89_a	6.345	4.725	10.211	4.858				0.89	
90	5.801	4.07	9.665	5.13	0.67	1.653	26.74		30.04
95	5.801	4.06	9.644	5.14	0.67	1.653	26.74		
99_a	6.345	4.6	9.963	4.978				0.88	
100	5.801	4.03	9.579	5.18	0.68	1.677	26.34		29.93
110	5.801	4.05	9.613	5.15	0.70	1.736	25.59		

a - Photographs at these temperatures are taken in presence of magnetic field 5.81 K.Gauss of oriented sample.

TABLE 10.11

Sample: PCBAV.

Mean Intensity and normalised distribution function at different temperatures.

θ, β, (deg.)	I (θ) for temp. °C				f (β) for temp. °C			
	69	79	89	99	69	79	89	99
0	44	33.8	38.25	41.88	14.51	15.27	12.786	12.556
5	41.45	29.78	35.79	39.81	13.32	13.96	11.999	11.561
10	33.06	24.13	30.96	32.49	10.36	10.75	9.938	9.12
15	24.93	18.75	23.63	25.53	6.996	7.22	7.331	6.416
20	18.13	13.80	17.11	20.28	4.391	4.62	4.925	4.379
25	13.30	9.73	12.08	15.15	2.852	3.13	3.150	3.159
30	9.69	6.73	8.58	11.14	2.019	2.25	2.034	2.368
35	7.19	4.50	6.23	8.19	1.439	1.49	1.368	1.657
40	5.13	3.03	4.36	5.46	0.954	0.811	0.932	1.017
45	3.94	1.80	2.84	3.81	0.622	0.401	0.613	0.598
50	2.81	1.38	2.13	2.83	0.456	0.283	0.388	0.424
55	1.80	0.88	1.45	2.01	0.354	0.264	0.252	0.347
60	1.13	0.63	0.99	1.41	0.227	0.181	0.173	0.238
65	0.65	0.38	0.59	0.89	0.096	0.059	0.116	0.114
70	0.31	0.20	0.31	0.53	0.025	0.003	0.064	0.05
75	0.13	0.10	0.13	0.26	0.020	0.023	0.023	0.049
80	0	0.05	0.06	0.50	0.024	0.038	0.003	0.047
85	0.	0	0	0	0.004	0.008	0.001	0.015
90	0	0	0	0	-0.011	-0.016	0.003	-0.006

TABLE 10.12

Sample: PCBAV.

Order parameters at different temperatures.

Temp. °C	$\langle P_2 \rangle_V$	$\langle P_2 \rangle$	$\langle P_2 \rangle_{M.F}$	$\langle P_4 \rangle_V$	$\langle P_4 \rangle$	$\langle P_4 \rangle_{M.F}$
69	0.64	0.71	0.66	0.26	0.37	0.33
79	0.68	0.74	0.62	0.32	0.40	0.32
89	0.66	0.71	0.58	0.29	0.37	0.28
99	0.62	0.68	0.54	0.25	0.33	0.23

TABLE 10.13

Sample: PCBAV.

a_L and b_L (for L = 2 & 4) values at different temperatures.

Temp. °C.	Temp. °K	a_0	a_2	a_4	a_6	a_8	a_{10}	b_2/k	b_4/k
69	342	-1.880	4.765	-1.333	1.197	-0.096	0.018	-2312	1247
79	352	-2.028	4.718	-0.43	0.076	-0.926	0.654	-2260	375
89	362	-2.151	5.370	-2.014	2.082	-1.306	0.634	-2726	1961
99	382	-1.497	3.908	-0.596	0.601	-0.104	0.122	-2489	672

References:

1. A.J.Leadbetter and E.K. Norris, Mole. Physics, 38, 669, (1979).
2. A. J. Leadbetter and P.G. Wrighton, J. de Physiq Colloq., 40 C3-234 (1979).
3. D. Demus & L. Richter, Texture of Liquid Crystals, VEB Deutscher, Verlag Chemie (1978).
4. B. Bhattacharjee, S. Paul and R. Paul, Mol. & Physics, 44, 1391 (1981).

4a. Basana Bhattacharjee, Sukla Paul and Ranjit Paul, Mol.Cryst.Liq.Cryst. 89, 181-192 (1982).

5. Same as ref. No. 2 in chapter 7.
6. Same as ref. No. 2 in chapter 7.
7. Same as ref. No. 8 in chapter 7.
8. W.L.McMillan, Phys. Rev. A6 936, (1972).

CHAPTER 11.

X-RAY DIFFRACTION STUDIES ON THE MESOPHASES OF p-p-CYANOBENZYLIDENE p-OCTYLOXY ANILINE (CBOOA IN SHORT) IN MAGNETIC FIELD.

CHAPTER 11.

X-RAY DIFFRACTION STUDIES ON THE MESOPHASES OF n-b-CYANOBENZYLIDENE p-OCTYLOXY-ANILINE (CBOOA IN SHORT) IN MAGNETIC FIELD.

1. Introduction

The mesophases and the crystalline phases of CBOOA have been studied previously by X-ray diffraction studies[1-3] but there is no reported work on determination of orientational ordering of CBOOA on magnetic field. McMillan[4-7] has done X-ray diffraction studies on ordered CBOOA and has calculated the anisotropic liquid structure factor and inferred that the smectic - Nematic phase transition in CBOOA is of the 2nd. order. The same conclusion has been reached by many other workers using a different techniques[8-9]. However, according to Torza and Cladis[10], this transition is weakly of 1st. order.

The structural formula of CBOOA is given in chapter 2.

In the pa present work the X-ray diffraction photographs of CBOOA both in presence of magnetic field (in the set up No.3, of chapter 2) and in absence of magnetic field (in the set up No.1 of chapter 2) were taken at different temperatures.

By X-ray diffraction studies and texture analysis the transition path of CBOOA is found to

$$C \underset{\sim 46^{\circ}C}{\overset{73{\cdot}2^{\circ}C}{\rightleftharpoons}} S_A \overset{82{\cdot}8^{\circ}C}{\rightleftharpoons} N \overset{107^{\circ}C}{\rightleftharpoons} I$$

The transition temperature agree well with the literature values[11].

2. Experimental results and discussions:

As with the other compounds described in earlier chapters we have analysed the data obtained from the X-ray diffraction photograph to obtain intermolecular distance, apparent molecular length of the molecule (layer thickness in case of S_A phase), degree of ordering at different temperatures with the variation of magnetic field, the orientational distribution function $f(\beta)$ and orientational order parameter $\langle P_2 \rangle$ and $\langle P_4 \rangle$. Details of experimental procedure have been described in chapter 2. In case of CB00A the magnetic field used for the oriented sample is 4.2 kilogauss and the exposure time is 3 to 4 hours. Further details of the experimental technique and alignment of the S_A phase in presence of magnetic field have been discussed in chapters 7 and 9.

Texture studies of the compound CB00A under polarizing microscope (as described in chapter 2) indicate the phase transition at different temperatures during heating and cooling and thus the supercooled phase is observed. Typical polygonal fan shaped and occasional focal conic texture indicates the smectic phase is of A type.

Photographs of oriented nematic at 86°C and smectic phase at 60°C are shown in figure 11.1 and fig. 11.2 respectively. From the diffraction pattern of the oriented

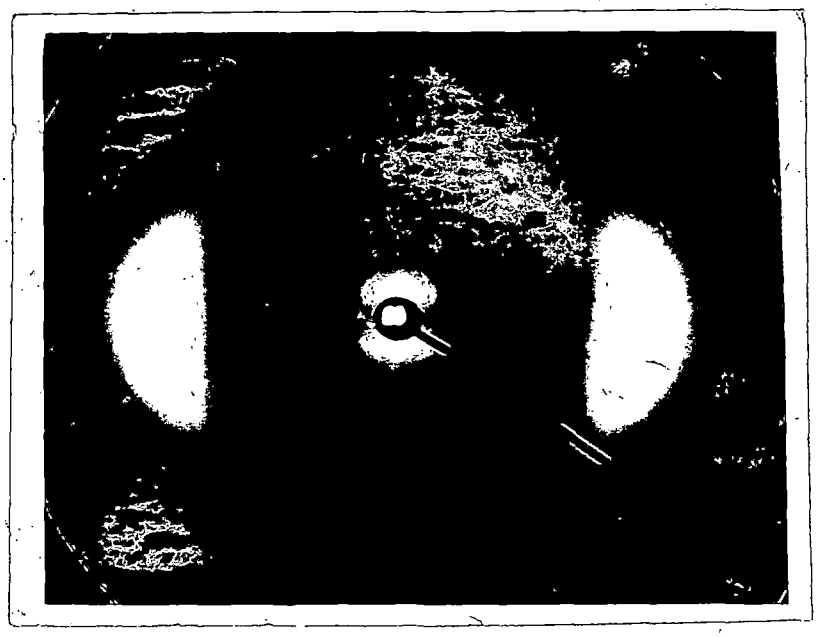

Fig.11.1. Photograph of oriented Nematic phase of CBOOA at 86°C.

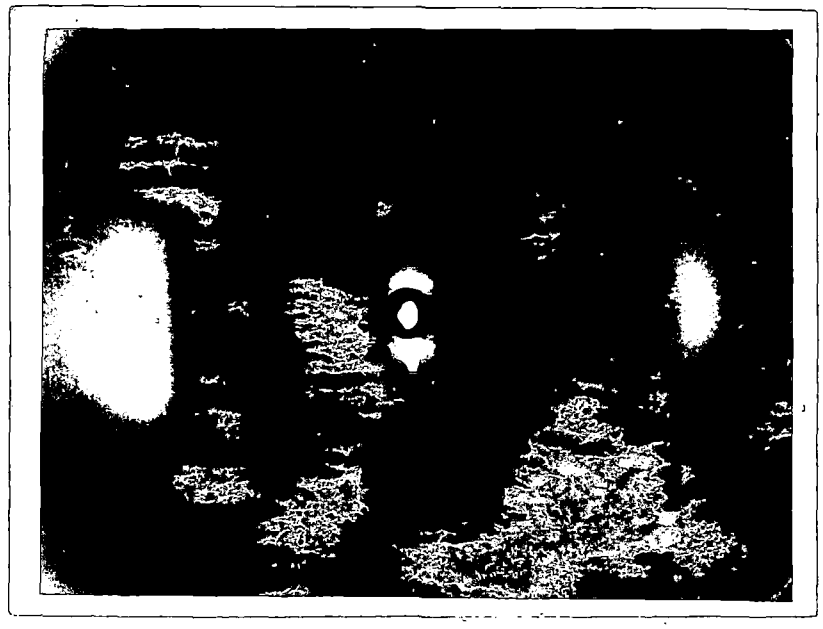

Fig. 11.2. Photograph of oriented S_A phase of CBOOA at 60°C.

phase it is obvious that the smectic phase is of A type, since the line joining the outer maxima is perpendicular to the line joining the inner maxima.

The linear scanning for all the films in absence of magnetic field are given in tables 11.1 - 11.14. The linear and angular scanning for all the films at different temperatures at magnetic field 4.2 kilogauss and for different magnetic fields only at temperature 86°C are presented in tables 11.15 - 11.28.

Intermolecular distance 'D' degree of ordering, apparent molecular length of the molecule 'ℓ', layer thickness 'd' in case of smectic.

The average intermolecular distance, apparent length of the molecule or layer thickness in case of smectics for oriented and unoriented samples are calculated by the procedure described in earlier chapters. For this a sample CBOOA, the degree of ordering are made in Vainshtein's approximation for each quadrant in each film. If the result of any quadrant showed large deviation, then this results was excluded. The mean of the value of $\langle P_2 \rangle$ for all the quadrants are taken and are plotted as function of the magnetic field in fig. 11.3. Fig. 11.4 represents the variation of intermolecular distance at three different temperatures with magnetic field. It is observed from the fig. 11.4 that 'D' decreases in low fields and reaches a constant value at about 1.2 kilogauss. The degree of ordering also reaches a satura-

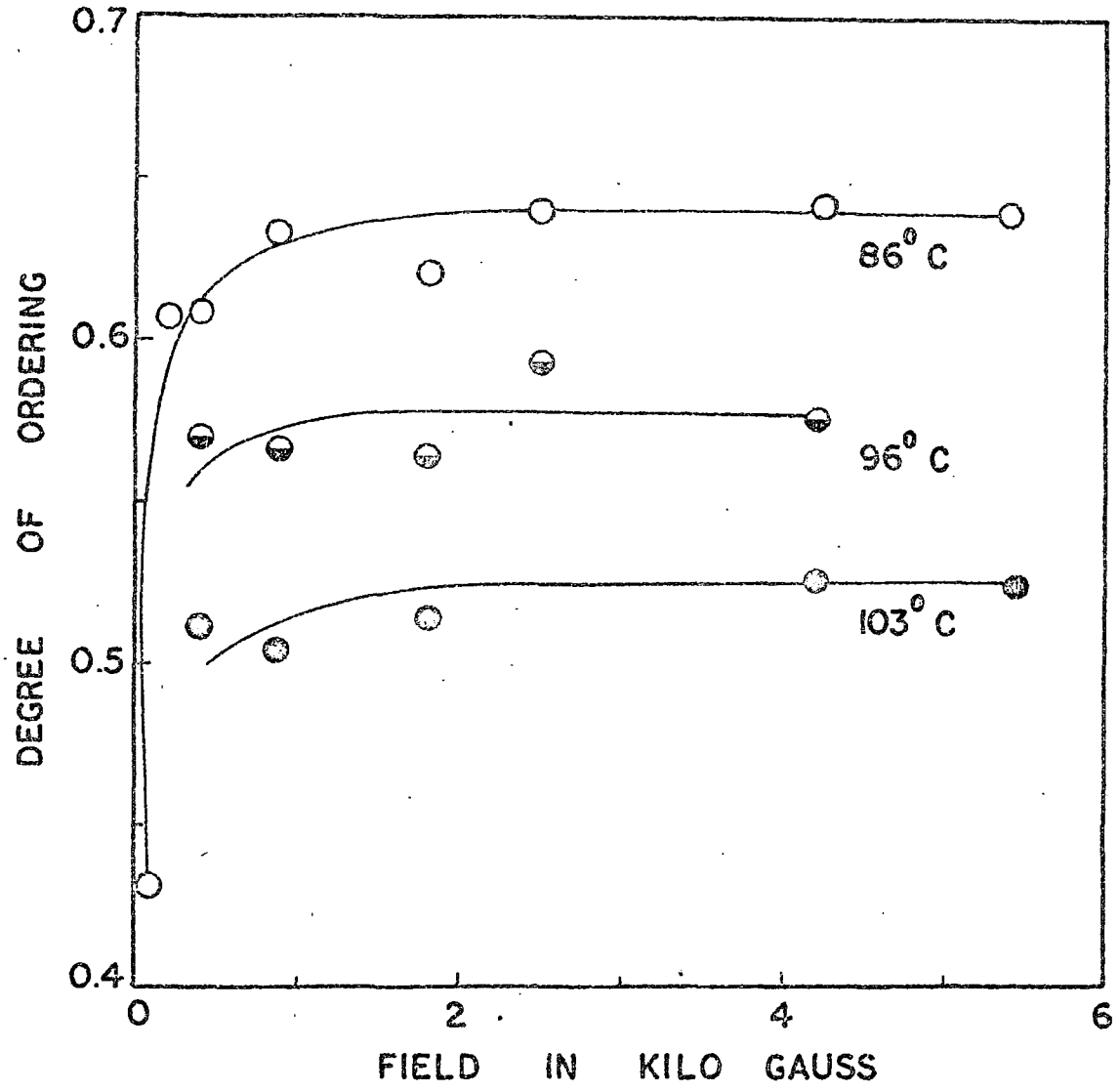
0.7
0.6
0.5
0.4
DEGREE OF ORDERING
0
2
4
6
FIELD IN KILO GAUSS
86° C
96° C
103° C

FIG. II.3.

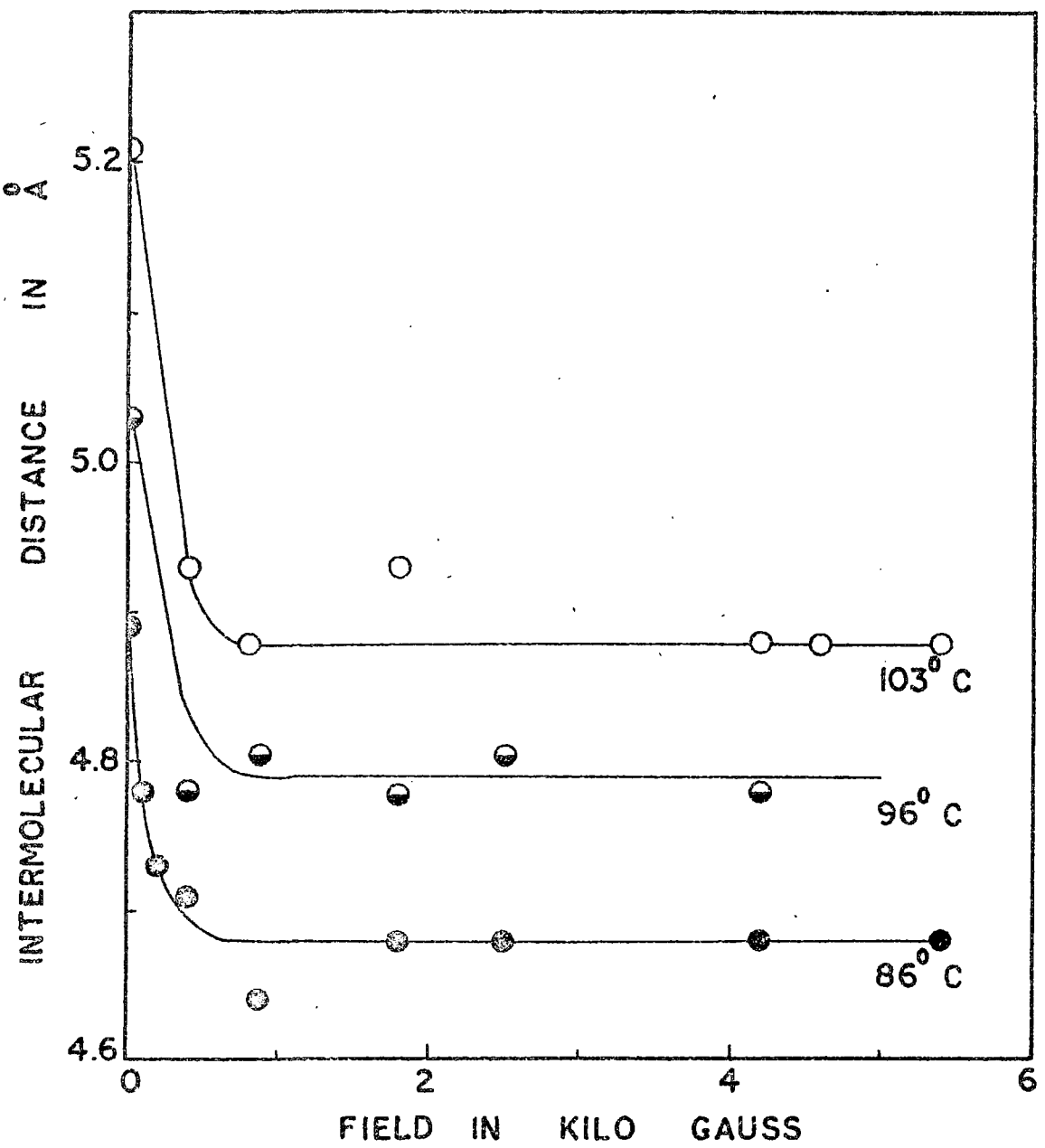
INTERMOLECULAR DISTANCE IN Å
5.2
5.0
4.8
4.6
0
2
4
6
FIELD IN KILO GAUSS
103° C
96° C
86° C

FIG. II.4.

tion value at this field. The 'D' values at zero magnetic field for particular temperature are taken from the graph 11.5 which shows the variation of 'D' with temperature in both smectic and nematic phase. There is a slight discontinuity at the smectic - nematic transition which can be observed from the fig. 11.5. It may indicate the weakly first order smectic - nematic transition in CBOOA. Because of experimental inaccuracy including the temperature control we can not confirm this statement. The table 11.29 includes the data for intermolecular distance and degree of ordering at different magnetic field strength.

The intermolecular distance 'D', layer spacings (d) in smectic phase and the apparent length of the molecule 'ℓ' in nematic phase in absence of magnetic field are given in table 11.30.

'd' and 'ℓ' values are plotted against temperature in figure 11.6.

The layers spacings 'd', within our experimental uncertainity, increases with temperature slightly, which can be taken as constant. The mean value of d is 34 $\pm$ 1.5 Å. The length 'L' of the CBOOA molecule is 25 Å. As discussed in chapter 9 we have tried to take into account the orientational disorder σ in the calculation of layer thickness in S_A phase. The values of d, $\langle\cos\theta\rangle$, $d/\langle\cos\theta\rangle$ ($\langle\cos\theta\rangle$ is calculated by the process described in chapter 9) at different temperatures are given in table 11.30. The mean

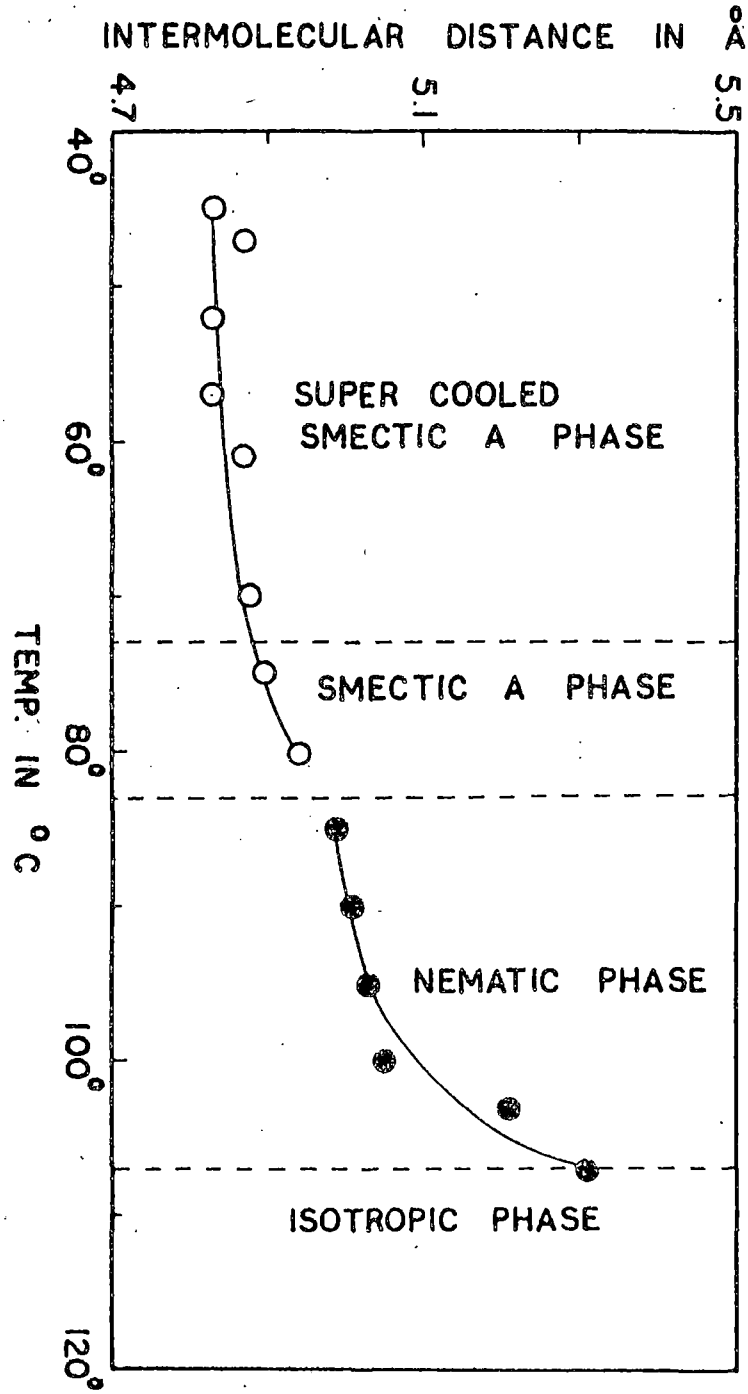
INTERMOLECULAR DISTANCE IN Å
4.7
5.1
5.5
40°
60°
80°
100°
120°
TEMP. IN °C
SUPER COOLED
SMECTIC A PHASE
SMECTIC A PHASE
NEMATIC PHASE
ISOTROPIC PHASE

Fig 11·5

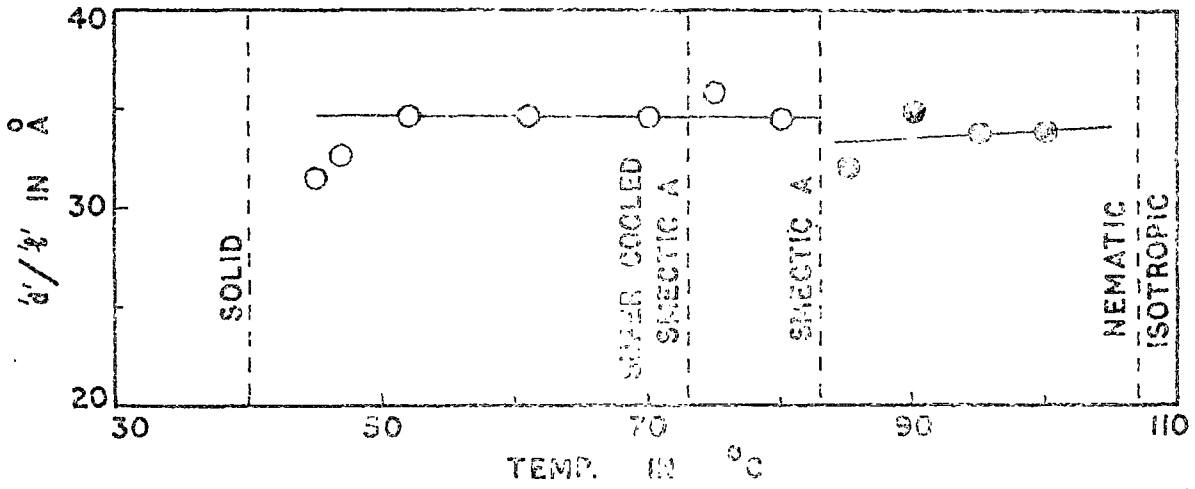
40
30
20
d'/2' IN Å
SOLID
SUPER COOLED SMECTIC A
SMECTIC A
NEMATIC
ISOTROPIC
30
50
70
90
110
TEMP. IN °C

FIG.II.6.

value of $d/\langle \cos\theta \rangle$ is 39.4 ± 0.6 Å. The ratio of the d and L valuesand $d/\langle \cos\theta \rangle$ and L valuesare 1.36 and 1.58 respectively. Evidently, the molecules of CBOOA form dimers with partial overlap of their rigid parts and the ratio of the dimer length to monmer length is 1.6 instead of 1.4. The similar case is observed in case of 8m SOCB (described in chapter 9) which is another cyano compound. The layer thickness in the smectic phase (before correction) and the apparent molecular length in the nematic phase both correspond to about 1.4 times the length of the molecule in accordance with some k earlier works on other cyano compounds and CBOOA[12-16]. Bilayer packing of molecules in the smectic phase have been considered to account for this layer thickness. Gladis et al[17] have proposed a model of partial bilayer with an overlapping of the aromatic systems for several cyanocompounds. As suggested by others[1] a bilayer structure must be formed in the smectic phase of CBOOA. Vani and Vijayan[3] have described the crystal structure of CBOOA. In the crystalline structure described by them, cyano groups of the neighbouring molecules are at a distance less than the sum of the w Vander Waal's radii. The CBOOA molecules associates in pairs about the centres of invertion and hence adjacent molecules in the unit cell are antiparallel to each other. The structure can therefore, be described as consisting of layers. The layer like stacking, k of the molecules in the solid phase probably explains

the smectogenic nature of the compound.

In the nematic phase the mean value of l is found to be 34.3 ± 1 Å, which is almost independent of temperature. The reason for the difference between the measured and apparent length of the CBOOA in the nematic phase is same for other cyano compounds such as 5OOB, 8OOB (chapter 5 and 9).

Distribution function, order parameters and pseudopotential.

As before $\theta - I(\theta)$ (i.e. the mean intensity value from the four quadrants at different θ from 0°-90°) values for the oriented samples at different temperatures are given in table 11.31 and the variation of normalized orientational distribution function $f(\beta)$ with β as obtained from $I(\theta)$ for different temperatures are shown in table 11.32. It has been found from the analysis of variation of $f(\beta)$ with β for different temperatures that the distribution function spreads out a higher temperatures, which is in accordance with other findings[16], as described in chapter 7, 8, 9 etc. $\langle P_L \rangle$ values are calculated using distribution functions as described in chapter 3. The temperature dependence of the order parameters $\langle P_2 \rangle$ and $\langle P_4 \rangle$ are shown in fig. 11.7 with Maier-Saupe mean field predictions. (T_{NI} is the nematic isotropic transition temperature). It is seen from the fig. that both $\langle P_2 \rangle$ and $\langle P_4 \rangle$ values

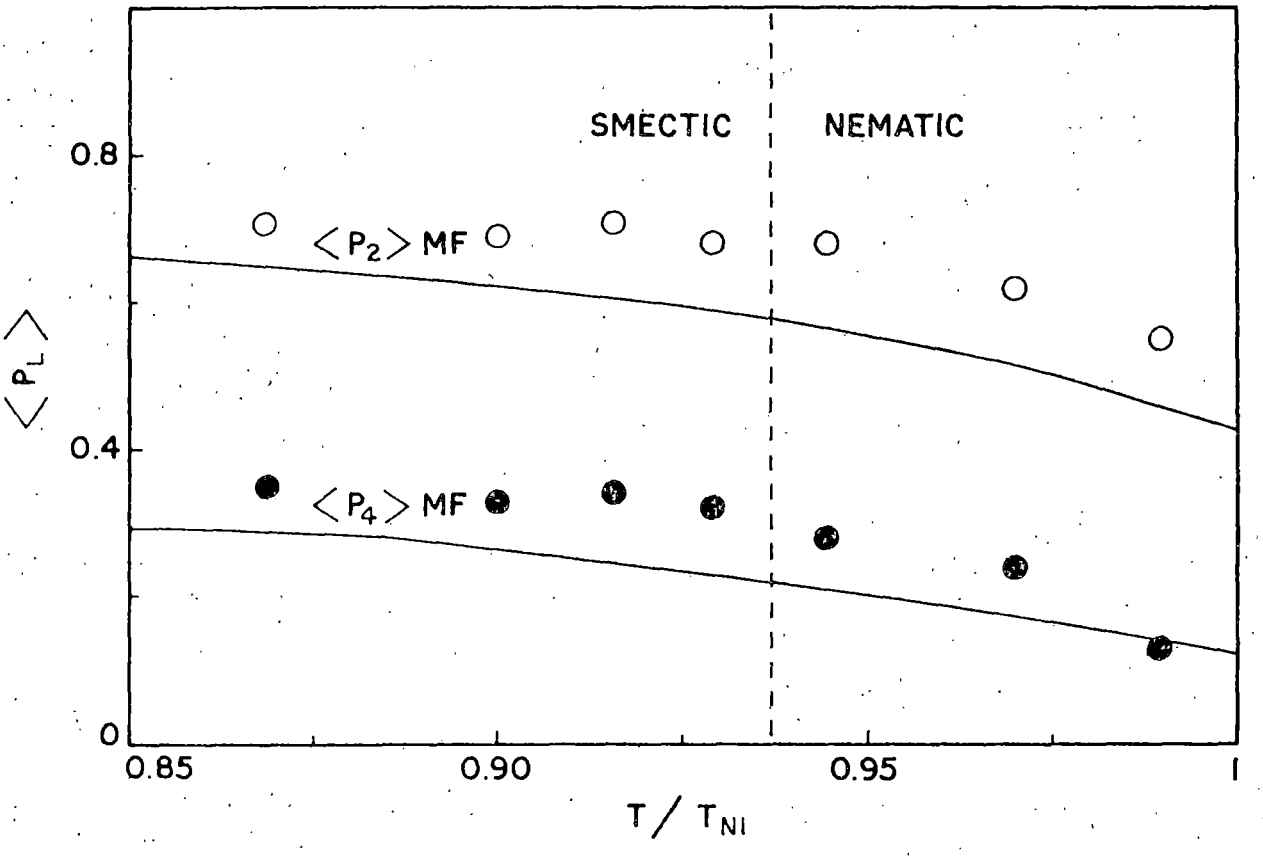

Fig II·7 Solid lines - $\langle P_2 \rangle$ M.F. & $\langle P_4 \rangle$ M.F.

Open circle -$\langle P_2 \rangle$ & Filled circle -$\langle P_4 \rangle$

are higher then those predicted by mean field theories. In our earlier work on PCBAV (chapter 10) we have found such descripancies in $\langle P_2 \rangle$ and $\langle P_4 \rangle$ values.

The higher values in ordering may be due to strong short range dipolar attractions because of the strong cyano-group along the long axis of the molecule.

$\langle P_2 \rangle$ and $\langle P_4 \rangle$ values determined are given in table 11.33 along with the a_L, b_L/k (for L = 2 & 4) values for smectic A and nematic phases. b_L values are calculated from a_L values as described in earlier chapters.

From the data for the four temperatures of the smectic phase and that from the table 11.33 the mean of the coefficients b_2/k and b_4/k and the standard deviations of the coefficients have been written in table 11.34 and similarly for three temperatures in the nematic range the coefficients b_2/k and b_4/k with their standard deviations are given in the same table.

The anisotropic part of the pseudopotential in the smectic and the nematic phase are given by

$$V(\beta)/k = -(2900 \pm 30)\langle P_2 \rangle P_2(\cos\beta) + (2600 \pm 300)\langle P_4 \rangle P_4(\cos\beta)$$

and

$$V(\beta)/k = -(2840 \pm 360)\langle P_2 \rangle P_2(\cos\beta) + (3800 \pm 1000)\langle P_4 \rangle P_4(\cos\beta)$$

respectively.

The normalized $f(\beta)$ values calculated with truncated potentials at 86°0 are shown in fig. 11.8. The nature of the curves are similar to those found in other compounds as described in earlier chapters. $f(\beta)$ values are also calculated from the potential neglecting the $P_4(\cos\beta)$ values and the values are plotted in the same fig. In conclusion the orientational distribution function obtained from the X-ray diffraction data do not agree well with the distribution function generated from the commonly accepted molecular field potential even after the inclusion of $P_4(\cos\beta)$ term. The possible causes for the discrepencies have been discussed in chapter 7.

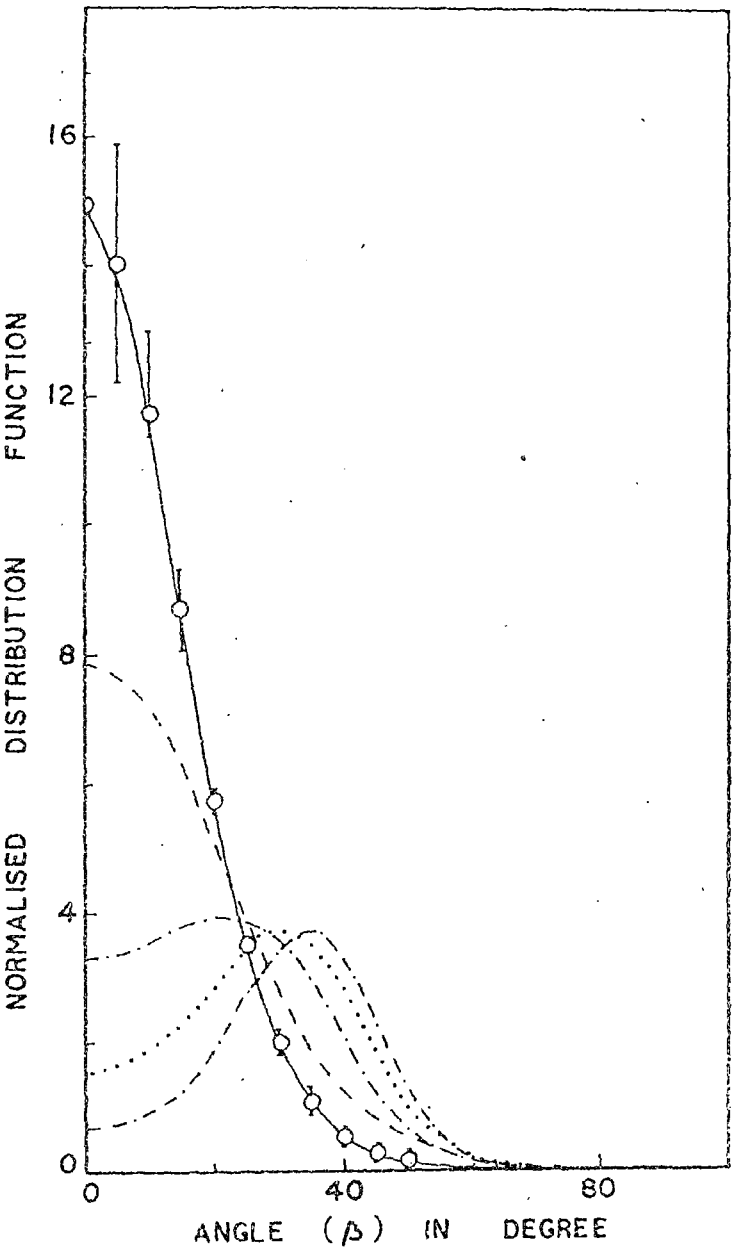

Fig II.8. Variation of normalised orientational distribution function $f(\beta)$ with angle β at temperature 86°C for CBOOA.

- – – – – – Experimental data.
- ——————— Calculated value with pseudopotential $-(2840 \pm 360)\ \langle P_2 \rangle\ P_2(\cos\beta)$.
- . . . . . Calculated value with pseudopotential $-(2840)\ \langle P_2 \rangle\ P_2(\cos\beta) + 3800\ \langle P_4 \rangle\ P_4(\cos\beta)$
- – . – . – . – Calculated value with pseudopotential $-2840\ \langle P_2 \rangle\ P_2(\cos\beta) + (3800 + 1000)\ \langle P_4 \rangle\ P_4(\cos\beta)$
- — . — . — . — Calculated value with pseudopotential $-2840\ \langle P_2 \rangle\ P_2(\cos\beta) + (3800 - 1000)\ \langle P_4 \rangle\ P_4(\cos\beta)$

Table - 11.1

Sample: CBOOA. Mag.Field Nil
Tempt.-45°C, Sample to
Film Distance 5.81 cm.

L in cm.	O. D.	L in cm.	O. D.
		2.8	0.53
	OUTER HALO	2.55	0.532
7.0	0.44	2.5	0.55
6.9	0.475	2.4	0.592
6.8	0.51	2.3	0.61
6.6	0.58	2.2	0.67
6.5	0.53	2.15	0.72
6.4	0.66	2.05	0.735
6.3	0.67	2.0	0.78
6.25	0.66	1.95	0.785
6.2	0.645	1.9	0.78
6.0	0.575	1.8	0.775
5.9	0.54	1.75	0.715
5.7	0.508	1.7	0.7
5.5	0.50	1.6	0.63
5.4	0.498	1.5	0.56
5.35	0.50	1.3	0.50
5.25	0.51	1.2	0.46
5.1	0.52		
4.9	0.54	INNER RING	
4.7	0.58		
4.6	0.615	4.6	0.625
4.475	0.64	4.5	0.66
4.45	0.665	4.45	0.78
4.4	0.66	4.4	0.82
4.3	0.415	4.375	0.835
4.25	0.43	4.35	0.84
4.2	1.145	4.325	0.845
4.15	1.52	4.3	0.41
4.1	1.95	4.25	0.405
4.05	1.50	4.2	0.865
4.0	1.41	4.125	1.63
3.95	0.42	4.1	1.985
3.85	0.365	4.075	1.99
3.75	0.472	4.05	1.86
3.62	0.632	4.0	1.7
3.6	0.63	3.9	0.47
3.55	0.61	3.85	0.415
3.5	0.598	3.8	1.0
3.4	0.57	3.755	1.30
3.2	0.555	3.725	1.29
3.0	0.54	3.7	0.82
		3.5	0.585

Table - 11.2

Sample: CBOOA. Mag.Field Nil
Temp. - 47°C, Sample to Film
Distance = 6.81 cm.

L in cm.	O. D.	L in cm.	O. D.
		2.8	0.625
	OUTER HALO	2.7	0.62
7.0	0.64	2.6	0.62
6.9	0.65	2.5	0.615
6.8	0.68	2.4	0.62
6.725	0.71	2.3	0.623
6.65	0.715	2.25	0.632
6.55	0.71	2.2	0.64
6.5	0.70	2.15	0.65
6.4	0.685	2.1	0.652
6.3	0.665	2.05	0.655
6.2	0.65	2.0	0.675
6.1	0.63	1.95	0.68
6.0	0.62	1.9	0.705
5.8	0.61	1.85	0.715
5.5	0.615	1.8	0.735
5.4	0.62	1.75	0.745
5.3	0.62	1.7	0.75
5.2	0.63	1.6	0.765
5.0	0.635	1.55	0.76
4.9	0.645	1.5	0.75
4.6	0.70	1.4	0.71
4.5	0.74	1.2	0.64
4.35	0.89		
4.3	0.835	INNER HALO	
4.2	0.665		
4.15	0.495	4.55	0.655
4.1	0.53	4.45	0.72
4.05	0.61	4.40	0.795
4.025	0.80	4.375	0.828
4.0	0.615	4.35	0.785
3.95	0.515	4.3	0.425
3.9	0.46	4.25	0.415
3.8	0.50	4.10	1.25
3.75	0.92	4.05	1.85
3.7	0.935	4.0	1.81
3.65	0.775	3.9	0.53
3.6	0.75	3.8	0.95
3.4	0.675	3.75	1.17
3.2	0.64	3.73	1.22
3.1	0.64	3.70	0.82
3.0	0.63	3.60	0.71
		3.50	0.61

Table 11.3

Sample: CB00A. Mag. Field nil
Temp. 52°C, Sample to
Film distance 6.81 cm.

L in cm.	O. D.	L in cm.	O. D.
OUTER HALO		3.35	0.655
		3.2	0.635
7.0	0.665	2.9	0.63
6.9	0.715	2.8	0.62
6.8	0.76	2.75	0.62
6.7	0.79	2.7	0.62
6.65	0.80	2.6	0.622
6.625	0.805	2.5	0.62
6.6	0.80	2.4	0.625
6.5	0.79	2.3	0.635
6.4	0.75	2.2	0.65
6.3	0.71	2.0	0.722
6.2	0.69	1.9	0.772
6.1	0.65	1.825	0.795
5.9	0.62	1.7	0.86
5.8	0.605	1.6	0.91
5.7	0.60	1.5	0.93
5.6	0.59	1.525	0.95
5.55	0.61	1.45	0.925
5.45	0.615	1.4	0.895
5.2	0.63	1.3	0.812
5.1	0.635	1.2	0.71
5.0	0.64	INNER HALO	
4.85	0.65	4.6	0.72
4.75	0.67	4.5	0.76
4.65	0.68	4.4	1.06
4.475	0.73	4.35	1.1
4.4	0.72	4.33	1.19
4.35	0.70	4.25	0.695
4.3	0.45	4.2	0.485
4.2	0.44	4.1	0.665
4.1	0.612	4.05	1.0
4.05	0.9	4.0	0.72
4.0	0.638	3.95	0.45
3.95	0.51	3.9	0.46
3.9	0.612	3.85	0.79
3.8	0.81	3.8	1.04
3.75	0.81	3.75	1.125
3.70	0.75	3.725	1.4
3.6	0.73	3.7	0.85
3.5	0.688	3.6	0.76
		3.5	0.70

Table - 11.4

Sample: CB00A. Mag.Field nil
Temp. 57°C, Sample to
Film distance 5.81 cm.

L in cm.	O. D.	L in cm.	O. D.
OUTER HALO		3.2	0.562
		3.05	0.55
7.0	0.435	2.9	0.535
6.8	0.498	2.8	0.53
6.6	0.57	2.7	0.53
6.4	0.68	2.6	0.54
6.3	0.69	2.5	0.56
6.25	0.68	2.3	0.61
6.2	0.675	2.15	0.72
6.15	0.645	2.05	0.74
6.0	0.598	2.0	0.77
5.9	0.56	1.95	0.775
5.7	0.522	1.9	0.772
5.6	0.508	1.85	0.755
5.55	0.508	1.8	0.715
5.45	0.508	1.6	0.60
5.4	0.51	1.5	0.55
5.3	0.512	1.25	0.46
5.2	0.52	INNER HALO	
5.0	0.54		
4.9	0.55		
4.7	0.595		
4.5	0.648		
4.4	0.69		
4.35	0.68		
4.3	0.46		
4.25	0.5		
4.2	0.65		
4.15	1.605		
4.075	1.97		
4.05	1.77		
4.0	1.54		
3.95	0.515		
3.9	0.41		
3.85	0.395		
3.8	0.425		
3.75	0.49		
3.7	0.65		
3.65	0.65		
3.6	0.645		
3.5	0.61		
3.35	0.575		

Table - 11.5

Sample: CBCOA. Mag.Field Nil
Temp. 61°C, Sample to
Film distance 6.81 cm.

L in cm.	O. D.	L in cm.	O. D.
		3.4	0.662
OUTER HALO		3.2	0.62
		3.0	0.61
7.0	0.68	2.9	0.605
6.9	0.735	2.65	0.60
6.7	0.80	2.5	0.59
6.65	0.815	2.4	0.59
6.6	0.81	2.3	0.59
6.5	0.80	2.15	0.59
6.4	0.775	2.05	0.60
6.3	0.752	2.0	0.605
6.2	0.715	1.9	0.61
6.0	0.65	1.65	0.632
5.9	0.635	1.60	0.645
5.8	0.625	1.5	0.638
5.5	0.615	1.3	0.61
5.4	0.62	1.2	0.59
5.2	0.63		
5.1	0.635	INNER HALO	
5.0	0.635		
4.85	0.64	4.6	0.69
4.8	0.653	4.5	0.725
4.7	0.67	4.45	0.802
4.6	0.69	4.40	0.89
4.5	0.72	4.35	0.96
4.45	0.77	4.325	1.33
4.4	0.82	4.30	0.80
4.35	1.12	4.20	0.49
4.275	0.88	4.10	0.46
4.2	0.45	4.05	1.12
4.1	0.48	4.0	1.20
4.05	0.99	3.95	1.135
4.025	1.02	3.9	0.55
4.0	1.01	3.85	0.59
3.9	0.50	3.8	0.905
3.85	0.70	3.75	1.06
3.775	0.79	3.72	1.38
3.725	1.03	3.675	1.19
3.7	0.97	3.65	0.96
3.6	0.785	3.6	0.87
3.5	0.7	3.5	0.71

Table 11.6

Sample: CBCOA. Mag.Field Nil
Temp. 70°C, Sample to
Film distance 5.81 cm.

L in cm.	O. D.	L in cm.	O. D.
		3.4	0.715
OUTER HALO		3.3	0.71
		3.2	0.69
7.15	0.592	3.1	0.68
7.0	0.612	3.0	0.675
6.9	0.622	2.9	0.67
6.8	0.64	2.8	0.66
6.7	0.68	2.6	0.66
6.6	0.692	2.4	0.662
6.5	0.725	2.35	0.67
6.4	0.75	2.2	0.68
6.3	0.79	2.1	0.69
6.25	0.795	2.0	0.695
6.2	0.80	1.95	0.698
6.15	0.798	1.90	0.70
6.1	0.792	1.85	0.692
6.0	0.77	1.8	0.69
5.9	0.735	1.7	0.68
5.8	0.705	1.6	0.655
5.7	0.68	1.5	0.645
5.6	0.67	1.15	0.615
5.5	0.665		
5.4	0.675	INNER HALO	
5.3	0.698		
5.2	0.69	4.7	0.7
5.15	0.665	4.6	0.71
5.1	0.668	4.5	0.748
5.05	0.67	4.4	0.83
4.9	0.678	4.3	1.085
4.8	0.682	4.25	0.98
4.7	0.70	4.2	0.855
4.6	0.715	4.1	0.61
4.5	0.74	4.05	-
4.4	0.80	3.95	0.89
4.3	0.79	3.9	0.60
4.05	-	3.85	0.61
3.85	0.62	3.8	0.66
3.8	0.975	3.78	1.115
3.75	0.95	3.75	1.1
3.7	0.9	3.7	1.085
3.55	0.755	3.6	0.795
		3.4	0.73

Table 11.7

Sample: CBOOA. Mag.Field Nil
Temp. 75°C, Sample to film distance 5.81 cm.

L in cm.	O. D.	L in cm.	O. D.
		3.5	0.59
OUTER HALO		3.35	0.58
		3.2	0.58
6.8	0.55	3.1	0.58
6.7	0.575	3.05	0.575
6.6	0.615	3.0	0.57
6.5	0.66	2.95	0.57
6.4	0.74	2.9	0.56
6.3	0.8	2.7	0.56
6.2	0.815	2.6	0.56
6.15	0.81	2.5	0.55
6.1	0.8	2.45	0.57
6.05	0.79	2.3	0.59
6.0	0.75	2.2	0.62
5.9	0.715	2.0	0.68
5.85	0.665	1.95	0.69
5.7	0.62	1.925	0.695
5.6	0.60	1.9	0.685
5.5	0.59	1.8	0.66
5.3	0.58	1.5	0.56
5.1	0.58	1.3	0.50
4.9	0.58	1.2	0.49
4.65	0.585		
4.6	0.59	INNER HALO	
4.55	0.60	4.5	0.61
4.5	0.60	4.4	0.64
4.45	0.60	4.35	0.65
4.4	0.595	4.325	0.70
4.35	0.58	4.3	0.78
4.3	0.44	4.25	0.66
4.2	0.4	4.2	0.42
4.1	0.46	4.1	0.41
4.05	0.63	4.05	0.60
4.0	0.56	4.0	0.70
3.95	0.44	3.95	0.69
3.9	0.5	3.9	0.42
3.85	0.55	3.85	0.43
3.8	0.63	3.8	0.735
3.75	0.635	3.7	0.725
3.7	0.62	3.65	0.66
3.65	0.61	3.6	0.65
3.6	0.605	3.5	0.61
		3.3	0.57

Table 11.8.

Sample: CBOOA. Mag.Field Nil
Temp. 80°C, Sample to film distance 5.81 cm.

L in cm.	O. D.	L in cm.	O. D.
		3.3	0.75
OUTER HALO		3.2	0.75
		3.1	0.745
7.0	0.59	3.0	0.74
6.9	0.615	2.9	0.73
6.8	0.64	2.8	0.73
6.7	0.67	2.7	0.73
6.6	0.705	2.6	0.74
6.5	0.75	2.5	0.748
6.4	0.805	2.4	0.772
6.3	0.85	2.3	0.78
6.2	0.91	2.25	0.815
6.1	0.92	2.2	0.825
6.05	0.91	2.15	0.855
6.0	0.885	2.1	0.87
5.9	0.86	2.05	0.90
5.8	0.82	1.95	0.912
5.7	0.772	1.9	0.912
5.6	0.75	1.85	0.912
5.5	0.735	1.8	0.90
5.4	0.725	1.7	0.88
5.3	0.725	1.6	0.85
5.2	0.75	1.55	0.77
5.1	0.74	1.3	0.69
5.0	0.74	1.2	0.665
4.9	0.745		
4.8	0.75		
4.7	0.76		
4.6	0.765		
4.5	0.772		
4.4	0.785		
4.3	0.68		
4.2	0.54		
4.1	0.58		
4.0	0.938		
3.95	0.888		
3.9	0.58		
3.8	0.82		
3.7	0.83		
3.6	0.81		
3.5	0.78		
3.4	0.76		

Table 11.9

Sample: CBCOA, Mag.Field Nil Tempt. 85°C, Sample to Film distance 6.81 cm.

L in cm.	O. D.	L in cm.	O. D.
		4.20	0.51
OUTER HALO		4.15	0.63
		4.10	0.73
6.95X	0.635	4.05	0.95
6.9	0.66	4.0	0.76
6.8	0.675	3.95	0.61
6.7	0.698	3.9	0.76
6.6	0.70	3.85	0.85
6.55	0.695	3.8	1.46
6.5	0.69	3.75	1.47
6.4	0.67	3.7	0.92
6.3	0.65	3.6	0.83
6.2	0.63	3.5	0.73
6.1	0.62	3.4	0.70
6.0	0.61	3.35	0.66
5.9	0.60	3.25	0.63
5.8	0.598	3.2	0.61
5.75	0.60	3.1	0.61
5.7	0.602	3.0	0.61
5.6	0.605	2.95	0.60
5.5	0.608	2.9	0.595
5.45	0.602	2.85	0.595
5.35	0.60	2.8	0.59
5.3	0.60	2.7	0.588
5.25	0.602	2.6	0.58
5.2	0.61	2.5	0.58
5.1	0.615	2.4	0.578
5.0	0.62	2.3	0.575
4.95	0.635	2.2	0.57
4.9	0.64	2.05	0.572
4.85	0.645	1.85	0.58
4.8	0.665	1.7	0.582
4.75	0.69	1.675	0.585
4.7	0.72	1.65	0.58
4.6	0.74	1.5	0.56
4.55	0.81	1.3	0.54
4.5	0.84	1.2	0.52
4.45	1.20		
4.4	1.32		
4.35	1.465		
4.325	1.365		
4.30	0.69		

Table 11.10

Sample: CBCOA, Mag.Field Nil, Tempt. 90°C, Sample to Film distance 6.81 cm.

L in cm.	O.D.	L in cm.	O.D.
		2.3	0.585
OUTER HALO		2.15	0.60
		2.0	0.64
7.1	0.65	1.9	0.67
7.0	0.685	1.8	0.68
6.9	0.728	1.7	0.70
6.8	0.75	1.65	0.695
6.725	0.775	1.5	0.665
6.70	0.78	1.3	0.57
6.60	0.785	1.2	0.555
6.55	0.778		
6.45	0.77		
6.4	0.745		
6.3	0.722		
6.2	0.688		
6.0	0.632		
5.9	0.615		
5.7	0.60		
5.55	0.605		
5.35	0.61		
5.1	0.612		
5.0	0.615		
4.65	0.66		
4.45	0.74		
4.325	0.772		
4.3	0.74		
4.2	0.54		
4.1	0.772		
3.95	0.43		
3.85	0.42		
3.8	0.61		
3.7	0.685		
3.65	0.71		
3.6	0.70		
3.45	0.66		
3.35	0.64		
3.2	0.615		
3.0	0.61		
2.9	0.6		
2.65	0.585		
2.5	0.58		
2.4	0.58		

Table 11.11

Sample: CBOOA. Mag. Field Nil
Temp. 95°C, Sample to
Film distance 6.81 cm.

L in cm.	O. D.	L in cm.	O. D.
		3.4	0.67
OUTER HALO		3.3	0.662
7.0	0.64	3.0	0.632
6.8	0.7	2.9	0.635
6.7	0.742	2.8	0.63
6.6	0.775	2.65	0.62
6.55	0.78	2.45	0.62
6.5	0.785	2.3	0.622
6.475	0.79	2.2	0.63
6.45	0.785	2.0	0.66
6.4	0.77	1.9	0.675
6.3	0.75	1.85	0.69
6.1	0.70	1.75	0.695
6.0	0.68	1.70	0.70
5.9	0.66	1.65	0.702
5.8	0.64	1.55	0.70
5.7	0.635	1.50	0.69
5.6	0.635	1.3	0.645
5.5	0.635	1.2	0.63
5.3	0.64	INNER HALO	
5.2	0.64		
5.1	0.645	4.5	0.76
4.9	0.64	4.45	0.778
4.85	0.65	4.4	0.86
4.75	0.66	4.37	0.88
4.7	0.66	4.3	0.82
4.6	0.672	4.25	0.50
4.5	0.70	4.2	0.49
4.4	0.71	4.15	0.58
4.35	0.70	4.1	0.85
4.3	0.665	4.05	1.09
4.2	0.51	4.025	2.0
4.1	0.545	4.0	0.72
4.05	0.712	3.95	0.58
4.025	1.3	3.9	0.6
4.0	0.93	3.85	0.665
3.9	0.72	3.8	0.85
3.8	0.61	3.75	0.88
3.7	0.72	3.7	0.86
3.6	0.72	3.6	0.74
3.55	0.705	3.5	0.69
3.5	0.69		

Table 11.12

Sample: CBOOA. Mag. Field Nil
Temp. 100°C, Sample to
Film distance 6.81 cm.

L in cm.	O. D.	L in cm.	O. D.
		2.35	0.61
OUTER HALO		2.2	0.61
7.0	0.655	2.15	0.615
6.85	0.685	2.1	0.62
6.7	0.71	2.05	0.622
6.65	0.715	1.95	0.645
6.60	0.718	1.8	0.65
6.55	0.715	1.6	0.655
6.45	0.71	1.45	0.635
6.4	0.70	1.30	0.615
6.25	0.68	INNER HALO	
6.1	0.658		
6.0	0.64	4.5	0.715
5.85	0.625	4.45	0.765
5.5	0.61	4.4	0.768
5.45	0.612	4.375	0.765
5.3	0.62	4.37	0.78
5.15	0.62	4.30	0.675
4.95	0.625	4.20	0.532
4.9	0.63	4.15	0.61
4.7	0.645	4.05	1.14
4.55	0.66	4.0	0.835
4.4	0.71	3.95	0.515
4.275	0.705	3.9	0.512
4.15	0.63	3.8	0.75
4.1	0.56	3.75	0.775
4.05	0.65	3.725	0.75
4.0	0.655	3.7	0.74
3.9	0.55	3.6	0.715
3.85	0.56	3.5	0.67
3.8	0.61		
3.7	0.715		
3.65	0.72		
3.6	0.70		
3.55	0.69		
3.45	0.68		
3.3	0.65		
3.05	0.63		
3.0	0.625		
2.9	0.618		
2.8	0.615		
2.65	0.61		

Table 11.13

Sample: CBCOA. Mag.Field Nil
Temp. 103°C, Sample to
Film distance 6.81 cm.

L in cm.	O. D.	L in cm.	O. D.
		2.65	0.612
OUTER HALO		2.5	0.61
7.0	0.655	2.4	0.605
6.8	0.69	2.3	0.612
6.7	0.70	2.15	0.62
6.6	0.715	2.0	0.63
6.55	0.712	1.95	0.632
6.5	0.71	1.9	0.63
6.2	0.67	1.8	0.625
6.0	0.64	1.6	0.612
5.8	0.62	1.3	0.565
5.5	0.62	1.2	0.56
5.4	0.62		
5.25	0.625		
5.1	0.63		
5.0	0.64		
4.8	0.675		
4.7	0.70		
4.6	0.72		
4.5	0.76		
4.45	0.772		
4.4	0.782		
4.35	0.77		
4.3	0.64		
4.25	0.54		
4.2	0.62		
4.15	0.89		
4.10	1.09		
4.05	1.14		
4.0	0.63		
3.9	0.525		
3.8	0.705		
3.7	0.78		
3.675	0.765		
3.65	0.75		
3.6	0.74		
3.5	0.70		
3.15	0.64		
3.0	0.63		
2.8	0.625		
2.7	0.61		

Table 11.14

Sample: CBCOA. Mag.Field Nil
Temp. 107°C, Sample to
Film distance 6.81 cm.

L in cm.	O. D.	L in cm.	O. D.
		3.5	0.74
OUTER HALO		3.3	0.67
		3.2	0.655
7.0	0.66	3.0	0.64
6.9	0.685	2.9	0.635
6.7	0.72	2.65	0.62
6.6	0.73	2.55	0.618
6.5	0.745	2.4	0.618
6.4	0.75	2.3	0.618
6.35	0.758	2.25	0.618
6.3	0.748	2.2	0.62
6.25	0.74	2.05	0.625
6.2	0.73	2.0	0.63
6.15	0.72	1.9	0.63
6.0	0.70	1.85	0.63
5.9	0.675	1.8	0.63
5.7	0.65	1.75	0.635
5.5	0.64	1.6	0.625
5.35	0.64	1.5	0.62
5.3	0.642	1.4	0.61
5.1	0.65	1.2	0.59
4.9	0.66	1.1	0.57
4.8	0.67		
4.6	0.72		
4.5	0.745		
4.4	0.76		
4.3	0.76		
4.25	0.685		
4.2	0.52		
4.15	0.53		
4.05	-		
4.0	0.79		
3.95	0.645		
3.9	0.55		
3.85	0.655		
3.8	0.68		
3.75	0.73		
3.7	0.788		
3.675	0.79		
3.65	0.788		
3.6	0.75		
3.55	0.74		

TABLE 11.15

Sample: COCOA. Mag. Field = 4.2 K.Gauss, Temp. = 60°C.
Background Optical Density 0.36.

LINEAR SCANNING				ANGULAR SCANNING		
L in cm.	O. D.	L in cm.	O. D.	θ in (deg.)	O. D.	Intensity.
7.15	0.56	1.6	0.84	355	0.09	1.2
7.1	0.58	1.5	0.78	0	0.09	1.2
7.0	0.60	1.4	0.71	15	0.09	1.2
6.8	0.72	1.3	0.69	20	0.10	1.4
6.7	0.78	1.2	0.635	37	0.10	1.4
6.6	0.81			50	0.15	1.95
6.55	0.825			60	0.215	2.78
6.5	0.820			70	0.305	4.0
6.45	0.815			75	0.38	5.1
6.3	0.73			80	0.45	6.5
6.1	0.64			85	0.49	7.3
5.9	0.565			90	0.52	8.1
5.8	0.55			92.5	0.53	8.35
5.7	0.545			95	0.52	8.1
5.6	0.54			100	0.49	7.3
5.5	0.55			105	0.44	6.35
5.4	0.55			110	0.38	5.1
5.3	0.55			115	0.32	4.2
5.2	0.55			120	0.26	3.35
5.1	0.54			130	0.175	2.2
5.0	0.53			140	0.12	1.55
4.9	0.525			150	0.09	1.2
4.8	0.525			160	0.08	1.1
4.07				180	0.075	0.9
3.5	0.56			200	0.08	1.0
3.4	0.55			210	0.08	1.0
3.3	0.55			223	0.10	1.3
3.2	0.55			230	0.125	1.6
3.1	0.57			240	0.17	2.2
3.0	0.575			250	0.26	3.3
2.9	0.58			260	0.375	5.0
2.85	0.582			265	0.42	5.8
2.8	0.578			270	0.435	6.2
2.7	0.572			272.5	0.44	6.3
2.6	0.572			280	0.42	5.8
2.5	0.58			285	0.38	5.1
2.4	0.60			290	0.33	4.3
2.3	0.61			295	0.275	3.5
2.2	0.66			300	0.19	2.4
2.1	0.72			310	0.14	1.8
2.0	0.79			320	0.11	1.4
1.9	0.855			330	0.09	1.2
1.8	0.87			340	0.085	1.1
1.75	0.88			350	0.085	1.1
1.7	0.875			0	0.088	1.15

TABLE 11.16

Sample: CB00A, Mag. Field = 4.2 K.Gauss. Temp. = 69°C,
Background Optical Density = 0.55

LINEAR SCANNING				ANGULAR SCANNING		
L in cm.	O. D.	L in cm.	O. D.	Θ in (deg.)	O. D.	Intensity.
7.1	0.99	2.0	1.255	350	0.2	2.5
7.0	1.03	1.9	1.34	357	0.195	2.45
6.9	1.11	1.8	1.365	2	0.2	2.5
6.8	1.20	1.7	1.42	25	0.2	2.5
6.7	1.28	1.6	1.40	30	0.21	2.6
6.6	1.36	1.5	1.34	40	0.25	3.15
6.5	1.40	1.4	1.21	50	0.31	4.05
6.45	1.40	1.3	1.18	60	0.42	5.8
6.4	1.375	1.2	1.09	70	0.60	10.5
6.3	1.32			80	0.78	16.0
6.2	1.26			85	0.835	17.7
6.1	1.12			90	0.865	18.7
6.0	1.10			92	0.870	18.8
5.9	1.04			95	0.855	18.4
5.8	1.01			100	0.805	16.9
5.7	0.985			105	0.75	15.2
5.6	0.97			110	0.64	11.8
5.5	0.97			115	0.56	9.2
5.4	0.97			120	0.465	6.7
5.3	0.98			125	0.39	5.3
5.2	0.98			130	0.34	4.4
5.2	0.98			140	0.26	3.35
5.15	0.978			150	0.22	2.75
5.1	0.97			160	0.20	2.5
5.0	0.96			177	0.20	2.5
4.9	0.94			197	0.21	2.55
4.8	0.94			210	0.23	2.85
4.7	0.95			220	0.265	3.4
4.04				230	0.335	4.4
3.4	0.965			250	0.62	11.2
3.3	0.95			260	0.8	16.6
3.2	0.95			265	0.825	17.4
3.1	0.96			270	0.84	17.95
3.0	0.97			272	0.842	18.0
2.9	0.98			275	0.84	17.8
2.8	0.982			280	0.81	17.0
2.8	0.98			290	0.65	12.1
2.75	0.98			295	0.55	9.18
2.7	0.98			300	0.465	6.78
2.6	0.97			310	0.33	4.3
2.5	0.98			320	0.265	3.4
2.4	1.005			330	0.21	2.55
2.3	1.01			340	0.2	2.5
2.2	1.05			350	0.2	2.5
2.1	1.13					

TABLE 11.17

Sample: CB00A. Mag.Field = 4.2 K.Gauss, Temp. = 75°C,
Background Optical Density = 0.42.

LINEAR SCANNING				ANGULAR SCANNING		
L in cm.	O. D.	L in cm.	O. D.	θ in (deg.)	O. D.	Intensity.
7.2	0.90	1.9	1.34	0	0.24	3.05
7.1	0.94	1.8	1.382	10	0.24	3.05
7.0	1.00	1.7	1.382	17	0.23	2.8
6.9	1.08	1.6	1.33	34	0.24	3.05
6.7	1.245	1.5	1.24	44	0.26	3.3
6.6	1.31	1.4	1.135	50	0.285	3.65
6.5	1.325	1.3	1.04	60	0.35	4.6
6.4	1.30	1.2	1.00	70	0.47	6.8
6.3	1.23			80	0.63	11.6
6.2	1.17			90	0.84	17.9
6.1	1.08			95	0.91	20.0
6.0	1.01			100	0.95	21.2
5.9	0.96			103	0.96	21.6
5.8	0.93			104	0.96	21.6
5.7	0.91			110	0.92	20.2
5.6	0.90			115	0.86	18.5
5.5	0.90			120	0.76	15.5
5.4	0.90			130	0.58	9.8
5.3	0.91			140	0.415	5.75
5.25	0.912			150	0.31	4.05
5.2	0.91			160	0.26	3.3
5.1	0.90			170	0.235	2.95
5.0	0.88			180	0.23	2.8
4.9	0.875			195	0.22	2.75
4.8	0.87			210	0.22	2.75
4.7	0.89			222	0.25	3.15
4.07				230	0.28	3.6
3.4	0.91			240	0.30	3.9
3.3	0.90			250	0.445	6.25
3.2	0.905			260	0.615	11.0
3.1	0.912			265	0.71	14.0
3.05	0.92			270	0.80	16.7
3.00	0.92			275	0.87	18.8
2.95	0.922			280	0.91	20.0
2.9	0.925			283	0.915	20.15
2.85	0.928			285	0.91	20.0
2.8	0.922			290	0.87	18.8
2.7	0.92			295	0.825	17.25
2.6	0.915			300	0.745	15.0
2.5	0.92			305	0.65	12.0
2.4	0.955			310	0.565	9.4
2.3	1.01			320	0.42	5.8
2.2	1.03			330	0.33	4.3
2.1	1.12			340	0.28	3.6
2.0	1.24			350	0.26	3.3

TABLE 11.18

Sample: CBCOA. Mag. Field = 4.2 K.Gauss, Tempk. = 80°C,
Background Optical Density = 0.34.

LINEAR SCANNING				ANGULAR SCANNING		
L in cm	O. D.	L in cm.	O. D.	θ in (deg.)	O. D.	Intensity
7.15	0.70	2.1	0.865	0	0.18	2.2
7.10	0.71	2.0	0.925	10	0.18	2.2
7.0	0.735	1.9	0.985	20	0.185	2.3
6.9	0.79	1.8	1.00	30	0.205	2.5
6.8	0.87	1.75	1.02	40	0.22	2.7
6.7	0.93	1.7	1.01	50	0.27	3.5
6.6	1.00	1.6	0.99	60	0.335	4.4
6.5	1.04	1.5	0.925	70	0.45	6.25
6.45	1.05	1.4	0.86	75	0.51	7.7
6.425	1.07	1.3	0.82	80	0.57	9.5
6.4	1.045	1.2	0.755	85	0.64	11.8
6.3	1.03			90	0.66	12.4
6.2	0.985			95	0.68	13.0
6.1	0.92			100	0.66	12.4
6.0	0.85			105	0.64	11.8
5.9	0.81			110	0.595	10.4
5.8	0.76			115	0.535	8.55
5.7	0.73			120	0.465	6.70
5.6	0.72			130	0.34	4.4
5.5	0.71			140	0.27	3.5
5.4	0.72			150	0.22	2.7
5.3	0.72			160	0.20	2.5
5.2	0.725			170	0.19	2.4
5.1	0.72			190	0.185	2.2
5.15	0.725			210	0.195	2.42
5.0	0.715			220	0.22	2.8
4.9	0.70			230	0.26	3.3
4.8	0.705			240	0.33	4.3
4.7	0.73			250	0.419	5.8
4.04				255	0.54	8.6
3.5	0.72			260	0.61	10.9
3.4	0.69			265	0.66	12.4
3.3	0.68			270	0.70	13.3
3.2	0.68			275	0.71	14.0
3.1	0.70			280	0.69	13.4
3.0	0.71			285	0.655	12.3
2.95	0.712			290	0.60	10.5
2.9	0.71			295	0.545	8.7
2.8	0.71			300	0.465	6.7
2.7	0.705			310	0.35	4.6
2.6	0.705			320	0.27	3.5
2.5	0.72			330	0.23	2.9
2.4	0.74			340	0.205	2.5
2.4	0.79			350	0.195	2.3
2.2	0.805			0	0.185	2.15

TABLE 11.19

Sample: CBOOA. Mag. Field = 0.10 K.Gauss, Tempt. 86°C, Background Optical Density = 0.27

LINEAR SCANNING				ANGULAR SCANNING		
L in cm.	O. D.	L in cm.	O. D.	θ in (deg.)	O. D.	Intensity
7.25	0.50	2.7	0.615	300	0.42	5.8
7.2	0.51	2.6	0.615	310	0.405	5.6
7.1	0.53	2.5	0.625	320	0.41	5.6
7.0	0.58	2.4	0.65	330	0.42	5.8
6.9	0.64	2.3	0.662	340	0.42	5.9
6.8	0.695	2.2	0.71	350	0.44	6.2
6.7	0.735	2.1	0.76	0	0.47	6.8
6.6	0.78	2.0	0.812	10	0.50	6.5
6.5	0.815	1.9	0.86	20	0.53	8.45
6.45	0.822	1.8	0.875	30	0.565	9.3
6.4	0.825	1.75	0.87	40	0.595	10.4
6.35	0.82	1.7	0.865	50	0.60	10.9
6.3	0.815	1.6	0.83	60	0.615	11.1
6.2	0.78	1.5	0.77	70	0.61	10.95
6.1	0.73	1.4	0.752	74	0.60	10.9
6.0	0.685	1.3	0.69	90	0.55	9.0
5.9	0.65	1.2	0.63	100	0.52	8.1
5.8	0.635			110	0.48	7.0
5.7	0.62			120	0.45	6.6
5.6	0.612			130	0.42	5.85
5.5	0.612			140	0.41	5.6
5.4	0.615			150	0.42	5.6
5.3	0.62			160	0.43	6.0
5.2	0.63			170	0.45	6.4
5.1	0.64			180	0.47	6.8
5.0	0.641			190	0.48	7.0
4.9	0.66			200	0.51	7.8
4.8	0.68			210	0.52	8.2
4.7	0.72			216	0.54	8.5
4.6	0.761			220	0.548	8.8
4.5	0.78			225	0.55	8.9
4.08				228	0.555	9.0
3.72	0.77			230	0.555	9.0
3.6	0.745			240	0.55	8.8
3.5	0.70			245	0.545	8.8
3.4	0.66			250	0.538	8.6
3.3	0.64			255	0.535	8.5
3.2	0.63			260	0.52	8.1
3.1	0.625			265	0.51	7.7
3.15	0.625			270	0.50	7.5
3.05	0.622			275	0.48	7.0
3.00	0.620			280	0.46	6.6
2.95	0.62			285	0.45	6.5
2.9	0.618			290	0.44	6.3
2.8	0.615			295	0.43	6.1

TABLE 11.20

Sample: CBOOA. Mag.Field = 0.20 K.Gauss, Temp. = 86°C,
Background Optical Density = 0.27

LINEAR SCANNING				ANGULAR SCANNING		
L in cm.	O. D.	L in cm.	O. D.	θ in (deg.)	O. D.	Intensity
7.15	0.50	2.5	0.525	0	0.30	3.8
7.1	0.51	2.4	0.54	20	0.30	3.8
7.0	0.548	2.3	0.545	36	0.30	3.80
6.9	0.59	2.2	0.575	45	0.31	4.0
6.8	0.615	2.1	0.605	50	0.31	4.0
6.7	0.66	2.0	0.650	63	0.33	4.3
6.6	0.705	1.9	0.675	74	0.35	4.6
6.5	0.752	1.8	0.68	80	0.37	4.95
6.45	0.76	1.75	0.686	85	0.388	5.2
6.4	0.765	1.7	0.684	90	0.40	5.6
6.35	0.762	1.65	0.68	95	0.414	5.7
6.3	0.755	1.6	0.655	100	0.42	5.8
6.2	0.72	1.5	0.61	105	0.42	5.8
6.1	0.67	1.4	0.56	110	0.42	5.8
6.0	0.62	1.3	0.55	120	0.42	5.8
5.9	0.60	1.2	0.55	125	0.41	5.65
5.8	0.565			130	0.39	5.3
5.7	0.545			140	0.375	5.0
5.6	0.535			150	0.365	4.8
5.5	0.535			160	0.342	4.4
5.4	0.535			170	0.33	4.3
5.3	0.54			180	0.33	4.3
5.2	0.55			190	0.33	4.3
5.1	0.555			200	0.34	4.5
5.0	0.555			210	0.35	4.6
4.9	0.56			220	0.36	4.8
4.8	0.565			230	0.37	4.95
4.7	0.58			240	0.395	5.35
4.6	0.60			245	0.40	5.6
4.5	0.625			250	0.42	5.8
4.46	0.64			255	0.44	6.2
4.06				260	0.46	6.6
3.62	0.70			270	0.48	7.0
3.5	0.63			275	0.49	7.3
3.4	0.58			280	0.51	7.8
3.3	0.555			285	0.495	7.45
3.2	0.55			290	0.482	7.05
3.15	0.54			295	0.475	6.95
3.1	0.538			300	0.46	6.6
3.05	0.538			310	0.415	5.75
3.0	0.535			320	0.37	4.95
2.9	0.53			330	0.34	4.5
2.8	0.525			336	0.33	4.3
2.7	0.52			340	0.32	4.2
2.6	0.52			350	0.31	4.0

N.B.:-The quadrant 190°-280° has been excluded in calculating $\langle P_2 \rangle$

TABLE 11.21

Sample: CS00A. Mag. Field = ~~0.40~~ 0.40 K.Gauss,
Temp. = 86°C, Background Optical Density = 0.29.

LINEAR SCANNING				ANGULAR SCANNING		
L in cm.	O. D.	L in cm.	O. D.	Θ in (deg.)	O. D.	Intensity
7.15	0.48	2.1	0.60	10	0.21	2.65
7.1	0.50	2.0	0.65	40	0.21	2.65
7.0	0.52	1.9	0.69	50	0.23	2.85
6.9	0.56	1.8	0.698	60	0.26	3.3
6.8	0.58	1.75	0.712	75	0.31	4.1
6.7	0.635	1.7	0.712	80	0.34	4.5
6.6	0.675	1.65	0.705	85	0.37	4.95
6.55	0.69	1.6	0.70	90	0.385	5.25
6.50	0.718	1.55	0.655	95	0.40	5.5
6.45	0.728	1.4	0.61	100	0.40	5.5
6.425	0.718	1.3	0.59	106	0.405	5.6
6.4	0.715	1.2	0.55	110	0.395	5.4
6.35	0.695			115	0.372	5.0
6.3	0.62			120	0.35	4.6
6.2	0.62			125	0.325	4.3
6.1	0.58			130	0.30	3.8
6.0	0.550			140	0.245	3.2
5.9	0.54			150	0.215	2.7
5.8	0.52			160	0.20	2.5
5.7	0.515			170	0.19	2.4
5.6	0.51			180	0.17	2.2
5.5	0.51			208	0.17	2.2
5.4	0.515			220	0.18	2.25
5.35	0.515			230	0.20	2.5
5.3	0.515			240	0.22	2.8
5.2	0.515			250	0.26	3.3
5.1	0.515			255	0.29	3.7
5.0	0.515			260	0.32	4.25
4.9	0.515			265	0.35	4.65
4.8	0.52			270	0.38	5.1
4.7	0.54			275	0.39	5.3
4.05				280	0.41	5.65
3.5	0.56			286	0.422	5.95
3.4	0.54			290	0.41	5.65
3.3	0.53			295	0.402	5.5
3.2	0.53			300	0.385	5.25
3.15	0.525			305	0.36	4.75
2.9	0.525			310	0.34	4.5
2.8	0.52			320	0.30	3.8
2.7	0.52			330	0.25	3.2
2.6	0.52			340	0.23	2.85
2.5	0.515			350	0.222	2.8
2.4	0.53			0	0.22	2.8
2.3	0.535			10	0.22	2.8
2.2	0.56					

TABLE 11.22

Sample; CB00A. Mag. Field = 0.88 K.Gauss, Temp. 86°C,
Background Optical Density = 0.29.

LINEAR SCANNING				ANGULAR SCANNING		
L in cm.	O. D.	L in cm.	O. D.	θ in (deg.)	O. D.	Intensity.
7.15	0.53	2.1	0.70	340	0.14	1.7
7.1	0.55	2.0	0.76	10	0.14	1.7
7.0	0.58	1.9	0.82	22	0.15	1.9
6.9	0.63	1.8	0.84	30	0.17	2.1
6.8	0.67	1.7	0.865	40	0.205	2.6
6.7	0.745	1.65	0.862	50	0.235	2.95
6.6	0.815	1.6	0.85	60	0.31	4.0
6.5	0.86	1.5	0.80	65	0.425	4.9
6.45	0.865	1.4	0.74	70	0.48	7.0
6.4	0.86	1.3	0.71	75	0.52	8.0
6.3	0.85	1.2	0.65	80	0.56	9.2
6.25	0.842	[illegible]	[illegible]	85	0.58	9.8
6.2	0.82			88	0.595	10.2
6.1	0.77			90	0.584	10.0
6.0	0.695			95	0.56	9.1
5.9	0.640			100	0.52	8.1
5.8	0.62			105	0.47	6.8
5.7	0.590			110	0.425	6.0
5.6	0.58			120	0.33	4.3
5.5	0.58			130	0.25	3.1
5.4	0.585			140	0.21	2.6
5.3	0.59			150	0.19	2.4
5.2	0.59			160	0.17	2.2
5.1	0.59			170	0.17	2.2
5.0	0.59			180	0.16	2.0
4.9	0.585			190	0.16	2.0
4.8	0.595			200	0.165	2.05
4.7	0.61			210	0.18	2.3
4.6	0.63			220	0.22	2.8
4.5	0.63			230	0.29	3.7
4.0				240	0.39	5.3
3.5	0.64			250	0.49	7.3
3.4	0.61			255	0.535	8.5
3.3	0.60			260	0.57	9.5
3.2	0.595			262	0.58	9.8
3.1	0.595			265	0.575	9.45
3.0	0.60			270	0.56	9.2
2.9	0.60			275	0.528	8.2
2.8	0.60			280	0.488	7.2
2.7	0.59			290	0.38	5.2
2.6	0.59			300	0.29	3.7
2.5	0.595			310	0.225	2.8
2.4	0.618			320	0.18	2.3
2.3	0.62			330	0.16	2.0
2.2	0.65			340	0.14	1.7

TABLE 11.23

Sample: CBOOA. Mag. Field = 1.8 K.Gauss, Temp. = 86°C,
Background optical density = 0.31.

LINEAR SCANNING				ANGULAR SCANNING		
L in cm.	O. D.	L in cm.	O. D.	Φ in (deg.)	O. D.	Intensity
7.15	0.55	2.1	0.705	0	0.12	1.5
7.10	0.57	2.0	0.775	20	0.12	1.5
7.0	0.605	1.95	0.778	28	0.13	1.6
6.9	0.65	1.9	0.83	40	0.15	1.8
6.8	0.705	1.85	0.835	50	0.19	2.4
6.7	0.725	1.8	0.84	60	0.255	3.2
6.6	0.78	1.775	0.85	70	0.235	4.4
6.55	0.81	1.75	0.848	75	0.39	5.3
6.5	0.81	1.7	0.842	80	0.44	6.2
6.475	0.81	1.6	0.80	85	0.485	7.1
6.45	0.805	1.5	0.74	90	0.51	7.8
6.4	0.80	1.4	0.68	95	0.52	8.2
6.3	0.75	1.3	0.66	100	0.51	7.8
6.2	0.72	1.2	0.60	105	0.47	6.8
6.1	0.67			110	0.425	6.0
6.0	0.625			115	0.38	5.1
5.9	0.58			120	0.335	4.4
5.8	0.565			125	0.285	3.6
5.7	0.56			130	0.24	3.0
5.6	0.55			140	0.175	2.2
5.50	0.55			150	0.14	1.8
5.3	0.56			160	0.125	1.6
5.2	0.56			170	0.12	1.5
5.1	0.56			180	0.11	1.4
5.0	0.555			195	0.11	1.4
4.9	0.555			205	0.12	1.5
4.8	0.56			215	0.13	1.6
4.7	0.58			230	0.17	2.1
4.6	0.595			240	0.24	3.0
4.1				250	0.33	4.3
3.5	0.58			255	0.38	5.05
3.4	0.56			260	0.41	5.7
3.3	0.55			265	0.47	6.8
3.1	0.555			270	0.495	7.4
3.0	0.555			275.5	0.505	7.55
2.9	0.555			280	0.482	7.1
2.8	0.555			285	0.455	6.6
2.7	0.55			290	0.42	5.8
2.6	0.55			295	0.365	4.8
2.5	0.558			300	0.31	4.0
2.4	0.58			310	0.235	2.7
2.3	0.595			320	0.18	2.2
2.2	0.645			330	0.15	1.8
2.1	0.705			340	0.14	1.7
2.2	0.775			350	0.13	1.6

N.B. Two quadrants 5-95° and 275-50° have been excluded for the calculation of $\langle P_2 \rangle$ %.

TABLE 11.24.

Sample: CBCOA. Mag. Field = 2.5 K.Gauss, Temp. = 86°C,
Background Optical Density = 0.42.

LINEAR SCANNING				ANGULAR SCANNING		
L in cm.	O. D.	L in cm.	O. D.	θ in (deg.)	O. D.	Intensity.
7.15	0.715	2.1	0.83	0	0.175	2.2
7.1	0.73	2.0	0.885	10	0.175	2.2
7.0	0.76	1.9	0.94	20	0.18	2.25
6.9	0.81	1.8	0.96	30	0.19	2.4
6.8	0.87	1.75	0.99	40	0.22	2.7
6.7	0.915	1.7	0.992	50	0.26	3.3
6.6	0.94	1.65	0.995	60	0.32	4.1
6.5	0.995	1.6	0.99	70	0.410	5.6
6.45	1.002	1.5	0.95	80	0.49	7.2
6.4	1.01	1.4	0.90	85	0.52	8.1
6.35	1.01	1.3	0.88	90	0.55	8.95
6.3	1.01	1.2	0.83	93.5	0.56	9.1
6.2	0.98	1.17	0.82	95	0.556	9.1
6.1	0.97			100	0.55	8.85
6.0	0.865			105	0.53	8.25
5.9	0.81			110	0.49	7.2
5.8	0.78			115	0.455	6.5
5.7	0.75			120	0.41	5.6
5.6	0.735			125	0.34	4.5
5.5	0.715			140	0.265	3.3
5.4	0.72			145	0.24	3.0
5.3	0.725			150	0.22	2.7
5.2	0.73			160	0.20	2.5
5.1	0.73			170	0.20	2.5
5.0	0.728			180	0.20	2.5
4.9	0.728			190	0.21	2.6
4.8	7.35			200	0.21	2.6
4.7	0.755			210	0.21	2.6
4.6	0.78			220	0.215	2.65
4.02				230	0.26	3.3
3.5	0.78			240	0.34	4.5
3.4	0.75			250	0.43	6.0
3.3	0.74			260	0.53	8.35
3.2	0.735			265	0.565	9.2
3.1	0.738			270	0.58	9.85
3.0	0.74			277	0.59	10.2
2.9	0.74			280	0.585	10.0
2.8	0.742			285	0.56	9.1
285	0.74			290	0.52	8.1
2.7	0.735			300	0.42	5.85
2.6	0.732			310	0.33	4.3
2.5	0.735			320	0.26	3.3
2.4	0.75			330	0.22	2.7
2.3	0.76			340	0.20	2.5
2.2	0.785			350	0.19	2.4

TABLE 11.25.

Sample: CB00A. Mag. Field = 5.4 K.Gauss, Tempt. = 86°C,
Background Optical Density = 0.25

LINEAR SCANNING				ANGULAR SCANNING		
L in cm.	O. D.	L in cm.	O. D.	θ in (deg.)	O. D.	Intensity.
7.15	0.355	1.85	0.455	0	0.065	0.8
7.1	0.36	1.8	0.458	27	0.065	0.8
7.0	0.365	1.75	0.464	40	0.07	0.85
6.9	0.375	1.7	0.464	60	0.12	1.5
6.7	0.40	1.65	0.462	70	0.14	1.75
6.6	0.422	1.6	0.45	80	0.17	2.1
6.5	0.445	1.5	0.43	85	0.188	2.35
6.45	0.462	1.4	0.42	90	0.205	2.55
6.4	0.468	1.3	0.395	95	0.215	2.65
6.35	0.465	1.2	0.38	99	0.215	2.75
6.3	0.461	1.25	0.375	105	0.21	2.65
6.25	0.46			110	0.19	2.35
6.2	0.455			115	0.175	2.2
6.1	0.435			120	0.155	1.95
6.0	0.42			130	0.122	1.5
5.8	0.388			140	0.10	1.3
5.6	0.375			150	0.085	1.1
5.5	0.375			160	0.07	0.85
5.4	0.378			170	0.07	0.85
5.3	0.380			213	0.07	0.85
5.2	0.386			220	0.075	1.0
5.1	0.395			230	0.085	1.1
5.0	0.405			240	0.12	1.5
4.9	0.41			250	0.14	1.75
4.8	0.42			260	0.17	2.1
4.7	0.44			265	0.19	2.35
4.6	0.47			270	0.202	2.5
4.05				275	0.212	2.66
3.5	0.472			280	0.21	2.65
3.4	0.445			285	0.20	2.5
3.3	0.435			290	0.19	2.35
3.2	0.415			295	0.175	2.2
3.1	0.405			300	0.155	1.95
3.0	0.395			310	0.12	1.5
2.9	0.385			320	0.095	1.2
2.8	0.385			330	0.08	1.0
2.7	0.37			340	0.07	0.85
2.6	0.37			35	0.07	0.85
2.5	0.372			0	0.07	0.85
2.4	0.375					
2.3	0.38					
2.2	0.39					
2.1	0.41					
2.0	0.43					
1.9	0.44					

TABLE 11.26

Sample: CB00A. Mag. Field = 4.2 K.Gauss, Tempt. = 86°C, Background Optical Density = 0.40.

LINEAR SCANNING				ANGULAR SCANNING		
L in cm.	O. D.	L in cm.	O. D.	θ in (deg.)	O. D.	Intensity.
7.15	0.865	1.8	1.25	0	0.24	3.0
7.1	0.90	1.75	1.3	5	0.225	2.8
7.0	0.96	1.7	1.3	15	0.23	2.9
6.9	1.02	1.65	1.29	28	0.23	2.9
6.7	1.12	1.6	1.28	31	0.24	3.0
6.6	1.25	1.5	1.20	40	0.25	3.2
6.5	1.30	1.4	1.10	50	0.34	4.5
6.45	1.31	1.3	1.07	60	0.37	5.0
6.4	1.312	1.2	0.98	70	0.615	11.0
6.2	1.21			75	0.70	13.6
6.1	1.12			80	0.775	15.9
6.0	1.05			85	0.84	17.95
5.9	0.985			90	0.89	19.50
5.8	0.95			97	0.90	19.7
5.7	0.91			100	0.89	19.5
5.6	0.89			105	0.86	18.5
5.5	0.885			110	0.79	16.4
5.4	0.885			120	0.64	10.8
5.3	0.89			125	0.56	9.2
5.25	0.895			130	0.49	7.3
5.2	0.892			140	0.37	4.9
5.15	0.892			150	0.28	3.45
5.1	0.888			160	0.24	3.0
5.0	0.88			170	0.225	2.8
4.9	0.88			175	0.22	2.75
4.8	0.89			190	0.215	2.7
4.7	0.92			200	0.23	2.9
4.05				220	0.28	3.45
3.5	0.905			230	0.345	4.5
3.4	0.88			240	0.465	6.7
3.3	0.87			250	0.60	10.5
3.2	0.88			260	0.765	15.6
3.1	0.88			270	0.89	19.5
3.0	0.89			275	0.915	20.2
2.9	0.89			278	0.92	20.3
2.8	0.89			280	0.915	20.2
2.7	0.885			285	0.885	19.0
2.6	0.885			295	0.76	15.5
2.5	0.895			300	0.68	13.0
2.4	0.92			305	0.595	10.4
2.3	0.93			310	0.525	8.8
2.2	1.00			320	0.41	5.7
2.1	1.06			330	0.33	4.3
2.0	1.14			340	0.28	3.45
1.9	1.23			350	0.25	3.2

TABLE 11.27

Sample: CBOOA. Mag. Field = ~~96°C, Tempt.~~ 4.2 K.Gauss,
Tempt. = 96°C, Background Optical
Density = 0.36

LINEAR SCANNING				ANGULAR SCANNING		
L in cm.	O. D.	L in cm.	O. D.	θ in (deg.)	O. D.	Intensity.
7.2	0.62	2.0	0.87	0	0.125	1.55
7.1	0.65	1.9	0.92	10	0.12	1.45
7.0	0.695	1.85	0.928	30	0.125	1.55
6.9	0.76	1.8	0.928	40	0.14	1.8
6.8	0.82	1.75	0.92	50	0.17	2.2
6.7	0.85	1.7	0.918	60	0.215	2.6
6.6	0.91	1.6	0.865	70	0.30	3.8
6.55	0.916	1.5	0.795	80	0.39	5.3
6.5	0.914	1.4	0.725	90	0.49	7.2
6.45	0.90	1.3	0.71	95	0.52	8.2
6.4	0.89	1.2	0.65	100	0.54	8.6
6.3	0.825			103	0.542	8.7
6.2	0.825			105	0.54	8.6
6.1	0.77			110	0.53	8.3
6.0	0.73			115	0.50	7.5
5.9	0.713			120	0.455	6.5
5.8	0.68			125	0.40	5.5
5.7	0.675			130	0.355	4.0
5.6	0.675			140	0.26	3.3
5.5	0.682			150	0.205	3.6
5.4	0.692			160	0.17	2.1
5.3	0.70			170	0.13	1.6
5.2	0.70			180	0.12	1.4
5.15	0.70			190	0.13	1.6
5.1	0.695			200	0.12	1.4
5.0	0.69			210	0.12	1.4
4.9	0.67			220	0.13	1.6
4.8	0.67			230	0.16	2.1
4.7	0.69			240	0.21	2.6
4.07				250	0.28	3.5
3.5	0.70			260	0.39	5.3
3.4	0.68			270	0.49	7.2
3.3	0.68			280	0.55	8.9
3.2	0.69			283.5	0.57	9.5
3.1	0.70			285	0.555	9.1
3.0	0.71			290	0.545	8.8
2.9	0.708			295	0.52	8.2
2.8	0.70			300	0.485	7.1
2.7	0.69			305	0.425	6.0
2.6	0.685			310	0.37	4.8
2.5	0.69			320	0.27	3.4
2.4	0.71			330	0.21	2.6
2.3	0.72			340	0.16	2.1
2.2	0.76			350	0.14	1.8
2.1	0.82					

TABLE 11.28.

Sample: CB00A. Mag. Field = 4.2 K.Gauss, Tempt. = 103°C,
Background Optical Density = 0.31.

LINEAR SCANNING				ANGULAR SCANNING		
L in cm.	O. D.	L in cm.	O. D.	θ in (deg.)	O. D.	Intensity.
7.2	0.505	2.2	0.625	0	0.175	2.2
7.1	0.515	2.1	0.67	10	0.17	2.15
7.0	0.53	2.0	0.70	20	0.17	2.15
6.9	0.56	1.9	0.72	30	0.18	2.25
6.8	0.575	1.85	0.732	40	0.20	2.5
6.7	0.61	1.8	0.735	50	0.22	2.75
6.6	0.635	1.75	0.74	60	0.27	3.45
6.5	0.67	1.7	0.745	70	0.312	4.05
6.4	0.70	1.65	0.735	80	0.355	4.65
6.35	0.713	1.60	0.70	85	0.385	5.1
6.3	0.718	1.5	0.68	90	0.40	5.5
6.25	0.715	1.4	0.635	95	0.415	5.75
6.2	0.715	1.3	0.59	100	0.422	5.9
6.15	0.705	1.2	0.55	103	0.42	5.85
6.1	0.690	1.15	0.53	105	0.418	5.8
6.0	0.67			110	0.40	5.5
5.9	0.64			115	0.385	5.2
5.8	0.62			120	0.37	4.9
5.7	0.605			130	0.325	4.25
5.6	0.60			140	0.28	3.6
5.5	0.592			150	0.24	3.0
5.4	0.595			160	0.21	2.6
5.3	0.60			170	0.195	2.45
5.2	0.615			180	0.19	2.35
5.1	0.64			190	0.19	2.35
5.0	0.65			200	0.20	2.4
4.9	0.665			210	0.205	2.45
4.8	0.685			220	0.212	2.7
4.7	0.71			230	0.25	3.1
4.6	0.745			240	0.28	3.55
4.28	0.98			250	0.325	4.25
4.0				260	0.38	5.05
#3.57	0.84			265	0.40	5.5
3.4	0.75			270	0.41	5.6
3.3	0.70			275	0.418	5.8
3.2	0.662			280	0.418	5.8
3.1	0.635			285	0.41	5.6
3.0	0.62			290	0.40	5.5
2.9	0.595			295	0.39	5.3
2.8	0.595			300	0.37	4.9
2.7	0.585			308	0.31	4.2
2.6	0.58			320	0.27	3.45
2.5	0.582			330	0.23	2.85
2.4	0.595			340	0.20	2.5
2.3	0.60			350	0.19	2.35

TABLE 11.29

Sample: CB00A.

Data for intermolecular distance (D) and degree of ordering (in Vainshtein's approximation)).

Sample to film distance = 6.2044 cm.

Temp. °C.	Field in K. Gauss	Outer halo: Dia. in cm.	Outer halo: Bragg angle (deg.)	Outer halo: D in Å	Degree of ordering (2nd. order) in Vainshtein's approximation.	Phase
60	4.2	4.80	10.57	4.69	0.68	
69	4.2	4.775	10.52	4.71	0.69	Smectic
75	4.2	4.75	10.47	4.74	0.68	
80	4.2	4.675	10.32	4.81	0.62	
	0.10	4.6	10.17	4.88	0.44	
	0.20	4.65	10.27	4.83	0.61	
	0.40	4.675	10.32	4.81	0.61	
86	0.88	4.75	10.47	4.74	0.65	Nematic
	1.8	4.70	10.37	4.78	0.65	
	2.5	4.7	10.37	4.78	0.65	
	4.2	4.7	10.37	4.78	0.66	
	5.4	4.7	10.37	4.78	0.65	
	0	4.45	9.86	5.02		
	0.400	4.7	10.37	4.78	0.57	
	0.88	4.675	10.32	4.81	0.57	
96	1.8	4.7	10.37	4.78	0.56	"
	2.5	4.675	10.32	4.81	0.59	
	4.2	4.7	10.37	4.78	0.58	
	0.40	4.55	10.07	4.92	0.51	
	0.88	4.6	10.17	4.88	0.50	
	1.8	4.55	10.67	4.92	0.51	
103	4.2	4.6	10.17	4.88	0.53	"
	4.6	4.6	10.17	4.88	0.53	
	5.4	4.6	10.17	4.88	0.52	

TABLE 11.30.

Sample: CBOOA. Intermolecular distance (D), Layer spacing (d) smectic phase and length of the molecule (ℓ) in nematic phase (in absence of magnetic field).

Phase	Temp. °C.	Sample to film distance	Outer halo			Inner halo			$\langle\cos\theta\rangle$	$\frac{d}{\langle\cos\theta\rangle}$
			Dia. in cm.	Bragg angle	D in Å	Dia. in cm.	'Bragg angle (deg.)	'd' or 'ℓ' in cm.		
	45	5.81	4.35	10.26	4.83	0.57	1.404	31.42		
	47	6.81	5.05	10.17	4.87	0.645	1.356	32.55		
	52	6.81	5.1	10.26	4.83	0.605	1.271	34.71		
Smec-	57	5.81	4.35	10.26	4.83	-	-	-		
tic	61	6.81	5.05	10.17	4.87	0.605	1.271	34.71	0.89	39.0
	70	5.81	4.3	10.15	4.88	0.52	1.281	34.44	0.88	39.14
	75	5.81	4.275	10.10	4.90	0.50	1.232	35.81	0.89	40.24
	80	5.81	4.25	10.04	4.94	0.52	1.281	34.44	0.88	39.14
	85	6.81	4.925	9.94	4.99	0.60	1.261	34.98		
	90	6.81	4.9	9.89	5.01	-	-	-		
	95	6.81	4.875	9.85	5.03	0.62	1.303	33.86		
Nema-	100	6.81	4.85	9.80	5.05	0.62	1.303	33.86		
tic	103	6.81	4.7	9.51	5.21	-	-	-		
	107	6.81	4.6	9.33	5.31	-	-	-		

TABLE 11.31

Sample: CROCA.

Mean Intensity I (θ) for different θ values at different temps.

θ (deg.)	I (θ) for temperatures °C.						
	60	69	75	80	86	96	103
0	6.25	16.10	18.05	11.30	17.15	7.30	3.66
5	5.79	15.5	17.46	10.75	16.75	7.00	3.54
10	5.08	14.06	15.91	9.83	15.32	6.32	3.22
15	4.13	11.68	13.55	8.12	13.48	5.4	3.02
20	3.13	8.70	10.36	6.15	11.01	4.35	2.66
25	2.26	6.20	7.53	4.33	8.32	3.32	2.28
30	1.55	4.15	5.08	3.2	6.10	2.55	1.91
35	1.13	2.86	3.37	2.25	4.31	1.98	1.58
40	0.81	1.90	2.31	1.70	2.91	1.47	1.26
45	0.50	1.32	1.52	1.20	1.96	1.20	0.96
50	0.33	2.89	0.95	0.85	1.24	0.87	0.70
55	0.19	0.53	0.61	0.55	0.71	0.62	0.49
60	0.11	0.28	0.36	0.36	0.38	0.45	0.31
65	0.06	0.13	0.23	0.23	0.21	0.25	0.18
70	0.02	0.03	0.15	0.13	0.07	0.15	0.11
75	0	0	0.05	0.06	0.03	0.08	0.08
80	0	0	0	0.02	0	0.03	0.04
85	0	0	0	0	0	0	0
90	0	0	0	0	0	0	0

TABLE 11.32.

Sample: CBCOA.

Normalized distribution function for different temperatures.

β (deg.)	f(β) for temperature (°C).						
	60	69	75	80	86	96	103
0	11.31	9.84	9.10	9.49	7.82	8.27	5.73
5	10.72	9.46	8.90	9.21	7.65	7.95	5.51
10	9.13	8.43	8.24	8.35	7.13	7.08	4.94
15	7.06	6.99	7.07	6.92	6.25	5.84	4.25
20	5.05	5.37	5.49	5,16	5.09	4.50	3.64
25	3.43	3.71	3.83	3.45	3.83	3.28	3.11
30	2.29	2.22	2.45	2.18	2.69	2.31	2.60
35	1.52	1.14	1.51	1.43	1.81	1.64	2.09
40	1.01	0.650	0.957	1.03	1.19	1.19	1.62
45	0.659	0.617	0.622	0.758	0.774	0.895	1.23
50	0.413	0.695	0.384	0.504	0.484	0.671	0.920
55	0.245	0.588	0.216	0.298	0.280	0.482	0.643
60	0.133	0.291	0.121	0.181	0.147	0.322	0.396
65	0.063	0.021	0.079	0.127	0.070	0.197	0.213
70	0.025	0.060	0.050	0.082	0.030	0.109	0.116
75	0.008	-0.002	0.021	0.021	0.010	0.054	0.077
80	0.002	0.040	0.002	0.002	0.002	0.021	0.077
85	0	0.009	-0.001	-0.001	0	0.004	0.012
90	-0.001	-0.020	0.001	0.004	0	-0.001	-0.006

TABLE 11.33

Sample: CBOOA.

a_L $\langle P_L \rangle$, and $b_{L/k}$ (for L = 2 and 4) at different temperatures.

Phase	Temp. °C	Temp. °K	a_0	a_2	a_4	a_6	a_8	a_{10}	$\langle P_2 \rangle$	$\langle P_4 \rangle$	$b_{2/k}$	$b_{4/k}$
	60	333	-2.520	6.169	-2.536	1.930	-0.973	0.393	0.71	0.35	-2893	2412
	69	342	-7.413	17.347	-14.765	11.867	-0.286	1.539	0.69	0.33	-8598	15302
Smec-	75	348	-2.372	5.866	-2.340	2.053	-1.719	0.829	0.71	0.34	-2875	2395
tic	80	353	-2.176	5.636	-2.636	2.544	-1.94	0.950	0.68	0.32	-2926	2908
	86	359	-2.433	6.175	-2.801	1.910	-1.243	0.499	0.68	0.28	-3260	3591
Nema-	96	369	-1.528	4.422	-1.849	1.737	-1.154	0.543	0.62	0.24	-2632	2834
tic	103	376	-1.189	3.945	-1.667	0.985	-1.537	0.338	0.55	0.13	-2629	4823

TABLE 11.34

Sample: OBOOA.

Coefficients of pseudopotential.

Coefficients	Smectic phase		Nematic phase	
	Mean	Standard deviation	Mean	Standard deviation
$b_{2/k}$	-2898	26	-2840	364
$b_{4/k}$	2572	291	3749	1004

References:

1. D. Guillon, P. Seurin and A. Skoulers, Mol.Cryst. Liq. Cryst. 51, 149 (1979).
2. R. Ribotta, J. de Physics. C3, 149 (1976).
3. G.V. Vani and K. Vijayan, Mol.Cryst.Liq.Cryst.42 249 (1977).
4. W.L.McMillan, Phys. Rev. A4, 1238 (1971).
5. W.L.McMillan, Phys. Rev. A6, 936 (1972).
6. W.L.McMillan, Phys. Rev. A7, 1419 (1973).
7. K.C.Chu and W.L.McMillan, Phys.Rev. A11, 1059 (1975).
8. H.M.Conrad, W.Krasser, H.H.Stiller, A.Wergin, Liquid Crystals, Proceedings of an International Conference, Editors, S.Chandrasekhar, Heyden, London (1979),p. 429.
9. H.M. Conrad, F. Mezei, Reference 8, p. 441.
10. S.Torza and P.E.Cladis, Phys. Rev.Lett.32, 1046(1974).
11. Eastman Kodak Company Catalog No.11 963 .
12. P.E.Cladis, Ref. 8 p. 105
13. G.W.Gray and J.E.Lydon, Nature (London) 252, 221(1975).
14. J.E.Lydon and C.J.Oakley, J.Phys.(Paris) 36 C1-45(1975).
15. A.J.Leadbetter, J.L.Durrant and M.Rugman, Mol.Cryst. Liq.Cryst.Lett. 34, 231 (1977).
16. P.E.Cladis, R.K. Bogardus, and D.Aadsen, Phys. Rev.A18, 2296 (1979).
17. P.E.Cladis, R.K.Bogardus, W.B.Daniels and G.N.Taylor, Phys. Rev.Lett.34, 231 (1977).
18. B.Bhattacharjee, S.Paul, & R.Paul, Mol.Phys. 44 1391 , 6,(1981).

CHAPTER 12.

THE ORDER PARAMETER OF DYE MOLECULES AS GUEST IN NEMATIC LIQUID CRYSTALLINE HOST IN PRESENCE OF ELECTRIC FIELD.

CHAPTER 12

THE ORDER PARAMETER OF DYE MOLECULES AS GUEST IN NEMATIC LIQUID CRYSTALLINE A HOST IN PRESENCE OF ELECTRIC FIELD.

1. Introduction and Outlines of the theoretical backgroundi

A systematic study of the relationship between molecular structure and the electrical properties of nematic liquid crystals has recently led to the discovery that cooperative alignment of certain mesomorphic "host" compounds by external electric fields can be used to orient pleochroic dye molecule guests[1]. This orientation results in changes in the optical density of the material and consequently in the colour of light transmitted through the medium. A display technique in which a dye was dissolved in a liquid crystal matrix was first suggested by Heilmeier and Zanoni[1] of the R.C.A. laboratories in 1968. A detailed study of the optical density changes as a function of field strength and dye concentration for one guest host system is presented by Heilmeier et al[2] in 1969.

In the first report Heilmeir has coined the name guest-host interaction cells and this has remained until the present.

The principle behind the display of guest-host (GH) cell is very simple and has not changed substantially since its inception in 1968. A small amount of dichroic dye dissolved in a nematic liquid will be aligned with its long

axis parallel to the long axis of the liquid crystal. The solution is then aligned either homeotropically or parallel to transparent electrodes depending upon the electrode surface treatment. If, for example, the nematic liquid crystal is aligned in a parallel mode and has a positive dielectric anisotropy, the cell will be colored in the off position and become colourless on application of a field across the electrodes which is shown schematically in the fig.12.1 (a and b).

A number of investigations by different workers have been concerned with the properties of pleochroic dyes in nematic liquid crystalline host[3-7]. A.Bloom et al have shown first that order parameter S, of a dye in a nematic host is greatly affected by the structure of the dye[8] and then again shown the effect of host on dye order parameter[9]. Bloom et al also determined the order parameters of cholesteric azo dyes in several nematic hosts[10].

The G-H interactions of pleochroic dyes dissolved in nematic liquid crystals has been reviewed by R.J.Cox[11], particularly with respect to the application in electro-optic displays. The role of the dye structure and the liquid crystal mixture is considered with respect to factors such as order parameters, absorption spectra and solubility.

Uchida et al[12] did an investigation of dyes suitable for display cells by determining the order parameter for a number of dyes in a single liquid crystal host having

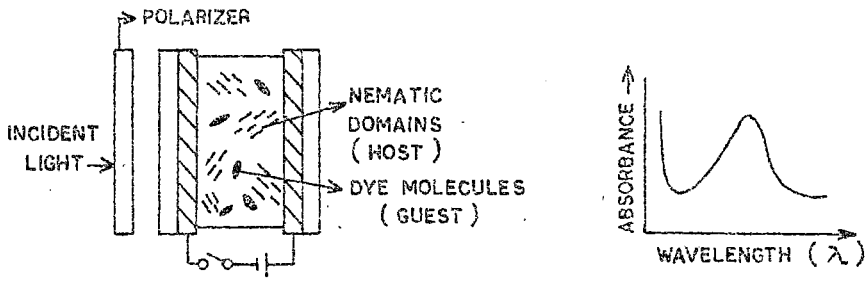

(a) GUEST - HOST SYSTEM NO FIELD.

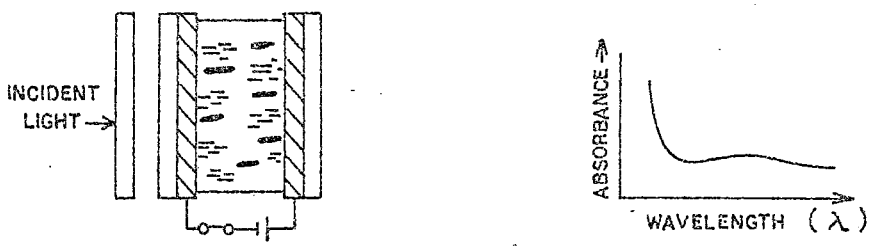

(b) GUEST - HOST SYSTEM WITH FIELD.

FIG. 12.1 (a) and (b). SCHEMATIC REPRESENTATION OF ELECTRO OPTIC GUEST - HOST CELL.

a positive dielectric anisotropy and confirmed that the longer dyes had higher order parameters and comparing three types of dye it was found that the order parameters of the azo and azomethines were greater than comparable methine dyes.

Several classes of organic dyes have been found to exhibit pleochroism. The dye used for guest-host interaction are long, rod like molecules which possess highly polarizable terminal groups and aromatic rings. These features resemble those of mesomorphic compounds and thus make the molecule compatible with nematic hosts. The extremely important criterion for the selection of dye is that the dye must be non-ionic.

In this thesis attempt has been made for the determination of order parameters for five different azo dyes in different nematic liquid crystalline host by guest-host interaction.

Fundamental behaviour of the Guest-Host cell is described in details by T.Uchida and M. Wada[12]. When rod like dichroic molecules are doped in liquid crystals, they tend to align parallel to the liquid crystal molecules. In actual practice, however the direction of the dye molecules as well as liquid crystal molecules deviate from the direction of the direction as shown in fig. 12.2, because of thermal fluctuation. If the deviated angle of each dye molecule is denoted by θ , the order parameter S can be

expressed by the average of $\cos^2\theta$ as

$$S = \frac{(2\langle\cos^2\theta\rangle + 1)}{3} \qquad \ldots (1)$$

The angle between the directions of transition moment C and of the molecular axis B is denoted by β and the angle between director A and the direction of electric field of the incident polarized light D is denoted by ψ, which are indicated in fig. 12.2.

Then the absorbances A as a function of β and ψ is represented by[13]

$$A(\beta,\psi) = K_M c d \left\{(S/2)\sin^2\beta + (1-S)/3 + (S/2)(2-3\sin^2\beta)\cos^2\psi\right\} \qquad \ldots (2)$$

where K_M is a coefficient relating to magnitude of the transition moment, d is the thickness of the layer of mixture of the dye and liquid crystal and c is the concentration.

The dka dichroic dye usually has a transition moment parallel to its molecular axis which is called positive dichroic dye or p-type dye. This type absorbs a polarized light component $L_{\parallel}$ whose polarized direction is parallel to the molecular axis. Let $A_{\parallel}$ and $A_{\perp}$ k be absorbances of the dye in a liquid crystal for the polarized light whose polarized directions are parallel and perpendicular to the director, respectively.

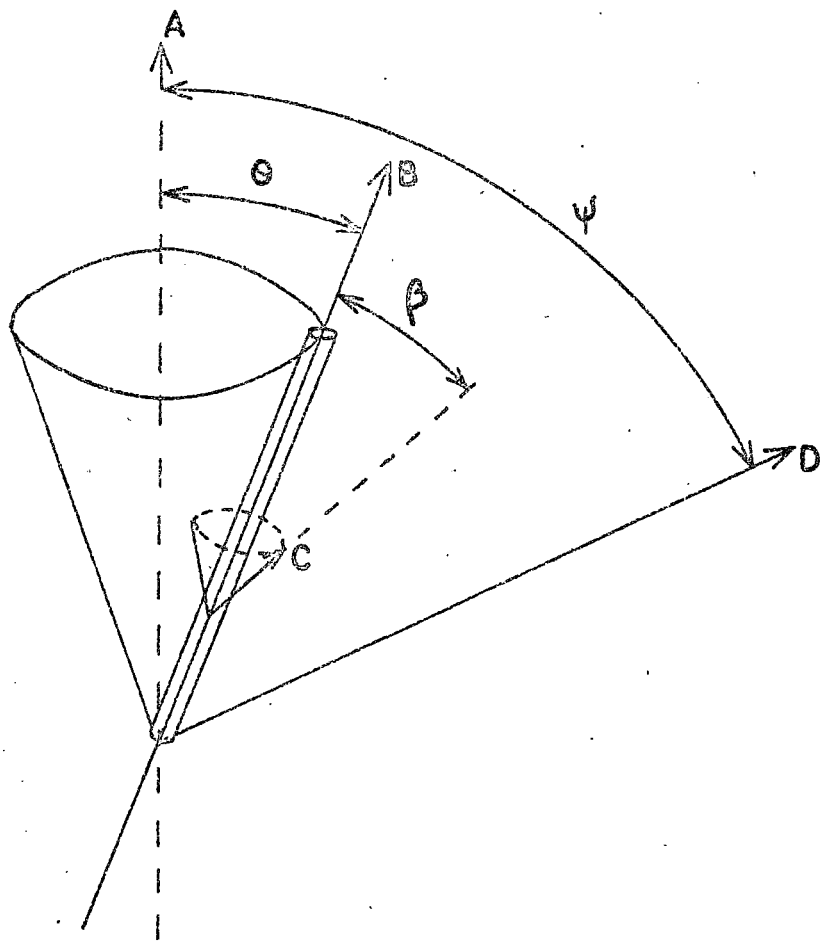

FIG. 12.2. GEOMETRICAL RELATIONSHIP OF DIRECTIONS OF DIRECTOR, 'A' MOLECULAR AXIS OF DYE 'B', TRANSITION MOMENT 'C' AND ELECTRIC VECTOR OF POLARIZED LIGHT 'D'.

The values a for $A_{\parallel}$ and $A_{\perp}$ can be obtained from equation (2)

$$A_{\parallel} = A\ (\beta = 0,\ \psi = 0) = K_M cd\ (1+2S)/3 \quad ...(3)$$

$$A_{\perp} = A\ (\beta = 0,\ \psi = \pi/2) = K_M cd\ (1-S)/3 \quad ...(4)$$

where the direction of transition moment is assumed to be completely parallel to the molecular axis.

If we consider the case of negative dichroic dye (π type dye) which has been reported lately[14] it is found that the dye has a transition moment almost perpendicular to its molecular ~~ax~~ axis but its direction of the moment rotates in a nematic liquid crystal, because the nematic state has freedom in rotation. Therefore, in case of π type dyes, the dye absorbs the perpendicularly polarized light.

$A_{\parallel}$ and $A_{\perp}$ for π type dye are represented from the eqn. (2) as -

$$A_{\parallel} = A\ (\beta = \pi/2,\ \psi = 0) = K_M cd\ (1-S)/3 \quad ...\ (5)$$

$$A_{\perp} = A\ (\beta = \pi/2,\ \psi = \pi/2) = K_M cd\ (2+S)/6 \quad ...\ (6)$$

From the eqn. (3) to (6) dichroic ratios of the σ type and π type dyes D_p and D_n obtained are respectively

$$D_p = \frac{A_{\parallel}}{A_{\perp}} = \frac{1+2S_p}{1-S_p} \quad ...(7)$$

and

$$D_n = \frac{A_{\perp}}{A_{\parallel}} = \frac{2+S_n}{2(1-S_n)} \quad ...(8)$$

From the eqn. (7) the order parameter for p type of dye S_p (or S) can be written as

$$S = \frac{A_{\parallel} - A_{\perp}}{2A_{\perp} + A_{\parallel}} \qquad \ldots(9)$$

As we are using only p type of dyes here, the order parameter S_p is written as S. $A_{\parallel}$ and $A_{\perp}$ are the optical density of the dye at its absorption maxima when aligned parallel to the liquid crystal director, and as measured by plane polarised light perpendicular to the liquid crystal director respectively i.e. for homogeneous alignment $A_{\parallel}$ is the optical density of the dye at absorption maxima in the field off position and $A_{\perp}$ is the optical density of the dye at absorption maxima in the field on position.

It has been suggested by a number of workers[5,7,9] that it is appropriate to correct the dye order parameter for the refractive index anisotropies of the host

$$S_{corr} = \frac{A_{\parallel} n_{\parallel} - A_{\perp} n_{\perp}}{2A_{\perp} n_{\perp} + A_{\parallel} n_{\parallel}} \qquad \ldots (10)$$

where $n_{\parallel}$ is the refractive index of the host in the alignment direction and $n_{\perp}$ is the refractive index of the host perpendicular to the alignment direction and by studying different cases it has been found that the corrected S value is 0.03 to 0.05 higher than the observed S value.

2. Experimental

Liquid Crystals and dye used.

Four different nematic hosts used for our experimental purpose are given below:

I. RO-CN 1540)

p-Cyanophenyl-p-n-heptylbenzoate (CPHB in short)

Nematic range (43.5°C to 56°C)

II- RO-CB 5315.

p-n-pentyloxy-p-biphenylcarbonitrile (5OCB in short)

Nematic range - (47.5°C to 67.5°C).

III. RO-CP 7334

5-p-(n-Butyl phenyl)-2-(p-Cyanophenyl)-pyrimidine

Nematic range - (93.6°C $\gtrless$ 244.7°C).

IV. p-Butyloxybenzal-p-ethylaniline.

m.p. 103°C

For the guest molecules we used five different azo dyes as given below:-

I. Methyl red

II. 2-Hydroxy (benzene Azo)2'-hydroxynepthol.

III. 2-Chloro (benzene azo) 3'-methyl phenol

IV. Dispersol scarlet B.

V. Dispersol Rubine B.

The liquid crystals I, II and III are obtained from M/s. Hoffmann-La-Roche & Co., Basle, Switzerland and the IV is obtained from Prof. A. de Vries, Kent State University, Ohio, U.S.A.

The L. C. sample I, II, III are recrystallized from acetone and the IV is used without further purification.

The dyes I, II and III are synthesized and purified in the chemistry department of North Bengal University and the dyes IV and V are obtained from M/s. Imperial Chemical Industries (U.K.), which are used without further purification.

The chemical structure of different Liquid Crystals and dyes are given below:

Liquid Crystals

I. 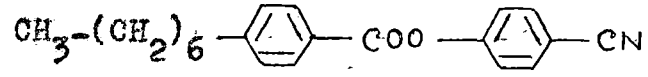

II. 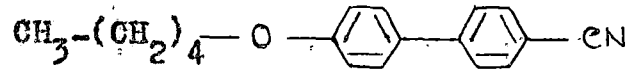

III. 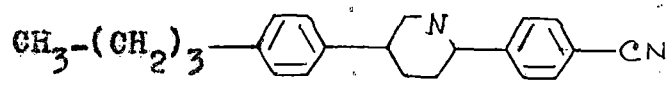

IV. 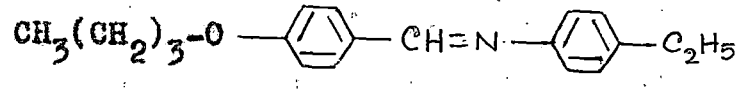

Dyes:-

I. 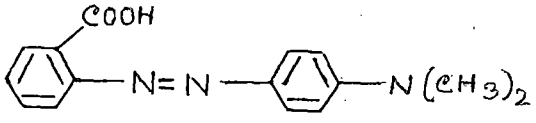

II. 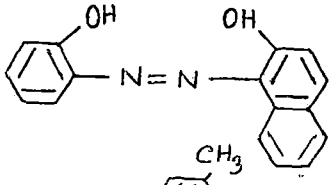

III. 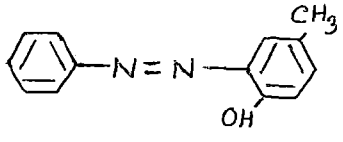

IV. 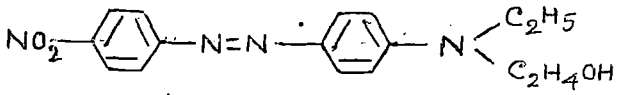

V. 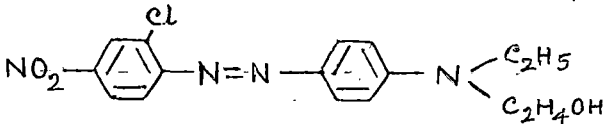

Guest-host mixtures are prepared by mixing different dyes of small amount (0.05 - 0.1%) by wt.) with different liquid crystals and fifteen different guest-host mixtures are prepared for experimental purpose.

Apparatus:-

The apparatus used for this particular experiment is an electro-optic cell or guest-host cell (GH cell in short) with a high temperature attachment and a spectrophotometer for obtaining the absorption spectra in the visible range. The spectrometer used in our laboratory is "Spektromom 202" by which absorption spectra can be obtained both in the UV and visible region. For this experiment the absorption spectra is obtained only in the visible range.

The technique used for the preparation of the GH cell required for our experimental purpose is described below. The cells used consisted of two glass plates 2.5 cm. x 2.5 cm. in area, and 1 mm. in thickness. Each glass plates having one surface transparent conductive layer of a mixture of indium oxide and tin oxides. The conducting glass plate were purchased from M/s. Agrwal Industries, U.P. (India). Some coated glass plates were prepared for us by Prof.K.L. Chopra at I.I.T. Delhi.

To have optical axis parallel to the glass plates and in one specified direction, the surface treatment of the glass plates are necessary. For this reason, the conducting surface of the glass plate is rubbed against a

drawing paper sheet in one well maintained direction for 100 strokes. The conducting surface is coated with 1% aqueous poly vinyl - alcohol solution and the surface is again rubbed against paper for several storkes. After this treatment when the nematic liquid crystal put into contact with the plate, will set its optic axis parallel to the rubbing direction. The cells were made by separating the conducting glass plates with a spacer (a thin glass piece cut from a cover slip of thickness 160 μm) fixed with araldite (Trade name of an epoxy resin). The plates were joined by using araldite outside the spacer such that the araldite could never touch the liquid crystal. Colloidal silver (Silver conducting epoxy) was used for joining the metallic wires. The two glass plates are displaced relative to each other in order to facilitate the filling of the cell by capillarity and to provide space to apply contacts to metallic wires.

Two identical cells are used for experimental purpose. One is kept empty and the other is filled with mixture of dye and liquid crystal. Homogenous alignment of the nematic liquid crystal in GH cell was observed under polarising microscope.

A high temperature attachment to contain the Guest-host cell is designed by us and then fabricated in our workshop which can be inserted into the sample compartment, of the Spectromom. A polarizer was attached to the window of the spectromom and the visible part of the radiation was used for our experimental purpose.

After taking the readings for absorbance with one guest host cell the spectromom was found to be malfunctioning and ultimately we had to stop our experiment with that instrument.

Then we started our experiment with a double beam Spectrophotometer [Shimadzu UV-visible Spectrophotometer] , in Indian Association for the Cultivation of Science, Jadavpur, Calcutta - 32. A new high temperature attachment was designed by us for inserting the GH cell in the sample compartment of the double beam spectrophotometer and is fabricated in our workshop. The part of the high temperature attachment is shown in the fig. 12.3.

As we are using a double beam spectrophotometer the empty cell and the guest host cell are used simultaneously. A brass chamber is made with two separate glass cell containers having two windows for the entrance of light from spectrophotometer. The inner cavity of the cell holder is 2.8 cm. wide, 2.6 cm. deep and 5 mm. in thickness.

The heating element is kept over the middle portion of the brass chamber covered with asbestos as shown in the fig. 12.3 and then insulated with pieces of mica. The whole arrangement is kept inside a tightly closed box made of bakelite having two identical windows for entrance of radiation. Four pieces of optically plane glass plates are kept in between brass and bakelite chamber for maintaining steady temperature. A copper constantan thermocouple is inserted at the lower portion of the brass chamber on the side in which the guest host cell is kept. The connecting wires,

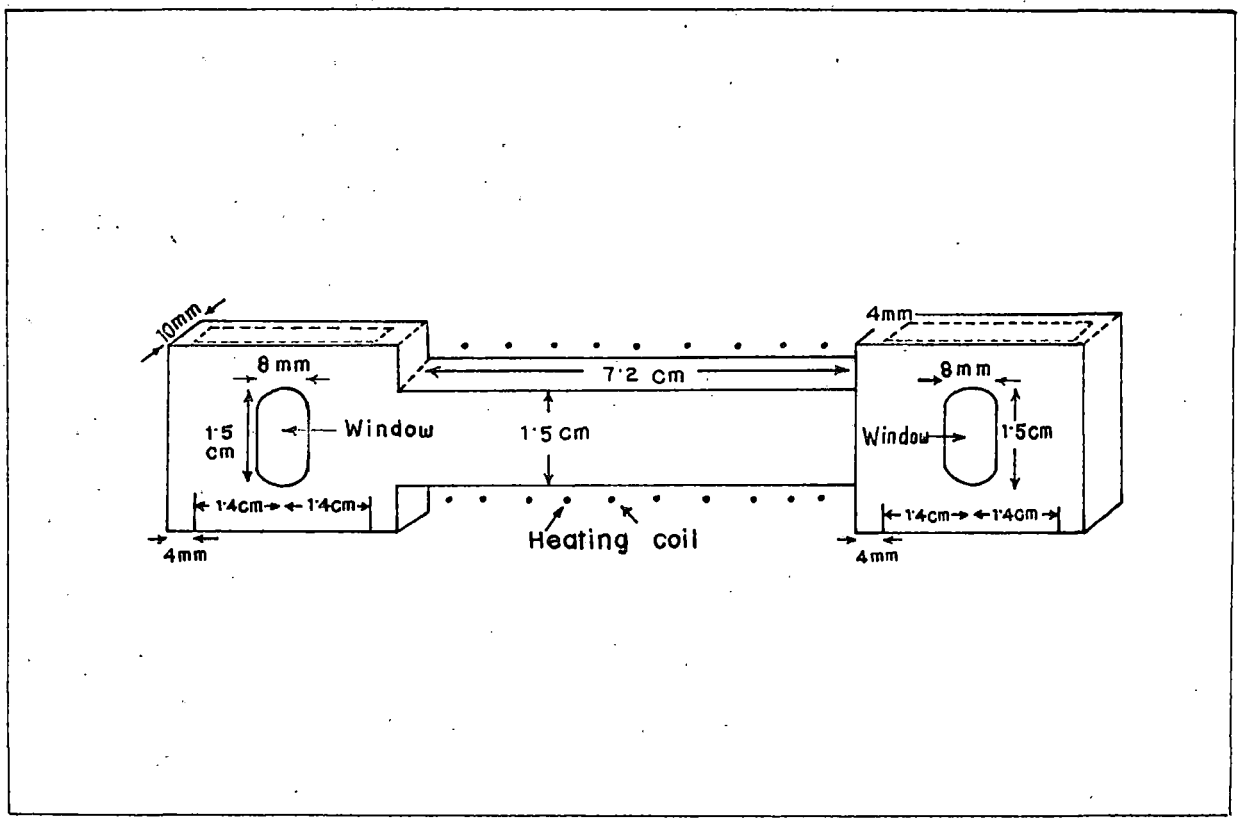

Fig.12·3. Brass chamber for inserting GH cell.

heating coils and the two ends of the thermocouple are brought outside by making holes on the bakelite box. Some metallic pieces with windows of equal size as in the brass chamber are kept inside the cavity of the brass chamber after inserting the glass cell in it to attain the steady temperature.

The thermocouple is calibrated with three samples of known melting point as described in chapter 2. Polarizers are attached on separate ebonite cases to the outer part of the bakelite box. The temperature was regulated within ± 1° to 2°C. The D.C. electric field applied to the guest host cell is 10 volts-50 volts.

3. Results and Discussions:

Absorption spectra in the visible region for different guest host cells were obtained from the recorder attached with the double beam spectrophotometer. Absorption spectra of all the guest host cells were obtained in the electric field off and on position with the polarized light component whose polarized direction is parallel to the molecular axis. The optical density of the dye at its absorption maximum (λ^{max}) is obtained from both the spectrum i.e. in the field off and on position, and thus $A_{\parallel}$ and $A_{\perp}$ values are obtained. Then using the eqn. 9, the order parameter values 'S' are calculated.

The order parameter values S along with $A_{\parallel}$ and $A_{\perp}$ values for fifteen different guest host mixtures are shown in Table 12.1. This table also includes particular temperature

of the guest host mixture and also the λ^{max} values in nm.

From table 12.1, it is found that the order parameter values varies from 0.02 to 0.49 and in general much lower than the expected order parameter values from the mean field theory, which indicates that in most of the cases the guest molecules have very poor ordering with the nematic hosts.

From the table it can be observed that S values are lowest for the dye I in all the nematic hosts. One reason for this may be cited as poor solubility of the dye I. It could be visually observed that some fine particles of dye are present in the guest host mixture. Dye II and III have almost identical length and structure. The S value is maximum for the mixture no. 9 (i.e. dye III in L.C. II) and next value is for mixtures no. 5 (dye II in L.C.II).

For the poor ordering of the guest molecules a different factors may be responsible.

Solubility of the dye molecules in the hosts used by us are not very good in general.

The field applied is d.c. field in this experiment. Application of A.C. field could have yield better results. This field used for cell thickness 0.16 mm. is only from 10 volts to 50 volts which may not be sufficient for the maximum alignment of the guest molecules. However, in this range of applied field we could not observe any significant change.

Some impurity present in the dye used which may be one of the causes for lowering the S values.

Structures of the dye used for experimental purpose show that they are not sufficiently long and some branches along the side chain are present. This implies that the guests will not be able to align perfectly in the direction of the hosts.

The order parameter of oriented nematic liquid crystals I & II have been determined by X-ray diffraction as given in chapter 7 and chapter 8. One thing can be definitely said that the order parameter determined from the guest host interactions are not same as the order parameter for nematic hosts.

Three of our liquid crystals have permanent dipole moments and the interactions between the host dipole and the guest dipole may cause some local cluster formation resulting in lower value of 'S'. However, we think this is not the main reason in our case since the maximum value of 'S' was obtained with a polar liquid.

From the table 12.1, it is found that there is no systematic variation of order parameter 'S' with temperature this may be due to the change in solubility of dye molecules or there are factors involved which we cannot explain.

The experiment could have been repeated by using thinner spacers in the GH cell and taking cautions for all other above mentioned factors. Unfortunately it was not p possible as the experiment had to be performed in a distant laboratory with limited access to the spectrophotometer. Also, all efforts to repair our 'Spectromom 202' were unsuccessful.

TABLE 12.1.

Mixture No.	Dye	L.C.	Temp. °C.	λ_{max} (nm)	$A_{\parallel}$	$A_{\perp}$	Order parameter (S)
1	I	I	45	485	2.004	1.803	0.03
			48	485	2.100	1.92	0.03
			53	485	2.235	2.138	0.02
2	I	II	48	480	2.406	2.184	0.05
			52	480	2.258	2.01	0.03
			56	480	2.244	2.055	0.03
3	I	III	98	488	1.41	1.098	0.09
			105	488	1.38	1.08	0.08
			112	488	1.35	1.095	0.07
			117	488	1.38	1.155	0.07
4	II	I	45	425	1.64	0.69	0.19
			48	425	0.878	0.60	0.13
5	II	II	50	0.520	0.984	0.396	0.33
			55	0.520	0.705	0.6	0.08
			60	0.520	0.69	0.6	0.05
			65	0.520	0.72	0.6	0.06

Contd.....

Table 12.1 (Contd.)

Mixture No.	Dye	L.C.	Temp. °C	λ_{max} (nm)	$A_{\parallel}$	$A_{\perp}$	Order parameter (S)
6	II	III	95	522	0.306	0.219	0.11
			100	522	0.285	0.21	0.11
			105	522	0.36	0.285	0.12
			110	522	0.573	0.48	0.06
			115	522	0.585	0.54	0.03
7	II	IV	104	520	0.645	0.45	0.126 ≃ 0.13
8.	III	I	48	520	0.345	0.225	0.15
			52	520	0.24	0.21	0.05
			55	520	0.243	0.213	0.05
9.	III	II	54	524	0.57	0.306	0.22
			58	524	0.547	0.308	0.21
			60	524	0.504	0.30	0.19
			62	524	0.495	0.126	0.49
10.	III	III	95	520	0.45	0.28	0.17
			100	520	0.45	0.42	0.02
			105	520	0.45	0.42	0.02
			110	520	0.465	0.42	0.03
			115	520	0.465	0.426	0.03
			120	520	0.435	0.396	0.03

Contd.....

Table 12.1 (Contd.)

Mixture No.	Dye	L. C.	Temp. °C	λ_{max} (nm)	$A_{\parallel}$	$A_{\perp}$	Order parameter (S)
11.	II	IV	104	522	0.675	0.48	0.12
12.	IV	I	47	520	0.5	0.381	0.09
			51	520	0.67	0.46	0.13
13.	IV	II	49	485	0.78	0.52	0.14
			55	485	0.77	0.455	0.19
			63	485	1.02	0.655	0.15
14.	V	I	44	425	0.48	0.43	0.04
			51	425	0.365	0.322	0.04
			54	425	0.485	0.445	0.03
15	V	II	49	520	0.36	0.225	0.17
			55	520	0.575	0.405	0.12
			65	520	0.7	0.6	0.06

References:

1. G.H.Heilmeir and L.A. Zanoni, Appl. Phys. Lett. 13,91 (1968).
2. G.H.Heilmeier, J.A. Castellano and L.A. Zanoni, Mol.Cryst. Liq.Cryst. 8, 293 (1969).
3. G.H.Heilmeier, J.A. Castellano and L.A. Zanoni, Liq.Cryst. 2, Part II, G.H. Brown, Ed. Gordon and Breach, London (1970), pp. 763-74.
4. D.L.White and G.N.Taylor, J.Appl.Phys. 45, 4718 (1974).
5. L.M.Blinov, V.A. Kized, V.G.Rumyantsev, and V.V.Titov, J.Phys. (Paris) 36 (Cl.Suppl.3), 69 (1975).
6. J.Constant, E.P. Raynes, I.A. Shanks, D.Coates, G.W.Gray and D.G.McDonnell, Abstracts, Sixth International Liquid Crystal Conference, Kent, Ohio, August, 1976, HOK-11.
7. H.Wedel and W.Haase, Ber.Bun. Ges. 80, 1342 (1976).
8. A. Bloom and P.L.K. Hung, Mol.Cryst.Liq.Cryst., 1977, 40, pp. 213 (1977).
9. A. Bloom, P.L.K. Hung and D. Meyerhofev, Mol.Cryst. Liq. Cryst. (Lett.) 41, Po. 1-4, (1977).
10. A. Bloom, P.L.K. Hung, Mol.Cryst.Liq.Cryst. 44,p.323 (1978).
11. R.J.Cox, Mol.Cryst.Liq.Cryst. 55, p.1-32 (1979).
12. T.Uchida and M.Wada, Mol.Cryst.Liq.Cryst., 63, p.19-44 (1981).
13. K.Toda, S. Nagura, T.Watanabe; M. Sukigara, and K.Honda, Nippon Kagaku, Kaishi, No.3, 459 (1975).
14. D. Demus, B. Kricke, F. Kuschel, H.V.Nothnick, G.Pelzl, and H. U Zaschke, Mol.Cryst.Liq.Cryst.Lett., 56, 115 (1979).

CHAPTER 13.

SUMMARY AND CONCLUSIONS.

CHAPTER 13

SUMMARY AND CONCLUSION

In the present work, I have reported X-rays, spectroscopic and textural studies on several liquid crystals in Nematic, Smectic and Cholesteric phases.

I have designed a hot stage to study the textures and the phase transitions between different mesophases under polarising microscope. I have been able to obtain the transition temperatures of seven different mesomorphic compound and also to identify different mesophases by texture analysis under polarising microscope. The existence of S_A, S_B and cholesteric phases in MBAC sample were confirmed by texture analysis. The sample PCBAV possesses only S_A phase, both 8OCB and CB0OA possess S_A as well as nematic phase and the three other samples (MBBA, CPHB and 5OCB) possess only nematic phases which were observed under polarising microscope.

A high temperature X-ray, camera for taking flat plate photographs of liquid crystal samples in magnetic field is designed and fabricated in our laboratory[1]. Utilizing this camera, I have been able to take X-ray photographs of aligned samples of five liquid crystal compounds over their entire mesomorphic temperature range (including the supercooled phase)[2,5,3a,3b].

The X-ray diffraction photograph of MBBA sample in a glass capillary oriented by recycling (i.e. by heating and cooling) prbesess is taken at room temperature using a Universal camera[4,5]. As MBBA breaks down very easily photographs

at different temperature could not obtained. Most probably due to presence of cholesteric phase, sample MBAC[6] could not be aligned by the application of magnetic field of about 6 Kilo gauss. So the unoriented photographs of the sample MBAC in absence of magnetic field were taken by utilizing another high temperature X-ray diffraction camera designed and fabricated in our laboratory. Photographs of ± other mesomorphic compounds in absence of magnetic field are also taken ± by this camera.

The photographic optical density values were measured with a microdensitometer and were converted to relative intensity values using a standard calibration method. The X-ray intensity data have been analysed to give the normalized distribution function, $f(\beta)$ in a power series of $\cos^2\beta$ and the orientational order parameters $\langle P_2 \rangle$ and $\langle P_4 \rangle$. In principle, we could obtain $\langle P_6 \rangle$ and $\langle P_8 \rangle$ etc. from our data, however experimental uncertainties and truncation errors involved in series representation, would make the value of these higher order parameters unreliable.

I have compared these experimentally obtained $f(\beta)$ values with those obtained from the Maier-Saupe mean field potential by taking the potential containing P_2 term only as well as the potential containing both P_2 and P_4 terms for the four cyno compounds (CPHB, 5OCB, 8OCB and CBOOA). The agreement between the Maier-Saupe theoretical values and the experimental values for the strongly polar cyano compounds are not good except for the sample 8OCB. For all the substances the agreement between the experimental and theoretical values

become worse if the P_4 term in the potential is included. It seems that for strongly polar molecules the Maier-Saupe theory does not give a good distribution function. Also, the introduction of the P_4 term in the mean field potential fails to account for the permanent dipole-permanent dipole interaction.

The order parameter $\langle P_2 \rangle$ and $\langle P_4 \rangle$ values have also been compared with Maier-Saupe theoretical predictions.

In case of nematic mesophase of CPHB the $\langle P_2 \rangle$ values were found to be larger than the Maier-Saupe theoretical value, whereas $\langle P_4 \rangle$ values are significantly lower than the M.S. theoretical predictions PCBAV having S_A phase only shows higher experimental values for both $\langle P_2 \rangle$ and $\langle P_4 \rangle$. The experimental $\langle P_2 \rangle$ values for both the compounds 50CB and 80CB are found to be larger than M.S. theoretical values and the experimental $\langle P_4 \rangle$ values for 50CB and the nematic phase of 80CB are lower than the M.S. theoretical values. In S_A phase of 80CB the experimental $\langle P_4 \rangle$ values seem to agree with theoretical values within experimental uncertainity. In CBOOA the experimental values of $\langle P_2 \rangle$ and $\langle P_4 \rangle$ are higher. For MBBA $\langle P_2 \rangle$ shows a good agreement with theoretical value within experimental uncertainity, but $\langle P_4 \rangle$ value found experimentally is much lower than the theoretical value. However, the $\langle P_4 \rangle$ value is positive and is much larger than the values obtained by Shen Jen[7] et al and is in good agreement with the $\langle P_4 \rangle$ obtained by Kobinata[8] et al.

Translational order parameter τ_1 and the average value of the equare of the root mean square displacement $\langle z^2 \rangle^{1/2}$ of S_A phase of PCBAV at one particular temperature is determined as the second order reflection is obtained prominently. In case of S_A phase of 8OCB and CBOOA as the second order x reflections are not observed in the photographs of S_A phase the translational order parameters could not be determined. The photographs of S_A and S_B phase of MBAC showed second order reflection line, but due to the low intensity, calculation of translational order parameter is not possible. In case of MBAC the orientational order parameters also could not be determined as x I could not get the photograph of the oriented sample in the magnetic field.

The X-ray data have also been analysed to obtain apparent molecular length/layer thickness and intermoleculer distance in the mesophases. The layer thickness of MBAC in its smectic phase is found to be little larger than the length of the molecule in its completely stretched form, the probable reason for which is given in chapter 5. The apparent molecular length/layer thickness in case smectic phase of the four cyano compounds (CPHB, 5OCB, 8OCB and CBOOA) in the mesophases are much longer than their expected length, which can be explained by the formation of association of molecules (due to the strong dipole moment of the $C \equiv N$ group) in the mesophase. This type of association has been found by Leadbetter[6] and x others in the different

cyano compounds. For PCBAV sample the layer thickness of the molecule is almost same as the length of the molecule in its completely extended form. We have also corrected the apparent molecular lengths, as obtained in the smectic phases, for thermal vibrations, as suggested by de Vries[9].

The intermolecular distances are in expected range 4.8 Å to 5.2 Å in all the compounds studied except for the cholesteric phase of MBAC, where the intermolecular distance is 5.2 Å to 5.4 Å. However for all the substances, the intermolecular distance seems to decrease with the increase in the applied magnetic field. Though the effect is quite small (2% to 3%), its persistence in all the compounds and its saturation with the magnetic field forces us to believe it to be a real effect. The diameter of the outer halo which determines the intermolecular distance, were measured at different angles to the equatorial line without observing any change from the equatorial diameter. Of course, for aligned samples, the intensity of the outer halo falls off rapidly away from the equator, so this procedure can be accurately done only within ± 20° of the equatorial x line. At about 1 K.Gauss, magnetic field the saturation of the intermolecular distance occurs irrespective of the temperature of the sample. The degree of ordering also reaches saturation value at this field which implies apparently that the intermolecular distance is dependent on the degree of ordering (However this change in intermolecular distance does not produce any volume change). Why the intermolecular

distance (lateral) should change with magnetic field could not be explained.

I have designed and fabricated a high temperature attachment for the Guest Host cell with a view to get an a idea about ordering of dye molecules in different nematic liquid crystalline hosts. As the spectrophotometer in our laboratory started malfunctioning after a ~~fx~~ few readings, I had to use the spectrophotometer at the Optics Department of Indian Association for the Cultivation of Science, Jadavpur, Calcutta-32. I had to redesign the high temperature attachment to suit the new spectrophotometer used. Though, I could measure the absorption spectra of five different guest dyes in four different nematic hosts at different temperatures the results obtained are not quite expected because, in most of the cases I could get very poor ordering of the dyes; the probable reasons for which are described in chapter 12.

Most probably, many phenomena in my work are left unexplained, however, it is sure that future research workers will try to tackle these problems and will come up with the solutions sooner or later.

References:

1. Reference No. 2 of Chapter 2

2. Reference No. 3 of Chapter 7

3. Reference No.4a of Chapter 10

3a. Reference No.3a of Chapter 9

3b. B.Jha, B.Bhattacharjee, S. Paul and R.Paul, Phys. Stat.Sol.(a) 76, 1983 (In Press).

4. Reference No. 4 of Chapter 6

5. Reference No. 5 of Chapter 6

6. B.Bhattacharjee, R.Paul and S. Paul, Mol.Cryst.Liq. Cryst. 65, p.61 (1981).

7. Reference No. 1 of Chapter 6.

8. Reference No. 2 of Chapter 6

9. Reference No. 7 & 8 of Chapter 9.

List of Publications

1. The order parameter of 4-Methoxy-4-n-Butylbenzylidene-Aniline (MBBA) from X-ray Diffraction Data. Basana Bhattacharjee, Ranjit Paul and Sukla Paul, Jap. J. Appl. Phys. Vol.18, No.5 (1979).

2. X-ray Diffraction studies of (-)-2-Methylbutyl p-(n-(P-Methoxy Benzylidene) Amino) Cinnamate. Basana Bhattacharjee, Ranjit Paul and Sukla Paul, Mol. Cryst. Liq.Cryst. Vol.65, pp. 61-72 (1981).

3. Structure of the smectic phase of 4'-(n-(p-Pentyloxy Carbonyloxy Benzylidene) Amino) valerophenone, B.Bhattacharjee, A. Zeminder and S.Paul, Proc. Nucl. Phys. and Solid State Phys. Symposium, Vol.21C (Solid State Physics) p. 420 (1978).

4. Order parameter of 4'-n-Pentyloxy-4-Biphenyl carbonitrile in nematic phase, B. Bhattacharjee, R. Paul and S. Paul, Proc. Nucl. Phys. & Solid State Phys. Symposium (Solid State Physics), (1980).

5. Order parameter and the orientational distribution function for 4-cyanophenyl-4'-n-heptyl benzoate in the nematic phase, B.Bhattacharjee, S.Paul and R.Paul, Mol. Phys. Vol.44, No.6, 1391-1398 (1981).

6. Order parameters and distribution function of 4'-(n-(p-Pentyloxy carbonyloxy-Benzylidene) Amino) Valerophenone in smectic phase from X-ray Diffraction measurements, Mol.Cryst.Liq.Cryst.Vol.88, pp.245-254(1982), B. Bhattacharjee, R. Paul and S. Paul.

8

7. Orientational Distribution Function and order parameters of two 4'-Alkoxy-4-Cyanophenyls in Mesomorphic phase, Basana Bhattacharjee, Sukla Paul and Ranjit Paul, Mol. Cryst. Liq.Cryst. Vol. 69, pp 181-192 (1982).

8. Orientational Distribution Function and order parameters for MBBA, Basana Bhattacharjee, Sukla Paul and Ranjit Paul, Presented at Ninth International Conference on Liquid Crystals, Bangalore, India (1982) Abstract B-21P.

9. X-ray diffraction studies on the mesophases of n-p-Cyanobenzylidene-p-Octyloxy Aniline in Magnetic field, B. Jha, B.Bhattacharjee, S.Paul and R. Paul, Phys. Stat. Sol.(a) 76, (1983) (In Press).

NORTH BENGAL
UNIVERSITY LIBRARY
RAJA R[illegible]PUR